Northumbria Research Link

SYNTROPHIC INTERACTIONS IN THE DIGESTION OF FUNGAL β-GLUCAN BY THE GUT MICROBIOTA

P J FERNÁNDEZ JULIÁ

PhD

2022

SYNTROPHIC INTERACTIONS IN THE DIGESTION OF FUNGAL β-GLUCAN BY THE GUT MICROBIOTA

PEDRO JESÚS FERNÁNDEZ JULIÁ

A thesis submitted in fulfilment of the requirements of the University of Northumbria at Newcastle for the degree of Doctor of Philosophy in Human Nutrition

Research undertaken in the Faculty of Health and Life Sciences and in collaboration with Quorn®, Northumberland

November 2022

Abstract

The human gut microbiota (HGM) contributes to the physiology and health of the host. The health benefits provided by dietary manipulation of the HGM require knowledge of how glycans are metabolized. β-glucans are polysaccharides that can be obtained from different sources, and which have been described as potential prebiotics since they support the growth of gut-associated bacteria, including members of the genera *Bacteroides*, *Bifidobacterium* and *Lactobacillus*. Nevertheless, the mechanism of action underpinning these health effects has been subject to debate and revision. By using alkaline extraction, β-glucan was purified from the fungi *Fusarium venenatum,* and it was consumed by certain members of the genus *Bacteroides* as primary degraders, although the ability to degrade the intact polysaccharide was also tested in some members of the genera *Roseburia*, *Akkermansia* and *Victivallis*. It was shown that *Bacteroides cellulosyliticus* WH2, *Bacteroides thetaiotaomicron* VPI 5482 and *Bacteroides vulgatus* ATCC 8482 express specific enzymes to degrade *Fusarium* β-glucan, thereby releasing short-chain fatty acids and oligosaccharides into the growth medium. Using a cross-feeding approach, those oligosaccharides were purified and then utilized as carbon source for members of the genera *Bifidobacterium* and *Lactiplantibacillus*, which acted as secondary degraders. Finally, they were grown in cocultures with *Bacteroides* species. Using colony counting and qPCR, it was shown that both primary and secondary degraders grew in the coculture by establishing syntrophic interactions when *Fusarium* β-glucan acted as carbon source. The data obtained points out the potential prebiotic effect that *Fusarium* β-glucan may have as a polysaccharide substrate for different members of the Human Gut Microbiota.

List of Contents

List of Tables

List of Figures

Covid 19 impact

Due to the Covid-19 pandemic, my access to the laboratory was suspended from 23rd March 2020 until 22nd September 2020. Moreover, on 12th November 2020 I was diagnosed with Covid-19, and I had to stay self-isolated until 23rd November 2020, losing ten more days of lab work. Apart from the six months when the labs were closed and the period when I was infected, I had to stay at home for either two weeks or ten days anytime I came back from visiting my family in Spain. Furthermore, I had to stay at home when some lab colleague or friend reported me as a close contact when he/she got the infection. In addition, the delays in the delivery and acquisition of reagents and instruments must be considered as well. For all these reasons, the total amount of time inwhich lab work could not be developed is estimated in nine months. That means a fourth part of the total time of this thesis.

Even though the lab work is essential for carrying out the project, my research training and development was also affected. I couldn't attend several conferences such as the "2nd European Conference in Biocatalysis" (Utrecht July 2020) or the "Mycoprotein Research Conference 2020" (London, 2020) which were canceled. My placement for 3 months in the department of Biochemistry at the University of Cambridge was canceled as well.

Therefore, I adjusted my objectives and changed the project plan to finish my research within the original deadline, trying to not request any extension. This unprecedented pandemic was one more problem to deal with, making even harder my PhD because of the fear and pressure of getting infected at any moment. In conclusion, all the mentioned facts should be considered before judging the quality and extension of my research work.

List of Publications

- **P. J. Fernandez-Julia**, J. L. Munoz-Munoz, D. van Sinderen, The impact of β-glucan metabolism by Bacteroides and Bifidobacterium species as members of the gut microbiota, *Int. J. Biol. Macromol.*, (2021). doi: https://doi.org/10.1016/j.ijbiomac.2021.04.069.

- J. Munoz-Munoz, D. Ndeh, **P. Fernandez-Julia**, G. Walton, B. Henrissat, H. J. Gilbert, Sulfation of arabinogalactan proteins confers privileged nutrient status to *Bacteroides plebeius*, *Mbio*, (2021). doi: https://doi.org/10.1128/mbio.01368-21.

- **P. J. Fernandez-Julia**, D. M. Commane, D. van Sinderen, J. Munoz-Munoz, Cross-feeding interactions between human gut commensals belonging to the *Bacteroides* and *Bifidobacterium* genera when grown on dietary glycans, *Microbiome Res. Rep.*, (2022). doi: https://doi.org/10.20517/mrr.2021.05.

- **P. Fernandez-Julia,** G. Black, W. Cheung, D. Van Sinderen, J. Munoz-Munoz, Fungal β-glucan-facilitated cross-feeding activities between *Bacteroides* and *Bifidobacterium* species, *Commun. Biol.* (2023). doi: https://doi.org/10.1038/s42003-023-04970-4.

List of Conferences

- Poster presentation of my PhD project **"Syntrophic interactions in the digestion of fungal β-glucan by the gut microbiota"** in the **Microbiology Society Annual Conference 2022** (Belfast, 6th April 2022).

- Poster presentation of my PhD project "**Syntrophic interactions in the digestion of fungal β-glucan by the gut microbiota**" in the fourth annual **Harvard Chan Microbiome in Public Health Center (HCMPH) symposium** (online, 16th May 2022).

- Oral presentation of my PhD project "**Syntrophic interactions in the digestion of fungal β-glucan by the gut microbiota**" in the 3 min thesis competition 2022 (Northumbria University), 21st June 2022).

Authors' Contributions

In the publication **"A comprehensive review on the impact of β-glucan metabolism by *Bacteroides* and *Bifidobacterium* species as members of the gut microbiota"**, I wrote the original draft. Prof Van Sinderen and Dr Munoz-Munoz review it, being responsible for the editing and conceptualization.

In the publication **"Sulfation of Arabinogalactan Proteins Confers Privileged Nutrient Status to *Bacteroides plebeius"***, I developed the protein mutagenesis and subsequent analysis of co-cultures of *Bacteroides plebeius* and *Bacteroides cellulosyliticus*. Dr Munoz carried out protein expression, growth studies of monocultures, biochemical analysis of the enzymes, transcriptomics, experimental design. Batch fermentations of the human microbiota were carried out by Dr Munoz-Munoz and Dra Walton. rRNA profiling of the HGM was done by Dr Nelson employed by NU-OMICS (Northumbria University). Prof Gilbert wrote the manuscript, which was revised by Dr Henrissat and Dr Munoz-Munoz.

In the publication **"Cross-feeding interactions between human gut commensals belonging to the *Bacteroides* and *Bifidobacterium* genera when grown on dietary glycans"**, I wrote the original draft while Dr Commane, Prof van Sinderen and Dr Munoz-Munoz were responsible for reviewing, editing, and conceptualization.

In the publication **"Fungal β-glucan-facilitated cross-feeding activities between *Bacteroides* and *Bifidobacterium* species"** I cloned, expressed, and purified recombinant

enzymes; conducted and analysed kinetics for hydrolysis of polysaccharides, oligosaccharides, and chromogenic substrates; determined hydrolysis products in the HPLC; performed growth curves of all anaerobic bacteria; carried out cross-feeding experiments; and wrote the article. Dr Cheung conducted and analysed the proteomics data and wrote the proteomics section in the manuscript. Prof Black, Prof van Sinderen and Dr Munoz-Munoz directed research and co-wrote the article with input from all authors.

Acknowledgments

Firstly, I would like to thank my supervisors Dr Jose Munoz-Munoz, Prof Gary Black and Dr Daniel Commane for the opportunity to complete my PhD studies at NorthumbriaUniversity. Moreover, thank you specially to my first supervisor Dr Jose Munoz-Munoz for all the support through the stressful times, many nights and weekends in the lab. I would also like to extend my thanks to the team at Quorn®, for all the help that Dr Tim Finnigan has offered during all this project.

Secondly, would like to thank my mother, my father, my sister and, specially, my beloved Ana who has been my best support and the reason why I never gave up. Without you all,I would never have been able to complete my studies. Thanks to the rest of my family and friends for helping me despite the long distance between us.

Further thanks to my lab mates Migena, Effie and Joe, for understanding and helping each other in many afternoons and nights in the lab.

Finally, I would like to dedicate this thesis to my grandparents. I know the three of you take care of me from up there.

Declaration

I declare that the work contained in this thesis has not been submitted for any other award and that it is all my work. I also confirm that this work fully acknowledges opinions, ideas and contributions from the work of others. The work was done in collaboration with Quorn®.

Any ethical clearance for the research presented in this commentary has been approved. Approval has been sought and granted through the Researcher's submission to Northumbria University's Ethics Online System on 22nd November 2022.

I declare that the Word Count of this Thesis is 58,002words.

Name: Pedro Jesús Fernández Juliá

Signature:

Date: 30/11/2022

1 Introduction

The diverse community of microorganisms that inhabit the human gastrointestinal (GI) tract make up the human gut microbiota (HGM) (Thursby et al., 2017). The HGM consists of protozoa, archaea, eukaryotes, viruses and bacteria and these organisms have evolved to exist symbiotically within the host, exerting various beneficial roles including protection from invading pathogens, development of host systems, maintaining gut homeostasis and modulating the immune system. The Human Gut Microbiota (HGM) forms a recently considered novel organ of the human body that impacts human health in a variety of ways (Nishida et al., 2018; Quigley, 2017). It is made up mainly of three main phyla: Bacillota, Bacteroidota and Actinomycetota (Figure 1).

Figure 1. Diagram for the most abundant microbial components of the human microbiota in the colonic section of the gut.

The HGM in both worldwide populations represents a complex microcosm of trillions of microorganisms. In Western populations, Bacteroidota and Bacillota are the most dominant phyla, while Actinomycetota, Proteobacteria and Verrucomicrobiota are less abundant (Qin et al., 2010; Yang et al., 2009) (Figure 2). Nonetheless, such minor components may still represent important ecological players in the complexity of HGM, specially for the metabolic interactions they offer to members of the Bacteroidota and Bacillota phyla (Cani et al., 2017; Hou et al., 2020).
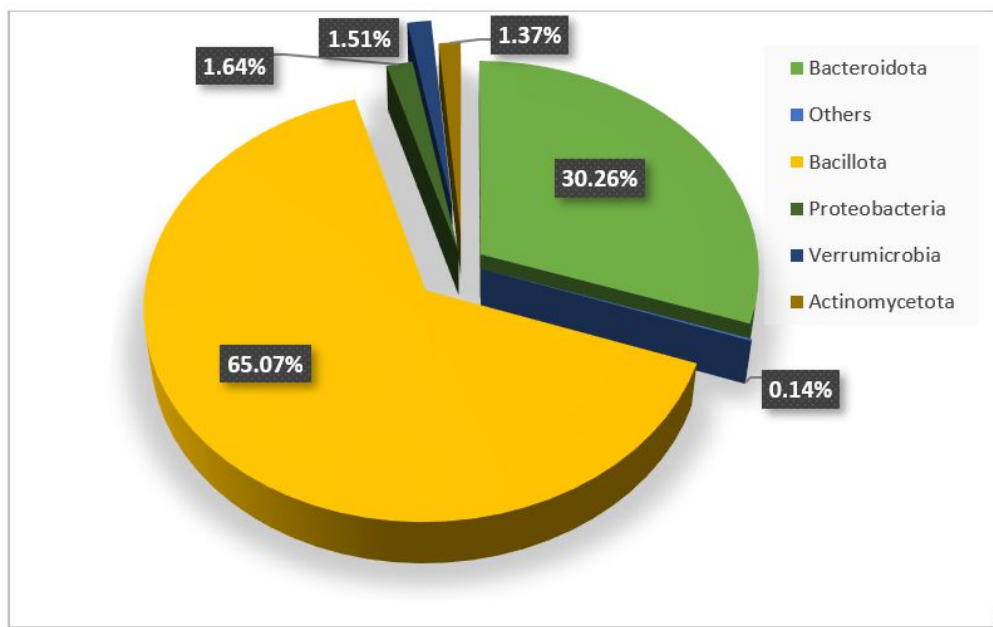
Figure 2. Percentages of the predominant phyla according to their relative abundance in the human gut (Yang et al., 2009).

1.1 *Bacteroides* genus

Bacteroides is the main genus within the Bacteroidota phylum. Most of the *Bacteroides* members are common gut commensals, but, under some conditions, they can act as opportunistic pathogens (Colov et al., 2020; Maraki et al., 2020). *Bacteroides* are widely spread in different natural niches and human populations and possess a lot of mechanisms to adapt to various competitive environments (Arumugam

et al., 2013; De Filippo et al., 2010; Kelsen et al., 2012; Koropatkin et al., 2012; Wexler et al., 2017).

Bacteroides species are broadly known for their role as primary glycan degraders since their genomes dispose of polysaccharide utilization loci (PULs) (Figure 3) which lie in clusters of genes, all of them behind the same regulon, and involved in the detection and digestion of a specific polysaccharide. To date, all sequenced *Bacteroides* genomes contain PULs, which typically encode surface glycan-binding proteins (SGBPs), enzymes for carbohydrate degradation (glycoside hydrolases, GHs, and polysaccharide lyases, PLs), TonB-dependent transporters (TBDT) which are of vital importance for the transport of nutrients into the cell, and transcriptional sensors/regulators that act as modulators for the gene expression.(Cantarel et al., 2012; El Kaoutari et al., 2013; Grondin et al., 2017).
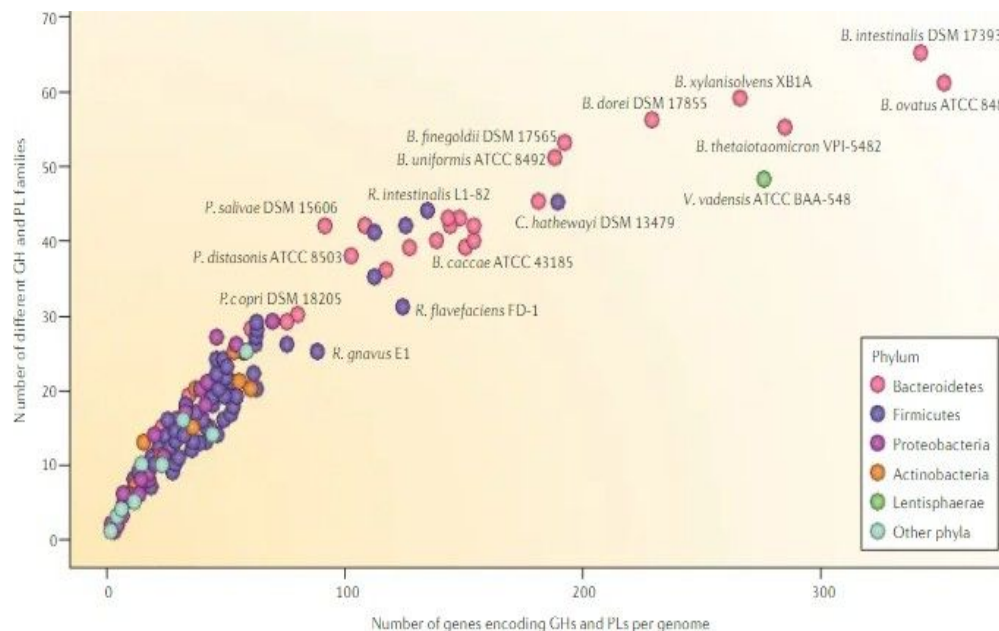
Figure 3. Distribution of genes encoding glycan-cleaving enzymes (GHs and PLs) in the genomes of different members of the HGM, and the numbers of GHs and PLs families located in these genomes (El Kaoutari et al., 2013).

For this reason, they can access a broad range of complex carbohydrate substrates (Eilam et al., 2014). For example, for the case of *Bacteroides thetaiotaomicron*, which is the model for the study at *Bacteroides* genus (see Figure 4 below), around the 18% of its genome content is devoted to carbohydrate metabolism. This fact points out the huge metabolic capacity and versatility of *Bacteroides* sp. to use different types of polysaccharides (Grondin et al., 2017; McNulty et al., 2013; Terrapon et al., 2018). Furthermore, the degradation of dietary fibre by the Human Gut Microbiota results in the production of beneficial substances such as postbiotics which are functional bioactive compounds that are generated through microbial fermentation and they have the potential to benefit the health of the host (Wegh et al., 2019).
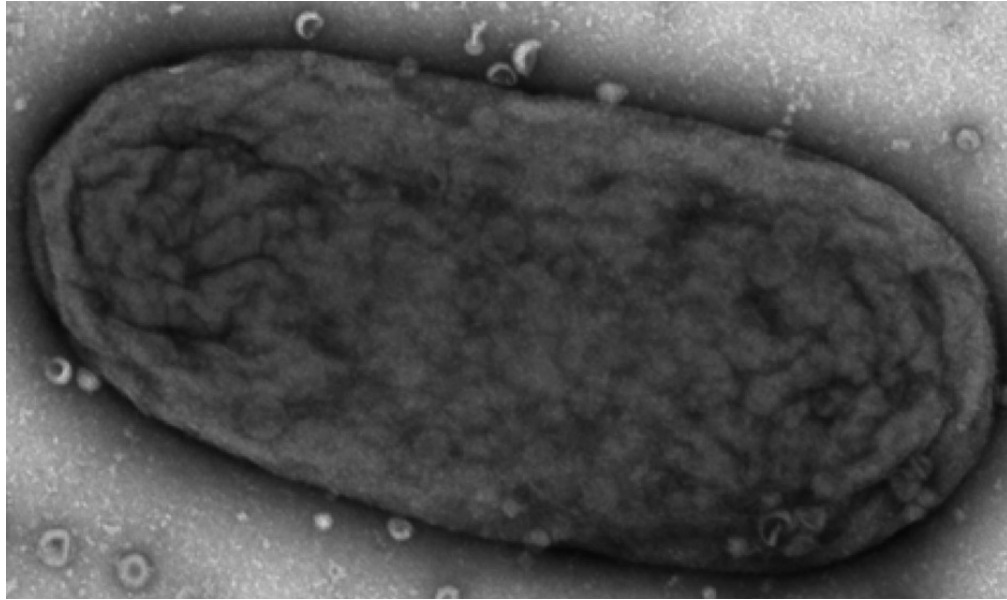
Figure 4. Transmission electron microscopy of a single cell of *Bacteroides thetaiotaomicron* VPI 5482 (Valguarnera et al., 2018).

Polysaccharide breakdown usually begins at the cell surface by a GH or PL via degradation of the complex intact polysaccharide into oligosaccharides. After this, these released oligosaccharides are then transported into the periplasm by pairs of SusC/SusD-like TBDT proteins (Glenwright et al., 2017). However, they may also be utilized by other bacteria as substrates through cross-feeding, a common phenomenon observed for complex polysaccharides but also with essential cofactors such as folates or corrinoids (Briggs et al., 2020; Cantarel et al., 2012; El Kaoutari et al., 2013; Seth et al., 2014). In the periplasm, several exo- and endo-glycosidases are responsible for further hydrolysis of the internalized oligosaccharides, and this degradation commonly releases a signal molecule (normally a di-/tri-/tetrasaccharide), which binds to the regulator, thereby triggering transcriptional induction of the corresponding PUL. The final step of this degradative process involves the incorporation of monosaccharides into the cytoplasm where they are channelled into central carbon catabolism. The first PUL described was the starch utilization system (Figure 5) which is composed of eight genes, *susRABCDEFG*, whose encoded proteins make up a complex and cell envelope-associated apparatus which is highly specialized in starch catabolism (Anderson et al., 1989; Brown et al., 2020; Cameron et al., 2014; Cameron et al., 2012; Cho et al., 2001; Foley et al., 2016; Koropatkin et al., 2010; Shipman et al., 2020). The SusC/D complex is predominantly responsible for starch binding with SusE and SusF being involved in increasing the efficiency of the binding process. SusG generates internal hydrolytic cuts in the bound starch, releasing oligosaccharides that are transported into the periplasmic compartment by SusC (Cameron et al., 2014; Cameron et al., 2012; Foley et al., 2016). Here, SusA and SusB, both glycoside hydrolases, degrade these malto-oligosaccharides to glucose, which is then transported into the cytosol (Cameron et al., 2014; Cameron et al., 2012; Foley et al., 2016).

Transcriptional regulation of the whole process is accomplished by SusR in response to starch availability (Cameron et al., 2014; Cameron et al., 2012; Foley et al., 2016).
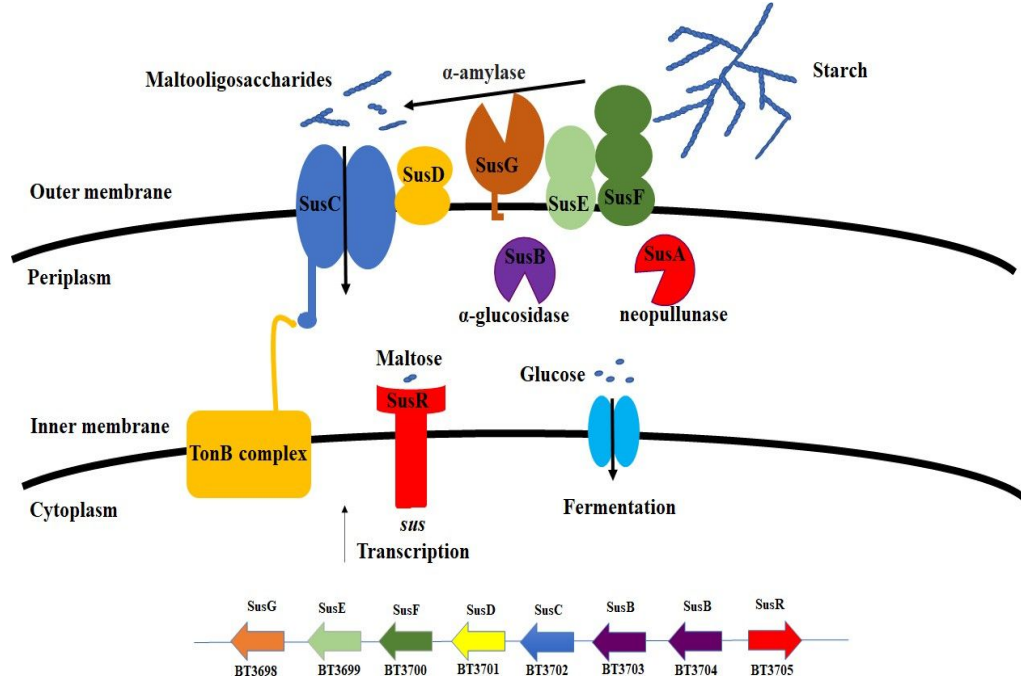
Figure 5. Cartoon representation of starch utilization system model in *Bacteroides thetaiotaomicron* VPI 5482 (Brown et al., 2020; Foley et al., 2016; Koropatkin et al., 2010). The degradation of starch is initiated at the outside surface of the cell by SusG (alpha-amylase), thereby generating oligosaccharides. These oligosaccharides are incorporated into the periplasm by the SusC/SusD pair which allows further degradation to glucose by other glycoside hydrolases, and which generates a signal molecule for the TonB receptor, which is SusR, causing transcriptional activation of the entire PUL. B. The genomic content of the starch PUL in *Bacteroides thetaiotaomicron* VPI 5482 is shown below (Brown et al., 2020; Foley et al., 2016).

Due to the huge range of diversity in the structure of the polysaccharides, several proteins/enzymes are involved in their degradation, as is the case of Bacteroidota with the above-mentioned PULs. The composition of PULs within the genome of a specific *Bacteroides* species is connected to substrate availability and the establishment of the microbial ecosystem within the gut (Flint et al., 2012). The diversity of the monosaccharide subunits and glycosidic linkages results in the high level of complexity of carbohydrate molecules whose breakdown requires a vast array of

specific enzymes. The carbohydrate-active enzymes (CAZymes) (Consortium, 2018) are encoded by a large number of genes in the gut microbiota. The CAZy database groups enzymes based on amino acid sequence into families of glycoside hydrolases (GHs), glycosyltransferases (GTs), polysaccharide lyases (PLs), carbohydrate esterases (CEs), redox auxiliary activities (AAa) and associates non-catalytic carbohydrate-binding molecules (CBMs) (Carbohydrate Active Enzymes database, http://www.cazy.org). Within CAZy, the polysaccharide utilization loci database (PULDB) is used to predict PULs in isolated *Bacteroides* species as well as those that are described in the literature (Terrapon et al., 2018). Within CAZyme families, the structural fold, the catalytic mechanism, and residues involved in the catalysis of the enzymes, are highly conserved (Gloster et al., 2008). The system used to classify CAZymes can be used in some cases for the prediction of the target based on the family of enzymes it is assigned to (Cantarel et al., 2012; Lombard et al., 2010). Therefore, this means that there could be potential to use the DNA sequence of an organism to predict its glycobiological profile. However, too little is currently known about the relationship between sequence and substrate specificity of the CAZyme families since some CAZymes have not been assigned to any function yet, and CAZymes, within the same families, act upon different substrates, causing difficulties in the annotation of CAZyme-related genes. Additionally, a cross-genome study of PULs (Lapébie et al., 2019) proposed that the degradation of glycans involved combinations of different enzymes and those enzymes encoded by PULs can give an insight into the structure of the polysaccharide, supporting the hypothesis that Cantarel and colleagues first discussed in 2012 (Cantarel et al., 2012).

1.2 *Lactobacillus* genus

Lactobacillus constitutes one of the diverse bacterial genera within the Bacillota phylum. *Lactobacillus* genus gathers Gram-positive bacteria which are catalase negative and acid-tolerant organisms (Figure 6). Even though they are described as facultatively anaerobic, they often grow better under microaerophilic conditions (Goldstein et al., 2015; Lebeer et al., 2008). Lactobacilli are ubiquitous commensals of the normal human flora and are only occasionally found in clinical infections (O'Callaghan et al., 2013) being traditionally associated with caries development and progression (Byun et al., 2004). They are present in several human niches such as the gastrointestinal tract in the case of *Lactiplantibacillus plantarum, Lacticaseibacillus casei*, and *Lactobacillus rhamnosus* (Goldstein et al., 2015; Roos et al., 2005) or in the vagina as *Lactobacillus crispatus* or *Lactobacillus gasseri* (Scillato et al., 2021).

The World Health Organization and Food and Agriculture Organization of the United Nations (WHO/FAO, 2007) described probiotics as live microorganisms which can confer a health benefit to the host when administrated in adequate amounts. In fact, probiotics may be used as potential treatments of gastroenteritis, urogenital and respiratory tract infections inflammatory bowel syndrome, prevention of allergies or various cancers, among many others (Goldin et al., 2008; WHO/FAO, 2007). However, to date, no product or bacterial strain has been approved for an official health claim by the European Food Safety Authority (EFSA).
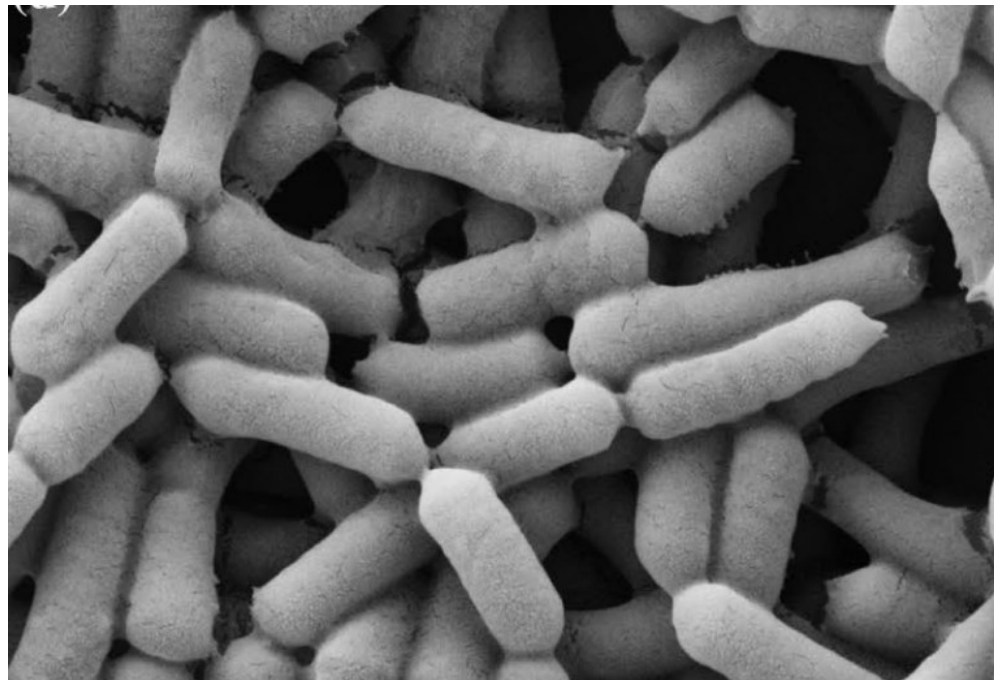
Figure 6. Scanning electron microscopy of the *Lactobacillus rhamnosus* CRL 1332 biofilm (Leccese-Terraf et al., 2016).

Many bacterial strains which fulfil this definition belong to *Lactobacillus* or *Bifidobacterium* genus previously described above (Collado et al., 2009). For example, *Lacticaseibacillus casei*, *Lactobacillus acidophilus*, *Bifidobacterium bifidum*, *Bifidobacterium longum* subsp. *longum* and *Bifidobacterium longum* subsp. *infantis* have been identified as possessing probiotic properties, and many have been used to treat gastrointestinal diseases since they have been shown to exert either bacteriostatic or bactericidal activity against several pathogens. Moreover, lactobacilli have been worldwide included in industrial use as starters in the manufacturing of fresh fermented milk products such as yogurt, fermented milk or fermented juices and also

as a freeze-dried encapsulated powder in health supplements (Nguyen et al., 2022; Varela-Pérez et al., 2022).

Lactobacillus sp. are widely described as defenders of the vaginal flora homeostasis since several species (e.g., *Lactobacillus gasseri*, *Lactobacillus jensenii*, *Lactobacillus iners*, and *Lactobacillus crispatus*) produce hydrogen peroxide, lactic acid, bacteriocins and biosurfactants that act as inhibitors for the growth of harmful organisms (Petrova et al., 2015) helping the maintenance of a healthy state and avoid the appearance of vaginal bacteremia caused by anaerobic pathogens such as *Gardnerella vaginalis* (Bautista et al., 2016). Additionally, it has also been reported the beneficial probiotic effect of *Lactobacillus* sp. in diabetes (Abdelazez et al., 2018) and bacteremia (Panpetch et al., 2018).

Specially remarkable is the case of *Lactiplantibacillus plantarum,* a probiotic strain with a huge research interest due to its ability to regulate the immune response by down-regulating multiple proinflammatory factors and up-regulating anti-inflammatory factors, affecting the intestinal health and gut microbiota homeostasis (Hao et al., 2021; Wang et al., 2021; Zhao et al., 2021). It has been described as an important means to prevent diabetes (Yang et al., 2021) obesity (Yoshitake et al., 2021), atherosclerosis (O'Morain et al., 2021) and colitis (Hao et al., 2021).

Furthermore, several studies have described the ability of *Lactobacillus* sp. to grow via fermentation of β-glucan. In the case of cereal β-glucan, the utilization of oat β-glucan and its hydrolysates promoted the growth of faecal counts of *Lactobacillus* sp. (Dong et al., 2017). Furthermore, the degradation of oat β-glucan by *Lactobacillus rhamnosus* was related to antioxidant and anti-inflammatory potentials (Yau et al., 2020). Within the ambit of cereal β-glucan*,* also *Lactiplantibacillus plantarum* has been extensively

described as a good user of barley β-glucan with an associated reduction of lipid accumulation (Gu et al., 2021; J. Zhang et al., 2022; Zhao et al., 2020). Compared with other lactobacilli species, *Lactiplantibacillus plantarum* shows a stronger carbohydrate utilization capability, allowing an extensive ability to persist in diverse environments with different carbohydrates (Cui et al., 2021).

Nonetheless, the β-glucan utilization by *Lactobacillus* sp. is not limited to cereal types, but also extended to fungal β-glucan. For instance, yeast β-glucan may act as a modulator of the gastrointestinal microbiome, modifying bacterial populations with an increase in the abundance of the genus *Lactobacillus* (Venardou et al., 2021; Zhen et al., 2021). The utilization of fungus β-glucan from *Schizophyllum commune* increased the abundance of the *Lactobacillus* genus (Vu et al., 2022) and *Lactobacillus rhamnosus* L34 promoted the attenuation of uremia caused by β(1,3)-glucan from *Candida albicans* and it decreased intestinal injury through the reduction of *Candida,* improving intestinal bacteremia symptoms (Panpetch et al., 2021).

Even so, more studies need to be carried out to provide a broader perspective of the role played by *Lactobacillus* sp. as polysaccharide degraders, specially for fungal β-glucans, in the Human Gut Microbiota.

1.3 *Roseburia* genus

The genus *Roseburia* also belongs to the phylum Bacillota and includes five species (*Roseburia intestinalis, Roseburia hominis, Roseburia inulinivorans, Roseburia faecis* and *Roseburia cecicola*) of anaerobic Gram-positive bacteria with rod-shaped and multiple flagella (see Figure 7 below) (Tamanai-Shacoori et al., 2017). *Roseburia* sp. metabolize complex polysaccharides as dietary components producing butyrate as the final SCFA product (Hillman et al., 2020), which acts as an important immunomodulator with positive effects against health disorders such as Type II diabetes, ulcerative colitis or colon cancer (Machiels et al., 2014; Rivière et al., 2016; Si et al., 2018).
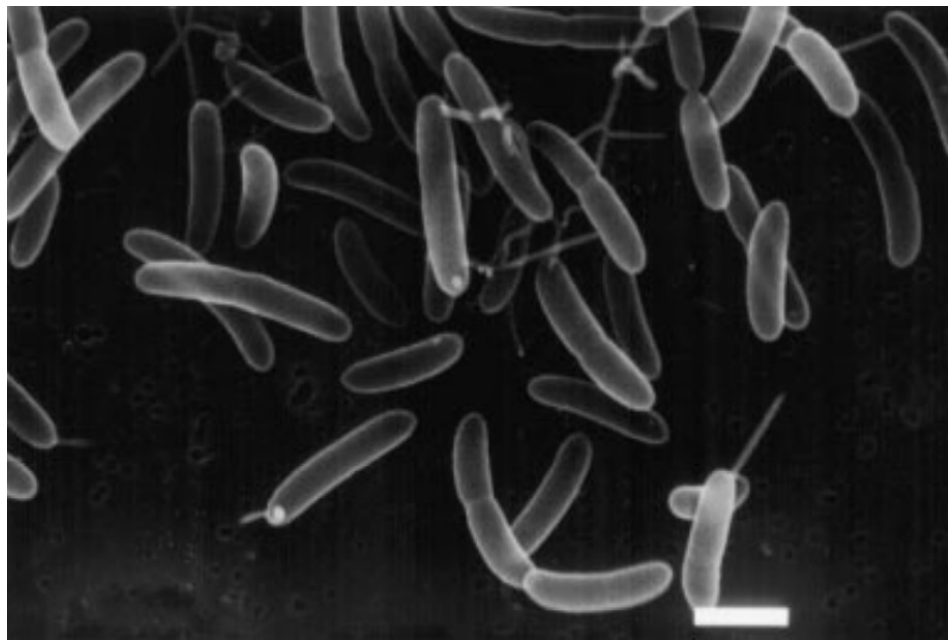
Figure 7. Scanning electron micrograph of *Roseburia intestinalis* (Duncan et al., 2002).

It is remarkable that *Roseburia intestinalis* (*R. intestinalis*), one of the most abundant butyrate producers of human faeces (Duncan et al., 2002), protects against digestive diseases (Nie et al., 2021). *R. intestinalis* can activate the immune system of the host

due to the presence of flagelin, a microbial protein that forms the flagellum. This protein is detected by the immune system producing the activation of the gut barrier and modulating the immune response via Toll-like receptor 5 (Seo et al., 2020).

R. intestinalis flagellin presents anti-inflammatory effects by increasing cytokine expression, including TNF-a, IL-1b, IL-6 and IL-12, but not TNFb (Quan et al., 2018). Furthermore, *Roseburia intestinalis* also plays an important role in the activation of regulatory T lymphocytes (Arpaia et al., 2013) exerting a deep immune effect in the gut.

The modulation of the immune system is also present in the case of *Roseburia inulinovorans* (*R. inulinovorans*), which may decrease inflammation via inhibition of nuclear factor kB (NF- kB) or activation by histone deacetylation (Ananthakrishnan et al., 2017; Canani et al., 2011; Hamer et al., 2008; Inan et al., 2000). For instance, Ananthakirshnan et al. (2017) found that Chron' disease patients presented higher levels of *Roseburia inulinivorans,* which remarks the anti-inflammatory and immune-stimulator role of this bacterium (Ananthakrishnan et al., 2017).

Furthermore, the presence of flagellum supposes a powerful advantage because it increases its chemotaxis and attachment capacity, which allows *Roseburia* sp. to get access to a wide range of insoluble substrates (Scott et al., 2011). *Roseburia* sp. are among those with the highest number of glycoside hydrolases within the phylum Bacillota, being only exceeded by the Bacteroidota phylum (El Kaoutari et al., 2013; Sheridan et al., 2016). For this reason, the *Roseburia* genus can use different kinds of polysaccharides. In this sense, long-chain arabinoxylan can stimulate different bacterial groups including *Roseburia* sp. (Van den Abbeele et al., 2011). *R. inulinovorans* can ferment inulin and fructooligosaccharides, showing a high level of specialisation in short-chain and long-chain fructans (Duncan et al., 2006; Falony

et al., 2009; Ho et al., 2019; Munoz et al., 2020; Scott et al., 2011; Scott et al., 2014). It has also been reported as a resistant starch degrader (Walker et al., 2011).

It has also been reported that *Roseburia* sp. can be supported by fungal glucan as well. For instance, the addition of β(1,3)/(1,6)-glucan isolated from *Schizophyllum* sp. increased the content of *Roseburia* sp. (Muthuramalingam et al., 2020). The administration of chitin-β(1,3)glucan complex from the fungus *Aspergillus niger* allowed the total recovery of *Roseburia* sp. levels, which were previously depleted by high fat diet administration (Neyrinck et al., 2012). Calatayud et al. (2021) reported the specific increase of *Roseburia hominis* (*R. hominis*) and *R. inulinivorans* when the substrate was chitin-β(1,3)-glucan (Calatayud et al., 2021). An intervention with humans increased *Roseburia* sp. as well as the rise in butyric and vaccenic acid concentrations (Rodriguez et al., 2020). Two glucans, characterized as a β(1,3) and β(1,6)-linked and a β(1,3)-linked β-D-glucans, obtained from the fungus *Cookeina speciosa,* promoted marked increases in *Roseburia* sp.

Bioinformatic approaches have shown that *Roseburia* sp. are specialized in the utilization of carbohydrates, with species sharing a communal core, but also showing species specialisation: while *R. intestinalis* shows disposition for the degradation of plant cell wall polysaccharides such as arabinoxylan, *R. inulinivorans* would prefer host-derived carbohydrates such as mucin instead, and in the case of *R. hominis*, this bacterium is predicted to be specialized in arabinogalactan degradation (Sheridan et al., 2016). To summarize, a huge number of studies have highlighted the potential of *Roseburia* sp. as probiotic microorganisms, because of their ability to metabolize different types of polysaccharides as carbon sources as well as to promote the activation of the immune system in the host.

1.4 *Bifidobacterium* genus

Bifidobacterium is a genus belonging to the Actinomycetota phylum whose species are distributed in several ecological niches (Turroni et al., 2019; Turroni et al., 2011). *Bifidobacterium* sp. are commonly found in adults, such as *Bifidobacterium adolescentis*, but many others such as *Bifidobacterium bifidum* (Figure 8) or *Bifidobacterium breve*, are usually isolated from faecal samples of breastfed infants (Duranti et al., 2016; Turroni et al., 2012). Various studies have shown the positive impact and thus probiotic effects of certain bifidobacterial species, for example *Bifidobacterium breve*, *Bifidobacterium longum* or *Bifidobacterium bifidum* (Gani et al., 2018; Zhao et al., 2013).
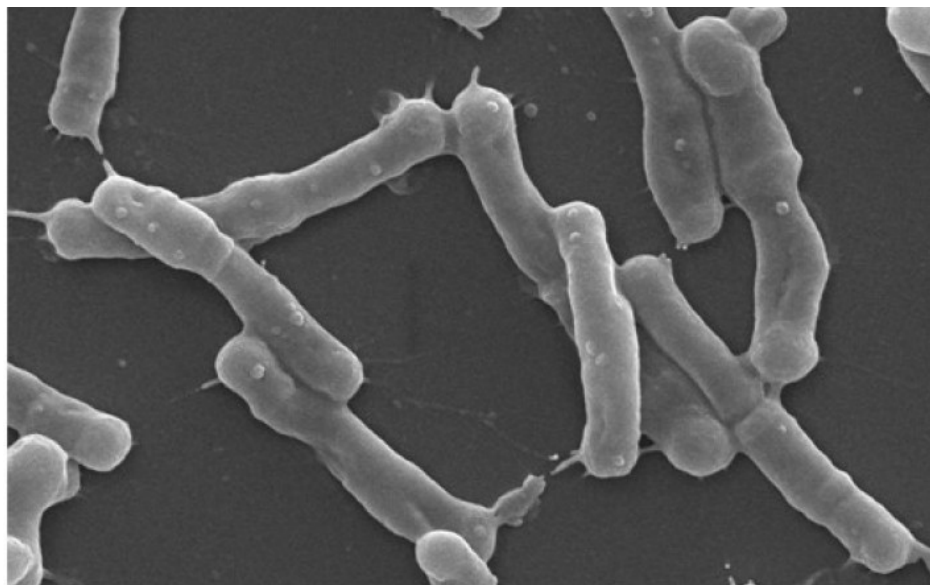
Figure 8. Scanning electron micrograph of *Bifidobacterium bifidum* MG731 (Kang et al., 2019).

Bifidobacteria contain a number of gene clusters dedicated to the metabolism of a specific poly/oligosaccharide (Pokusaeva et al., 2010). These clusters encode ABC transporters (most frequently observed), permeases or proton symporters to facilitate

the transport of mono-/oligosaccharides, such as fucosyllactose, fucose or galactooligosaccharides, into the cytoplasm. Once internalized, these oligosaccharides are degraded into monosaccharides by intracellular glycoside hydrolases, channelling these hexoses or pentoses into the central carbohydrate metabolic pathway for energy generation (Figure 9) (James et al., 2019).
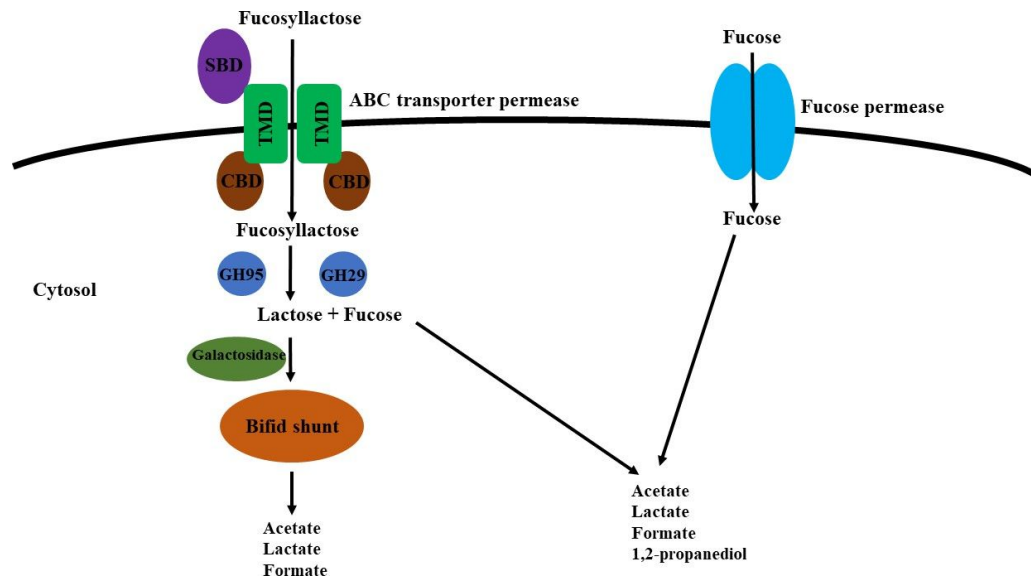
Figure 9. Schematic representation of the fucose and fucosyllactose utilization system in *Bifidobacterium kashiwanohense* (James et al., 2019).

Although *Bifidobacterium* sp. can degrade certain simple carbohydrates, they are generally unable to metabolize more complex polysaccharides. Studies have reported evidence of cross-feeding behaviours between members of the *Bifidobacterium* genus with other organisms to completely metabolize complex glycans (Singh, 2019). An example of this is the interspecies cross-feeding relationship between *Bifidobacterium bifidum* (*Bi. bifidum*) and *Bifidobacterium breve* (*Bi. breve*) when co-cultured on sialyllactose (Egan et al., 2014). In this study, the authors showed how *Bi. breve* was

able to cross-feed on sialic acid, the product of 3'-sialyllactose degradation by *Bi. bifidum*.

Bifidobacterium sp. have also been shown to cross-feed with members of the butyrate-producing Bacillota (Turroni et al., 2015). This evidence is of great significance as the production of the SCFA butyrate is regarded as highly beneficial to the host. Therefore, the Gram-positive genus *Bifidobacterium* present in the gut is well known to provide positive health benefits to the host, while the reduction of *Bifidobacterium* during infection within the gastrointestinal tract suggests that these organisms play a role in maintaining gut homeostasis (Gerritsen et al., 2011).

Members of the *Bifidobacterium* genus have been shown to have probiotic effects. *Bi. longum* subsp. *longum* BB536 is well known as a multifunctional probiotic and studies have highlighted its role in the modulation of gut metabolism, stability of the gut microbiome and elimination of pathogens by competition (Wong et al., 2019). During infancy, *Bifidobacterium* sp. are prevalent in the gut due to their ability to degrade human milk oligosaccharides (HMOs), being the most common species *Bi. breve*, *Bi. bifidum* and *Bi. longum* (Gerritsen et al., 2011). However, the introduction of solid food to the diet, mainly at the age of 4 years old, causes the composition of *Bifidobacterium* to change, with the dominant species becoming *Bi. adolescentis, Bi. catenulatum* and *Bi. longum* in the adult gut microbiome.

Bifidobacterium in the gut is saccharolytic and is involved in the metabolism of dietary and host-derived carbohydrates through the action of a large range of genes encoding for carbohydrate degrading enzymes (Milani et al., 2014). Unlike other saccharolytic organisms, *Bifidobacterium* sp. lack the enzymes aldolase and glucose-6-phosphate

NADP$^+$ oxidoreductase that are involved in the typical glycolysis pathway in the metabolism of carbohydrates (Gupta et al., 2017). Alternatively, *Bifidobacterium* sp. degrade hexose sugars through a unique pathway known as the "bifid shunt" which produces SCFAs and generates adenosine triphosphate (ATP). This pathway focuses on the phosphoketolase enzymes responsible for the metabolism of fructose-6-phosphate (F6P) and xylulose-5-phosphate (X5P). These two groups of enzymes (XFPK) metabolize F6P to erythrose-4-phosphate and acetyl phosphate. They also carry out the phosphorolysis of X5P to acetyl phosphate and D-glyceraldehyde-3-phosphate and, through the action of F6P metabolism, links this pathway with the phosphoketolase pathway which is typical of the lactic acid bacteria (LAB). This metabolic pathway is exclusively found in *Bifidobacterium* and so the presence of the XFKP enzyme, which displays activity towards F6P, can be used to identify bifidobacterial organisms. The bifid shunt provides an evolutionary advantage to *Bifidobacterium* as it generates much more energy than other sugar metabolic pathways (Gupta et al., 2017).

The genomes of the *Bifidobacterium* contain genes that encode membrane GH enzymes for the initial degradation of polysaccharides, together with solute binding proteins (SBPs) for the recognition of the initially degraded oligosaccharides before importing them into the cytoplasm where they are further degraded in the "bifid shunt" pathway (Singh, 2019). These SBPs are associated with an ATP-binding cassette (ABC) transporter, which utilizes the energy from the hydrolysis of ATP to transport molecules across the cell membrane. ABC transporters are the primary system for translocation of glycans into the cytoplasm of *Bifidobacterium* cells and the affinity of

the ABC transporter for the substrate is specified largely by the SBP (Berntsson et al., 2010).

For example, the utilization of arabinoxylooligosaccharides (AXOS) in *Bifidobacterium* (*Bi. animalis*) subsp. *lactis* Bl-04 is mediated by the SBP *Bl*AXBP (Ejby et al., 2013). Research shows that this protein has a highly broad range of specificity for both AXOS and xylooligosaccharides (XOS), with a preference for xylotetraose and arabinoxylotriose. The crystal structure showed that this specificity was increased by a spacious binding pocket where glycan decorations of different positions can bind as well as a lid-like loop that allows the oligosaccharides to bind in different conformations. Using phylogenetic analysis, the authors concluded that *Bl*AXBP is highly conserved among the *Bifidobacterium* genus, however, it is not present in other members of the HGM, which demonstrates the functional advantage of this glycan transport system within the *Bifidobacterium* genus which allows them to successfully compete with other organisms in the HGM. Similarly, in further research (Ejby et al., 2016) the authors found that the structure of the SBP *Bl*G16BP from *Bi. animalis* subsp. *lactis* Bl-04 displays significant ligand binding plasticity when bound to the trisaccharides raffinose and panose. This protein was shown to recognize α-1,6-diglycoside such as isomaltose and melibiose and the study highlighted that homologs of this protein were primarily present in *Bifidobacterium* and lacking in other members of the HGM (see Figure 10 below). *Bacteroides ovatus* ATCC 8483 (*Ba. ovatus* ATCC 8483), a dominant organism in the HGM in adults, was outcompeted by *Bi. animalis* subsp. *lactis* Bl-04 when growing in co-culture on raffinose as compared with its efficient growth in a monoculture.
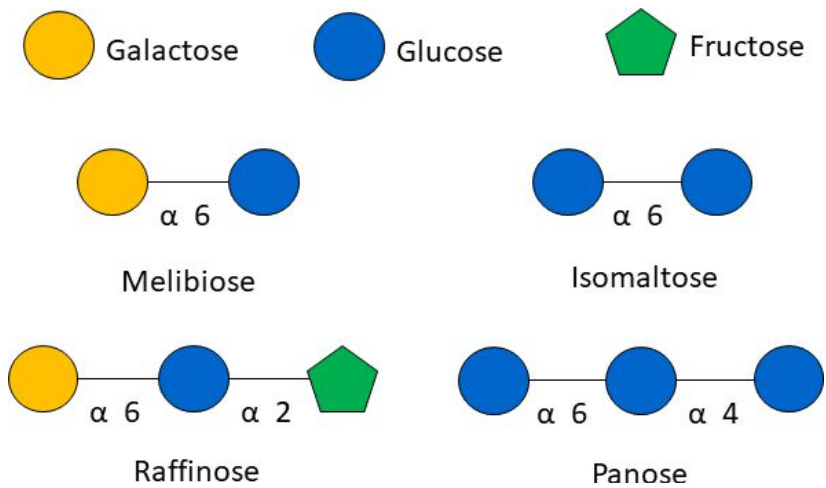
Figure 10. Schematic representation of the oligosaccharides recognized by *Bl*G16BP (Ejby et al., 2016).

The success of *Bi. animalis* subsp. *lactis* ATCC 27673 over *Ba. ovatus* ATCC 8483 was also observed in a more recent study by (Ejby et al., 2019) where the presence of the SBPs *Bl*MNBP1 and *Bl*MnBP2 associated with the ABC transporter allowed for the organism to outcompete a more dominant member of the HGM when growing in co-culture on β-mannan. This evidence further supports previous studies in which the recognition and uptake of the substrate via the ABC-transporter system provide *Bifidobacterium* sp. with a competitive advantage over other members of the HGM that do not possess this transport system.

Although ABC transporters act as the primary transporter of glycans, other transport systems in the *Bifidobacterium* genus include the phosphoenolpyruvate-phosphotransferase transport system (PEP-PTS) as well as the secondary transporters' major facilitator superfamily (MFS) and the glycoside-pentoside-hexuronide (GPH) cation symporter (Turroni et al., 2012). The number of genes predicted by the Transporter Classification Database that encodes proteins involved in transport systems in *Bifidobacterium* is relatively low (TCDB, https://www.tcdb.org/). *Bi.*

bifidum PRL2010 contains just 25 genes involved in the uptake of glycans; however, other bifidobacterial species are predicted to contain between 35 and 68 of these genes.

Previous studies have proved that *Bifidobacterium* sp. use a range of methods for the uptake and utilization of glycans. Nevertheless, more research needs to be carried out to fully understand the mechanisms of the transport and glycan utilization systems. The strategies developed by these organisms have provided them with a competitive advantage over other members of the HGM such as the more dominant *Bacteroides* as well as some pathogens. This has allowed for the establishment of a specialized ecological niche and the development of symbiotic relationships with other organisms.

1.5 *Victivallis vadensis*

Victivallis vadensis ATCC BAA-548 (*V. vadensis*) is a Gram-negative bacterium, strictly anaerobic, which constitutes the first coccus-shaped bacterium (see Figure 11 below) isolated from human faeces belonging to the phylum Lenthispaerae (van Passel et al., 2011; Zoetendal et al., 2003). It is a non-motile slime-producing bacterium whose first described carbon source was cellobiose, but with the ability to grow in a wide range of monosaccharides such as glucose, galactose or xylose and disaccharides such as lactose, maltotriose or melibiose, among others (Temuujin et al., 2012; Zoetendal et al., 2003). In glucose fermentation, it is described to produce ethanol, acetate, hydrogen and bicarbonate (Zoetendal et al., 2003).
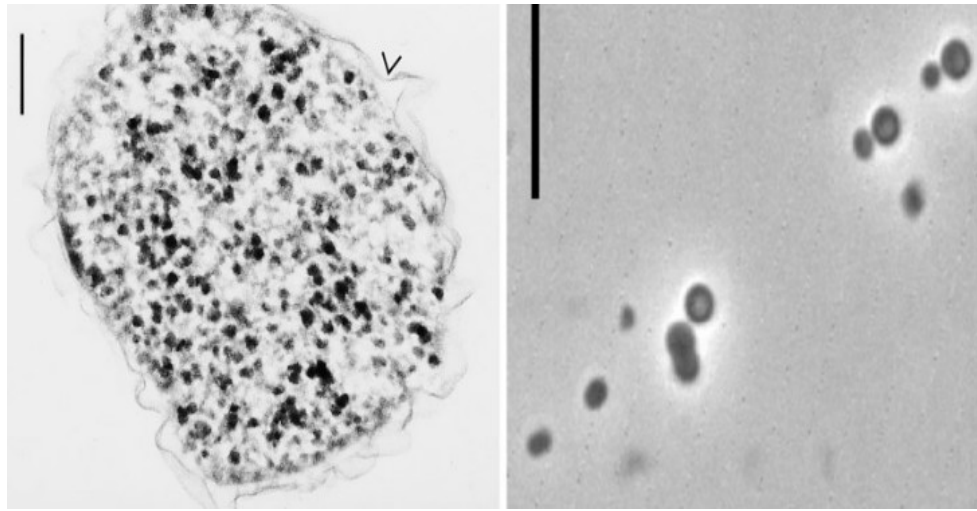
Figure 11. Phase-contrast micrograph of *Victivallis vadensis* (Zoetendal et al., 2003).

Some studies described the increase of *Victivallis vadensis* in different conditions in which the homeostasis was altered. For instance, its abundance seems to be higher in HIV-exposed seronegative individuals (Lopera et al., 2021), in cerebral ischemic stroke patients (Li et al., 2019) and in gastric cancer patients (Lin et al., 2018).

A small number of studies have reported polysaccharide utilisation by *V. vadensis.* For instance, two different starch dietary interventions showed an increase in its abundance (Nilholm et al., 2022; Zhang et al., 2019). It was also positively correlated with the utilization of exopolysaccharides from *Lacticaseibacillus paracasei* (Bengoa et al., 2020) and tea polysaccharides (Li et al., 2020).

Despite this, the ability of *V. vadensis* for the degradation of bacterial and fungal glucans remains almost unknown. This is surprising, given this bacterium has 275 different genes encoding GHs and PLs with 261 GHs and 14 PLs proteins, respectively (El Kaoutari et al., 2013). These numbers represent one of the highest GHs and PLs number of genes per genome for all predominant phyla in the Human Gut Microbiota, excluding Bacteroidota (El Kaoutari et al., 2013)

Even though the actual data reveals that *V. vadensis* possesses many genes for polysaccharide degradation, the mechanisms underlined its degradative pathways and potential targets are still unclear. Its low percentage of abundance and the small number of studies about it makes even more difficult to study its interactions and feasible cross-feeding with other bacteria in the gut.

In any case, *V. vadensis* supposes an unknown but fascinating member of our flora, who has shown many possibilities as a potential probiotic. Further studies are essential to amplify the spectrum of its substrates and its relationship with other bacteria. This will help clarify its role as an important agent within the Human Gut Microbiota and its implication in health as a main polysaccharide degrader.

1.6 *Akkermansia muciniphila*

Akkermansia muciniphila (*A. muciniphila*) is a Gram-negative bacterium, strictlyanaerobic with an oval shape (Figure 12) belonging to the phylum Verrucomicrobiota (Derrien et al., 2004; Geerlings et al., 2018). It was first isolated from human faeces, and it can colonize the intestinal tract in the early stages of life (Derrien et al., 2017). From that moment, it becomes one of the most abundant species in the Human Gut Microbiota (Abuqwider et al., 2021). This bacterium shows a strong interaction with the mucosal layer in the intestine because of its ability to ferment mucin as a carbon and nitrogen source, a process that leads to the production of propionate and acetate asmain metabolites (Zhai et al., 2019).

A. muciniphila acts as an essential factor in the maintenance of the thickness of the mucosal layer, keeping the integrity of the intestinal epithelial cells (Reunanen et al., 2015). A feasible explanation is that *Akkermansia muciniphila* might help the

promotion of intestinal stem cells to develop the intestinal epithelium. This helps the production of the mucus layer which acts as a barrier to upgrade the gut function, providing support against pathogens and inflammation (Reunanen et al., 2015; Zhou et al., 2021).
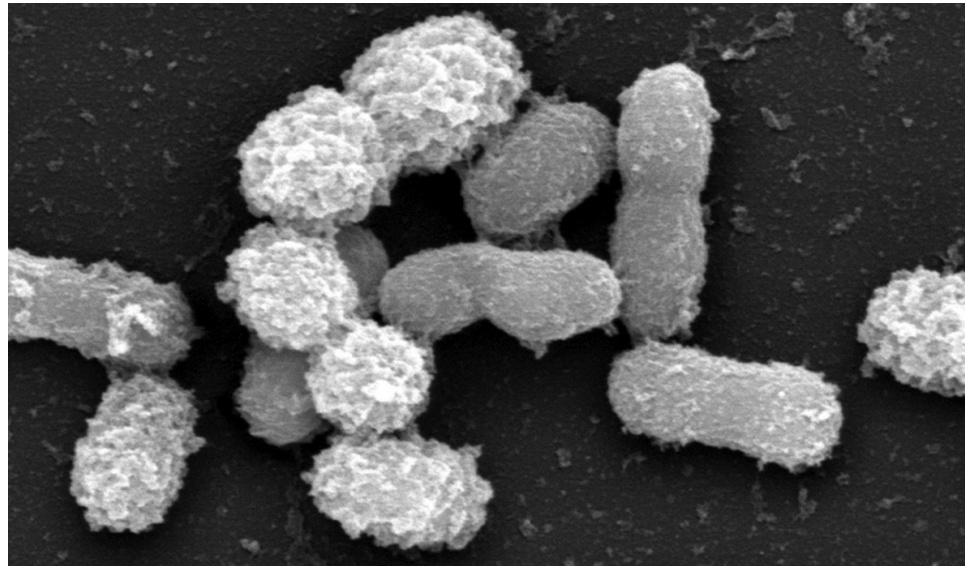
Figure 12. Scanning electronic micrograph of *Akkermansia muciniphila* (Derrien et al., 2017).

For this reason, it has been described as a next-generation probiotic (Cani et al., 2017) because it seems to be inversely associated with ulcerative colitis (Rajilić-Stojanović et al., 2013), diabetes (Hansen et al., 2012; Plovier et al., 2017; Zhang et al., 2013), obesity (Dao et al., 2016; Depommier et al., 2020), hepatic inflammation (Grander et al., 2018) or atherosclerosis (Li et al., 2016; Shen et al., 2016). The research on the mechanism of *Akkermansia*'s beneficial effects is large and growing fast every day, albeit it still demands further in-depth study.

Akkermansia has been proved to have beneficial effects when it is supplemented via oral administration, for example decreasing body weight (Everard et al., 2013),

improving glucose tolerance and insulin sensitivity (Sanjiwani et al., 2022) or maintaining the gastrointestinal balance by modulating the immune response and increasing the abundance of beneficial bacteria to ameliorate pathogens (Wu et al., 2022). Several studies have underlined the range of substrates that *Akkermansia muciniphila* can target. In addition to the well-described ability to digest mucus and mucin-derived o-glycans (Belzer et al., 2017; Pruss et al., 2021), the utilization of human milk oligosaccharides by *Akkermansia* has been reported as well (Kostopoulos et al., 2020; Luna et al., 2022). Depommier et al. (2021) found that the same positive enrichment in *Akkermansia muciniphila* was achieved when using hyaluronan supplementation (Depommier et al., 2021), and Fu et al. (2021) studied the growth of the bacterium with alginates oligosaccharides obtained by enzymatic reaction of seaweed polysaccharides from *Laminaria japonica* (Fu et al., 2021).

The ability for polysaccharide degradation in *Akkermansia* sp. is wide and diverse. Jin et al. (2022) demonstrated how the utilization of β-glucan from barley helped the expulsion of the helminth *Trichinella spiralis* by modulating the microbiota, recovering its healthy composition, and increasing the abundance of *Akkermansia muciniphila*. This allowed the bacterium to interact with the mucus layer and promote the host immunity (Jin et al., 2022). Huo et al. (2021) described how two novel polysaccharides from *Gastrodiaelata*, a Chinese orchid, favoured *Akkermansia* (Huo et al., 2021). The structure of the mentioned polysaccharides was a combination of α- and β-bonds with different spatial conformation and level of branching, and they both promoted the growth of *Akkermansia* (Huo et al., 2021). A similar increase in *Akkermansia muciniphila* was also achieved using oat β-glucan (Ryan et al., 2017).

Additionally, a purified polysaccharide from the herb *Polygonatum sibiricum* was used to prevent different Alzheimer's symptoms such as memory deficit, intestinal

deposition of Aβ plaques and inflammatory response via increasing *Akkermansia muciniphila* (Luo et al., 2022). In a separate study, an inulin-type β-D-fructan polysaccharide from the plant *Ophiopogon japonicus* was revealed as a good substrate for the enrichment of *Akkermansia* abundance (Zhang et al., 2022). The beneficial effects related to the action of *Akkermansia* sp. in the human gut, in conjunction with its capability to digest a big diversity of polysaccharides from many different sources, make this bacterium useful probiotic and an important participant in the role of the Human Gut Microbiota.

1.7 Cross-feeding interactions

The complexity of host and diet-derived glycans and the variability of feeding preferences of HGM organisms mean that the mechanisms of degradation of these molecules are highly specialized (Seth et al., 2014). As a result, different microbial communities have co-evolved to maintain a balanced and dynamic network of metabolic interactions, which enables them to adapt and thrive within the human gastrointestinal tract (GIT). The competition for nutrients between members of the HGM has resulted in the evolution of ecological feeding strategies that increase the efficiency of glycan utilization (Smith et al., 2019).

Although there are many different variations of the definitions of these interactions in the literature, Smith et al (2019) have defined bacterial metabolic cross-feeding as "an interaction between bacterial strains in which molecules resulting from the metabolism of one strain are further metabolized by another strain". The term "microbial syntrophy" is a closely related term to cross-feeding which describes the obligately mutualistic metabolism of microorganisms whereby processes are carried out through metabolic interactions between organisms that are mutually dependent

upon one another (Morris et al., 2013). These syntrophic interactions can result in the metabolism of complex molecules, which would otherwise be unable to be degraded by the action of just one organism.

1.7.1 *Bacteroides-Bacteroides* interactions

The ability of the *Bacteroides* to utilize polysaccharides has been well documented (Schwalm et al., 2017). Upon the breakdown of these complex polymer molecules comes the release of polysaccharide breakdown products (PBPs) which hold the potential to become available to other organisms that are otherwise unable to metabolize the carbohydrate. Rakhoff-Nahoum and colleagues investigated this theory in 2014 (Rakoff-Nahoum et al., 2014) and found that different *Bacteroides* species were able to break down different plant-derived polysaccharides to varying degrees, thus producing differing amounts of PBPs. Interestingly, they observed that *Bacteroides ovatus* ATCC 8483 and *Bacteroides vulgatus* ATCC 8482 (*Ba. ovatus* ATCC 8483 and *Ba. vulgatus* ATCC 8482) released only oligosaccharide PBPs on the breakdown of xylan which contradicts the findings of Salyers et al. (1981) who previously described the production of xylose on the breakdown of xylan by these organisms (Salyers et al., 1981). They then went on to look at how these PBPs were utilized by members that were unable to metabolize the carbohydrate alone. They performed growth experiments on conditioned mediums that were derived from the growth of organisms that produce PBPs and concluded that the ability of these organisms to produce these PBPs varies greatly among the different *Bacteroides* sp. investigated. Additionally, these breakdown products were not universally utilized by the non-polysaccharide-utilizing organisms meaning that the use of PBPs is

dependent upon the producer strain as well as the PBPs produced.

The ability of the non-utilizing strains to grow on these PBPs suggests that they posses PULs that encode the CAZymes required to metabolize the breakdown products and the non-utilizing strains lack only the GH and PL enzymes required for the initial degradation of the polysaccharide as well as the proteins required for PBP release from the cell. The observation of the breakdown of amylopectin in extracellular zones would suggest that rather than the release of just PBPs by the utilized strains, GH and PL CAZymes are also secreted. Communication between Gram-negative bacteria via outer membrane vesicles (OMVs) allows for the secretion of enzymes to extracellular regions where polysaccharide degradation can take place. This was demonstrated in this study using western immunoblot analysis which revealed that GH and PL enzymes were present in OMVs from *Ba. ovatus* ATCC 8483 and that their release supported the growth of *Ba. vulgatus* ATCC 8482 on inulin. This provides evidence that this interaction between the two species results in increased growth of a non-utilizing species (Salyers et al., 1981).

This evidence is supported by a further study by Rakoff-Nahoum and colleagues in 2016 (Rakoff-Nahoum et al., 2016), which found that there is a cooperation between different *Bacteroides* sp. in the breakdown of carbohydrates. *Ba. ovatus* ATCC 8483 is the primary degrader of inulin and releases a duo of GH enzymes (BACOVA_04502 and BACOVA_04503) that are not necessary for its metabolism. It is thought that *Ba. ovatus* ATCC 8483 expresses these enzymes for the feeding of other organisms in their microbial community and this process is beneficial for various members of the group. *Ba. ovatus* ATCC 8483 was grown in co-culture with *Ba. vulgatus* ATCC 8482 which cannot digest inulin but utilizes the breakdown products of this polysaccharide for growth.

In co-culture, *Ba. vulgatus* ATCC 8482 grew with increased fitness and, in return, increased the fitness of *Ba. ovatus* ATCC 8483 possibly due to the production of molecules that support the growth of *Ba. ovatus* ATCC 8483 or by the detoxification of substances that inhibit its growth.

In contrast, the degradation of amylopectin and levan by *Bacteroides thetaiotaomicron* VPI 5182 (*Ba. thetaiotaomicron* VPI 5182) showed no benefit to other species. These studies highlighted the interactions between members of the *Bacteroides* genus that allow the growth of organisms that do not possess the necessary degradative enzymes for the utilization of carbohydrates. These interactions may be key in the establishment of a dynamic and stable community of microorganisms in the human GIT.

1.7.2 *Bifidobacterium-Bifidobacterium* interactions

Bifidobacterium sp. have also been known to interact with one another to cooperatively break down carbohydrates (Turroni et al., 2015). The differing abilities of strains to utilise glycans have been thought to result in the evolution of cross-feeding activities between bifidobacterial strains. Studies have shown that *Bifidobacterium* sp. able to secrete GH enzymes (Milani et al., 2015). It is predicted that 10.9% of the GH enzymes encoded by *Bifidobacterium* sp. are extracellular, of which 24% are predicted to be of the GH43 family which acts as β-xylosidases and α-L-arabinofuranosidases. Extracellular GH enzymes were identified in 43 bifidobacterial species, with the most prevalent being *Bifidobacterium biavatii* (*Bi. biavatii)* which was identified to secrete 17 GHs, *Bifidobacterium scardovii* (*Bi. scardovii*) secreting 11 GHs and *Bifidobacterium bifidum* (*Bi. bifidum*) also secretes 11 GHs.

This fact provides strong evidence for the glycan-sharing abilities of bifidobacterial strains. Co-cultivation of *Bi. bifidum* PRL2010 with *Bi. breve* 12L, *Bifidobacterium adolescentis* 22L (*Bi. adolescentis* 22L) and *Bifidobacterium thermophilum* JCM1207 (*Bi. thermophilum* JCM1207) showed increased growth of *Bi. bifidum* PRL2010 (Turroni et al., 2015), supporting the idea of the ability of bifidobacterial strains to engage in cross-feeding. They found that the metabolic activity of *Bi. bifidum* PRL2010 was enhanced when co-cultivated with other bifidobacterial species and the transcription of genes involved in carbohydrate metabolism was induced. When grown in monoculture, *Bi. bifidum* PRL2010 was not able to utilize starch or xylan. However growth was observed when this strain was cultured alongside *Bi. breve* 12L or *Bi. adolescentis* 22L. Conversely, a decrease in the growth of *Bi. breve* 12L and *Bi. thermophilum* JCM1207 was noted, suggesting that the utilization of starch or xylan by *Bi. bifidum* PRL2010 respectively did not benefit these strains and resulted in them being outcompeted. The reduction in lactate and acetate production by *Bi. breve* 12L when grown in co-culture as opposed to monoculture supports the idea that the growth of this strain is hindered by the presence of another *Bifidobacterium*. Transcriptomics analysis showed that the genes encoding for an ABC-transporter and MFS transporter in *Bi. bifidum* PRL2010 was upregulated when grown in co-culture. It was suggested that this upregulation was due to the production of carbohydrates by *Bi. breve* 12L and *Bi. adolescentis* 22L which act as PBPS that can be utilised by *Bi. bifidum* PRL2010. Interestingly, upregulation of 21 genes of *Bi. breve* 12L was observed when co-cultured with *Bi. bifidum* PRL2010 on starch and 42 genes when grown on xylan. This upregulation provides evidence for a mutualistic cooperative relationship between these two strains (Turroni et al., 2015).

As well as evidence for cross-feeding between bifidobacterial species on plant-derived glycans, members of the *Bifidobacterium* genus are involved in the metabolism of host-derived glycans and human milk oligosaccharides (HMOs). *Bi. breve* UCC2003 is a known utilizer of mucin and sialic acid which is a monosaccharide derived from HMOs, along with *Bi. bifidum* PRL2010 which produces a big number of GH enzymes involved in the metabolism of mucin (Egan et al., 2014; Turroni et al., 2010). The production of sialic acid from the degradation of the HMO 3'-sialyllactose by *Bi. bifidum* PRL2010 was shown to support the growth of *Bi. breve* UCC2003 in another study (Egan et al., 2014). The sialic acid is released from the 3'-sialyllactose molecule by sialidase enzymes and it was previously shown that the genome of *Bi. bifidum* PRL2010 encodes for two extracellular exo-α-sialidases (Turroni et al., 2010). Egan et al. (2014) demonstrated that sialic acid is released as a PBP by *Bi. bifidum* PRL2010 was completely utilized by *Bi. breve* UCC2003, although they found that *Bi. breve* UCC2003 does produce an intracellular sialidase, but it was unable to utilize 3'- or 6'-sialyllactose, so these molecules are not the substrate for this enzyme.

A further study carried out by these authors supported this evidence by finding that *Bi. breve* UCC2003 could only grow on a mucin-based medium in the presence of *Bi. bifidum* PRL2010 (Egan et al., 2014). They demonstrated using HPAEC-PAD and transcriptome analysis that PBPs were released by *Bi. bifidum* PRL 2010 and they were utilized by *Bi. breve* UCC2003, including sialic acid, fucose, galactose, and containing oligosaccharides from mucin degradation. The upregulation of transcription of genes responsible for the uptake of fucose was observed as well as genes encoding for an ABC transporter system. The ability of *Bi. breve* UCC2003 to scavenge on these PBPs of mucin highlights its adaptability in the gut and shows that this strain can utilize a range of carbon sources depending on their availability.

1.7.3 *Bacteroides-Bifidobacterium* interactions

Research has shown that *Bacteroides* and *Bifidobacterium* have co-evolved to share a mutually symbiotic relationship in the utilization of dietary and host-derived carbohydrates via syntrophic metabolic interactions of their glycan utilization systems. The sharing of partially degraded oligosaccharides, intermediary molecules and genes by lateral gene transfer has allowed these organisms to carry out this relationship and contribute to the complex, dynamic nature of the human gut. *Bacteroides* often act as the primary degraders of carbohydrates in the gut, which are then in turn further metabolized by secondary degrader organisms (Fischbach et al., 2011). The action of cross-feeding has allowed for the less dominant organisms such as *Bifidobacterium* to utilise glycans as a source of nutrition without being out-competed by bacterial strains that are present in the gut in much higher numbers.

Investigation into the interactions between members of the *Bacteroides* and *Bifidobacterium* genera in the utilization of different carbon sources was carried out by Rios-Covian et al. (2013). They grew different combinations of co-cultures of two strains of *Bacteroides* and two strains of *Bifidobacterium* using exopolysaccharide (EPS), inulin or glucose as the carbon source to observe how this affected growth of the organisms. They found that *Bi. longum* NB677 and *Bi. breve* IPLA2004 were able to utilize glucose as a carbon source however showed no growth on more complex polysaccharides.

Conversely, *Bacteroides thetaiotaomicron* DSM 2079 (*Ba. thetaiotaomicron* DSM 2079) and *Bacteroides fragilis* DSM 2151 (*Ba. fragilis* DSM 2151) were able to utilize all the carbon sources and grow well. The authors found that the growth of *Ba. thetaiotaomicron* DSM 2079 on glucose was inhibited by the presence of *Bi. breve*

IPLA2004, suggesting that the interaction between these organisms in the breakdown of carbohydrates is not mutualistic in this case. *Ba. fragilis* DSM 2151 increased the fitness of *Bi. longum* NB677 on the other hand. No effect on growth was seen in co-cultures of *Bacteroides* and *Bifidobacterium* on complex carbohydrates suggesting that no PBPs were produced by the *Bacteroides* that could be utilized by the bifidobacterial strains. These results show that the behaviour of the co-cultures of different species is not universal and depends upon the bacterial strains and carbon source present.

The support of bifidobacterial growth by *Bacteroides* sp. on XOS has been previously observed (Rogowski et al., 2015). *Bi. adolescentis* ATCC 15703 is unable to utilize xylans however it can degrade simple XOS such as linear arabinoxylooligosaccharides. Simple xylans such as wheat arabinoxylan (WAX) are primarily degraded by *Ba. ovatus* ATCC 8483 and then further metabolized by *Bi. adolescentis* ATCC 15703. However, this glycan sharing was not observed with more complex xylans such as corn bran xylan (CX). The authors of this study suggested that this could be since *Bi. adolescentis* ATCC 15703 does not possess the necessary utilization systems for this complex xylan rather than the idea that *Ba. ovatus* ATCC 8483 does not support its growth due to an inadequate release of PBPs. To investigate this, they created a mutant strain of *Ba. ovatus* ATCC 8483 that lacked a functioning GH98 xylanase CAZyme (ΔGH98) thus preventing the cleavage of the backbone of CX and inhibiting its growth. When the ΔGH98 mutant was co-cultured with wild-type *Ba. ovatus* ATCC 8483 on CX media, growth of both strains was observed which provides evidence that the wild-type strain releases PBPs from the breakdown of CX, which are then utilized by the mutant. This confirms the inability of *Bi. adolescentis* ATCC 15703 to degrade complex xylans is due to its absence of the extensive glycan utilization machinery that is present in the *Bacteroides* sp. (see Figure 13 below).
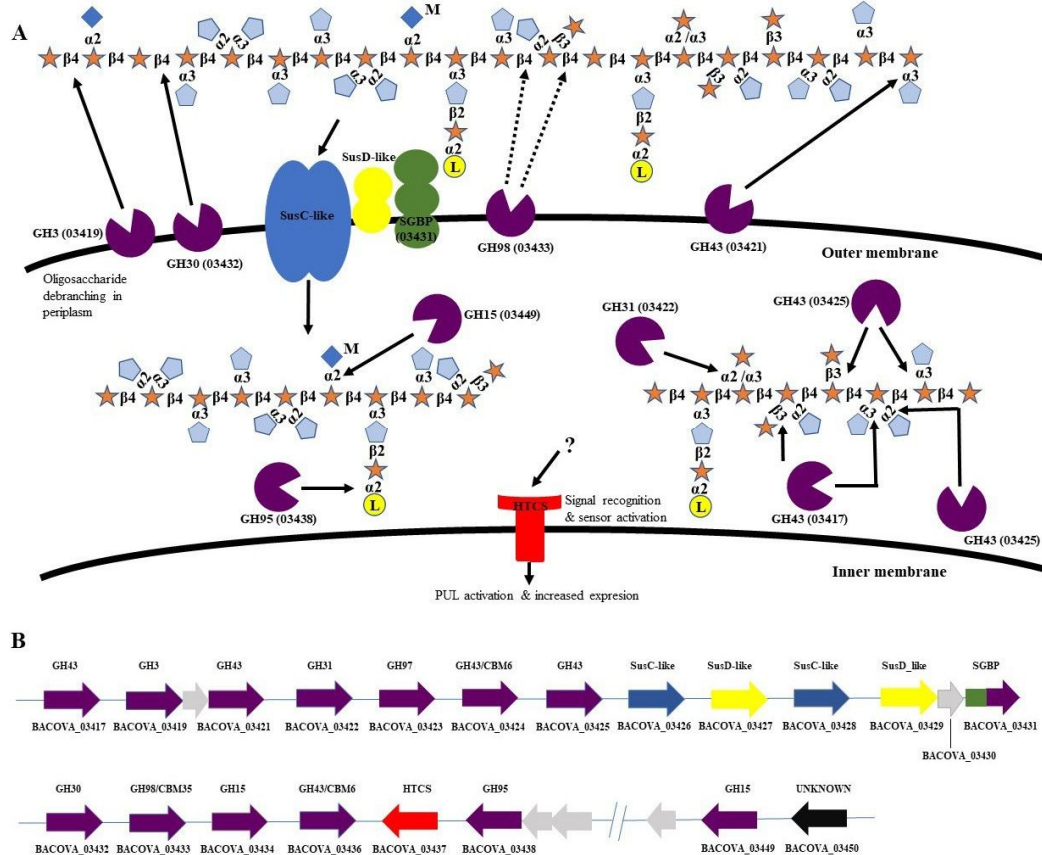
Figure 13. (A) Schematic representation of the glucuronoarabinoxylan utilization system in *Ba. ovatus* ATCC 8483. The substrate is bound by lipoproteins at the cell surface where it is primarily degraded to oligosaccharides and then transported to the periplasm where it is further hydrolysed to monosaccharides which can then be transported to the cytoplasm of the cell. (B) Genomic content of *Ba. ovatus* ATCC 8483 PUL in its action on corn arabinoxylan (Rogowski et al., 2015).

Further studies into the utilization of XOS by *Bacteroides* and *Bifidobacterium* strains in co-culture have supported the findings of the previous study by Rogowski et al. (2015) (Rogowski et al., 2015; Zeybek Rastall, 2020). In vitro and co-culture fermentation experiments were carried out and demonstrated the inability of bifidobacterial strains to utilise XOS in monoculture, with only *Bi. animalis* subsp. *lactis* as an exception. In monoculture, the two *Bacteroides* strains, *Ba. ovatus* ATCC 8483 and *Ba. xylanisolvens* XB1A were able to utilize all the substrates including xylose, XOS, beechwood xylan and corncob xylan. However, four of the five *Bifidobacterium* strains: *Bi. bifidum, Bi. breve, Bi. longum* subsp. *infantis* and *Bi.*

34

longum subsp. *longum* could not. *Bi. animalis* subsp. *lactis* was able to utilize only XOS. Nevertheless, the co-culture of *Bi. animalis* subsp. *lactis* with both the *Bacteroides* strains showed growth on beechwood and corncob xylans whilst the other *Bifidobacterium* strains showed no growth on any of the substrates in co-culture. These results highlight the differences in xylan-type polysaccharide fermentation abilities of different bifidobacterial species as is the case in the degradation of inulin-type fructans (Falony et al., 2009). The growth of *Bi. animalis* subsp. *lactis* in co-culture provides evidence for a cross-feeding relationship between this species and the *Bacteroides* which couldbe due to the release of XOS as a PBP on the hydrolysis of xylan by the *Bacteroides* species which is subsequently utilized by *Bi. animalis* subsp. *lactis*. This explains the lack of growth of the other *Bifidobacterium* to grow in co-culture as they were unable to utilize XOS alone.

Cross-feeding behaviours between *Ba. cellulosilyticus* DSM 14838 (*Ba.cellulosilyticus* DSM 14838) and some bifidobacterial strains were analysed in a study carried out by Munoz et al. (2020) where interactions between the genera were observed during the growth of plant-derived larch wood arabinogalactan (LW-AG, Figure 14). The authors of this study demonstrated how *Ba. cellulosyliticus* DSM 14838 primarily degrades LW-AG to release rhamnose and β-1,3-galactooligosaccharides which are further metabolized by certain bifidobacterial strains. *Bi. breve* UCC 2003 grown in co-culture with *Ba. cellulosilyticus* DSM 14838 was able to utilize LW-AG as a carbon source as compared with no growth detected in monoculture thus confirming the hypothesis of a cross-feeding relationship between the organisms. The carbohydrates β-1,3-galactobiose and β-1,3-galactotriose were utilized by *Bi. breve* UCC 2003 whereas rhamnose was not a viable growth substrate.

As well as *Bi. breve* UCC 2003, *Bi. longum* subsp. *infantis* ATCC 15697 was also able to utilize AG-derived oligosaccharides released by *Ba. cellulosilyticus* DSM 14838. The *bgaA* gene was identified in the genome of *Bi. breve* UCC 2003 and was predicted to encode a GH2 enzyme that is involved in the degradation of β-1,3-galactooligosaccharides. The active site of the BgaA enzyme was identified as being specific to β-1,3-galactobiose and β-1,3-galactotriose. Interestingly, this gene was not identified in the other bifidobacterial species examined including *Bi. breve* JCM 7017, *Bi. bifidum* LMG13195, and *Bi. longum* subsp. *longum* NCIMB8809 and this corresponds to their inability to cross-feed with *Ba. cellulosilyticus* DSM14838 thus confirming the function of the *bgaA* gene.
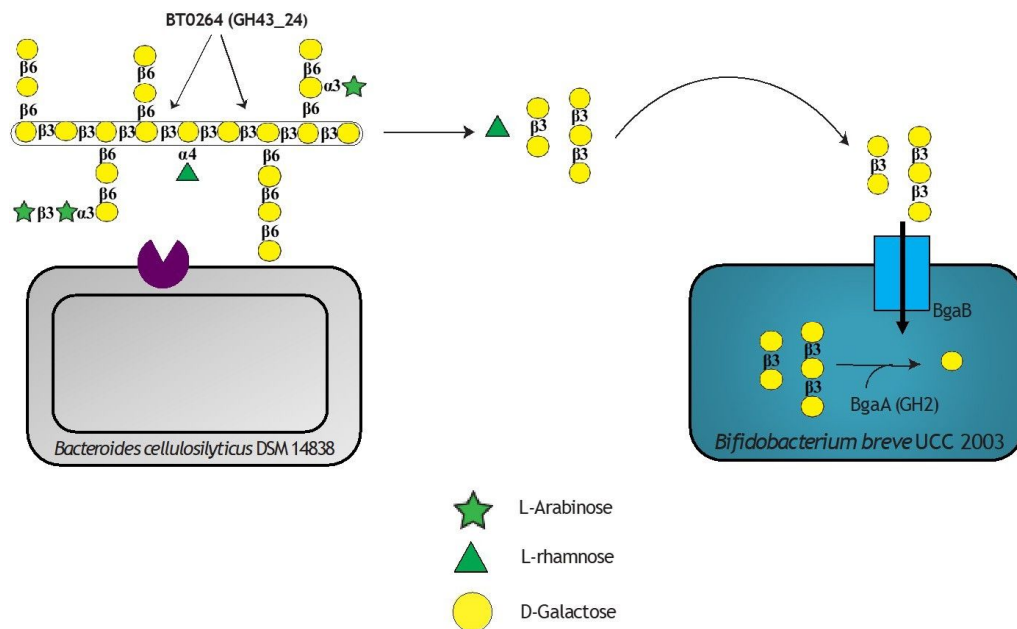
Figure 14. Biochemical analysis of cross-feeding behaviour between two common gut commensals when cultivated on plant-derived arabinogalactan (Munoz et al., 2020).

Another study (Liu et al., 2020) showed how *Bacteroides* and *Bifidobacterium* are involved in the breakdown of polysaccharides in co-culture, although no cross-feeding

interactions were observed. Three polysaccharide mixtures made up of different combinations of AX, xyloglucan, β-glucan and pectin were used as media for a co-culture of five different bacterial species including *Ba. ovatus* ATCC 8483 and *Bi. longum* subsp. *longum* ATCC 15707. Size-exclusion chromatography showed that the observed degradation of the polysaccharides was carried out by *Ba. ovatus* ATCC 8483 and *Bi. longum* subsp. *longum* ATCC 15707 and the other bacterial species did not utilize these carbohydrates. Further analysis identified the release of oligosaccharides by *Ba. ovatus* ATCC 8483 on the hydrolysis of β-glucan; however, these were not utilized by any of the other species in the co-culture. It was found that *Ba. ovatus* ATCC 8483 played a key role in the production of the SCFA succinate, which was utilized in the formation of propionate by other members of the co-culture, supporting the claim that *Bacteroides* species act as primary degraders of polysaccharides. This was also the case in the production of lactate by both *Ba. ovatus* ATCC 8483 and *Bi. longum* subsp. *longum* ATCC 15707 which was utilized by the other organisms. This study, along with previous studies discussed, highlights how the microorganisms in the human GIT can cooperatively interact in the breakdown of polysaccharides and benefit one another through PBPs and SCFAs production as well as providing benefit to the human host.

The identification of polysaccharide utilization loci in the dominant gut phylum *Bacteroides* has helped to increase knowledge of the complex system in which glycan molecules are broken down. It has allowed for further research into the utilization mechanisms as well as the ongoing characterization of carbohydrate-active enzymes that are produced by all glycan-degrading bacteria, including *Bifidobacterium*. Understanding enzyme function is essential to fully understand non-digestible carbohydrate utilization and may help us predict the production of postbiotics,

either SCFAs or other bioactive compounds such as vitamins, from a given substrate.

In the case of *Bacteroides* and *Bifidobacterium*, there is evidence for glycan-sharing and cross-feeding activities between certain members of these two genera, particularly during the breakdown of dietary fibre. As it has been discussed, interactions between these two genera have previously been studied. However, many other cross-feeding activities likely exist that have yet to be discovered. Interaction between *Bacteroides* and *Bifidobacterium* in the breakdown of arabinoxylan has been observed in a small number of studies; however, there is little to no literature available on possible cross-feeding activities on other dietary glycans, such as β-glucan, arabinogalactan, arabinan. Future research should investigate the interaction, if any, between *Bacteroides* and *Bifidobacterium* in the metabolism of dietary β-glucan and its effect on the human host. In addition, there are numerous other gut commensals, less dominant in the human large intestine such as *Lactobacillus reuteri*, which can be studied for their cross-feeding activities with *Bifidobacterium* (either involving dietary fibres or released mono-/oligosaccharides), but also for the conversion of metabolic end products of one species (for instance 1,2-propanediol or lactate) into other metabolites (propionate, butyrate). The experimental proof of the conservation of polysaccharide utilization loci involved in β-glucan degradation specifically, amongst *Bacteroides* genus, would allow us to identify the enzymes involved in the metabolism of these molecules, which would then provide a starting point to investigate whether *Bifidobacterium* genus has a role in the breakdown of this polysaccharide. Due to the complex nature of the human gut microbiota, and the complexity and variation in carbohydrate structure, more research is required for us to fully understand the roles of each member.

1.8 β-glucans

β-Glucans are complex polysaccharides composed of D-glucopyranosyl residues that are linked through β-bonds. These glucose polymers are present in cell walls of yeast, fungi, seaweed, bacteria and cereals (Du et al., 2019; Henrion et al., 2019) showing a different macromolecular structure of β-glucans according to the extraction source (Figure 15). For instance, cereal β-glucans have a backbone of single β(1,3)-bonds separating short sections of β(1,4)-bonds, while seaweed β-glucans typically consist of a mixture of β(1,3)-linkage backbone with single β(1,6) branching points, in which the resulting side chain contains β(1,3)-linkages. Additionally, mushroom-derived β-glucans typically represent polymers composed of β(1,6)-linked branches from a β(1,3) backbone, while bacterial β-glucans simply consist of a linear β(1,3) backbone (Dobrinčić et al., 2020; Jayachandran et al., 2018; Liu et al., 2019; Singh, 2019).
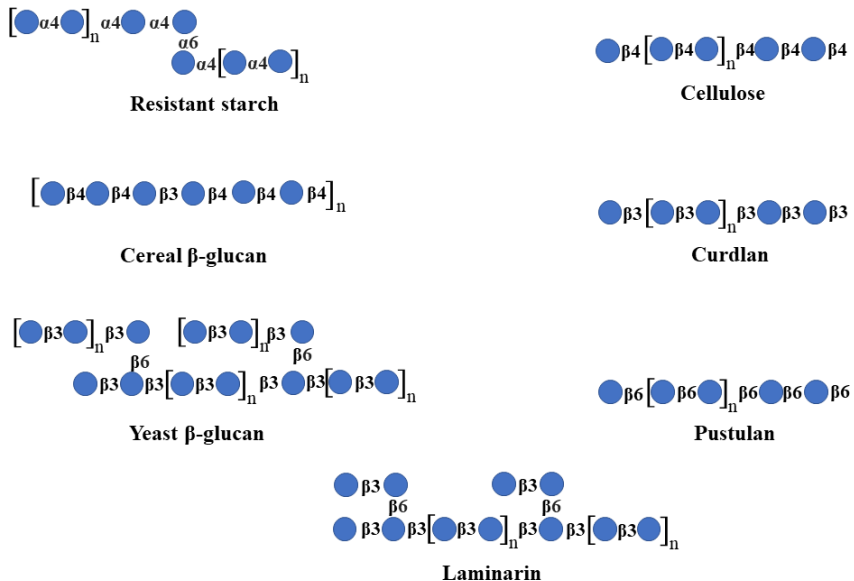
Figure 15. Structure of different types of α- (resistant starch) and β-glucans. The sources of β-glucans are varied: cereals, brown algae (Laminarin), *Saccharomyces cerevisiae* (Yeast), Fungi *Lasallia pustulata* (Pustulan), bacteria, e.g. *Alcaligenes faecalis* (Curdlan), and plants (Cellulose) (Singh, 2019).

β-glucans can be modified by physical, chemical, and biological methods, which affects its primary structure, spatial conformations, and bioactivity. Modification and transformation of β-glucans may not only improve their biological functionalities in the human gut but also their industrial applications as a prebiotic (Gibson et al., 2017; Kagimura et al., 2015; Wang et al., 2017). These types of processed β-glucans have been reported to reduce glucose and cholesterol blood levels, promote the production of short-chain fatty acids (SCFAs), which may act as important modulators of host immune function, decrease energy intake, and lower obesity, diabetes and cardiovascular risk (Cosola et al., 2017; De Vadder et al., 2014; Hooda et al., 2010; Hosseini et al., 2011; Rumberger et al., 2014; Shen et al., 2011; Zhu et al., 2016). Moreover, several studies have underlined a wide range of interesting properties of β-glucans, such as anticancer effects (Choromanska et al., 2015; Del Cornò et al., 2020; Geller et al., 2019; Zhang et al., 2018), immunomodulatory capacity (Stier et al., 2014), anti-inflammatory response (Schwartz et al., 2014), or their role as potential adjuvants for vaccine composition and development (Vetvicka et al., 2020) or as a delivery vehicle for probiotics (Gani et al., 2018).

1.8.1 Cereal β-glucans

Cereals are the most common and widespread source of β-glucan in the human diet and their chemical structures are widely conserved across cereal crops (Cameron et al., 2014; Cameron et al., 2012; Koropatkin et al., 2010). They are described usually as homoglucopolysaccharides with a backbone of single β(1,3)-bonds separating short sections of β(1,4)-bonds (Cameron et al., 2014; Cameron et al., 2012; Koropatkin et al.,2010).

Oat β-glucans

The effect of oat β-glucan ingestion was associated with a modest increase in bacterial richness (yet decreasing the *Bacteroides* population) in both ileal effluent and fecal samples when compared with intake of cellulose or carboxymethylcellulose (Metzler-Zebeli et al., 2010). The effect was viscosity-dependent, since low-viscosity oat β-glucan reduces the relative abundance of *Bacteroides* to a higher degree when compared to high-viscosity oat β-glucan. The same decreasing effect was observed in a similar study where oat β-glucan was compared with pectin, inulin and arabinoxylan (Yang et al., 2013).

However, in a subsequent study in BALB/c mice, oat β-glucan ingestion decreased bacterial biodiversity yet caused an increase in the relative abundance of the phylum Bacteroidota compared with the control and with a mixture oat β-glucan-cellulose. *Bacteroides* was found to be the predominant genus in the colon and it was associated with a higher concentration of beneficial short chain fatty acids (SCFAs) such as propionate and acetate (Luo et al., 2017). The increase in *Bacteroides* populations was also reported by Carlson et al. (2017) using Oatwell (oat-bran containing 28% oat β-glucan) (Carlson et al., 2017). Additionally, different studies have demonstrated the effect of oat β-glucans in *Bifidobacterium*. Wu et al. (2018) found that *Bifidobacterium* content was decreased by the dietary supplementation with oat β-glucans (Wu et al., 2018). Nevertheless, an in vitro fermentation study by Ji-lin et al. (2017) showed *Bi. longum* BB536 as a good degrader of raw and hydrolysed oat β-glucans hydrolysates, with a preference for the hydrolysed fractions (Ji-lin et al., 2017). Another study concluded that the addition of β-glucan to yogurt increased the survival probability of *Bi. longum* R0175 (Rosburg et al., 2010). Furthermore, *Bifidobacterium* abundance was demonstrated to increase significantly in rats fed with

oat whole meal or oat β-glucan compared with a control group, with rats exhibiting a higher growth rate when fed on pure oat β-glucan (Zhang et al., 2012).

Barley β-glucans

Supplementation with barley β-glucan in rats with a low or high-fat diet increased the production of SCFAs, reduced inflammation and cholesterol levels, and lowered the abundance of *Bacteroides fragilis* NCTC9343 in the caecum (Zhong et al., 2015). Additionally, in a study with polypectomyced patients (patients having colorectal polyps), no significant difference was observed during a 90-day feeding intervention using 3 g/day of barley β-glucan. Nevertheless, two weeks after cessation of the treatment, the abundance of the genus *Bacteroides* was found significantly decreased (Turunen et al., 2011). A similar negative correlation was observed in hypercholesterolemic rats fed with a medium molecular weight (530 kDa) barley β-glucan diet (Mikkelsen et al., 2017).

However, the application of 3 g/day of this medium molecular weight barley β-glucan in hypercholesterolemic human patients increased the relative abundance of Bacteroidota, while that of Bacillota was decreased. Interestingly, no significant differences were observed when patients received 3 g/day or 5 g/day of low molecular weight barley β-glucan. These findings, therefore, suggest that the promoting effect of Bacteroidota abundance by barley β-glucan is molecular weight-dependent (Wang et al., 2016).

One particular utilization locus was identified in *Bacteroides ovatus* ATCC 8483 (Bovatus_02740-Bovatus_02745) when this strain metabolizes barley-derived, mixed-linkage β-glucans (Figure 16) (Tamura et al., 2017). This locus encodes a GH16 *endo*-β-glucanase (BoGH16$_{MLG}$) which hydrolyses β(1,4)-linkages that are preceded by a

β(1,3)-linked glucosil residue, and a GH3 *exo*-glucosidase that digests the oligosaccharides released by BoGH16$_{MLG}$ to glucose. This PUL also encodes two SGBPs, BoSGBP$_{MLG}$-A (a SusD homolog) and BoSGBP$_{MLG}$-B. BoSGBP$_{MLG}$-A is essential for the growth of *Bacteroides ovatus* ATCC 8483 on barley β-glucan because it incorporates oligosaccharides originated by BoGH16$_{MLG}$ into the periplasm. However, BoSGBP$_{MLG}$-B is not essential for growth though it may assist in oligosaccharide scavenging Homologous PULs are also present in *Bacteroides xylanosolvens* XB1A and *Bacteroides uniformis* ATCC8492, which highlights the apparent prevalence of PULs dedicated to β-glucan metabolism among *Bacteroides* species (Tamura et al., 2017).

In addition, *Ba. ovatus* ATCC 8483 prioritizes the use of barley β-glucan in a mixture with pectin, xyloglucan and arabinoxylan, being able to use this substrate when it was the only carbon source in the medium. *Ba. ovatus* ATCC 8483 showed higher growth rates than *Bi. longum* subsp. *longum*, *Megasphaera elsdenii*, and *Ruminococcus gnavus*, but lower than *Veillonella parvula* (Liu et al., 2020).
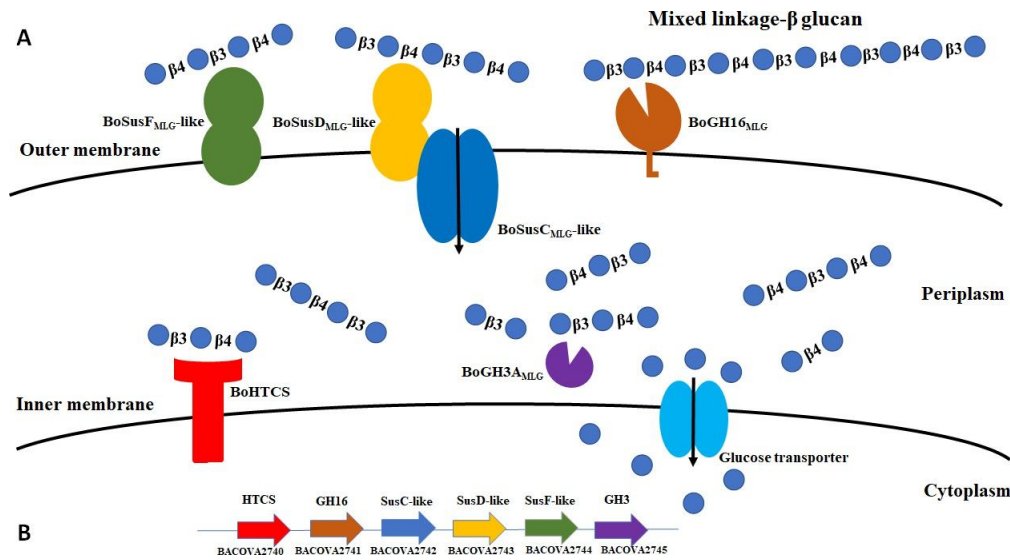
Figure 16. (A) Glycan utilization locus in *Ba. ovatus* ATCC 8483. Mixed linkage β-glucan is first degraded outside the cell by a cell surface-associated GH16, which generates oligosaccharides. The SusC/SusD-like pair incorporates these oligosaccharides into the periplasm, where a GH3 (β-glucosidase) degrades these internalized oligosaccharides into glucose monomers, which are then incorporated into the cytoplasm. **(B)** Genomic content of the MLG PUL in *Ba. ovatus* ATCC 8483 (Tamura et al., 2017; Tamura et al., 2019).

In *Bifidobacterium*, the bifidogenic effect of barley β-glucan supplementation in food/feed has been described in various publications. For instance, Arora et al. (2012) discovered that C57BL/6 mice, when maintained on a high-fat diet containing 10 % barley β-glucan for 8 weeks, showed a lower body weight gain and also an increase in the relative abundance of *Bifidobacterium* in both faecal and caecal samples (Arora et al., 2012). Similar results were found in rats fed on a low-fat diet supplemented with barley β-glucans for 25 days (Zhong et al., 2015) and, in a similar way, in other murine trial (Miyamoto et al., 2018).

Wheat β-glucans

In obese subjects with unhealthy dietary behaviour, wheat β-glucan was correlated with a relative abundance increase in members belonging to the Bacteroidota phylum and *Bacteroides* genus. It was also suggested that *Bacteroides* sp. reduces the levels of

inflammatory markers TNF-α and IL-6, and it plays a role in reducing pathologies associated with inflammation (Vitaglione et al., 2015). In a similar study, *Ba. cellulosyliticus*, *Ba. ovatus* and *Ba. stercoris* were described as predominantly wheat-brand β-glucan degraders, while *Ba. uniformis, Ba. dorei* and *Ba eggertii* were enriched in the β-glucans from wheat-lumen, so apparently not all *Bacteroides* species exhibit the same glycan utilization behaviour (De Paepe et al., 2017). Nevertheless, the use of whole grains instead of extracted β-glucan requires further studies for wheat.

Mix of different cereals

A dietary intervention using 3 g/d of durum wheat flour and whole-grain barley pasta for two months did not reveal any significant differences in the microbiota composition of the subjects (De Angelis et al., 2015). However, in another trial with wheat bran and barley in Japanese adults, a positive interaction was observed when both cereals were combined, causing an increase in the relative abundance of the genus *Bacteroides* and other butyrate-producing species (Aoe et al., 2018). Differences in the microbiota composition of distinct human populations because of varying diets and lifestyles may explain these conflicting findings (Hehemann et al., 2012; Nishijima et al., 2016; Sonnenburg et al., 2016).

Regarding *Bifidobacterium,* Shen et al. (2012) carried out a comparative study of the prebiotic efficacy of oat and barley β-glucan in rats. In the study, *Bifidobacterium* abundance increased using either of these cereals, with a more pronounced effect for oat β-glucan (Shen et al., 2012).

1.8.2 Seaweed β-glucans

Seaweeds are potential prebiotics rich in three polysaccharides depending on the seaweed source, being either brown, green, or red algae. In brown algae, fucoidan,

alginate and laminarin have been shown to act as an antioxidant, cognitive protective, anti-inflammatory, anti-angiogenic, anti-cancer, anti-viral, and anti-hyperglycemic agents, thus having very promising potential as a food additive and prebiotic (Collins et al. 2016; Patil et al., 2018). Laminarin (Figure 15) is a linear glucose-based homopolysaccharide with a β(1,3) backbone and β(1,6) branches at a 3:1 ratio, being isolated from the brown algae species *Laminaria* and *Alaria*, representing almost 50 % of algal dry matter. Laminarin is a type of β-glucan with special interest because of its proposed anticancer, antioxidant and immunomodulatory activities (Sellimi et al., 2018; Xia et al., 2014). For instance, in a recent study, both native laminarin and its enzymatic digestion products inhibited cell transformation on SK-MEL-28 human melanoma and DLD-1 human colon cancer cells, where the maximum anti-cancer effect was shown to be correlated with a high level of branching (Menshova et al., 2014).

Laminarin has been widely studied as a growth substrate for various marine *Bacteroides* species. An analysis of Bacteroidota-fosmids from ocean regions showed that 4 out of 14 identified PULs were laminarin-specific and were co-located with predicted β-glucosidase-encoding genes, thereby underscoring the role of laminarin as a common metabolic substrate for ocean-derived Bacteroidota species (Bennke et al., 2016).

At the species level, the degradation of laminarin in the marine bacterium *Zobellia galactanivorans* (*Z. galactanivorans*) has been described in different studies. Thomas et al., (2017) studied the gene transcription in *Z. galactanivorans* (Figure 17) when it grows on laminarin as a carbon source (Thomas et al., 2017). The authors suggested that this marine polysaccharide induced the expression of the cluster ZOBELLIA_209 to ZOBELLIA_214, which is predicted to encode two TonB-

dependent receptors (TBDR, ZOBELLIA_212 and ZOBELLIA _214) and their associated surface glycan- binding proteins (SGBP, ZOBELLIA_211 and ZOBELLIA_213), respectively. These tandems are characteristic of genomes in Bacteroidota (Grondin et al., 2017). This cluster encodes a predicted carbohydrate-binding module family 4 (CBM4, ZOBELLIA_209), whose family has been characterized to bind to β(1,3)-glucan, β(1,3-1,4)-glucan, β(1,6)-glucan, xylan, and amorphous cellulose (CAZy database, http://www.cazy.org/) (Consortium, 2018; von Schantz et al., 2012; Zhang et al., 2014). This cluster is involved in the recognition, binding, and incorporation of laminarin at the cellular surface of *Z. galactanivorans.* Together with the mentioned cluster*, Z. galactanivorans* induced transcription of ZOBELLIA_587, ZOBELLIA_588 and ZOBELLIA_589, which are predicted to be a periplasmic glucolactonase, a periplasmic gluconate transporter and a cytosolic galactonate dehydrogenase, respectively. Finally, *Z. galactanivorans* induced ZOBELLIA_3183, encoding a predicted polysaccharide lyase family 9, subfamily 4 (PL9_4) (Lombard et al., 2010). PL9_4 has only one characterized protein in the CAZy database from *Paenibacillus koleovorans* JCM11186, whose activity has been described as a thiopeptidoglycan lyase. Therefore, ZOBELLIA _3183 may represent a new activity in this subfamily 4 (Thomas et al., 2017).

On the other hand, two β-glucanases from *Zobellia galactanivorans*, *Zg*LamAGH16 and *Zg*LamCGH16, were described as laminarinases with residual activity on MLG (Labourel et al., 2014; Labourel et al., 2015). *Zg*LamAGH16 is a specific β(1,3)-glucanase with a unique extra loop in the active site, which is composed of 17 amino acids giving a bent shape in the cleft of the active site and adapting the enzyme to the U-shape topology of laminarin. This unique characteristic shows the enzyme as an evolution from the broad β-glucanase activities of the GH16 family (Viborg et al.,

2019), obtaining a very specific activity on β(1,3)-glucan. However, *Zg*LamCGH16 elicits preferential recognition and activity on branched laminarin. Altogether, these two GH16 enzymes in *Z. galactanivorans* are involved in the initial step of the metabolism of branched laminarin (*Zg*LamCGH16), while *Zg*LamAGH16 recognizes and efficiently attacks unbranched polysaccharide and oligosaccharide-derived laminarins (Labourel et al., 2014; Labourel et al., 2015). Another study showed that the incorporation of 2 % of brown algae laminarin in feed for a rat trial decreased the relative abundance of the Bacteroidota phylum in caecal microbiota populations. Specifically, the ratio of identified clones, based on 16S rRNA gene sequencing, of *Bacteroides capillosus* fell around 27 % compared to the control (An et al., 2013). By contrast, in a study with mice fed with high-fat diet compared with high-laminarin diet, the authors found that the diet without laminarin led to an increase in Actinomycetota, whereas dietary supplementation with laminarin witnessed an increase in the relative abundance of Bacteroidota, specially the genus *Bacteroides*, and a decrease in Bacillota. Laminarin ingestion shifted the microbiota at the species level towards a higher energy metabolism, increasing the *Bacteroides* species, and therefore increasing the number of carbohydrate-active enzymes. Laminarin also slowed weight gain in mice and decreased bacterial species diversity (Nguyen et al., 2016).

The same increase in Bacteroidota/Bacillota ratio was observed in a recent study with albino mice (Takei et al., 2020) in which laminarin was shown to be metabolized by *Ba*. *intestinalis* and *Ba*. *acidifaciens*, producing succinate and acetate as end-products, which are precursors of the beneficial SCFAs propionate and butyrate, respectively (De Vadder et al., 2016; Fernández-Veledo et al., 2019; Laserna-

Mendieta et al., 2018).
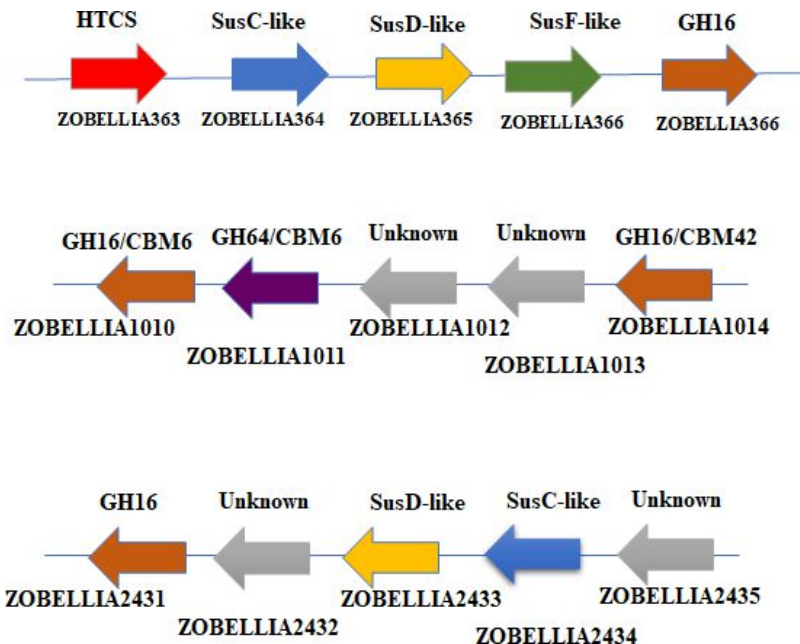
Figure 17. Genomic composition of the β(1,3)-glucan PUL in *Zobellia galactinovorans* DsijT (Thomas et al., 2017).

In contrast, several feeding studies have concluded that laminarin from *Laminaria digitata* does not affect the relative abundance of *Bifidobacterium* in the gut microbiota (Smith et al., 2011; Sweeney et al., 2012). Nevertheless, Lynch et al. (2010) reported a linear decrease in caecal *Bifidobacterium* in boars as a result of the addition of laminarin from *Laminaria* (Lynch et al., 2010). Though, further studies to deeply analyse the effect of laminarin on the HGM are still required.

Finally, a study on β(1,3)-glucan metabolism by *Bacteroides* sp. showed that *Ba*. *unformis* ATCC 8492, *Ba thetaiotaomicron* NLAE-zl-H207 and *Ba. fluxus* YIT12057 could use laminarin as a carbon source because of the defined PUL architecture where a GH158 is key in the release of oligosaccharides (Déjean et al., 2020).

1.8.3 Fungal β-glucans

Fungal β-glucans are polymers composed of a β(1,6) or β(1,3) backbone, with a variable branching degree (Figure 15). *Bacteroides* species have been reported as degraders of different types of fungal β-glucan. For example, when β-glucan from *Saccharomyces cerevisiae* (β-1,3-glucan with β-1,6-linked side chains) was supplied to C57BL/6 mice, it was shown to cause a reduction in bacterial diversity, but an increase in the relative abundance of the phylum Bacteroidota accompanied with higher levels of SCFAs such as acetic, propionic and butyric acid (Gudi et al., 2020). In another study, β(1,3)-glucan from *Candida albicans* increased the relative abundance of the *Bacteroides* genus when mice were administered live or heat killed-*Candida albicans* (Panpetch et al., 2017). Déjean et al. (2020) described a putative β(1,3)-glucan utilization locus in *Ba. uniformis* ATCC 8492 (BACUNI_01484-BACUNI_01490, see Figure 18 below) that encodes a TonB-dependent transporter (TBDT, SusC-homolog), two cell surface glycan-binding proteins (SGBP-A and SGBP-B), three glycoside hydrolases (GH16, GH158 and GH3) and a hybrid two-component system (HTCS) transcriptional regulator (Déjean et al., 2020).
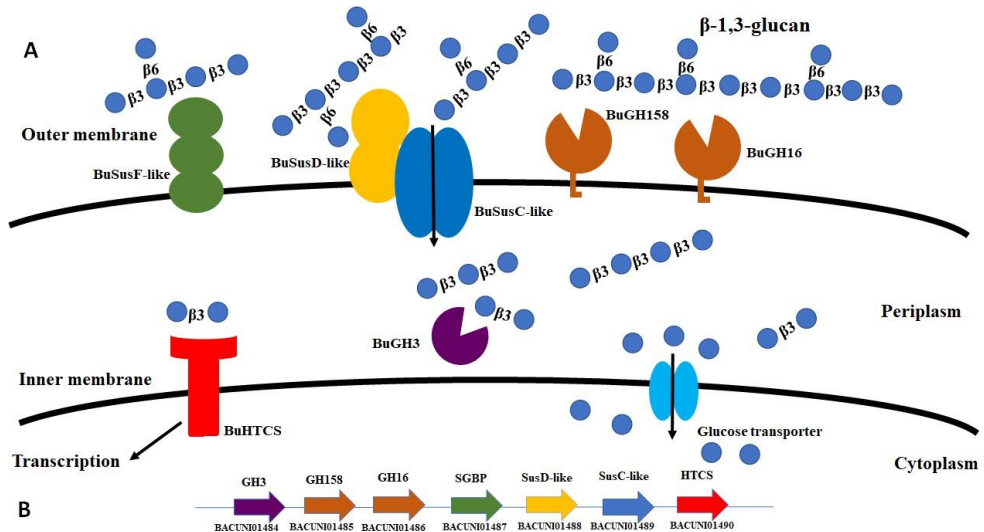
Figure 18. (A) Scheme of β(1,3)-glucan degradation by *Bacteroides uniformis* ATCC 8492, based on an analogy with the starch utilization system (Déjean et al., 2020). (B) Genomic content of the pustulan PUL in *Bacteroides uniformis* ATCC 8492 (Déjean et al., 2020).

One particular PUL (BT3309-BT3314) from *Ba. thetaiotaomicron* VPI 5182 has been associated with the degradation of pustulan, a fungal β(1,6)-glucan that is a common component of fungal cell walls of mushrooms and yeast (Temple et al., 2017). BT3312 represents an endo-β(1,6)-glucanase located at the cell surface accompanied by a SGBP (GH30_3, BT3313), a SusD-homolog (BT3311) and a β(1,6)-glucosidase (BT3314). *Ba. thetaiotaomicron* employs a very efficient mechanism to fully degrade pustulan as a carbon and energy source (Figure 19). The SGBP BT3313 starts the degradation process by recognizing and binding the intact polysaccharide to the cell surface of *Ba. thetaiotaomicron*. Following this, the GH30_3 cleaves the intact glycan into smaller glucooligosaccharides, which will then be internalized into the periplasm by BT3311 (SusD-homolog). In the periplasm, a GH3 (BT3314) will continue metabolism by degrading the internalized 1,6-glucooligosaccharides. Comparative genome analysis with other species revealed that homologous PULs are located in

genes of *Ba. uniformis* ATCC 8492, *Ba. ovatus* ATCC 8483 and *Ba. xylanosolvens* XB1A (Temple et al.,2017).
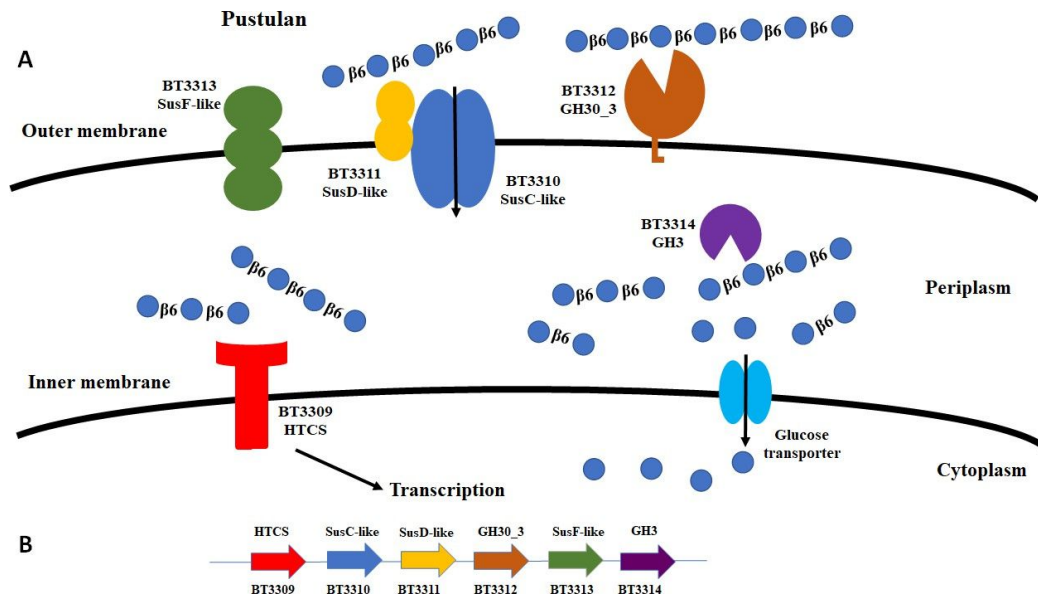
Figure 19. (A) Scheme of β(1,6)-glucan degradation by *Ba. thetaiotaomicron* (Temple et al., 2017). This linear β-glucan is degraded by a GH16 on the surface of *Ba. thetaiotaomicron* VPI 5482 and incorporated into the periplasm, where another GH3 (unspecific β-glucosidase) breaks the smaller oligosaccharides into single glucose monomers. B Genomic content of the pustulan PUL in *Ba. thetaiotamicron* VPI 5482 based on an analogy with the starch utilization system (Temple et al., 2017).

Several studies have addressed the role of fungal β-glucans in the *Bifidobacterium* genus. For instance, Wang et al. (2019) studied the relation between β-glucan obtained from the yeast *Saccharomyces cerevisiae* and immune response (Wang et al., 2019). Yeast β-glucans could alleviate the immune-suppression, favouring the proliferation of the *Bifidobacterium* genus (Wang et al., 2019).

Furthermore, the supplementation with yeast β-glucans in Alzheimer-induced mice led to an increase in the relative abundance of the genus *Bifidobacterium*, which was similar to that found in control mice (Xu et al., 2020). Alessandri et al. (2019) evaluated the growth ability of hundred bifidobacterial strains using glucan-chitin

complex from *Aspergillus niger* as the only carbon source. All strains were shown to exhibit some, though mostly modest growth with *Bi. breve* and *Bi. bifidum* strains to elicit the highest levels of growth (Alessandri et al., 2019). Zhao and Cheung showed that mushroom β-glucans elicit a prebiotic effect by enhancing the growth of *Bi. longum* subsp. *infantis* (Zhao et al., 2013). These authors studied the proteomic profile of this catabolic process, showing that this bifidobacterial species expresses 17 proteins that may be linked to mushroom β-glucan degradation. Pokusaeva et al. (2011) identified the cldC gene in *Bi. breve* UCC2003 to be involved in the metabolism of cellodextrins, which are β(1,4)-glucose hydrolysis products from cellulose (Pokusaeva et al., 2011). The authors showed the ability of this bacterium to use cellobiose, cellotriose, cellotetraose and cellopentaose through the cldEFGC gene cluster with a higher preference for cellobiose. Disruption of the cldC gene resulted in the inability of *Bifidobacterium breve* UCC2003 to use these cellodextrins as a carbon source, confirming that this gene cluster is unique in the bacterium for this metabolism. It is reasonable to assume that these enzymes would be able to degrade MLG oligosaccharides in a similar way to cellodextrin oligosaccharides. However, this hypothesis needs to be tested experimentally. Nevertheless, more studies are required to fully understand the impact of β-glucan oligosaccharides on bifidobacterial species.

1.9 Mycoprotein from *Fusarium venenatum*

The Food and Agriculture Organization (FAO) of the United Nations predicted in 2012 that the global demand for meat would reach 455 M metric tons by 2050 (Alexandratos et al., 2012). The steady increase in meat consumption around the world today suggests that there is still an issue for the environment and public health. For this reason, it is

crucial to find healthy and sustainable alternatives that allow meat substitution. These new methods of food production should combine novel agricultural techniques with environmentally friendly dietary modifications (Tuomisto, 2022). While some types of meats have been associated with the risk of cardiovascular diseases (Abete et al., 2014), meat alternatives, either plant-based products or fungus, may ease the reduction and prevention of coronary heart disease and stroke by reducing blood lipid levels (Pabois et al., 2020). They can simulate meat organoleptic features in appearance, and this may play an important role to enable a dietary change (Kumar etal., 2017). Even though meat alternatives have been available a long time ago, their popularity with consumers has increased rapidly in recent times since the change of marketing direction towards meat-eating consumers, rather than just vegans and vegetarians (Hu et al., 2019).

Quorn® mycoprotein is a nutritional replacement for animal meat protein substitute (Finnigan et al., 2019; Wilson et al., 2021) generated through industrial fermentation of the filamentous microfungus *Fusarium venenatum* A3/5 (See Figure 20 and Figure 21 below). Mycoprotein has all the necessary amino acids for human nutrition, and it is high in quality protein and fibre and low in fat. Mycoprotein is elaborated from the RNA depletion of the mycelium of the ascomycete (Finnigan et al., 2019). It typically contains 25 g of solids, including 11 g of protein and 6 g of fibre/100 g (nutritional profile available on https://www.quornnutrition.com/importance-of-micronutrients). The fibre part located in the cell wall is composed of 2/3 branched β(1,3/1,6)-glucan

and 1/3 chitin being specific to fungal mycelium (Finnigan et al., 2019) and not frequently present in human food (Bottin et al., 2016). For all this, mycoprotein has organoleptic characteristics that are comparable to those of meat, making it a well-known meat replacement that is widely used in diets across the world and which has been incorporated into the diet of many populations (Finnigan et al., 2019).
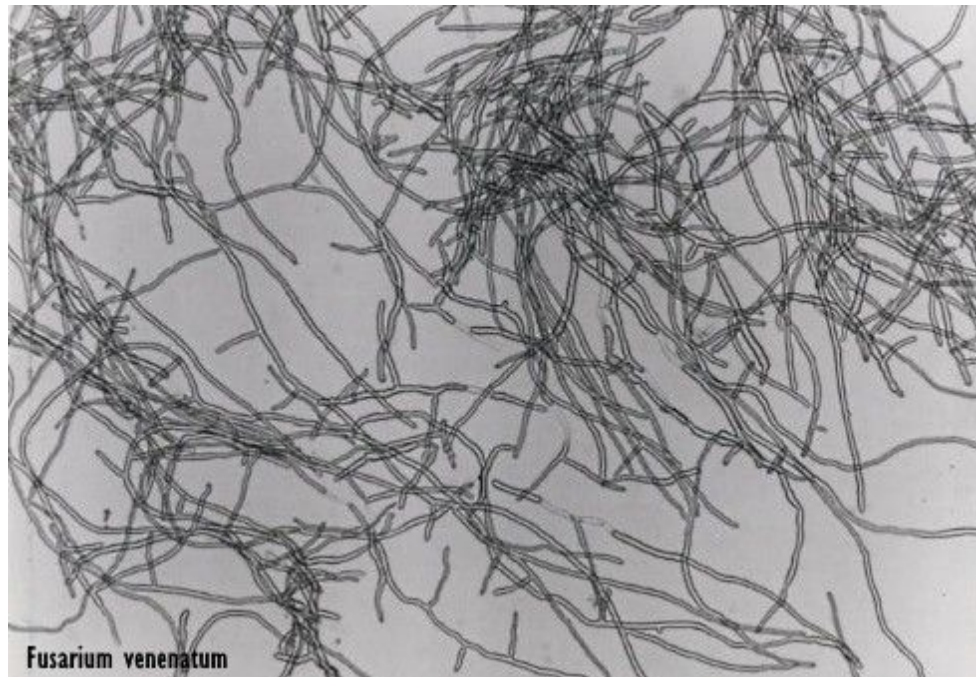
Figure 20. Image of *Fusarium venenatum* A3/5 (Ugalde et al., 2002).
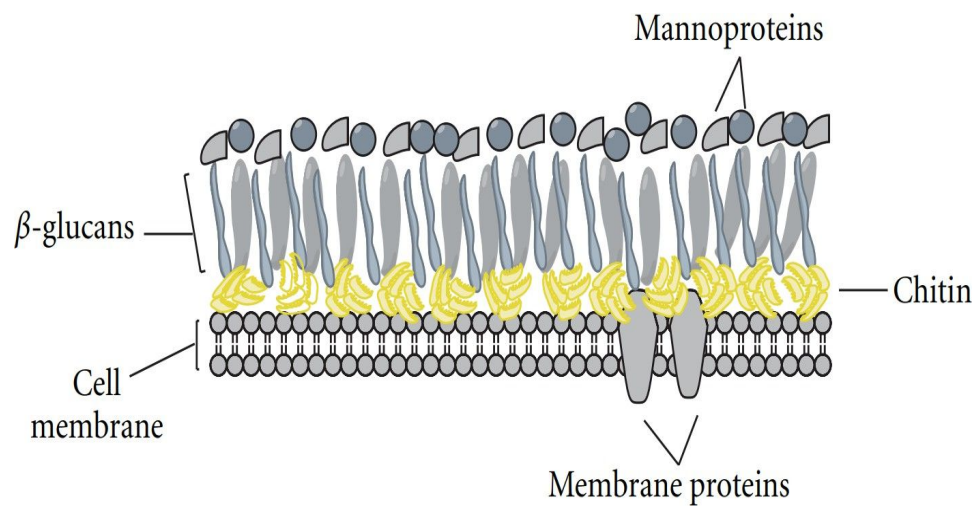
Figure 21. Cell wall and cell membrane of *Fusarium venenatum* A3/5 (Vega et al., 2012).

Mycoprotein is used to make a range of vegetarian meat replacements with a significantly lower environmental impact compared to that meat from beef (Kazer et al., 2021). Humpenöder et al. (2022) studied the environmental implications of replacing beef meat with mycoprotein analysing how this substitution would affect the level of several parameter such as production of greenhouse effect gases (N_2O, CH_4 and CO_2) and deforestation, among others (Humpenöder et al., 2022). Therefore, in the possible scenarios where the substitution of beef by mycoprotein was up to 20% 50% and 80% by 2050, the authors concluded that a 20% reduction would cause 56% less deforestation and 56% less net CO_2 emissions. For 50% and 80% of cases would imply drops of 82% and 93% in land destined for pasture and 83% and 87% less net CO_2 emissions, respectively (Humpenöder et al., 2022).

Several dietary beneficial effects of mycoprotein have been reported since it leads to lower plasma cholesterol levels and eases the reduction of different metabolic markers such as postprandial glucose, insulin output, energy intake, and lipolysis, compared with other protein sources (Burley et al., 1993; Cherta-Murillo et al., 2020; Colosimo et al., 2020; Turnbull et al., 1995; Turnbull et al., 1993). Coelho et al (2020) concluded that mycoprotein is a bioavailable source of high-quality protein and it could effectively affect daily glycaemic control and energy intake, stimulating muscle protein anabolism which consequently would enhance weight management (Coelho et al., 2020).

The mechanism by which the human body gets access to mycoprotein was studied by Colosimo et al. (2020). The results presented by the authors was referred only to *in vitro* models but they highlighted that protein bio-accessibility from mycoprotein was essentially an enzymatic process by which small intestinal proteases can permeate

56

through the fungal cell facilitating protein hydrolysis and release (Colosimo et al., 2020).

Another study (Wang et al., 2019) compared the relative abundance of different bacteria populations in anaerobic stirred batch cultures using four protein sources (casein, meat, mycoprotein, and soy protein). They concluded the existence of bacterial adaptation to different dietary sources because faecal bacteria from omnivores had insignificantly higher counts on meat, while faecal bacteria from vegetarians had higher counts on Quorn® extract. In the case of the specific genus, it is highly remarkable how *Bacteroides* and *Bifidobacterium* were supported by a mycoprotein diet, being related to higher concentrations of propionate and butyrate, respectively.

The positive relation between mycoprotein and SCFAs was also determined in another study (Harris et al., 2019). Mycoprotein led to higher levels of propionate compared with inulin and laminarin, and with significantly higher proportions of butyrate compared to rhamnose and oligofructose. The authors concluded that this preference for propionate and butyrate production is likely due to the β-glucan content, which has been previously shown to result in higher in vitro propionate and butyrate production (Hughes et al., 2008). Nevertheless, mycoprotein consists of a complex mixture of fibre, protein, and fat so it should not be considered an individual component.

At present there is still a big amount of research to be done on how the fungal components contained in Quorn® are metabolized in the human gut. Therefore, the analysis of the pure components of mycoprotein supposes the best manner to clarify what are their beneficial effects in the Human Gut Microbiota and to identify which bacteria populations show a predisposition to degrade mycoprotein from *Fusarium venenatum*, and, specially, β-glucan contained in it. This would allow bacteria to take

nutritious advantage from other microorganisms within the competitive environment that supposes the human gut. In conclusion, this would help to the clarification of the beneficial prebiotic effect that might be associated with the employment and increasing insertion of mycoprotein in the human diet.

1.10 Aims and objectives of this thesis

This thesis is focused on understanding different metabolic routes in the degradation and the metabolism of β-glucan from *Fusarium venenatum* by human gut *Bacteroides* sp., together with its secondary degradation via cross-feeding by *Bifidobacterium* sp. and *Lactobacillus* sp. Furthermore, the utilization of *Roseburia* sp.*, Akkermansia* sp. and *Victivallis* sp. as feasible primary degraders will expand the knowledge of how bacteria use fungal polysaccharides. Therefore, the main goal of this research is to clarify the potential impact that *Fusarium* mycoprotein, and, specially, *Fusarium* β-glucan, may have on human gut bacteria populations. Additionally, it will determine whether *Fusarium* mycoprotein may have any potential prebiotic effects that could influence the composition of the Human Gut Microbiota.

Understanding glycan metabolism may serve to evaluate how polysaccharides may affect the gut microbiota community, defining which bacteria species act as main degraders, developing a leading role, and which ones do not present this degradation capacity but anyhow can take advantage of the digestion products released by those previous ones. This understanding will help the development of nutraceutical-based strategies to increase the content of specific beneficial bacteria in the gut, increasing the associated health effects that the utilization of mycoprotein can have.

In summary, a combination of microbiology culture experiments, molecular biology techniques, enzymatic assays, proteomics and metabolomics, will show that the importance of mycoprotein goes further than being a simple ingredient in food products. It acts as a bacterial carbon and energy source which may also be considered as a potential regulator of our microbiota.

2 Material and Methods

2.1 Bacterial strains and vectors

2.1.1 *E. coli* strains for Cloning and Expression

Escherichia coli TOP10 (Invitrogen) was used as the cloning host and has the following genotype:

> *F- mcrA Δ(mrr-hsdRMS-mcrBC) φ80lacZΔM15 ΔlacX74 nupG recA1 araD139 Δ(ara-leu)7697 galE15 galK16 rpsL(Str^R) endA1 λ$^-$*

Escherichia coli BL21(DE3) (Novagen) was used as the expression host and has thefollowing genotype:

> *F– ompT gal dcm lon hsdSB(rB–mB–) λ(DE3 [lacI lacUV5-T7p07 ind1 sam7nin5]) [malB+]K-12(λS)*

2.1.2 Bacterial strains for the *Fusarium* β-glucan degradation

Bacteroides cellulosyliticus WH2
Bacteroides cellulosyliticus DSM 14838
Bacteroides thetaiotaomicron VPI 5482
Bacteroides ovatus ATCC 8483
Bacteroides vulgatus ATCC 8482
Roseburia inulinivorans DSM 16841
Roseburia intestinalis DSM 14610
Akkermansia muciniphila DSM 22959
Victivallis vadensis ATCC BAA-548
Bifidobacterium bifidum PRL2010
Bifidobacterium breve UCC03
Bifidobacterium breve JCM 7017
Bifidobacterium animalis subsp. *animalis* DSM 20104
Bifidobacterium longum subsp. *longum* NCIMB 8809
Bifidobacterium longum subsp. *infantis* ATCC 15697
Lactiplantibacillus plantarum WCFS1

Table 1. Bacterial strains for the *Fusarium* β-glucan degradation

2.1.3 Vectors

The commercially available plasmid pET-28 (+) (Novagen) was used as cloning vector for the experiments developed in this thesis.

2.2. Antibiotics stocks

All antibiotic stocks were prepared with autoclave sterilized 18.2 MΩ/cm H_2O, obtained from a Merck Milipore Milli-Q® water system in a 1000X concentration.

Media	Concentration
Kanamycin (Formedium)	50 µg/mL in 18.2 MΩ/cm H_2O
Gentamicin (Meldford)	20 µg/mL in 18.2 MΩ/cm H_2O
Ampicilin (Meldford)	20 µg/mL in 20% ethanol
Mupirocin (Sigma)	10 µg/mL 18.2 MΩ/cm H_2O
Vancomycin (Duchefa)	20 µg/mL in 18.2 MΩ/cm H_2O

Table 2. Antibiotics stocks used in this study.

2.3 Bacterial Growth Media

All growth media was prepared with distilled H_2O and then autoclaved at 120°C for 20 minutes. Liquid growth media were stored at room temperature and solid growth media at 4°C in the fridge.

Media	Composition
LB (Sigma)	10 g Tryptone (Sigma), 10 g NaCl (Formedium) and 5 g yeast extract (Melford). The final volume of 1L was achieved using 18.2 MΩ/cm H_2O.
LB Agar	25 g LB (LURIA-BERTANI) and 15 g Agar (Melford). A final volume of 100 mL was achieved using 18.2 MΩ/cm H_2O.
BIH (Melford)	17.5 g Brain Heart Infusion from solids (Melford), 10 g Pancreatic Digest of Gelatin (Sigma), 2 g Dextrose (Sigma), 5 g Sodium Chloride (Sigma) and 2.5 g Disodium Phosphate (Thermo). A final volume of 100 mL was achieved using 18.2 MΩ/cm H_2O.
MRS (Lab M) per Litre	It was purchased from the company and the final volume reached to 1L with 18.2 MΩ/cm H_2O.
Lactobacillus MRS media	It was purchased from the company and the final volume reached to 1L with 18.2 MΩ/cm H_2O.
Minimal media	1 g Ammonium sulfate (Thermo), 1 g Sodium bicarbonate (Thermo), 0.5 g L-Cysteine (Thermo), 100 mL 1 M K_3PO_4 pH 7.2 (Thermo), 50 mL Mineral solution (Sigma), 10 mL $FeSO_4$ (Melford), 1 mL Vitamin K (Thermo), 0.5 mL Vitamin B12 0.01mg/Ml (Sigma) 4 mL, Resazurin 0.25 mg/mL (Sigma) 1 mL Hemin solution (Fisher). A final volume of 100 mL was achieved using 18.2 MΩ/cm H_2O.

BIH Agar Plate	BIH (Melford) with 15 g per litre of Agar (Melford). A final volume of 100 mL was achieved using 18.2 MΩ/cm H_2O.
MRS Agar plate	MRS (Melford) with 15 g per litre of Agar (Melford). A final volume of 100 mL was achieved using 18.2 MΩ/cmH_2O.

Table 3. Culture media used in this study.

2.4 Glycerol stocks preparation

The glycerol stocks of all used bacteria were prepared at 25 % glycerol using 1 mL bacterial culture (OD_{600}=0,6-0,8) and 1 mL 50% glycerol (Thermo Fisher). The samples were stored at -80°C.

2.5 Preparation of Chemically Competent Cells

A 10 mL starter culture in LB was inoculated with 50 µL of either *Escherichia coli* BL21(DE3) or *Escherichia coli* TOP10 from their 50% (v/v) glycerol stock with no antibiotic. The culture was incubated for 16 hours at 37°C at 180 rpm. Then, a 2 L Erlenmeyer flask containing 1000 mL LB was inoculated with 5 mL of the starter and it was incubated at 37°C at 180 rpm until the OD_{600} reached 0.6-0.8. It was subsequently cool on ice for 30 minutes. The culture was then split equally between two pre-chilled sterile 500 mL (Nalgene) centrifuge pots centrifuged at 5000 rpm for 10 minutes in a Thermo Scientific Sorvall Evolution RC centrifuge in a SLA 3000 rotor. Consequently, the supernatant was poured aseptically and 100 mL $MgCl_2$ (0.1 M) added to both pellets. The pellets were resuspended and re-centrifugated at 4500 rpm for 10 minutes. The supernatant was discarded aseptically and 15 mL $CaCl2$ (0.1 M) was added to one of the

pellets. The pellet was resuspended and poured on top of the second pellet. The second pellet was then also resuspended. The final pot was then left on ice for 90 minutes and after the cooling period, 4.5 cold mL of sterile 50% glycerol (v/v) was added and mixed into the solution followed by overnight incubation.

To confirm the successful growth of *Escherichia coli*, three 2% LB agar plates were set up, one containing kanamycin (50 µg/µL), one ampicillin (100 µg/µL), and one with no antibiotic. 150 µL of the resuspended cells were spread on the agar plates with a sterile glass spreader. If the plate without antibiotic showed a confluent lawn of cell growth and both antibiotic-containing plates were free of colonies, the prepared cell resuspension was transferred into 150 µL aliquots in pre-chilled 1.5 mL microcentrifuge tubes and stored at -80°C.

2.6 Mycoprotein β-glucan extraction and purification

The fungus cell wall from *Fusarium venenatum* was extracted and the different glycan parts were purified by adapting a previously described method in yeast (Bzducha-Wróbel et al., 2012). An alkaline extraction with 3% NaOH at 75°C was done obtaining two different fractions: fraction 1 which included supernatant containing both mannoproteins and β(1,3-1,6)-glucan soluble in bases; and fraction 2, which included β-glucan/chitin insoluble in bases. Following this, Fraction 1 was neutralized with glacial acetic acid and then centrifuged at 15000 g for 30 min. Once the pellet of β(1,3-1,6)-glucan was dialyzed for 24 h, it was frozen-dried prior to its use.

2.7 PCR

Q5 hot-start DNA polymerase (NEB) was utilized in the amplification of target genes. The reaction components and conditions (see list of primers attached) are shown below:

Component	Volume	Final Concentration
Q5 DNA polymerase	0.5 µL	1X
5X Q5 reaction buffer	5 µL	1X
dNTPs (10 mM each)	1 µL	200 µM
Template DNA	1 µL	100 – 200 ng
10 µM forward primer	2.5 µL	0.5 µM
10 µM reverse primer	2.5 µL	0.5 µM
18.2 MΩ/cm H$_2$O	To 50 µL	N/A

Table 4. Reaction components for Q5 hot-start DNA polymerase.

2.8 qPCR

The time point aliquots of the bacterial cultures were harvested in triplicate with RNA protect (Qiagen) for immediate stabilization of RNA added, and then stored at -20°C. RNA was extracted and purified with the RNAeasy minikit (Qiagen), and RNA purity was assessed by spectrophotometry. Then, 1 µg of RNA was used for reverse transcription and synthesis of the cDNA (SuperScript VILO master mix; Invitrogen). Quantitative PCRs (20 µl final volume) using specific primers (see list attached) were performed with a Luna Universal qPCR Master Mix (Biolabs) on a Step One Plus Real-Time PCR system (Applied Biosystems). The reaction components and conditions are shown below:

Component	20 µL reaction	Final concentration
Luna Universal qPCR Mix	10 µL	30 seconds
10 µM forward primer	2.5 µL	0.5 µM
10 µM reverse primer	2.5 µL	0.5 µM
Template DNA	variable	50-100 ng
Nuclease-free water	To 20 µL	-

Table 5. Reaction components for Luna Universal qPCR Master Mix.

For the baseline reaction used as control, DNA template was replaced with sterilized UltraPure™ DNase/RNase-Free distilled water (Fisher).

2.9 Agarose Gel Electrophoresis of PCR Samples

A 1% agarose gel solution was prepared in a 100 mL Erlenmeyer flask and heated in a microwave until all agarose powder was dissolved. After cooling it, the gel was poured into a casting tray and inserting the combs, it was left to sit at room temperature for 30 minutes. Then, the gel tray was removed from the casting tray and placed into horizontal gel tank (BioRad) with 1X TAE buffer, and the comb was removed.

The DNA samples were prepared using 5 µL PCR sample and 1 µL 6X loading dye (NEB). The samples were then loaded into the agarose gel along with 1X 5 µL 1kb DNA ladder (NEB) per comb. The tank lid was closed, and the probes were plugged into the power pack (BioRad powerpack 300), and the power was set at 120 V for 45 minutes for a small gel (50 mL). After this electrophoresis, the gel was removed and submerged in ethidium bromide solution (10 µg/mL) and placed on a tank for 30 minutes at roomtemperature. The gel was moved to 18.2 MΩ/cm H2O for 15 minutes

and then visualized using a UV transilluminator (Cleaver Scientific).

Media	Concentration
TAE Buffer (50x working concentration)	242.0 g Tris base (Melford), 100 mL, EDTA (0.5 M, pH 8.0) (Sigma), 57.1 mL Glacial acetic acid (Sigma). A final volume of 100 mL was achieved using 18.2 MΩ/cm H_2O.
Small Agarose Gel 1% (w/v)	0.5 g Agarose (Melford), 49 mL 18.2 MΩ/cm H2O and 1 mL 50X TAE Buffer.
Medium Agarose Gel 1% (w/v)	1.2 g Agarose (Melford), 117.6 mL 18.2 MΩ/cm H_2O and 2.4 mL and 50X TAE Buffer.
Large Agarose Gel 1% (w/v)	2.4 g Agarose (Melford), 245 mL 18.2 MΩ/cm H_2O and 5 ml 50X TAE Buffer.
Gel Loading Dye Purple (6X)	Gel loading dye, a DNA loading buffer, was acquired from NEB. The PCR product was prepared according to the following ratio of DNA-loading dye: 5 μL PCR product and 1 μL gel loading dye. The loading dye ratio used for plasmid DNA was 2 μL loading dye for every 7 μL DNA.
Bromophenol Blue DNA Loading Dye 10X Concentrated Stock	It was made with 0.25 g Bromophenol blue (Sigma), 33 mL 150 mM Tris (pH 7.6), 60 mL Glycerol. A final volume of 100 mL was achieved using 18.2 MΩ/cm H_2O.

DNA Standard Ladder	1 kb DNA Ladder (New England Biolabs) was used throughout the study and comprised the following standard sizes: 0.5 kh, 1 kb, 1.5 kb, 2 kb, 3 kb, 4 kb, 5 kb, 6 kb, 8 kb, and 10 kb.
Ethidium Bromide	Ethidium bromide was used at a working concentration of 10 μg / mL, obtained by diluting a stock of 10 mg/mL in 18.2 MΩ/cm H_2O.

Table 6. Materials employed in agarose gel electrophoresis.

2.10 Agarose Gel Extraction

For the purification of DNA fragments (mainly PCR products), the electrophoresis was stopped, and the gel was put in staining in ethidium bromide. Following the staining the gel was sliced using a medical scalpel under a UV light (Cleaver Scientific transilluminator) and transferred to 1 mL Eppendorf tubes. The weight before and after the addition of the gel into tubes was recorded, and then, calculating the exact weight of the slice was. After this, DNA extraction was performed using the NZYTech Gelpure kit according to the manufacturer's instructions.

2.11 Restriction Endonuclease Digestions

For digestion of plasmid DNA, 50 µL of pET28b vector (50 µg), 6 µL of 10X restriction enzyme buffer Tango (ThermoFisher), 1,5 µL of NheI (ThermoFisher) and 1,5 µL XhoI (ThermoFisher) were added to a sterile 1.5 mL microcentrifuge tube. The tube was shacked and incubated for 2 hours at 37 °C.

For digestion of PCR products, 25 µL of PCR product (50 µg), 3 µL of 10X restriction enzyme buffer Tango (ThermoFisher), 1 µL of NheI (ThermoFisher) and 1µL XhoI (ThermoFisher) were added to a sterile 1.5 mL microcentrifuge tube. The tube was shacked and incubated for 2 hours at 37 °C.

Following this, the digestion products were analysed by agarose gel electrophoresis (section 2.9) to confirm complete digestion: 5 µL of the digestion was added to 1 µL 6X loading buffer (NEB). Following complete digestion, the total amount of digested product was analysed by agarose gel electrophoresis in 1% agarose gel (section 2.9). Finally, the plasmid was purified using agarose gel clean-up (see section 2.10).

2.12 Enzymatic reaction clean-up

After the PCR product was eluted in 50 µL elution buffer, the NZYtech Gelpure kit was used, following the manufacturer's protocol. The DNA was eluted in 50 µL of NZYtech elution buffer.

2.13 DNA Ligation and Transformation in *E. coli* TOP10

DNA ligation reactions were performed in 1.5 mL microcentrifuge tubes. The ligation components' concentration was calculated according to the next formula:

$$\text{Insert DNA (ng)} = \frac{\text{Insert Ratio X Insert size (bp) X Vector mass (ng)}}{\text{Vector size (bp)}}$$

5 µL vector using, 4 µL T4 ligation buffer (NEB) and 1 µL T4 Ligase (NEB) were always used, while the amount insert was variable but always keeping an insert to vector ratio between 1:3 to 1:6 was employed (see equation above). Ligations were incubated for 2 hours at 37 °C and then 7 µL of each was added to a 150 µL aliquot *E. coli* TOP10 competent cells and flicked once.

Transformations were left on ice for 20 minutes, and then heat shocked at 42 °C for 2 minutes, being consequently returned to the ice for a minimum of another 2 minutes. Subsequently, 150 µL LB was added to each transformation, and the cells were subject to incubation at 37°C. Finally, 200 µL was spread on a 2% LB agar plate containing 50 µg/mL kanamycin.

2.14 Mini-Prep Plasmid extraction

Following ligation and transformation (see previous section 2.13), one individual colony of *E. coli* TOP10 containing the target plasmid was inoculated in 5 mL sterile LB broth in a 30 mL glass universal put in incubation for 16-18 hours at 37 °C in a shaking incubator (New Brunswick Scientific) at 200 rpm. The day after, the plasmid was isolated following the manufacturers' instructions of the NZYTech kit. The DNA was eluted in 50 µL of elution buffer into a sterile 1.5 mL microcentrifuge tube and stored at -20°C.

2.15 Sequence Verification

To confirm the adequate inclusion of the insert in the vector, between 3 and 5 colonies were picked from the ligation-transformation agar plate and the plasmid was isolated following the manufacturers' instructions of the NZYTech kit (see previous sections 2.13 and 2.14). Following this, 10 µL of the purified construct was allocated for enzymatic restriction endonuclease digestion (see section 2.11) and then analysed by DNA electrophoresis (see section 2.9) with adequate ladder size to check the correct insertion. The constructs obtained from the extraction and purification kit were confirmed by Sanger sequencing performed by Eurofins Genomics®.

2.16 Recombinant Protein Production

2.16.1 Transformation in *E. coli* BL21(DE3)

2 µL of plasmid was added to a 150 µL aliquot of chemically competent cells, BL21(DE3) and left on ice for 20 minutes. The cells were then heat-shocked at 42°C for 2 minutes and then placed back on ice for 2 minutes. Then, 150 µL of sterile LB media was added and the cells were incubated at 37°C for one hour. 200 µL of the cells were then spread on 1.5 % (w/v) LB agar plates containing 50 µg/mL kanamycin placed in a static incubator at 37°C for 16 hours.

2.16.2 Large Protein Expression

LB agar plates with *E. coli* BL21(DE3) colonies containing the plasmid of choice were acquired (see section 2.16.1). A colony from each plate was transferred into individual 30 mL glass universals containing 10 mL LB and 10 µL kanamycin (50 mg / mL). The universals were placed into an orbital incubator at 180 rpm at 37°C for 16 hours. The

10 mL overnight cultures were then inoculated into 1 L LB media with 1 mL kanamycin (50 mg/ml) contained in a 2 L Erlenmeyer flask. Subsequently, the flask(s) were transferred to an orbital incubator and incubated at 37 °C at 180 rpm until they reached an OD_{600} of 0.6-0.8. The absorbance was measured using 1 mL of aseptically removed culture transferred into a 1 mL cuvette, read at 600 nm in a WPA Colourwave CO700 Medical Colorimeter, using LB as blank. Once the culture reached an optimal OD, 1 mL of 1M isopropyl β-D-1-thiogalactopyranoside (IPTG) was added to a final concentration of 200 μM. Isopropyl ß-D-1-thiogalactopyranoside (IPTG) was prepared dissolving 1000 times the working concentration (1 M) in sterile 18.2 MΩ/cm H_2O and then storing it at -20 ºC. The final concentration employed was 200 μM to induce protein expression. In the end, the flask was transferred to a pre-conditionate shaker (INFORS HT) at incubated at 180 rpm at 16 °C for 16 hours.

2.16.3 Protein Harvesting

Cell cultures from the large protein expression were transferred into 1L tubes (ThermoScientific). The cultures were then centrifuged at 5000 rpm at 4°C in a Sorvall centrifuge (ThermoScientific). The pellet was resuspended in 10 mL Taloon Buffer and then the cell suspension was transferred to a 50 mL Falcon tube on ice, ready for sonication.

2.16.4 Sonication and CFE Preparation from Harvested Cells

Each sample placed in ice water was sonicated for a total of 2 minutes in 15 seconds intervals at 12 microns using a MSE Soniprep 150 Plus. After this, the sonicated samples were centrifugated at 15000 g for 30 min in a Sorvall (ThermoScientific).

Evolution RC centrifuge in a SLA 3000 rotor.

2.16.5 Immobilized metal affinity chromatography (IMAC) Purifications

10 mL of homogenized chelating Sepharose resin (BioRad), stored in 20% ethanol (v/v) was poured into clean and empty 10 mL IMAC columns. The bottom nipple was removed, allowing the resin to pack. After packaging, the columns were washed using 20 mL degassed 18.2 MΩ/cm H$_2$O. The column was then equilibrated by the addition of 20 mL of 1x Talon buffer. All columns were stored in 20% ethanol when not in use.

All IMAC purifications were performed on 10 mL IMAC columns. After column preparation, the total CFE containing the enzyme of interest (see section 2.16.4) was loaded to an IMAC column previously equilibrated with 20 mL Talon buffer, with all flow through collected in 30 mL plastic universals. Protein elution was completed using 5 mL Talon buffer, 5 mL 50 mM Imidazole buffer and 5mL 100 mM Imidazole buffer (See Table 7 below), collecting the 5 mL aliquots of flow through in 30 mL plastic universals. Protein fractions were stored in ice at 4 °C.

Media	Concentration
Talon buffer (pH 8) per litre	24.23 g Tris (Sigma) and 8.77 g NaCl (Sigma). A final volume of 100 mL was achieved using 18.2 MΩ/cm H$_2$O.
10 mM Imidazole Buffer (pH 7.5) per litre	0.68 g Imidazole (Sigma), 2.4 g HEPES (Sigma) and 24.2 g NaCl (Sigma). The final volume was reached to 100 mL with 18.2 MΩ/cm H$_2$O.
100 mM Imidazole Buffer (pH 7.5) per litre	6.8 g Imidazole (Sigma), 2.4 g HEPES

	(Sigma) and 24.2 g NaCl (Sigma). A final volume of 100 mL was achieved using 18.2 MΩ/cm H_2O.
Imidazole Wash Buffer (pH 6.75) per litre	6.8 g Imidazole (Sigma), 2.4 g HEPES (Sigma) and 24.2 g NaCl (Sigma). A final volume of 100 mL was achieved using 18.2 MΩ/cm H_2O.

Table 7. Buffers employed in IMAC purification.

2.16.6 Size exclusion Chromatography

All purified enzyme fractions were concentrated using centrifugal filters with 5 kDa cut off (Amicon Ultra 4) and then subjected to size exclusion chromatography using an AKTA explorer system (Holmes Analytical) with a HiLoad 16/60 Sephacryl S-200 HR column and 2 mL loop. The column was equilibrated with 1.5 times column volumes with Talon buffer and the loop was rinsed with 2.5 mL of 20 % ethanol before injecting and then the 2 mL of sample. The protein was eluted using Talon buffer, collecting 1 mL the fractions in 10 mL tubes which were then analysed by SDS electrophoresis to check the total purity of the protein.

2.16.7 SDS-PAGE Electrophoresis

The purified proteins (see section 2.16.5 and section 2.16.6) were separated using recently prepared SDS-PAGE. Gels within adequate cores were placed into a Biorad mini-PROTEAN® tetra system SDS-PAGE gel tank. The tank was filled with 1X SDS running buffer to the required volume. The comb from each gel was then carefully extracted and all wells were flushed with 1X SDS running. The SDS-PAGE gel samples were prepared and loaded into the wells using and the tank was then connected to a BioRad Powerpack 300 and run at 200 V for 45 min. Following completion, the gels were removed from the cores and the glass plates separated. The gels were then placed into a clean container and submerged in SDS-PAGE Coomassie blue stain solution (see Table 8 below) for 20 minutes. After staining, the gels were transferred to destain solution (see Table 8 below) and placed for 20 minutes.

Media	Concentration
10X Stock SDS-PAGE Running Buffer	144 g Glycine (Sigma), 30.3 g Tris-HCl (Melford) and 10 g SDS (Thermo). The final volume of 1L was achieved with 18.2 MΩ/cm H_2O.
Resolving Buffer	325 mL 2 M Tris-HCl pH 8.8, 20 mL 10% (w/v) SDS and 18.2 MΩ/cm H_2O.
Stacking Buffer	250 mL 1 M Tris-HCl pH 6.8, 20 mL 10% (w/v) SDS and 230 mL H_2O.
10X SDS-PAGE Loading Buffer	0.25 mL 14.4 mM β-mercaptoethanol (Sigma), 0.3 mL 60 mM Tris-HCl (pH 6.8), 1.0 mL 10% SDS (w/v), 2.5 mL 50% glycerol

	(v/v) and 1.8 mg Bromophenol blue (Sigma).
APS 10% (w/v)	It contained 1g APS (Melford) with 10 mL 18.2 MΩ/cm H_2O.
Destain Solution (per litre)	100 mL glacial acetic acid (Thermo) and 450 mL Methanol (Thermo).
SDS-PAGE Coomassie Blue Stain Solution per litre	0.24 g Coomassie brilliant blue R-250 (Sigma) and 80 mL Destain Solution.

Table 8. Buffers and solutions used for SDS-PAGE electrophoresis.

2.17 Enzymatic reactions

All enzyme assays were carried out in PBS pH 7.0, containing and performed in triplicate. Assays were carried out at 37 °C employing 1 μM enzyme previously purified using AKTA Explorer (see section 2.16.6) in the presence of 1 mg/mL β-glucan. Samples and products were assessed by TLC (see section 2.19) and high-pressure anion exchange chromatography (see section 2.20).

In the case of GH30_3 and GH157, polysaccharide hydrolysis was quantified using a DNSA (dinitrosalicylic acid) reducing-sugar assay (Rogowski et al., 2015). Assays were conducted in a final volume of 1 mL at the optimum pH and 37°C for 10 min. Reactions were terminated by the addition of an equal volume (1 mL) of DNSA reagent. The colour was developed by heating to 80°C for 20 min before reading absorbance at 540 nm. Glucose (25 to 150 μM) was used to generate a standard curve for quantitation. To determine Michaelis-Menten parameters, different concentrations of polysaccharide solutions were used over the range of 0.01 to 3 mg/mL with the

appropriate concentration of enzyme for 15 min and the numbers of reducing ends released were quantified as described above. The values were plotted using linear regression giving kcat/K_M as the slope of the line.

In the case of GH3s and GH2, different concentrations of polysaccharide solutions were used over the range of 0.025 to 3 mg/mL with the appropriate concentration of enzyme in a Helyos spectrophotometer (Spectronic Unicam) at a wavelength of 340 nm. The kit from Megazyme (Dublin, Ireland) for glucose release quantification.

2.18 TFA assays

To analyse the purity of β-glucan, 66 µL samples of 1 mg/mL β-glucan from mycoprotein were combined with 33 µL 1 M trifluoroacetic acid (Fisher) for two hours at 90 °C in thermo-block. The results were analyzed using High Performance Liquid Chromatography (see section 2.20).

2.19 Thin layer Chromatography (TLC)

In TLC assays of enzyme activity, 4 µL drops of each sample were spotted onto TLC Silica gel aluminium sheets (Merck) and resolved in butanol/acetic acid/water at a concentration of 2:1:1 and carbohydrate products were detected by spraying with 0.5% orcinol in 10% sulfuric acid and heating to 100°C for 10 min. The TLC buffer was prepared using 50 mL Butanol (Acros), 25 mL Glacial Acetic Acid (Fisher) and 25 mL 18.2 MΩ/cm H_2O. The orcinol stain was prepared with 5 g Orcinol (VWR), 375 mL Ethanol (Fisher), 16 mL H_2SO_4 (Fisher) and 107 mL 18.2 MΩ/cm H_2O.

2.20 High Performance Liquid Chromatography (HPLC)

The HPLC analysis was undertaken on a Dionex ICS-5000$^+$ DC (Thermo Fisher) using a Dionex CarboPac^{TM} PA200 BioLC^{TM}. A 100 µL loop was used to inject any sample per run. All analyses were performed in a 50-well circle sampler at 20°C with a permanent flow rate of 1 mL/min. Sugars (mono and short oligosaccharides) were detected using the carbohydrate standard quad waveform for electrochemical detection at a gold working electrode with an Ag/AgCl pH reference electrode (Thermo Scientific).

Buffer	Composition
Buffer A	1L 100 mM NaOH
Buffer B	1L 100 mM NaOH 1M sodium acetate (Melford)
Buffer C	1L 18.2 MΩ/cm H$_2$O
Buffer D	500 mM NaOH

Table 9. Composition of HPLC buffers.

The LC-MS method had a total run time of 80 minutes, with the first 10 minutes gradient starting with 80% Buffer A and 20% buffer C to 100% Buffer A. Then, a 40 min gradient from 0% buffer B to 40% Buffer B. Following this gradient, 100% buffer B continued to run for 10 minutes, and, in the next step, Buffer B was switched back to Buffer D during the next 10 minutes. Finally, a mix of 20% Buffer A and 80% Buffer C was used during the last 10 minutes.

2.21 Gas Chromatography and Mass Spectrometry

Growth medium supernatants from stationary phase were used to assess SCFAs production of *Bacteroides* sp., *Bifidobacterium* sp. and *Lactiplantibacillus plantarum* WCFS1. Co-cultures were sterilized (0.45 μM filter, Costart Spin-X column) and injected into an UltiMate® BioRS Thermo HPLC system (Thermo Fisher Scientific) provided with a refractive index detector system. This system was used to determine the production of acetate, lactate and butyrate as a result of carbohydrate fermentation. SCFAs concentrations were calculated based on known standards. Non-fermented medium containing glucose served as control. An Accucore™ C18 HPLC column was used and maintained at 65°C. Elution was performed for 25 min using 10 mM H_2SO_4 solution at a constant flow rate of 0.6 mL/min.

2.22 LC/MS of the supernatant containing the released oligosaccharides

The samples containing the oligosaccharides generated from the supernatant from *Bacteroides cellulosyliticus* WH2 (*Ba. cellulosyliticus* WH2) and *Bacteroides thetaiotaomicron* VPI 5482 (*Ba. thetaiotaomicron* VPI 5482) on β-glucan were primarily purified using a P2 gel column extra fine (Bio-Rad, <45 μm wet bead size, 100–1,800 MW fractionation range, 1 mL/min flow rate). This allowed the reduction of the number of peaks in the samples. Then, they were diluted 1:10 (v/v) with Buffer B (85% acetonitrile/15% 50 mM ammonium formate in water, pH 4.7) and 0.5 mL was analysed by liquid chromatography-mass spectrometry analysis via elution from a ZIC-HILIC (SeQuant, 3.5 μm, 200 Å, 150 × 0.3 mm, Merck) capillary column. The column was connected to a NanoAcquity HPLC system (Waters) and heated to 35 °C with an elution gradient as follows: 100% Buffer B for 5 min, followed by a gradient to 25% Buffer B/75% Buffer A (50 mM ammonium formate in water, pH 4.7) over 40

min. The flow rate was 5 µL min^{-1} and 10 column volumes of Buffer B equilibration were performed between injections. MS data were collected using a Bruker Impact II Qtof mass spectrometer operated in positive ion mode, 50–2000 m, with capillary voltage and temperature settings of 2,800 V and 200 °C respectively, together with a drying gas flow and nebulizer pressure of 6 L min^{-1} and 0.4 bar. The MS data were analysed using Compass Data Analysis software (Bruker).

2.23 Proteomics

The trypsin digestion was performed after running SDS-PAGE polyacrylamide gels. The stained protein bands were excised from the gel and placed in 1.5 mL microcentrifuge tubes (Eppendorf). The stained gel pieces with Coomasie were washed three times with 100 µL 100 mM ammonium bicarbonate followed by 60 µL 100 % acetonitrile during 15 minutes with agitation at room temperature. The gel pieces were then shrunk for 10 min by adding 200 µL 100 % Cerium (IV) ammonium nitrate. The gel pieces were rehydrated in 100 µL 20 mM Dithiothreitol for 30 min at 56 °C, followed by re-shrinking of the gel pieces using 100 % acetonitrile.

After this, the gel pieces were rehydrated by adding 100 µL 55 mM iodoacetamide in 100 mM ammonium bicarbonate and alkylated in the dark for 20 min at room temperature. The gel pieces were washed twice with 100 µL ammonium bicarbonate in room temperature with agitation. They were dehydrated with 100 µL acetonitrile for 15 min at room temperature and agitation and the acetonitrile was removed and gel pieces were dried in a vacuum centrifuge for 5 minutes. Following this, the gel pieces were dehydrated with 30 µL of 20 µg/mL trypsin solution (100 µg trypsin stock was diluted with 1 mL 50 mM acetic acid,) and placed on ice for 20 min to allow to absorb

solution. Then was diluted 5 times in 50 mM NH_4HCO_3 to give 20 µg/ml. After 20 min, 50 µL 50 mM NH_4HCO_3 were added and incubated 16-24 h at 37 °C.

After overnight incubation, 50 µL containing 50 % (v/v) acetonitrile/ 5 % (v/v) formic acid was added to stop the enzymatic reaction, incubating at room temperature with agitation. After this, the supernatant was pipetted of and transferred to another new Eppendorf tubes and the extraction was repeated by adding 50 µL 83 % (v/v) acetonitrile/0.2 % (v/v) formic acid. The supernatant was pipetted off and added to the Eppendorf tube and it was frozen at -80°C, then lyophilised, and finally stored at -80. In the last step, the lyophilised and frozen samples were resuspended in 20 µL 5 % (v/v) Cerium (IV) ammonium nitrate / 0.1 % (v/v) formic acid and analysed by LC-MS for proteomic analysis.

2.24 Cross-feeding experiments

2.24.1 Bacterial growth using supernatants as carbon source

Bacteroides sp. were grown using 50 mL minimal media supplemented with 1 mg/mL of β-glucan in 250 mL conical flasks, over a shaker (IKA KS 130 Basic) set at 80 rpm. The cultures started at 0.05 OD for each strain. After 24 h hours, the cultures were centrifuged in a SL 16R centrifuge (Thermo Fisher) at 5000 g for 10 min. Following this, the supernatant fractions were filtrated using 0.2 µm filters (Sarstedt).

Then, a volume of 100 µL of supernatant was mixed with 100 µL minimal media and 25 µL of *Bifidobacterium* sp. or *Lactiplantibacillus* sp. (0.05 initial OD) in a 96 wells plate (Greiner Bio-One) of 300 µL volume per well. The OD at 600 nm was measured every 15 minutes using a TECAN SPARK 10 M plate reader.

2.24.2 Bacterial growth using co-culture experiments

The co-cultures experiments were undertaken inside of an anaerobic cabinet (CoyLab) connected to an electronic gas infuser (CoyLab) which kept the inside atmosphere in permanent oxygen absence. For this purpose, the gas infuser injected an anaerobic growth mixture of 85% N_2, 10% CO_2 and 5% H_2. The temperature was set at 37°C with an air heater (CoyLab) placed inside the cabinet.

Bacteria strains were grown using 50 mL minimal media supplemented with 1 mg/mL of β-glucan in 250 mL conical flasks, over a shaker (IKA KS 130 Basic) set at 80 rpm. The cultures started at 0.05 OD for each strain, and then 1 mL was taken at 0h, 1h, 3h, 5h, 10h, 15h, 24h, 30h and 48h. Aliquots of 50 µL were plated in selective media for each bacteria: BHI supplemented with 20 mg/mL ampicillin to count *Bacteroides* sp. colonies, MRS supplemented with 10 mg/mL mupirocin in the case of *Bifidobacterium* sp. colonies and MRS supplemented with 10 mg/mL vancomycin in the case of *Lactiplantibacillus plantarum* WCFS1 (see section 2.2). The rest of the volume (900 µL) was destined for qPCR (see section 2.8).

2.25 Bioinformatics Methods

2.25.1 Expasy Protparam

The 6-frame translation of DNA sequences to their amino acid sequences was completed using the online tool ExPASy website for DNA Translation (https://www.expasy.org/). The DNA sequences were written in the query box and consequently, the 'TRANSLATE SEQUENCE' button was clicked. The output shows the open reading frames in all 6 frames. Only the reading frame which showed no stop sequence was chosen. ProtParam is embedded in the ExPASY online tool. ProtParam calculates the physical and chemical protein parameters such as molecular

weight, amino acid composition, theoretical pI, extinction coefficient, etc. The amino acid sequence of a given protein was pasted in the given field and the molecular weight and extinction coefficient parameters were calculated.

2.25.2 Primer Design

Different online bioinformatic tools were used for the design of all primers. Firstly, the locus tag for any enzyme was obtained in CAZy Database (http://www.cazy.org/). The locus was then typed on the browser of the Protein Database supported by NCBI (https://www.ncbi.nlm.nih.gov/protein/) to choose the DNA sequences corresponding to the bacterial enzymes which were studied in this thesis. Consequently, the 6-frame translation of DNA sequences to their amino acid sequences was completed using the online tool ExPASy website for DNA Translation (https://web.expasy.org/translate/).

The DNA sequences were written in the query box and consequently, the 'TRANSLATE SEQUENCE' button was clicked. The output shows the open reading frames in all 6 frames. Only the reading frame which showed no stop sequence was chosen. In the next step, the amino acid sequence from Expasy was typed on LipoP-1.0 (https://services.healthtech.dtu.dk/service.php?LipoP-1.0), an online server that produces predictions for the signal lipoproteins to avoid the inclusion of the signal peptide in the final sequence. After, the online tool NEBcutter V2.0 (http://nc2.neb.com/NEBcutter2/) allowed to find non-overlapping open reading frames using the *E. coli* genetic code and the sites for all Type II and Type III restriction enzymes that cut the DNA sequence just once. The final primer sequences were constructed using the OligoCalc website tool (http://biotools.nubic.northwestern.edu/OligoCalc.html).

For all primers, the specific restriction site, chosen following the desired cloning strategy, was added and then followed by a 6 bp non-palindromic sequence to support polymerase binding (GCGGCG). Afterward, the forward primers were designed to be identical to the first 18-21 bases at the 5' end of the 'sense' strand of the target gene. On the other hand, the reverse primers were designed to complement the last 18-21 of the 'sense' strand at the 3' end using the option 'swap strands'. All primers showed more than 40% of GC content and a melting temperature of around 70 °C.

2.25.3 Structural prediction with AlphaFold

3-D structure of proteins from proteomics data and kinetics assays were modelled using AlphaFold, an open access database that provides protein structures and it also can provide predictions for proteins whose structure has not been resolved yet.

2.25.4 Protein visualization

The molecular graphics system Pymol was used for the three-dimensional visualization and comparison of protein structures (The PyMOL Molecular Graphics System, Version 2.0 Schrödinger, LLC, https://pymol.org/2).

3 Results

3.1 β-glucan extraction and culture of polysaccharide degraders

3.1.1 Extracting and purifying β-glucan and chitin from mycoprotein

Since mycoprotein is a mix of different components (Finnigan et al., 2019), a continuous extraction and purification of β-glucan to isolate it from crude mycoprotein is essential (Figure 22). Once the extraction protocol was finished (Figure 23, Bzducha-Wróbel et al., 2012) a 1% solution of the last extracted fraction was mixed with trifluoroacetic acid (TFA). TFA can break the β-bonds between monomers inside the polymer chain, releasing glucose as a result. As the only expected substance is glucose, this protocol serves as a checking process for the purity of the extract, since it allows the detection of any contaminant.

Figure 22. Crude mycoprotein (left) and β-glucan fraction (right) obtained in the alkaline extraction protocol.
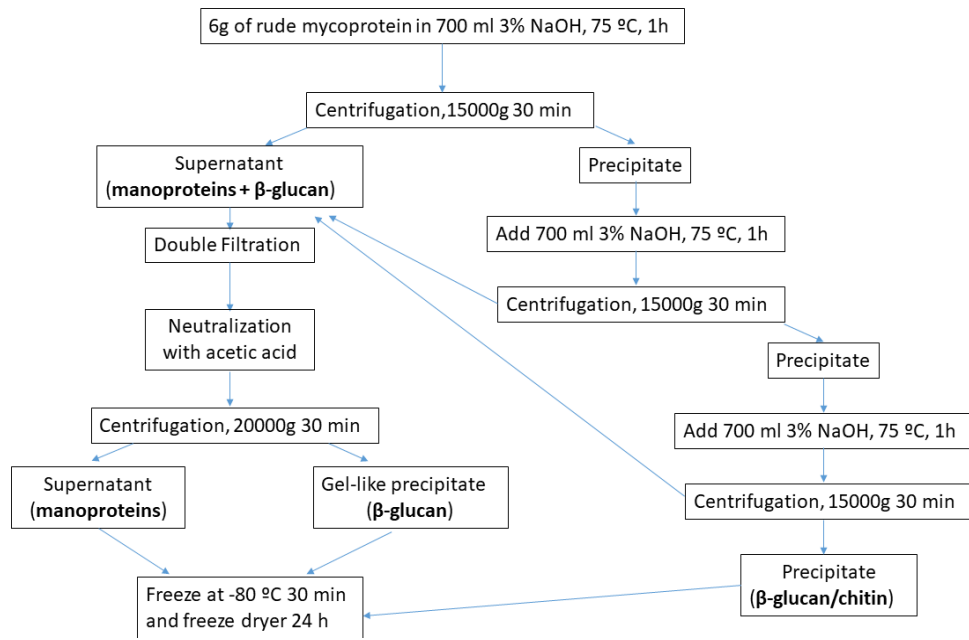
Figure 23. Extraction protocol for *Fusarium* β-glucan obtained from mycoprotein (Bzducha-Wróbel et al., 2012).

The HPLC (Figure 24) showed that only glucose was found in the extract, which means that other components, such as chitin or mannoproteins, were absent in the sample. This fact highlights the effectiveness of this method, and, for this reason, β-glucan was used as a potential carbon source for the studied bacteria in the next set of experiments.
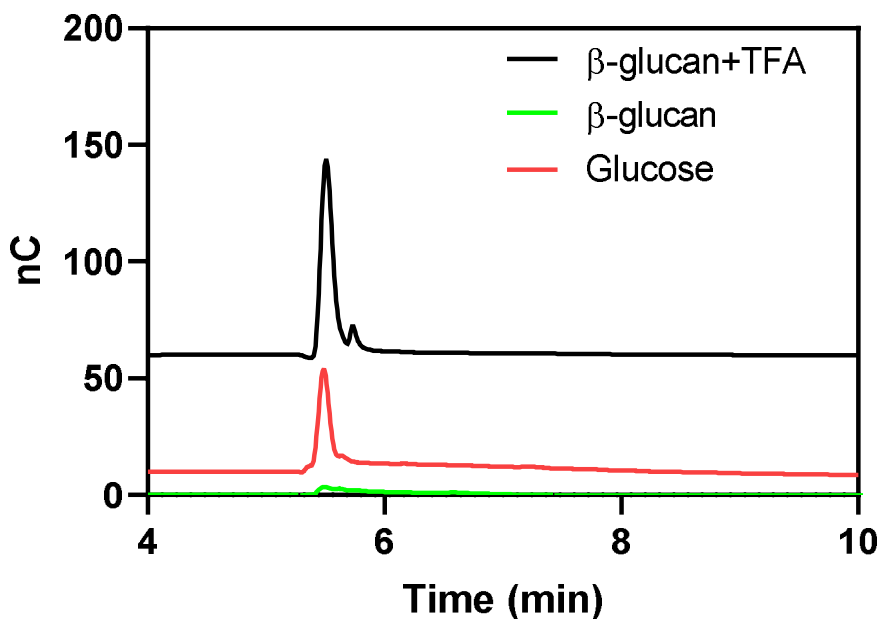
Figure 24. HPLC chromatogram for β-glucan analysis with TFA.

3.1.2 Determining the capacity of *Bacteroides* sp. and *Bifidobacterium* sp. for degrading *Fusarium* β-glucan

Firstly, three different *Bacteroides* species were tested (*Ba. cellulosyliticus* WH2, *Ba. thetaiotaomicron* VPI 5482 and *Ba. ovatus* ATCC 8483) using both the β-glucan and β-glucan/chitin fractions obtained previously in the alkaline extraction protocol (see Methods section 2.6). The election of these species instead of others was made taking into account two main reasons: first of all, it was impossible to study all the described *Bacteroides* sp. at present; and, secondly, these three species are reported to be users of polysaccharides from different sources, having a high number of described genes involved in the digestion of polysaccharides (El Kaoutari et al., 2013).

The results showed that all the species could use both fractions as carbon sources with a constant growth for 48 hours (Figure 25). This is due to the presence of Polysaccharide Utilization Loci (PULs) that are present in many *Bacteroides* species (Grondin et al., 2017). Since the bacterial growth was lower for fractions of β-glucan containing chitin, β-glucan without chitin was chosen as carbon source for the next experiments.
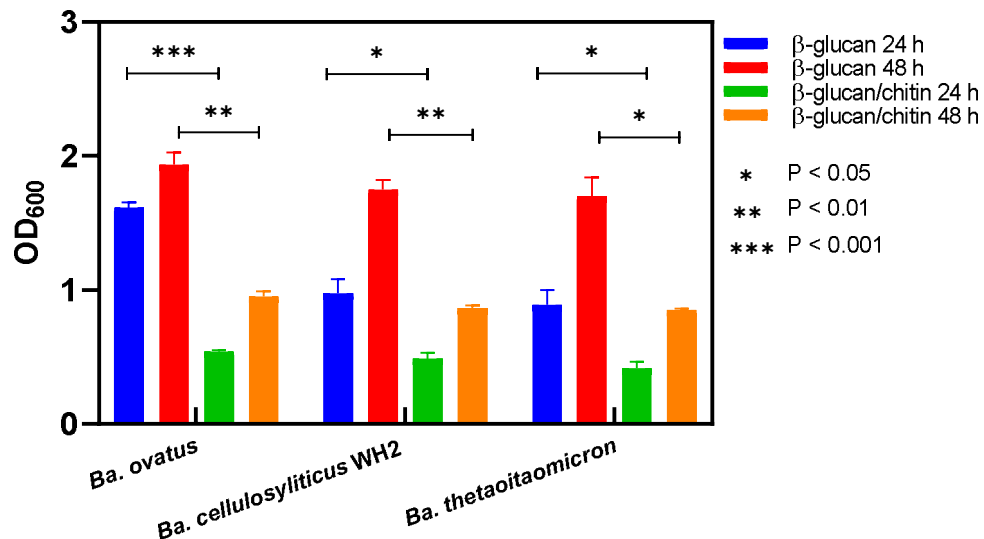
Figure 25. Growth of three *Bacteroides* species in different mycoprotein fractions.

After this experiment, the same method was repeated using six *Bifidobacterium* species (*Bi. bifidum* PRL2010*, Bi. breve* UCC2003*, Bi. breve* JCM7017*, Bi. animalis* subsp. *animalis* DSM 20104*, Bi. longum* subsp. *longum* NCIMB 8809 and *Bi. longum* subsp. *infantis* ATCC 15697). In this case, none of the six species of bacteria could use β-glucan as carbon source (Figure 26).
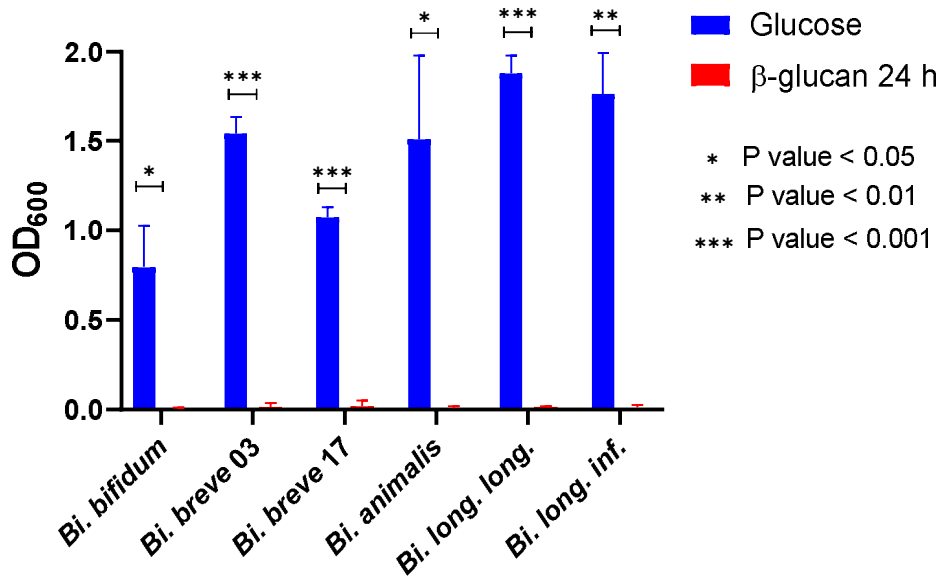
Figure 26. Growth of six *Bifidobacterium* species with different mycoprotein fractions.

The results observed in the graph above reflect the inability of *Bifidobacterium* to access intact *Fusarium* β-glucan, using glucose as positive control. This fact agrees with the inability of this bacteria genus for the utilization of intact polysaccharides, although *Bifidobacterium* sp. have been described as good oligosaccharide degraders (James et al., 2018).

Once described the differences in the primary degradation of intact *Fusarium* β-glucan by some *Bacteroides* sp. and *Bifidobacterium* sp., a similar experiment was developed with: *Ba. cellulosyliticus* WH2, *Ba. cellulosyliticus* DSM 14838, *Ba. thetaiotaomicron* VPI 5482, *Ba. ovatus* ATCC 8483 and *Ba. vulgatus* ATCC 8482). The utilization of *Fusarium* β-glucan was compared with yeast β-glucan from *Saccharomyces cerevisiae* and a positive control using glucose. The results are shown in the Figure 27 below
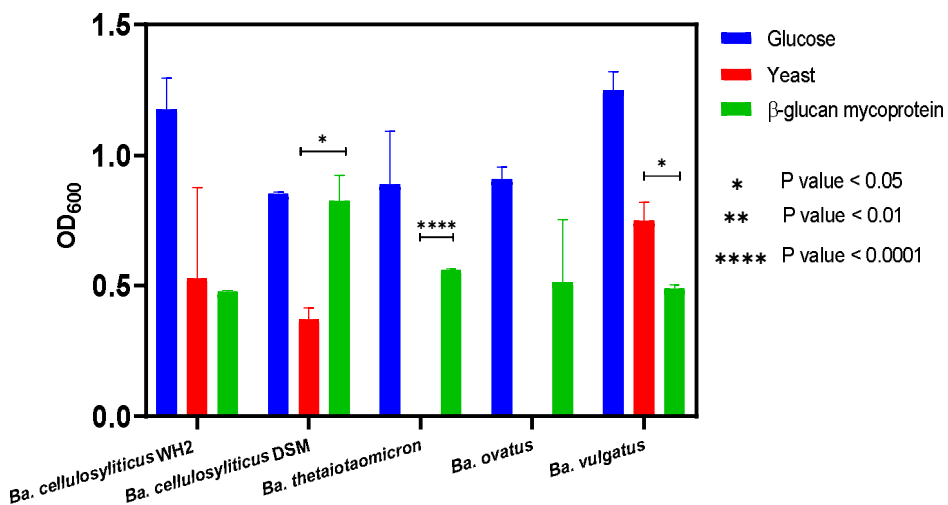
Figure 27. Growth of five *Bacteroides* species in *Fusarium* β-glucan compared with glucose and the yeast *Saccharomyces cerevisiae* β-glucan.

In general, *Bacteroides* sp. could persist in all the different substrates. On one hand, *Ba. vulgatus* grew better in yeast β-glucan than in *Fusarium* β-glucan. On the other hand, *Ba. cellulosyliticus* DSM and *Ba. thetaiotaomicron,* showed preference for *Fusarium* β-glucan. They all grew with the positive control better than the polysaccharides, which proves that bacteria spend more time and energy for the expression of the GHs encoded in the PULs rather than using the simple monosaccharide. In addition to this experiment, the previous *Bacteroides* sp. were grown in a plate reader measuring the optical density every 15 min for a total period of 24 hours. The results are shown in the Figure 28 below.
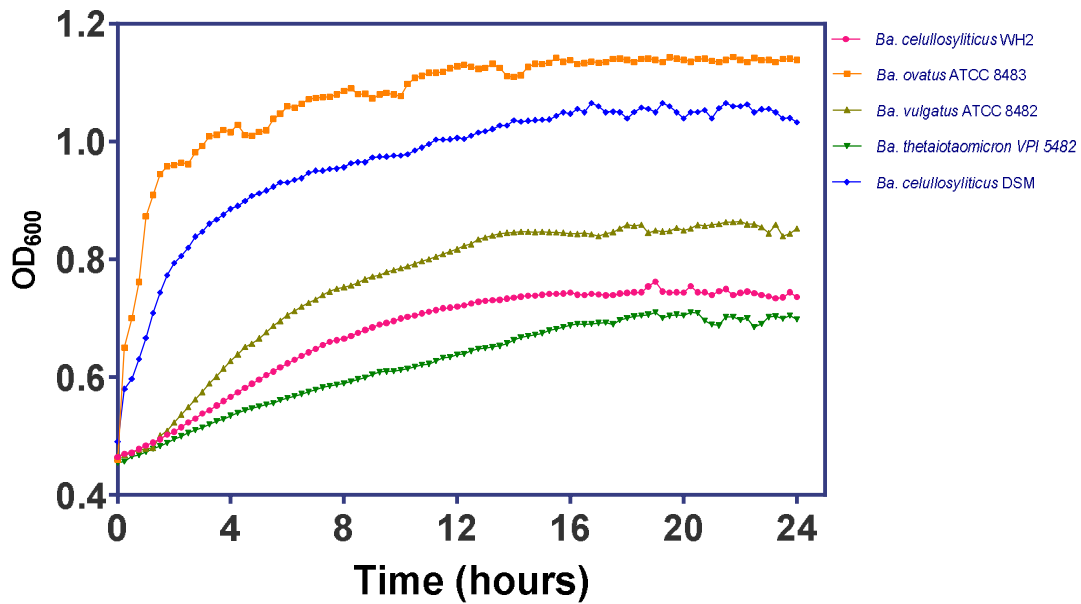
Figure 28. Growth in minimal media with of five *Bacteroides* species with *Fusarium* β-glucan as carbon source.

The growth curves showed that, although all the *Bacteroides* grew, each *Bacteroides* has a different growth rate and curve shape. This fact also underlines that the ability for the degradation of polysaccharides is widely extended within this bacteria genus, since they exhibit different genes encoding glycoside hydrolases belonging to several families. This confers *Bacteroides* genetic diversity and supposes a nutritional advantage among other bacteria populations.

3.1.3 Culturing other bacteria species in minimal media containing *Fusarium* β-glucan

Because of the tremendous complexity and diversity of the Human Gut Microbiota, the degradation of polysaccharides is not a unique quality of just one genus. For this reason, and to expand the range of bacteria in the study, different growth experiments were developed with bacteria species of three different genera: *Roseburia*, *Victivallis* and *Akkermansia*.

As previously described in the introduction, these bacteria have already been reported as polysaccharide users, but few studies have described them in the metabolism of fungal glucans. For this reason, the same protocol, previously applied for *Bacteroides* sp., was developed with these bacteria.

Roseburia intestinalis DSM 14610 and *Roseburia inulinovorans* DSM 16841

Both *Roseburia intestinalis* and *Roseburia inulinivorans* showed a good ability to degrade and grow with *Fusarium* β-glucan (Figure 29). It seems that *Roseburia inulinivorans* presented higher growth values values than *Roseburia intestinalis*, although the growth of both strains was quite similar. Since *Roseburia intestinalis* has an important number of GHs (El Kaoutari et al., 2013), it is reasonable that *Roseburia* sp. use *Fusarium* β-glucan with a similar capacity as in the case of *Bacteroides* sp.

Nevertheless, the election of *Bacteroides* sp. instead of *Roseburia* sp. as the main degrader for this study lies in the fact that *Bacteroides* sp. has been in more reports as better polysaccharides degraders than *Roseburia* sp.
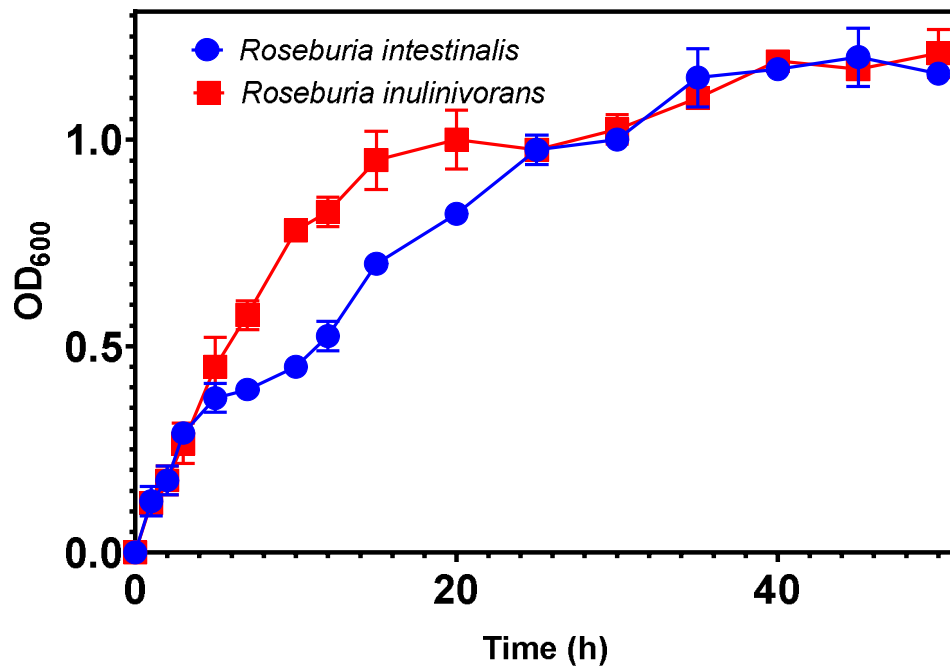
Figure 29. Growth curves of *Roseburia intestinalis* and *Roseburia inulinivorans* with *Fusarium* β-glucan.

Victivallis vadensis ATCC BAA-548

In the case of *Victivallis vadensis* ATCC BAA-548, this bacterium showed a good growth rate, even exceeding the values obtained for the positive control with glucose at the same concentration. The data previously gathered in the bibliography gave an idea of the huge genetic machinery for polysaccharide utilization that this bacterium possesses in its genome (El Kaoutari et al., 2013; Zoetendal et al., 2003). The data shown in the Figure 30 below is the first experimental approach of *Victivallis vadensis* using a fungus polysaccharide as a substrate. It seems clear the fact that *Victivallis vadensis* presents an incredible potential as a degrader of *Fusarium* β-glucan in the gut, although making a thorough analysis of its metabolic routes would be out of the scope of this thesis.
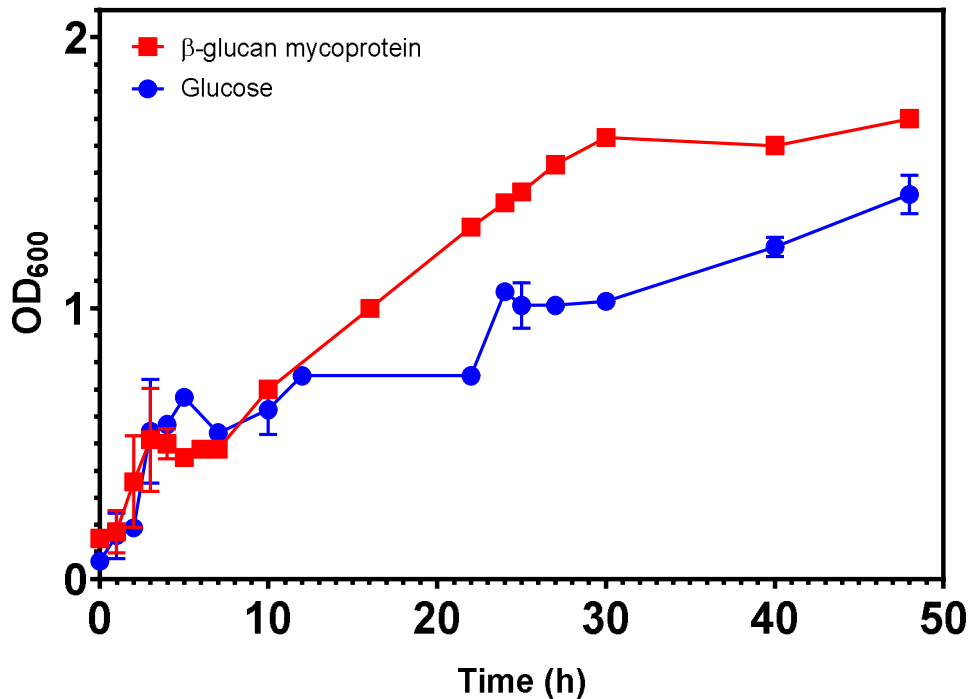
Figure 30. Growth curves of *Victivallis vadensis* with *Fusarium* β-glucan and glucose.

Akkermansia muciniphila DSM 22959

Even though *Akkermania muciniphila* DSM 22959 (*A. muciniphila* DSM 22959) could increase its abundance with *Fusarium* β-glucan as substrate, its capacity was lower than *Bacteroides* sp., *Roseburia* sp. or *Victivallis vadensis.* The growth values for this bacterium remained constant after five hours, while other main degraders usually can grow for 24 hours or longer (for example *Bacteroides* sp. or *Roseburia* sp.). Nevertheless, although bacteria can use different types of polysaccharides, they usually tend to show certain level of specialisation in some substrates, revealing unspecific activities in other substrates with a similar structure to those preferred. In the case of *Akkermansia*, that would be the case of mucin (Derrien et al., 2004).

94

A. muciniphila DSM 22959 does not possess a comparable number of GHs as in the case of *Bacteroides* sp. or *Roseburia* sp., since the total number of the diverse GHs families in *A. muciniphila* DSM 22959 is much lower than in the case of the other two bacteria (El Kaoutari et al., 2013). Even though *A. muciniphila* DSM 22959 grew on the substrate, it reached lower values of optical density compared with *Victivallis* or *Roseburia*. (Figure 31 below).

Although this bacterium shows the ability to degrade different polysaccharides, specially mucin, and it seems to play an important role in immune system regulation, the obtained data underlined the fact that *Fusarium* β-glucan may not be a potential substrate for *A. muciniphila* DSM 22959, which may act potentially as secondary degrader over the digestion products released by other bacteria such as *Bacteroides*. In any case, further experiments are needed to confirm this hypothesis.
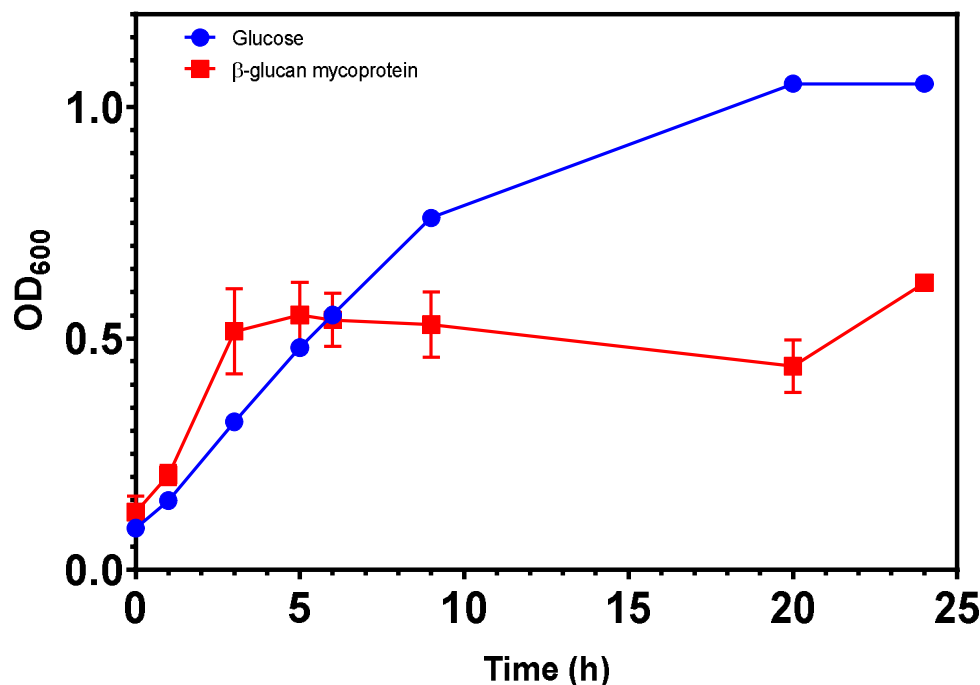
Figure 31. Growth curves of *Akkermansia muciniphila* DSM 22959 with *Fusarium* β-glucan.

3.2 Gene regulation and protein characterization

3.2.1 Determining the overexpression of encoded proteins in up-regulated genes when *Fusarium* β-glucan is the only carbon source

The study of the regulation of different genes from *Ba. cellulosyliticus* WH2 was focused on the differential expression of those genes when *Fusarium* β-glucan was the substrate, using glucose as positive control. After sample preparation and data analysis, it was remarkable that six different genes from two PULs showed a higher expression in *Fusarium* β-glucan than in glucose (Table 10). These PULs were previously predicted in CAZy, and, for that reason, they are numbered as 29 and 51, but the data shown here supposes the assignation of a new catalytic activity. This data reflects the fact that *Bacteroides* sp. specifically use some genes when *Fusarium* β-glucan obtained in the alkaline extraction protocol is the unique carbon source. The presence of the polysaccharide resulted in the activation of specific metabolic machinery involved in the polysaccharide digestion. This response leads to the overexpression of these proteins, which are mainly glycoside hydrolases (Consortium, 2018).

A good example of the activation of specific genes in response to the presence of a polysaccharide substrate is the starch utilization system, which is present in *Bacteroides thetaiotaomicron* VPI 5482 (Foley et al., 2016, Koropatkin et al., 2010).

PUL 29		
Locus Tag	**Family**	**Fold-change relative to minimal media with glucose**
BcellWH2_01926	GH3	54
BcellWH2_01927	GH3	41
BcellWH2_01928	SusD	55
BcellWH2_01929	SusC	57

BcellWH2_01931	GH157	89
BcellWH2_01932	HTCS	41

PUL 51		
Locus Tag	**Family**	**Fold-change relative to minimal media with glucose**
BcellWH2_02537	GH30_3	100
BcellWH2_02538	Unknown	89
BcellWH2_02539	SusC	80
BcellWH2_02540	SusD	65
BcellWH2_02541	GH2/CBM57	40

Table 10. Overexpressed proteins of *Ba. cellulosyliticus* WH2 with *Fusarium* β-glucan as carbon source. The difference in the expression was obtained by comparing the generated proteome data when grown on either of these carbon sources to identify proteins that exhibit increased expression when the strain is grown on *Fusarium* β-glucan.

As it can be appreciated in the Table 10 above, the proteome analysis revealed that all proteins encoded by both PULs, exhibit increased expression when *Ba. celulosyliticus* WH2 was grown on *Fusarium* β-glucan metabolism (when compared to growth on glucose). The genes that encode for the proteins are located consecutively in two different sets, separated one from the other within the genome of *Ba. cellulosyliticus* WH2. Furthermore, is remarkable that the maximum values of expression were obtained in the case of BcellWH2_02537 and BcellWH2_01931, a GH30_3 (the described activity for this family is β-1,6-glucosidase and endo-β-1,6-glucanase in CAZy database) and a GH157 (endo-β-1,3-glucanase/laminarinase in CAZy), respectively. The combination of enzymes that can attack the β-1,3 and the β-1,6 bonds, both present in the structure of the *Fusarium* polysaccharide, allows the degradation of both the backbone and the branching, which results therefore in the completed digestion of the β-glucan.

It is also remarkable the case of BcellWH2_02538, whose catalytic activity remains unknown in the CAZy database, but its expression is comparable with the two previous ones. This protein may act as a small size and soluble protein, maybe acting as a glycosidase that produces oligosaccharides of different sizes, promoting the expression and activity of other ones. Nevertheless, the completed description of its activity needs further investigation. The Figure 32 below reflects the up-regulation of SusC and SusD homolog genes for the two mentioned PULs in *Ba. cellulosyliticus* WH2.
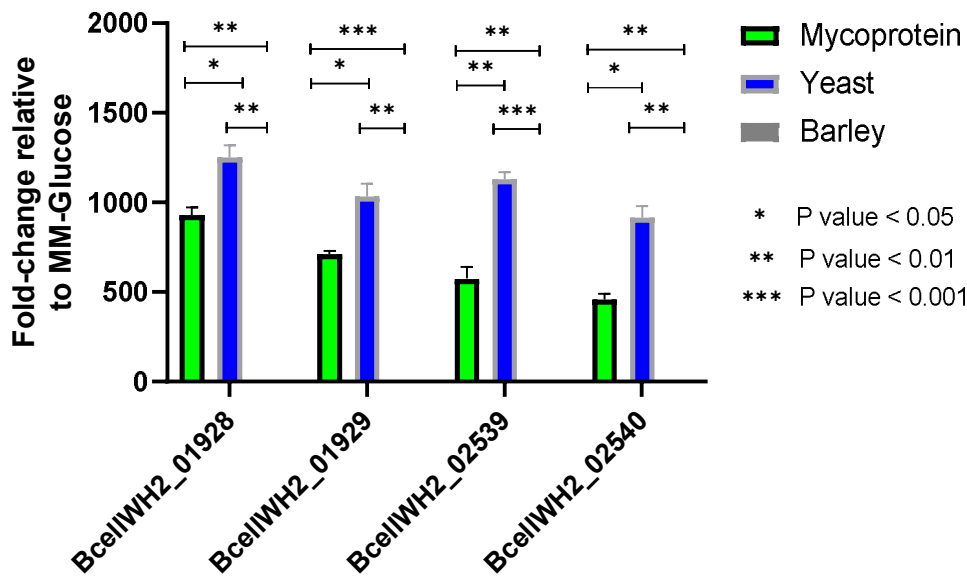
Figure 32. Upregulation of SusC homolog (BcellWH2_01929) and SusD homolog genes (BcellWH2_01928) of PUL29 and SusC homolog (BcellWH2_02539) and SusD homolog genes (BcellWH2_02540) of PUL 51 of *Ba. cellulosyliticus* WH2.

The same procedure was carried out for the case of *Bacteroides vulgatus*. This bacterium is less described in polysaccharide degradation than other *Bacteroides* sp., remaining almost unknown if we focus just on the case of fungus polysaccharides substrates. For this reason, the results obtained underline the importance of this study and the necessity of amplifying the research in the future.

As can be observed in the Table 11 below, the genes showed a higher expression compared with glucose and they appeared ordered in two separate PULs. Therefore, it can be concluded that these PULs, previously predicted as 24 and 33 in CAZy, are specialized in the β-glucan metabolism of *Fusarium venenatum*.

PUL 24		
Locus Tag	**Family**	**Fold-change relative to minimal media with glucose**
BVU_0839	HTCS	23
BVU_0840	Unknown	25
BVU_0841	SusC	80
BVU_0842	SusD	91
BVU_0843	GH30_4	67
BVU_0844	GH30_4	59
PUL 33		
Locus Tag	**Family**	**Fold-change relative to minimal media with glucose**
BVU_1150	HTCS	31
BVU_1151	GH2	48
BVU_1152	SusC	88
BVU_1153	SusD	102

Table 11. Overexpressed proteins of Bacteroides vulgatus ATCC 8482 in *Fusarium* β-glucan as carbon source. The difference in the expression was obtained by comparing the generated proteome data when grown on either of these carbon sources to identify proteins that exhibit increased expression when the strain is grown on *Fusarium* β-glucan.

For the first PUL, two GH30_4 (described as fucosidases in CAZy database) BVU_0843 and BVU_0844 (see Figure 33-35) respectively, showed a high level of

expression. In addition, there was an unknown protein, BVU_0840 (see Figure 33), for which no action mechanism was described. For this protein, the activity might correspond to another GH family, but that would require further studies in order to find a more a detailed explanation.
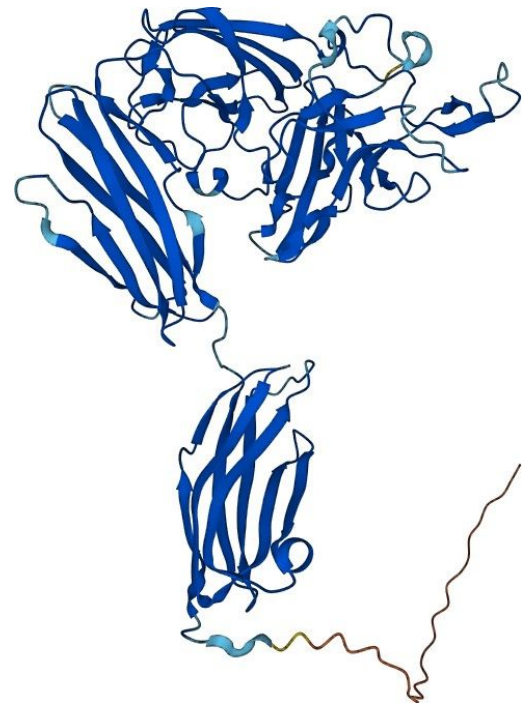
Figure 33. Structure prediction for the unknown protein BVU_0840.
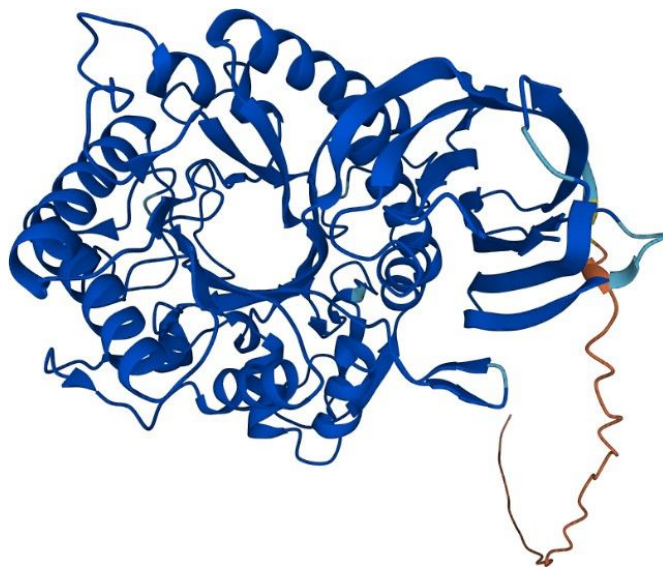
Figure 34. Structure prediction for BVU_0843 belonging to the family GH30 subfamily 4.
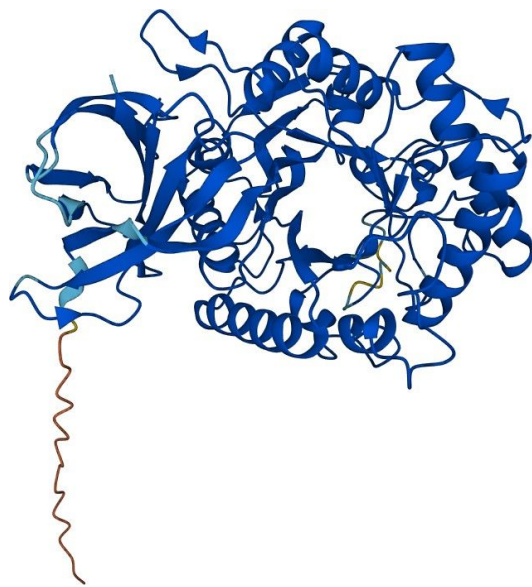
Figure 35. Structure prediction for BVU_0844 belonging to the family GH30 subfamily 4.

For the second PUL, the GH2 BVU_1151 (for this protein different activities are described such as β-glucosidase, β-galactosidase or β-mannosidase in CAZy database), was overexpressed, complementing the activities found in the proteins of the previous PUL. The structure is represented in the Figure 36 below.
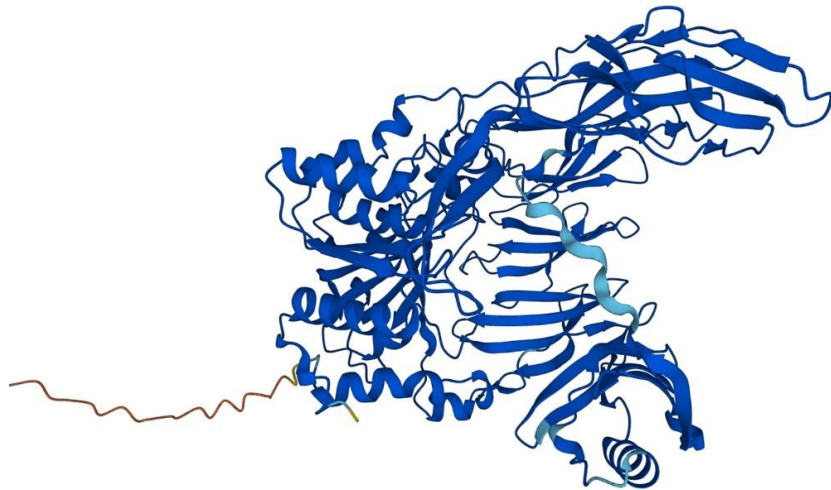
Figure 36. Structure prediction for BVU_1151, belonging to the family GH2.

3.2.2 Cloning and kinetic studies of carbohydrate-active enzymes such as glycoside hydrolases involved in *Fusarium* β-glucan degradation

Proteomics analysis gave important information about of how the utilization of β-glucan by two *Bacteroides* sp. entailed the overexpression of different PULs with several GHs genes involved. As a result, the primers for cloning the GHs allocated in these two PULs from *Ba. cellulosilyticus* WH2 were designed to carry out enzymatic reactions. The kinetics assays constitute an essential tool to study the enzymatic parameters and determine the mechanism of action of the enzymes.

Using the CAZy database as the reference for the sequences (Consortium, 2018), it was also studied the activity of three GH16_3 (β-glucosidase and endo-β-1,3-glucanase): BcellWH2_04354 from the PUL 105 of *Ba. cellulosilyticus* WH2,

BACELL_03483 located in the PUL 80 of *Ba. cellulosilyticus* DSM 14838; and, finally, Bovatus_03149 which is in the PUL 51 of *Ba. ovatus* ATCC 8483. Additionally, the process was extended for BT3312, BT3313 and BT3314 from the PUL 56 of *Ba. thetaiotaomicron* VPI 5482. All these proteins, together with the ones determined in the proteomics assays, formed the quorum subjected to this study.

Once the PCRs with Q5 polymerase were done, the ligations with the vector pET28a were conducted and, after, the consequent transformation using *Escherichia coli* BL21. Subsequently, the purification of the proteins using His-Tag columns and the AKTA Explorer exclusion chromatography system. The kinetic assays were carried out using a glucosidase activity kit (Megazyme) if the enzyme was described as a glucosidase in the CAZy database. The traditional DNSA method was used if the protein was described as endoglucanase.

GH16s from three different *Bacteroides* sp.

The GH16_3 subfamily is widely present in nature, and it is traditionally known as the laminariase subfamily because the more important catalytic functions found here are endo-β(1,3)-glucanase activity and endo-β(1,3)/β(1,4)-glucanase activity (Barbeyron et al., 1998, Vlborg et al., 2019).

Therefore, this subfamily is quite interesting to study algae or fungus β-glucan due to they both contain β(1,3) bonds. Mycoprotein consists basically of a β(1,3)- backbone with β(1,6) branches of variable length. The three enzymes BcellWH2_04354, BACELL_03483, and Bovatus_03149 have been described as GH16_3 enzymes. In the case of Bovatus_03149, it has already been proven its active role in the degradation of barley β-glucan (Martens et al., 2011). For all mentioned before, these three

proteins seemed to be good candidates to study their catalytic activity in the *Fusarium* β-glucan.
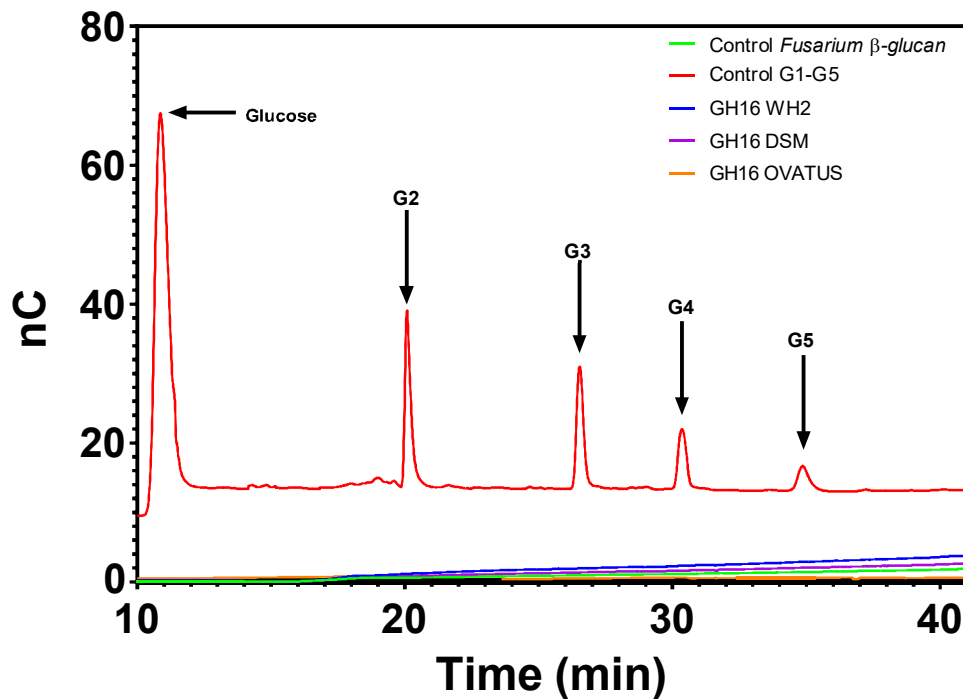
Figure 37. HPLC chromatogram of the enzymatic assays by three different GH16 of *Bacteroides* sp. in *Fusarium* β-glucan.

As it can be appreciated in the Figure 37 above, the chromatogram revealed a lack of activity in these three first candidates because oligosaccharides peaks were absent in all the studied samples while the glucose and the β(1,3)-standards were perfectly detected.

Bacteroides thetaiotaomicron **VPI 5482**

For *Bacteroides thetaiotaomicron* VPI 5482, the PUL 56 was cloned using the information provided by the CAZy database. In this PUL, there were three proteins with potential activity in *Fusarium* β-glucan: BT3312 (endo-β-1,6-glucanase, GH30_3 family, see Figure 38), BT3313 (unknown hypothetical protein, see Figure 39) and

BT3314 (β-glucosidase, GH_3 Family, see Figure 40). Any activity was found for BT3312 (Figure 41). BT3313 and BT3314 (see Figure 42 andFigure 43) were both active in *Fusarium* β-glucan. Nevertheless, it is a remarkable the fact that BT3313 was described as a hypothetical protein in the CAZy database, but the chromatograms obtained by HPLC showed activity in *Fusarium* β-glucan, β-glucan from yeast *Saccharomyces cerevisiae* and β(1,3)-glucan from *Euglena gracilis*.

In the case of BT3314, the results were similar, but any activity in β(1,3)-glucan from *Euglena gracilis* (see Figure 43). A globular structure is well defined in the case of both BT3312 and BT3314 (see Figure 38 and Figure 40), which were reported as GH30_3 and GH_3, respectively. Nevertheless, a very different structure is present in BT3313 (Figure 39), the unknown protein, where a small globular domain is linked to a β-fold tubular motif, likely to be attached to the cell membrane.

Since the time and resources of this project are limited, an in-depth study of the structure and function of the unknown BT3313 is not possible, but a wider clarification of the kinetics parameters and conformation of this novel protein would suppose an interesting and useful research in the future.

Figure 38. Structure of BT3312 belonging to the family GH30 subfamily 3. The protein was solved by Temple at al., 2017 (https://www.rcsb.org/structure/5NGK).
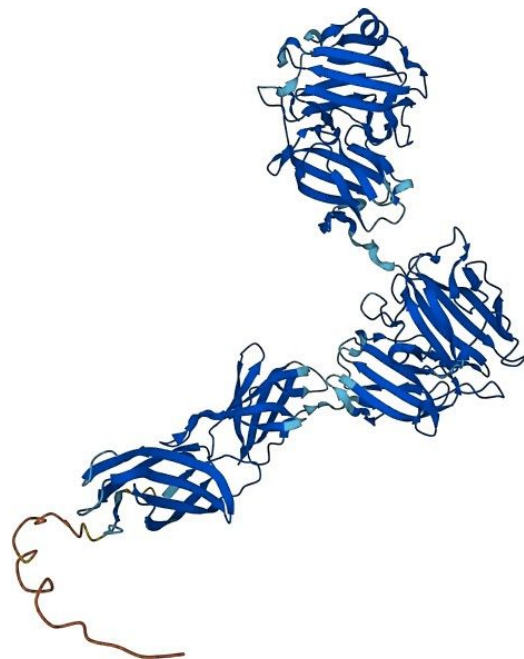
Figure 39. Structure prediction for unknown function protein BT3313.

106
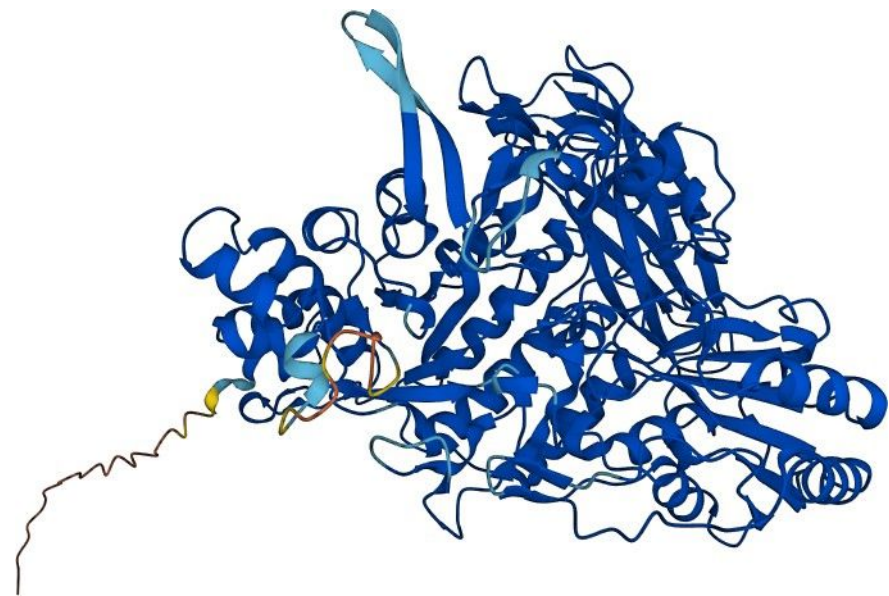
Figure 40. Structure prediction for BT3314, belonging to the GH3 family.
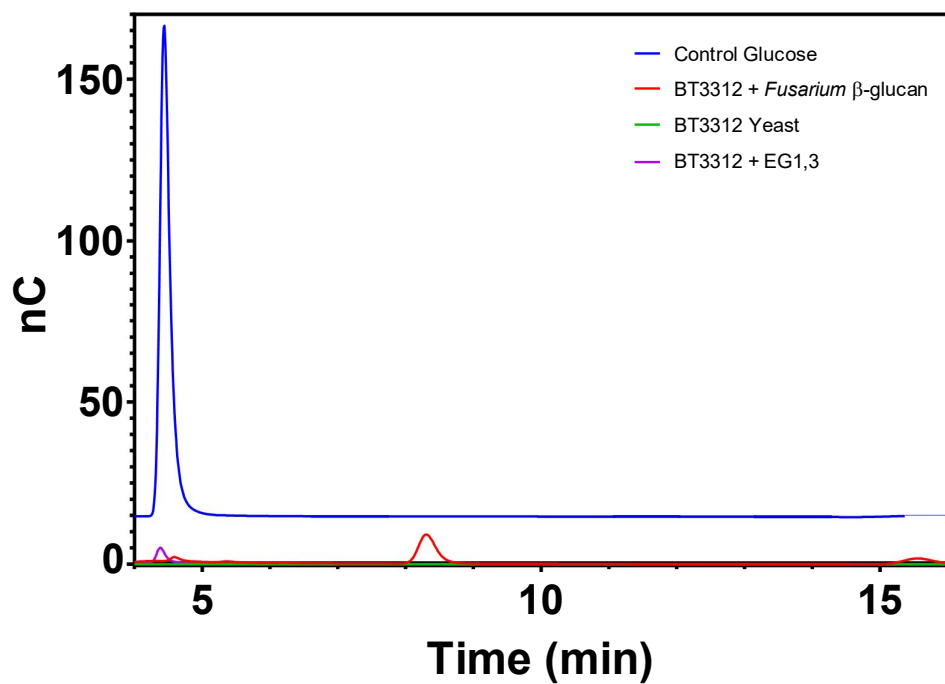
Figure 41. HPLC chromatogram of the enzymatic assays by BT3313 in *Fusarium* β-glucan.
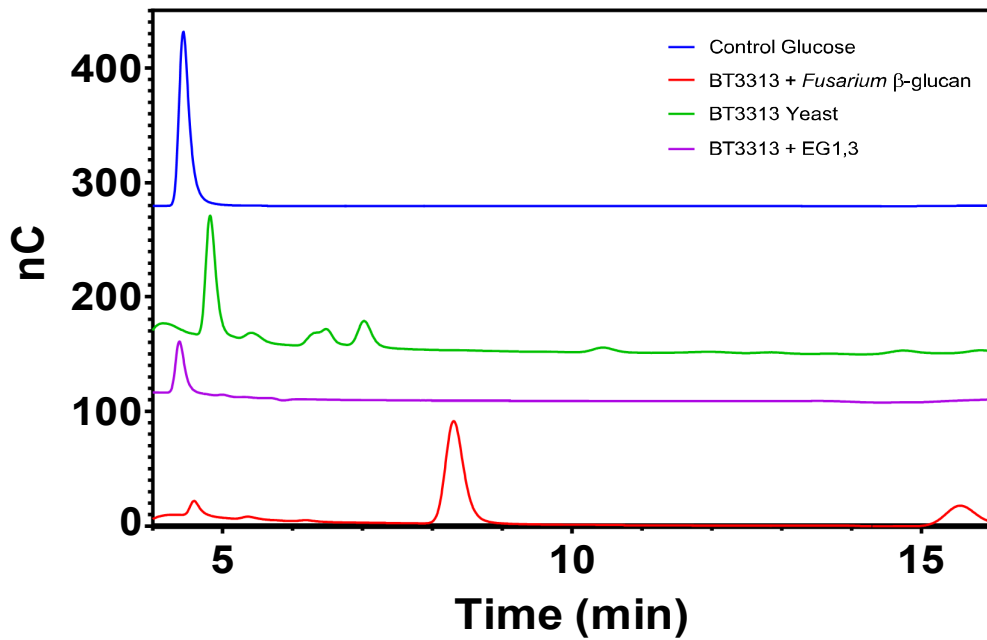
Figure 42. HPLC chromatogram of the enzymatic assays by BT3313 in *Fusarium* β-glucan.
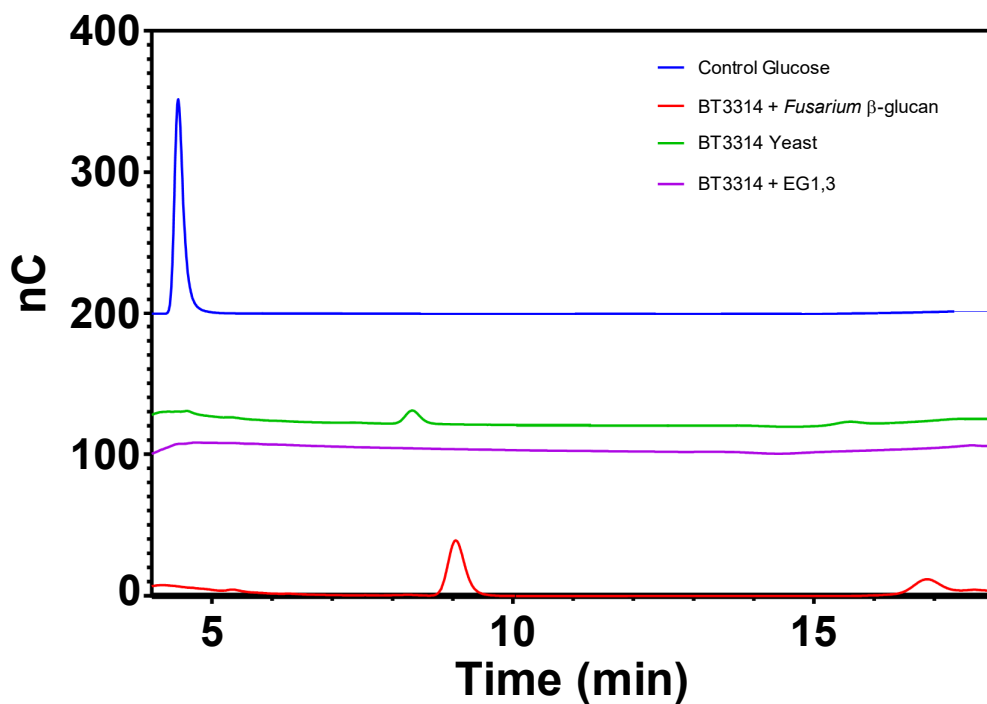
Figure 43. HPLC chromatogram of the enzymatic assays by BT3314 in *Fusarium* β-glucan.

Bacteroides cellulosyliticus **WH2**

Using the information provided by the proteomic assay, the activity of the six proteins in two different PULs was tested: on one hand, BcellWH2_01926 (GH3), BcellWH2_01927 (GH3) and BcellWH2_01931 (GH157, laminarinase) were found in the PUL 29; in the other hand, BcellWH2_02537 (GH30_3), BcellWH2_02538 (unknown) and BcellWH2_02541 (GH2/CBM57) were in the PUL 51 (see Figure 44).
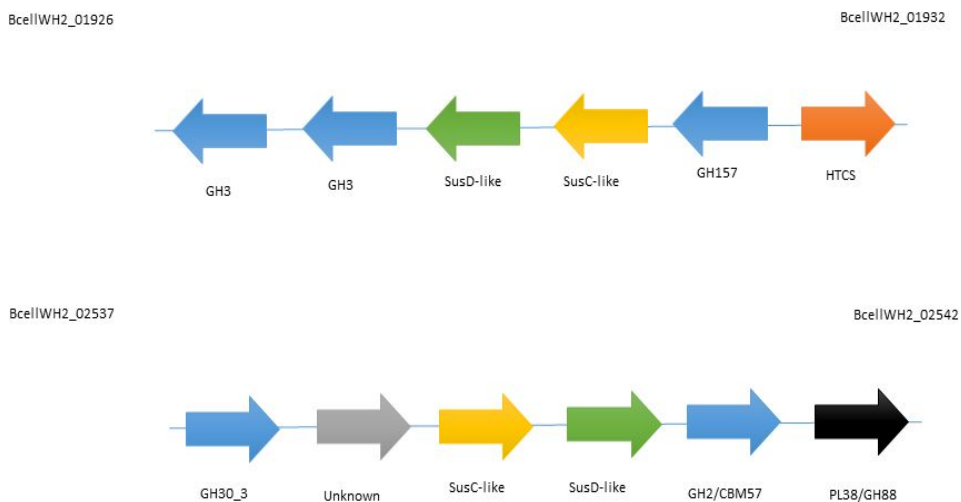
Figure 44. PULs studied in *Bacteroides cellulosyliticus* WH2.

In the first PUL, any activity was found for the protein BcellWH2_01926 (Figure 45). As it can be appreciated in the chromatogram below, the total absence of peaks corresponding with sugars released in the enzymatic reaction revealed that the protein did not act over the substrate. Although the preliminary data observed in the proteomics assays may invite us to think that it will act as an active enzyme, *in vitro* utilization of a single protein differs from the *in vivo* regulation of an entire PUL. Therefore, the obtained data does not mean on its own that BcellWH2_01926 has any activity on β-glucan. For example, it might act over the oligosaccharides produced

by other enzymes instead of the intact polysaccharide, acting maybe as a secondary glycosidase whose activity is preceded by other proteins within this PUL. Although the mutualism between several proteins is an important factor to consider when studying metabolic degradation by enzymes, the determination of the exact order and behaviour of all these proteins exceeds the scope of this thesis.
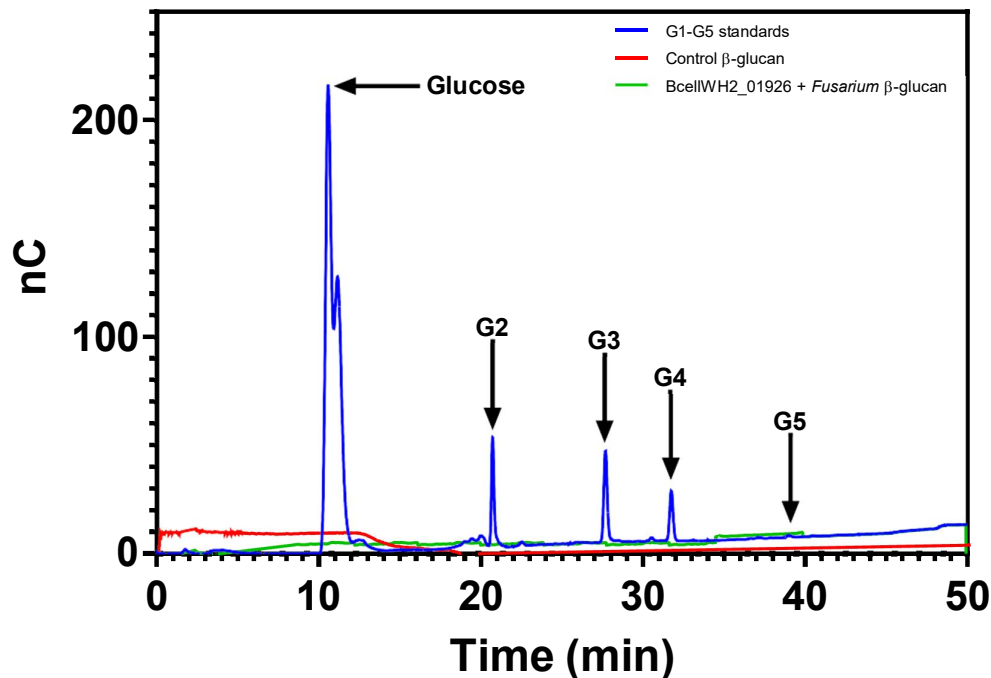
Figure 45. HPLC chromatogram of the enzymatic assays by BcellWH2_01926 in *Fusarium* β-glucan.

In addition, in the case of BcellWH2_01927, the PCR product was impossible to obtain, even after changing the design for the primers and the PCR conditions several times.

Furthermore, in the case of BcellWH2_01931 (GH157, Figure 46), both HPLC chromatogram (see Figure 47 below) and DNSA assays (Figure 48) were used to study the kinetics parameters. The HPLC data shows different peaks released during the reaction. One of them has a similar retention time than the glucose standard, while the

second one appeared later, before laminaribiose (G2). The last one seems to be like laminaritriose (G3), but the exact identity is impossible to detect with the employed technique. The presence of different products with a diverse range of sizes, together with the information contained in the CAZy database, may match an endoglucanase activity. This means that the protein, which shows a globular structure (see Figure 46), slices through the polysaccharide chain, from the inside to the outside, releasing firstly an oligo with high molecular size. After this happens, the first oligosaccharide is broken into smaller digestion products.
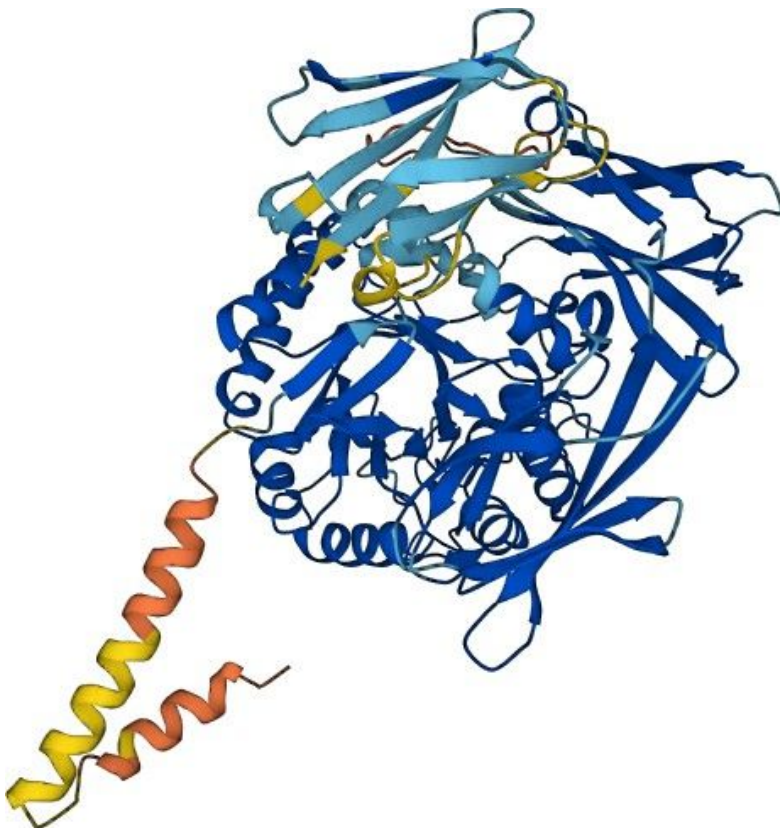
Figure 46. Structure prediction for BcellWH2_01931, belonging to the GH157 family.
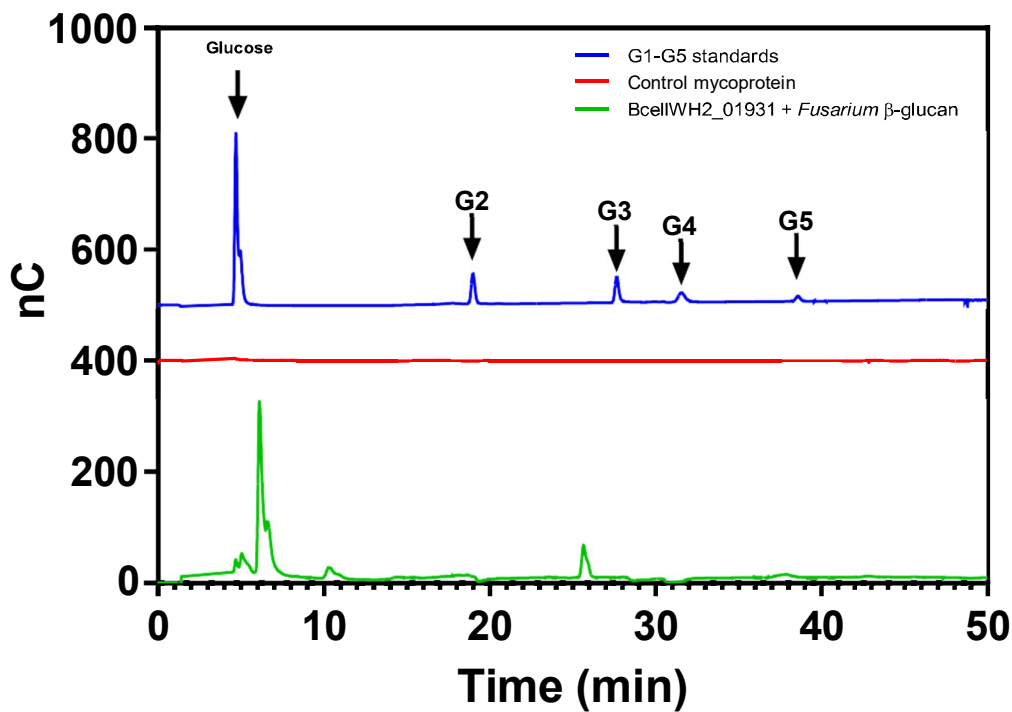
Figure 47. HPLC chromatogram for the enzymatic assay by DNSA method of BcellWH2_01931 with *Fusarium* β-glucan.

Using the DNSA method (see section 2.17), the kinetic parameters forBcellWH2_01931 were calculated, using β-glucan as substrate.
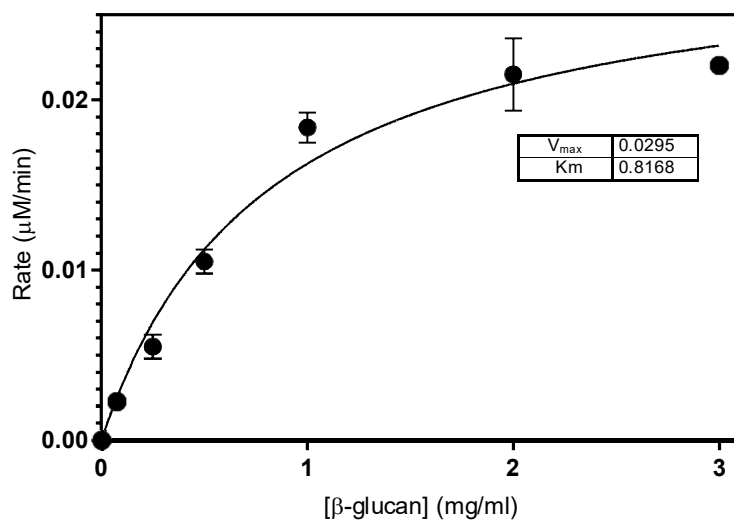
Figure 48. Kinetic assays by DNSA method in BcellWH2_01931.

For the proteins located in the second PUL, the first protein was BcellWH2_02537, which showed a globular structure (see Figure 49). The HPLC chromatogram (see Figure 50) for BcellWH2_02537 showed the presence of two peaks. The first one had a similar retention time to glucose, while the second one appeared after the glucose standard and before the laminaribiose (G2) standard. Since there were not any bigger peaks, a glucosidase activity might fit with BcellWH2_02537, according to the data previously reported in the CAZy database.
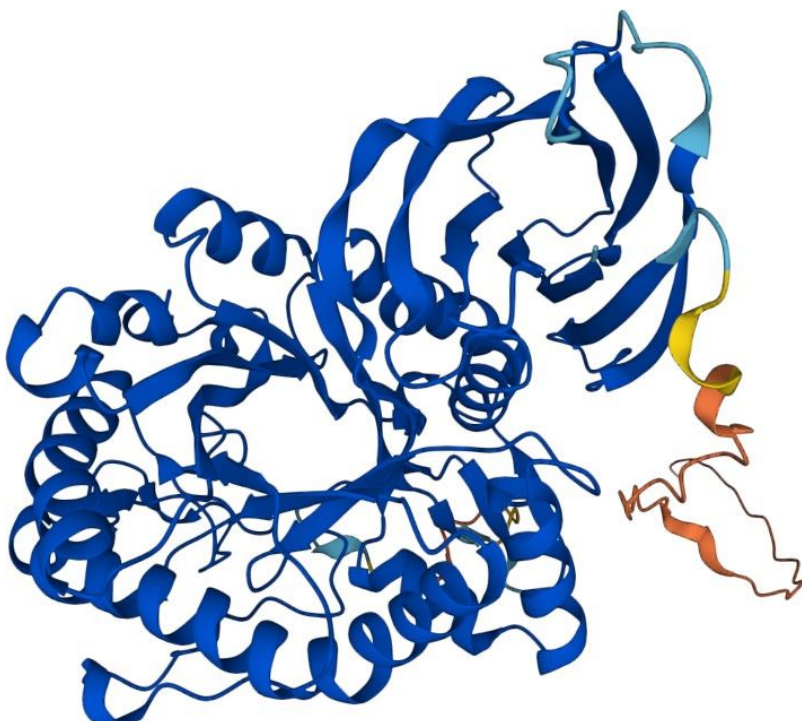
Figure 49. Structure prediction for BcellWH2_02537, belonging to the family GH30 subfamily 3.
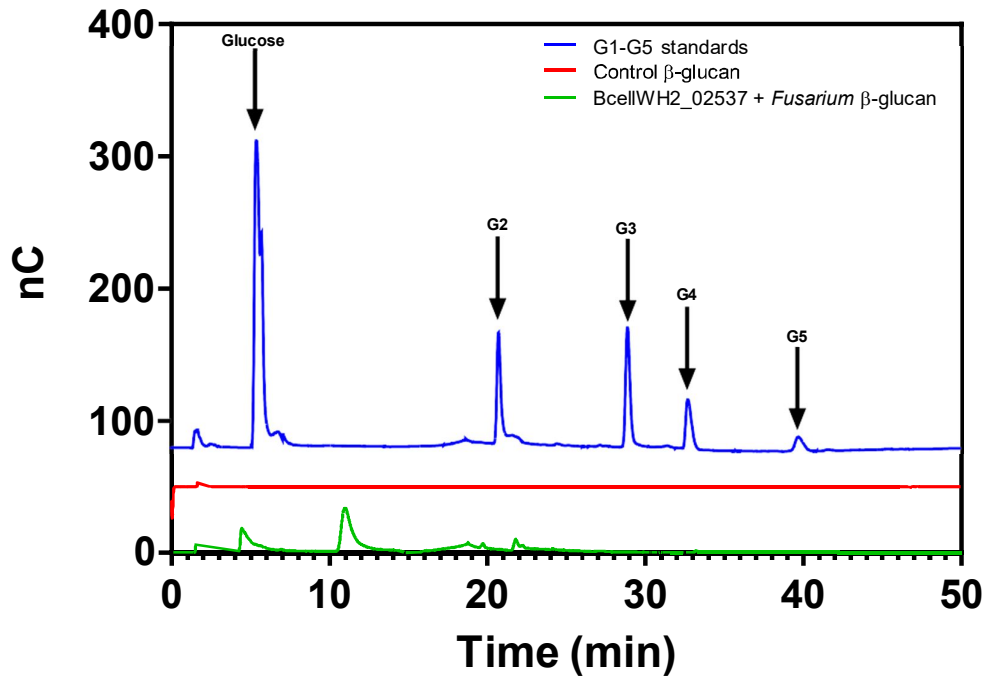
Figure 50. HPLC chromatogram for the enzymatic assay of BcellWH2_02537 with *Fusarium* β-glucan.

The kinetics assays were undertaken using β-glucan as substrate and measuring the appearance of NADPH at 340 nm (Figure 51 below).
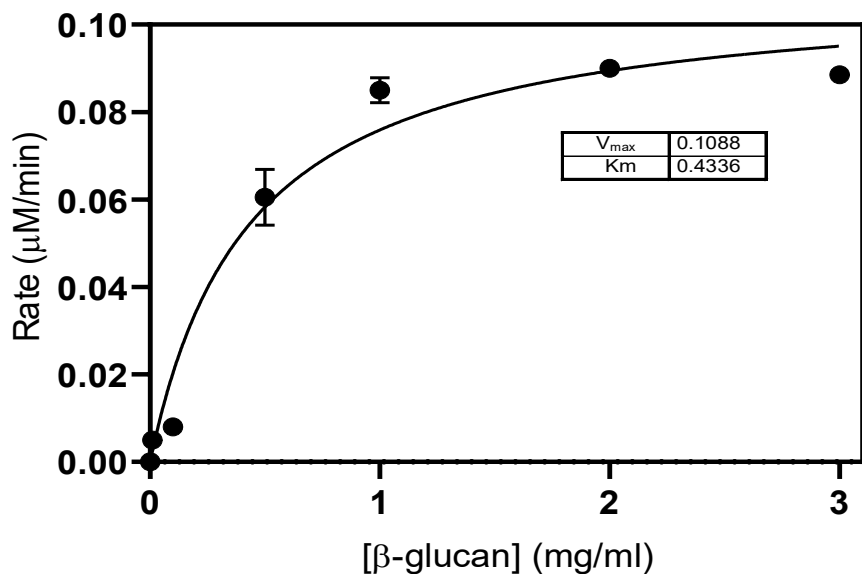
Figure 51. Kinetic assays in BcellWH2_02537.

In the case of BcellWH2_02538, it was an unknown protein whose catalytic activity was not described in the CAZy database, appearing as a hypothetical protein. It showed a tubular structure composed of different β-barrel motives linked, forming a tubular structure (see Figure 52 below). The enzyme reaction was injected into the HPLC (see Figure 53) revealing the existence of two peaks with similar retention times to the laminaribiose (G2) standard. For this reason, the same protocol used in BcellWH2_02537 was followed, since a potential glucosidase activity was the most probable activity. The subsequent kinetic assay was developed, and the obtained curve is shown in the Figure 54.
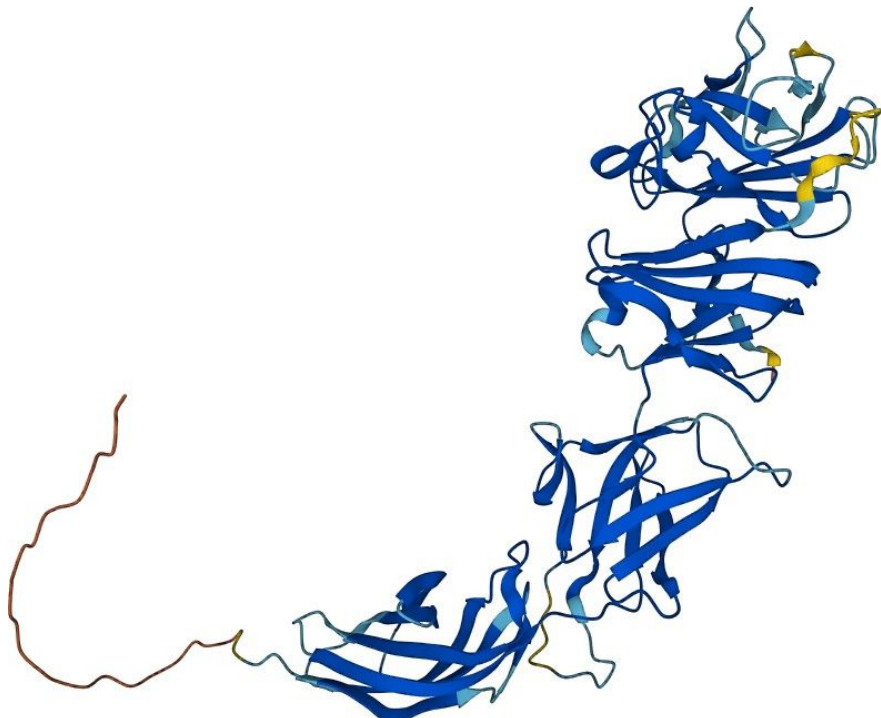
Figure 52. Structure prediction for the unknown function protein BcellWH2_02538.
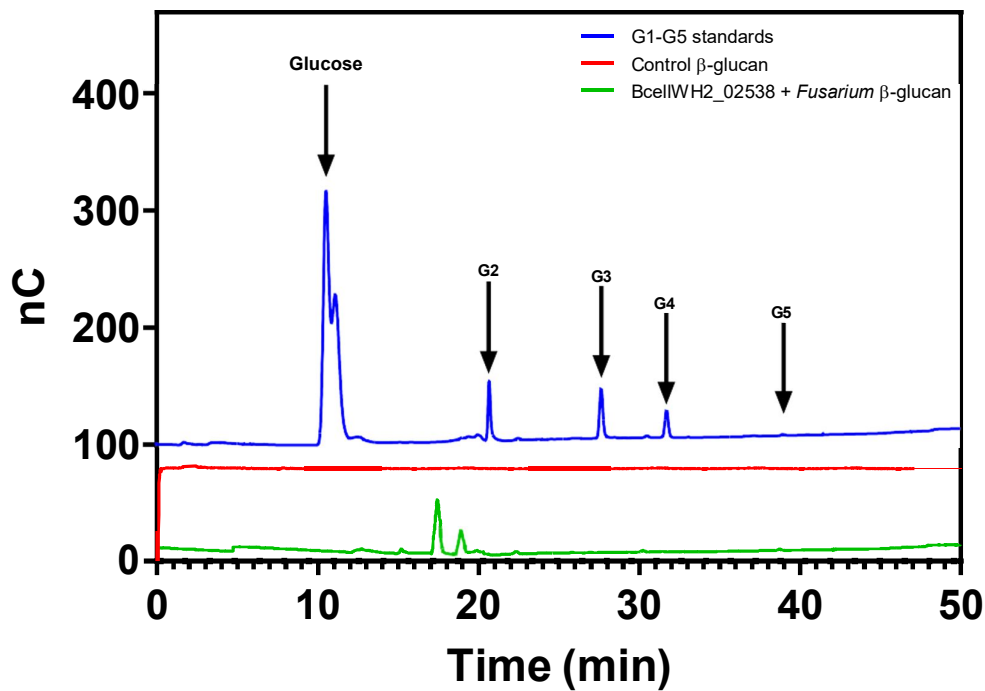
Figure 53. HPLC chromatogram for the enzymatic assay of BcellWH2_02538 with *Fusarium* β-glucan.

BcellWH2_02538

V_{max}	0.0295
Km	0.8168
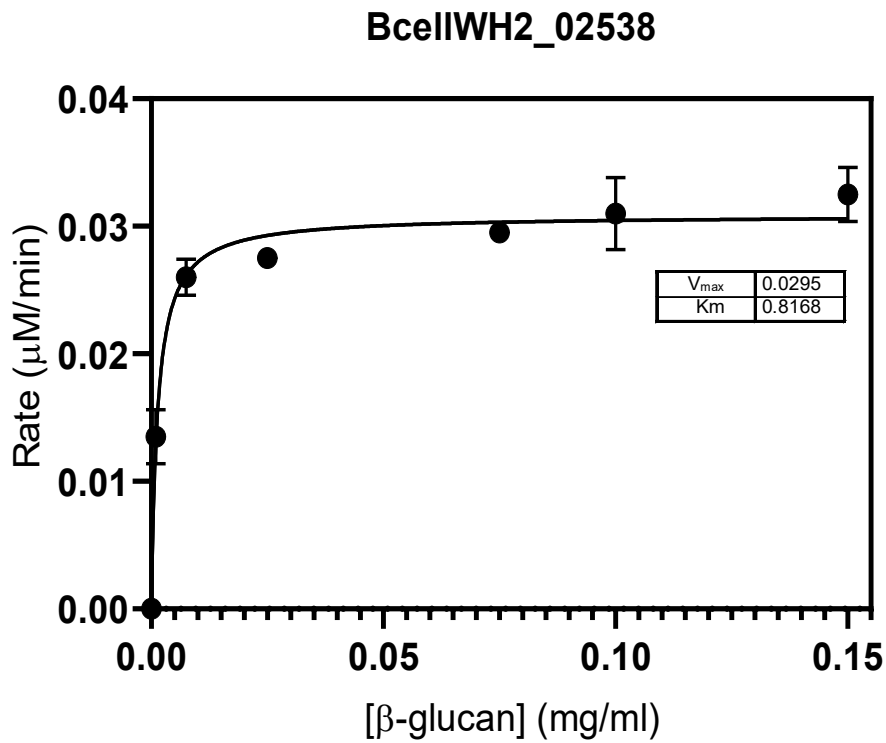
Figure 54. Kinetic assay in BcellWH2_02538.

Finally, for BcellWH2_2541 (GH2/CBM56) the HPLC (see Figure 55) revealed a lack of affinity in the presence of *Fusarium* β-glucan, as it can be easily appreciated in the absence of any oligosaccharide released to the media.
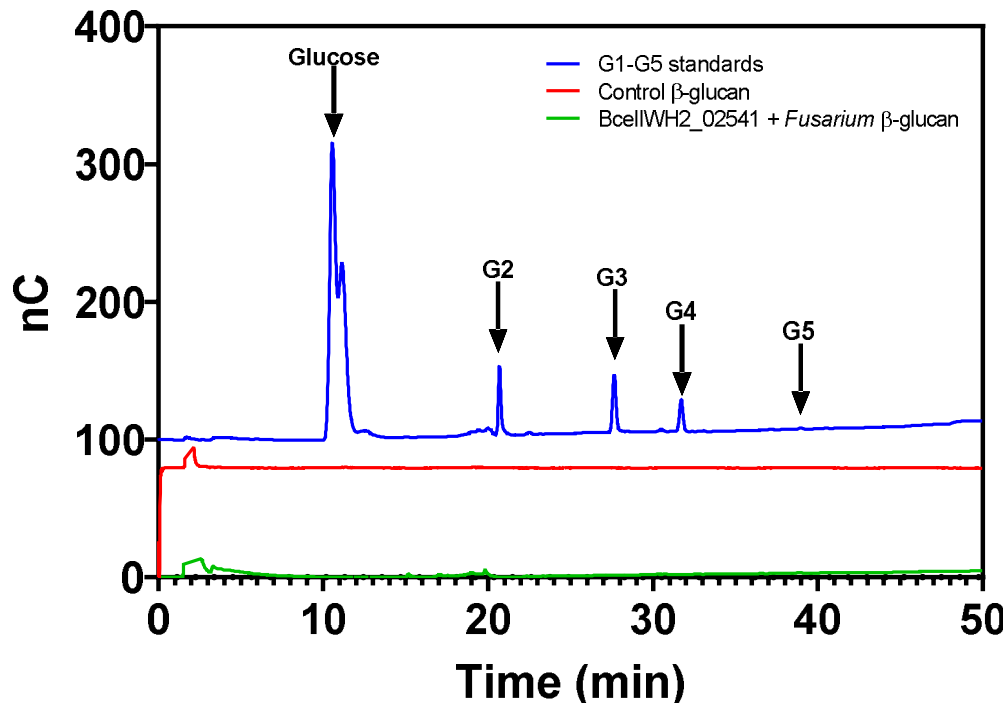
Figure 55. HPLC chromatogram for the enzymatic assay of BcellWH2_02541 with *Fusarium* β-glucan.

To sum up, in the case of *Bacteroides cellulosyliticus* WH2, three different proteins showed activity in *Fusarium* β-glucan. The values for the obtained kinetic parameters of each protein are shown in the Table 12 below.

Locus	V_{max} (mg mL^{-1} s^{-1})	K_M (mg mL^{-1})	k_{cat} (s^{-1})	k_{cat}/K_M (s^{-1}/mg mL^{-1})
BcellWH2_01931	0.02951	0.8168	5.98×10^3	7.3×10^3
BcellWH2_02537	0.1088	0.4336	4.5×10^3	1.03×10^4
BcellWH2_02538	0.03086	0.001354	1.43×10^3	1.06×10^6

Table 12. Kinetic parameters for the different GHs of *Bacteroides cellulosyliticus* WH2.

3.3 Cross-feeding experiments

3.3.1 Identification of released oligosaccharides when *Bacteroides* sp. degrade *Fusarium* β-glucan

The cultures from *Ba. cellulosyliticus* WH2, *Ba. thetaiotaomicron* VPI 5482*, Ba. vulgatus, Victivallis vadensis* ATCC BAA-548 and *Roseburia inulinovorans* were centrifugated (5000 g, 10 min) and filtrated with 0.2 μm filters for sterilization. Following this, the four samples were injected into the HPLC showing the presence of different peaks with similar retention times compared with the standards (see Figures 56-60 below).
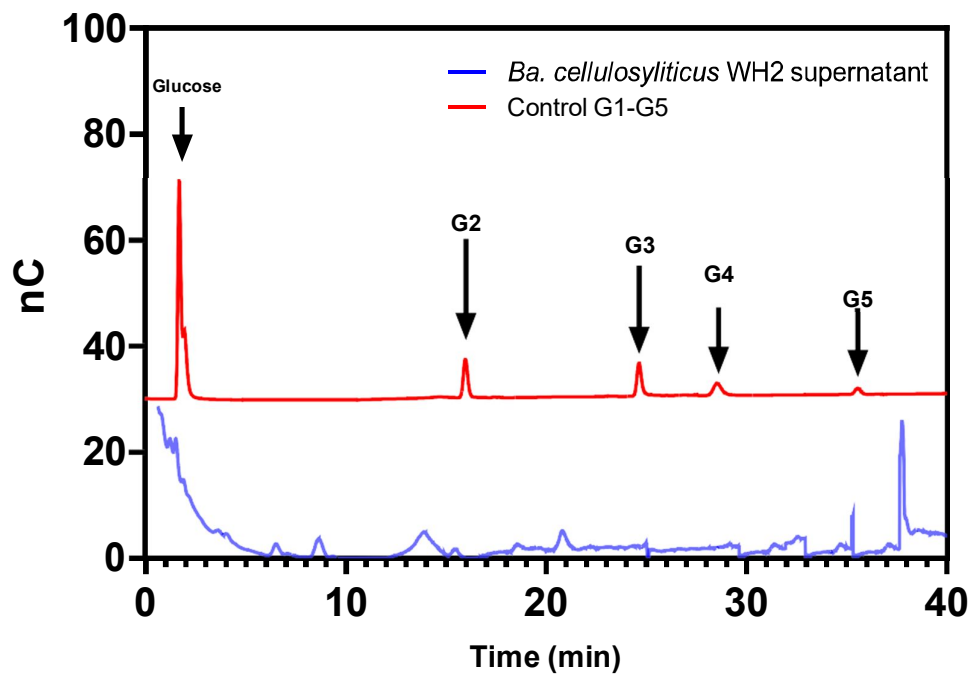
Figure 56. HPLC chromatogram for the filtered supernatant of *Ba. cellulosyliticus* WH2.
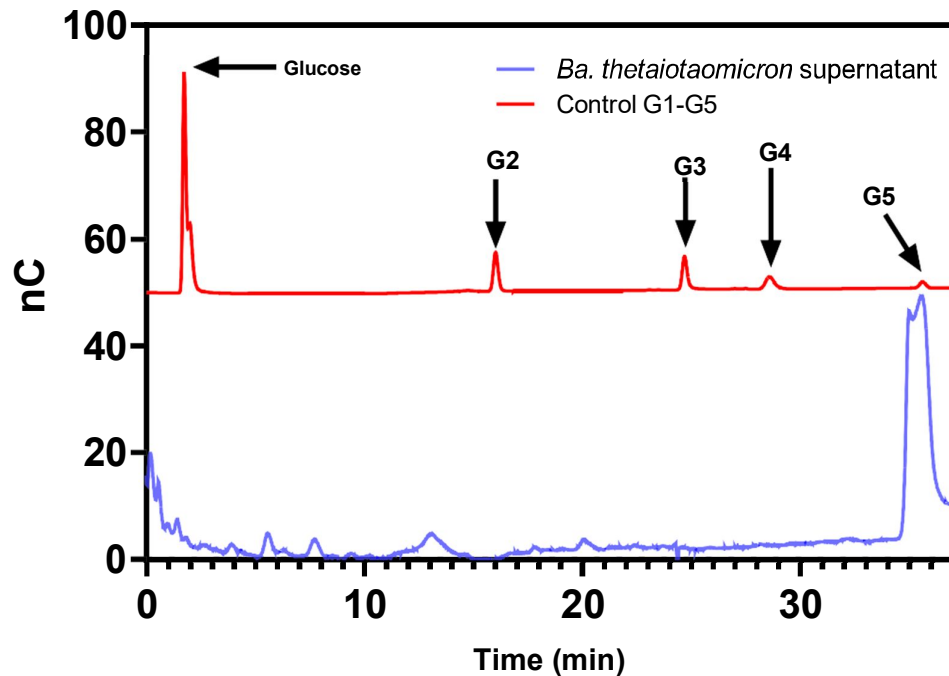
Figure 57. HPLC chromatogram for the filtered supernatant of *Ba. thetaiotaomicron* VPI 5482.
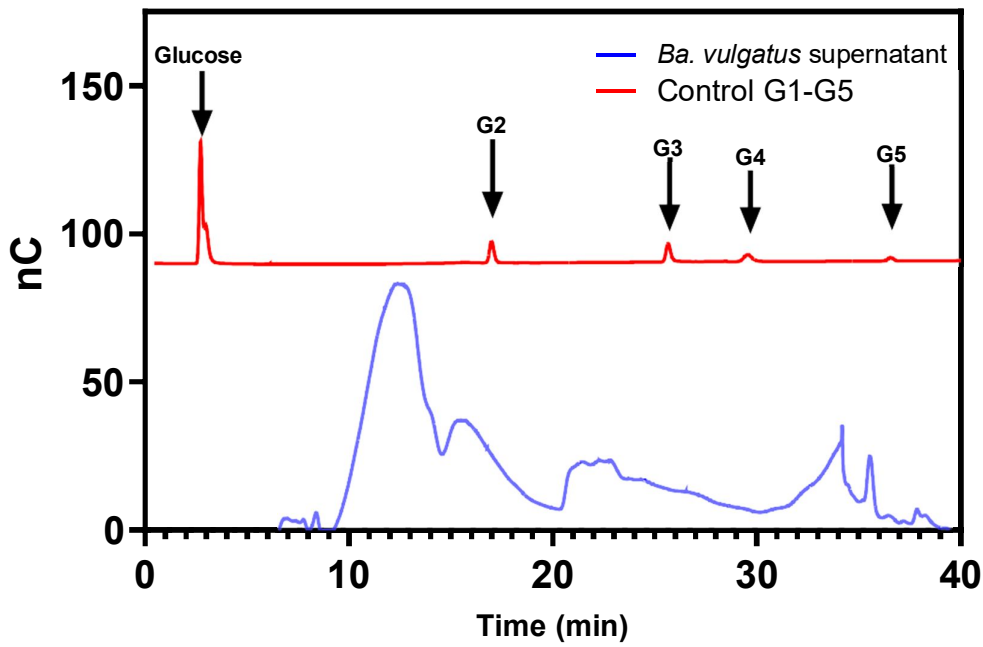
Figure 58. HPLC chromatogram for the filtered supernatant of *Ba. vulgatus*.
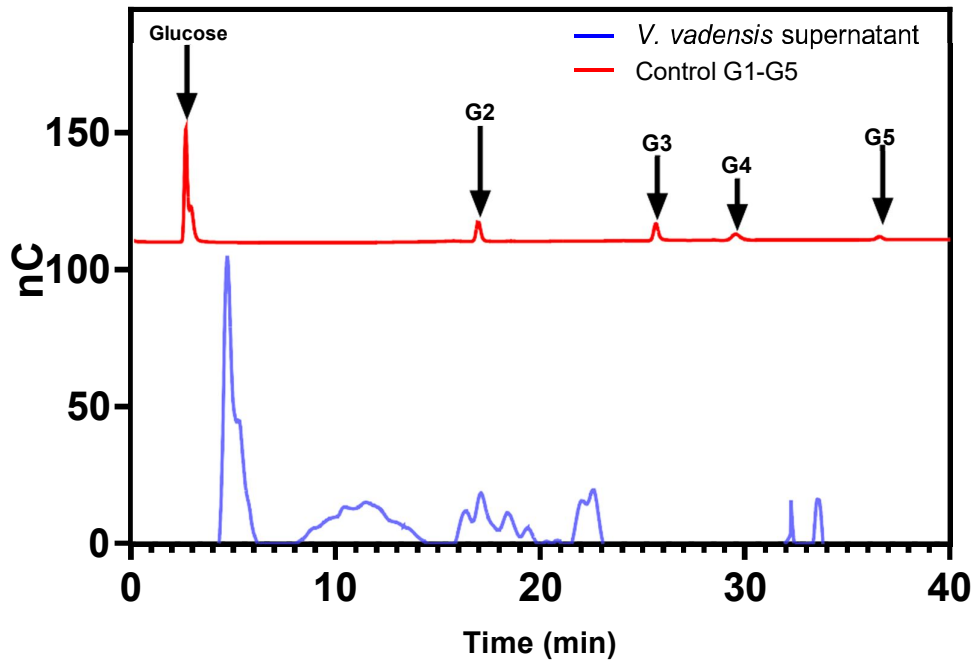
Figure 59. HPLC chromatogram for the filtered supernatant of *Victivallis vadensis*.
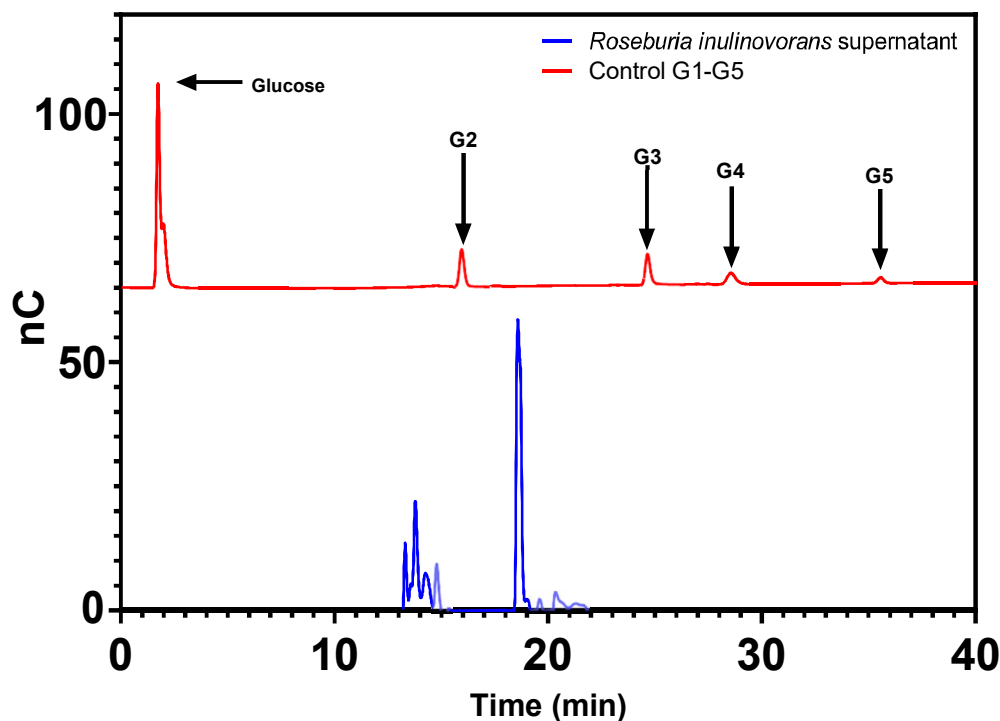
Figure 60. HPLC chromatogram for the filtered supernatant of *Roseburia inulinovorans*.

As it can be easily appreciated in the graphs above, each bacterium produced a different spectrum of oligosaccharides, with peaks appearing in diverse retention times. It seems logical to attribute this fact to the existence of several metabolic pathways corresponding to the studied bacteria. Differences in the production of oligosaccharides are due to variations in the type of enzymes involved in the degradation of the polysaccharide, as in its spatial location in the membrane or the periplasm.

The utilization of P2 exclusion chromatography (see Methods section 2.22) was used to obtain individual oligosaccharides instead of complex mixes. The application of this additional purification step allowed the reduction of the number of peaks in the samples (see chromatograms below) which increased the purity of the samples and, therefore, made easier their subsequent identification in the HPLC and the mass

spectrometry.

The HPLC revealed the presence of a variety of purified oligosaccharides for different bacteria. The results shown in the chromatograms below were compared with five standards corresponding to glucose, laminaribiose (G2), laminaritriose (G3), laminaritetrose (G4) and laminaripentose (G5). In the case of *Bacteroides cellulosyliticus* WH2 (see Figure 61 below), only one peak was collected after 40 minutes. The P2 column used cannot be considered a reliable technique to determine the exact molecular size of the sugars but only for an approximation of it. It was appreciated that the retention time for this peak was higher than the laminaripentose standard. For this reason, it should correspond with a mix of the oligosaccharides formed by six or more glucose monomers.
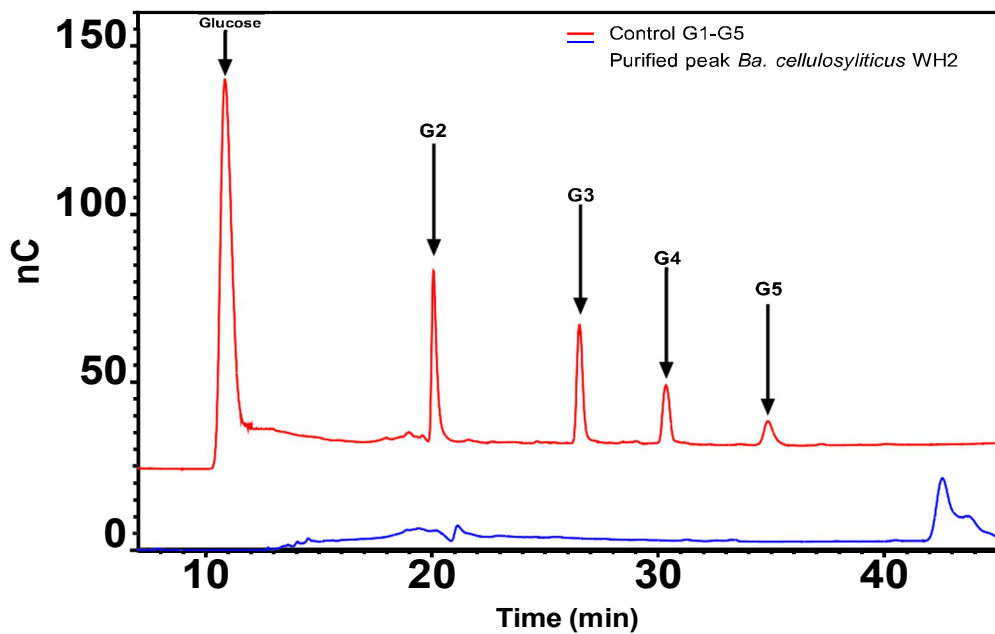
Figure 61. HPLC chromatogram of the oligosaccharides obtained from the filtered supernatant of *Bacteroides cellulosyliticus* WH2.

In the case of *Ba. thetaiotaomicron* VPI 5482 (see Figure 62 below), similar results were obtained since only one peak was collected after 40 minutes. The retention time for this peak was higher than the laminaripentose standard. For this reason, it should correspond with the oligosaccharides formed by six or more glucose monomers.
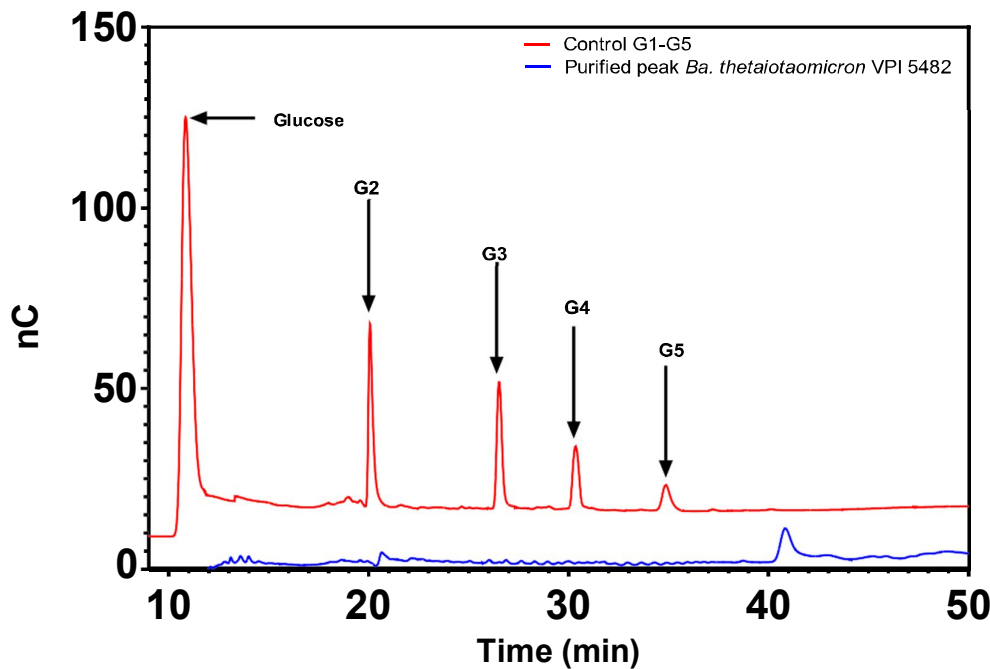
Figure 62. HPLC chromatogram of the oligosaccharides obtained from the filtered supernatant of *Ba. thetaiotaomicron* VPI 5482.

On the other hand, *Victivallis vadensis* showed bigger diversity since four peaks were appreciated. The first peak showed a similar retention time to glucose standard (See Figure 63 below) while two other peaks were found in the zone of laminaribiose standard (see Figure 64 and Figure 65 below). Finally, the last peak was found in a similar retention time to the ones found in *Bacteroides* sp. previously, appearing after the biggest oligosaccharide standard, the laminaripentose (Figure 66).
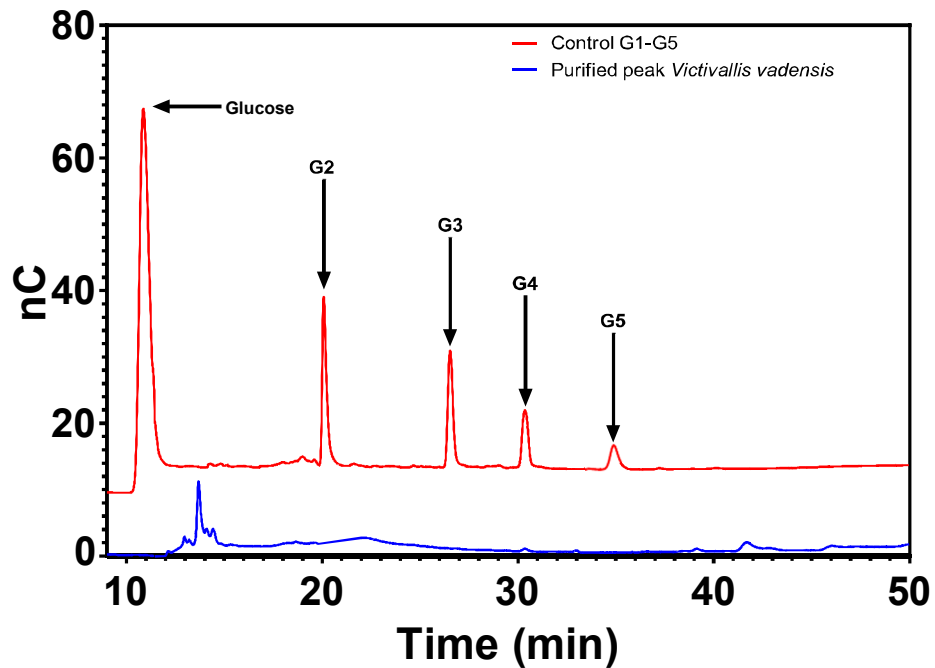
Figure 63. HPLC chromatogram of the first oligosaccharides obtained from the filtered supernatant of *Victivallis vadensis*.
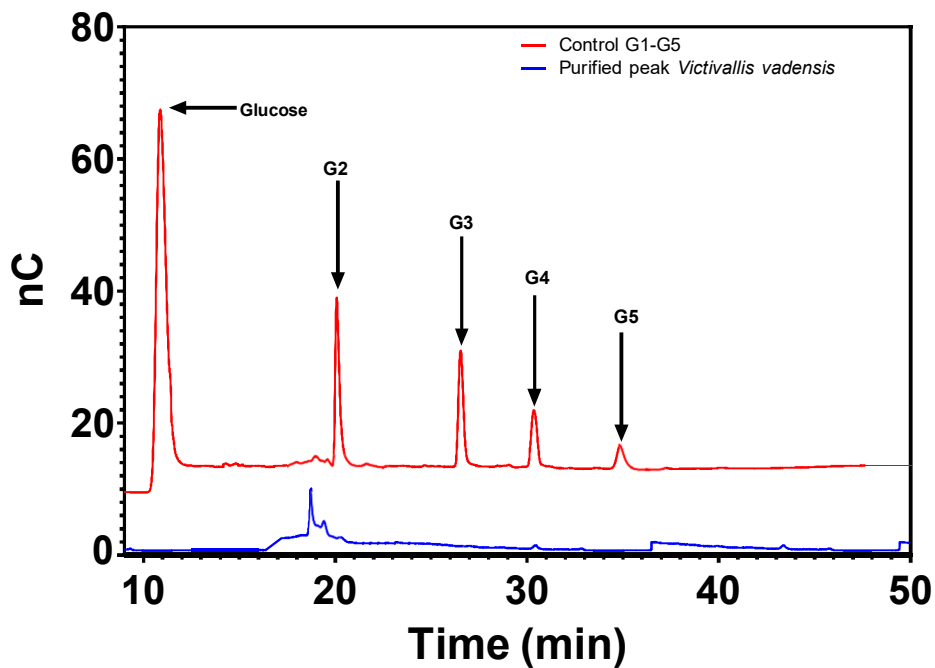
Figure 64. HPLC chromatogram of the second group of oligosaccharides obtained from the filtered supernatant of *Victivallis vadensis*.
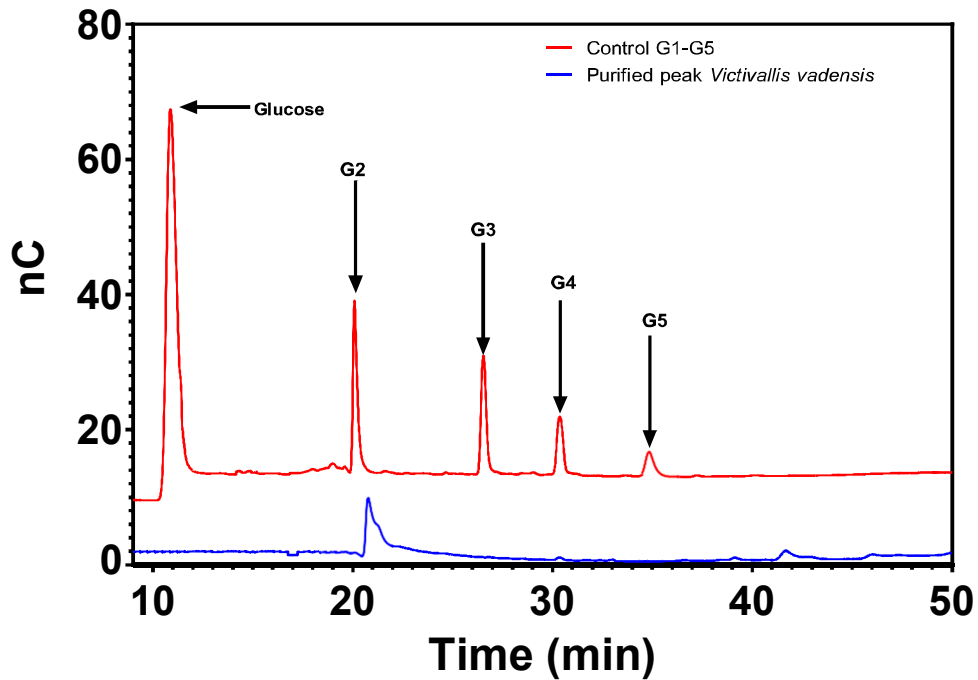
Figure 65. HPLC chromatogram of the third group of oligosaccharides obtained from the filtered supernatant of *Victivallis vadensis*.
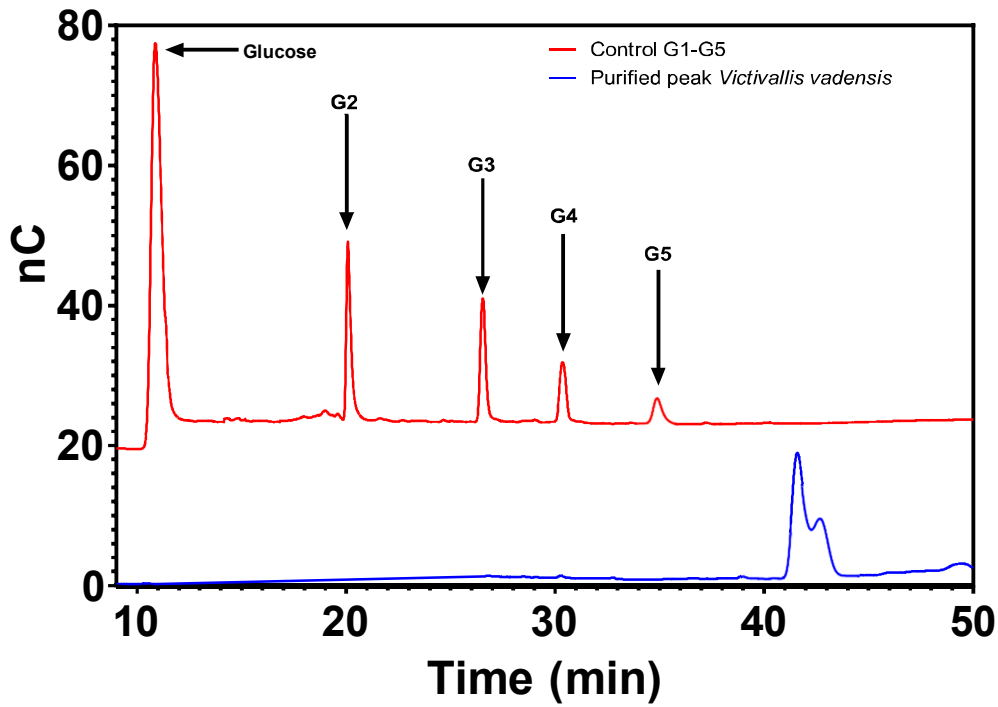
Figure 66. HPLC chromatogram of the biggest oligosaccharides obtained from the filtered supernatant of *Victivallis vadensis*.

The peaks from *Ba. cellulosyliticus* WH2 and *Ba. thetaiotaomicron* VPI 5482 were purified using the P2 column and then destined for LC/MS identification. This technique provided the exact mass/charge relation (m/z) of the peaks previously isolated in the P2 column, constituting an essential tool for their identification. Nevertheless, LC/MS does not supply any information regarding bond conformation. The structural conformation could be totally solved by using the NMR technique, but the preparation of samples and the interpretation of data would exceed greatly the resources and possibilities of this project. The data obtained with LC/MS is shown in the graphs below (Figure 67 and Figure 68).
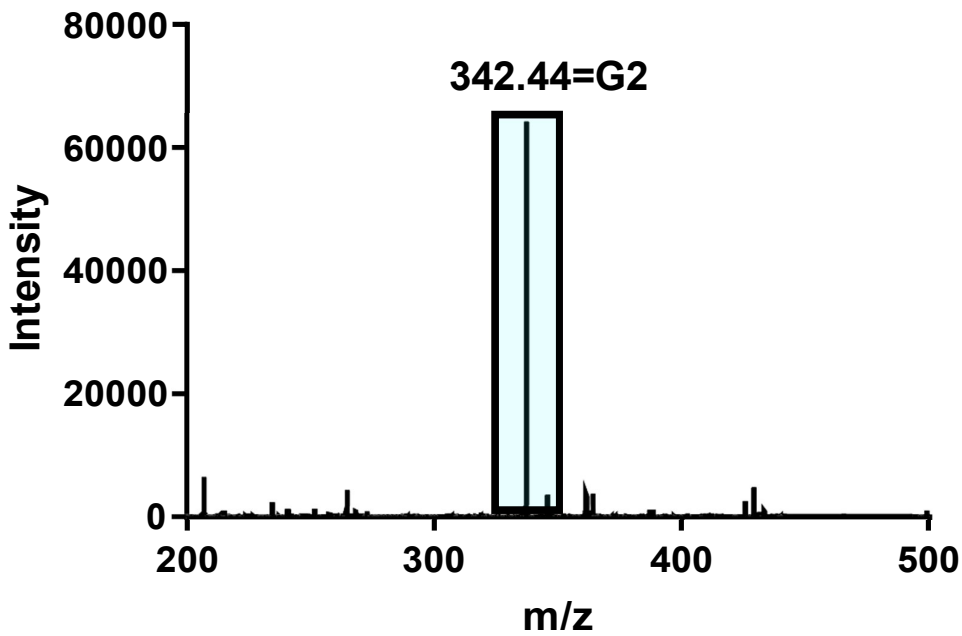
Figure 67. MS peak corresponding to the smallest oligosaccharide purified from *Ba. thetaiotaomicron* VPI 5482 supernatant.
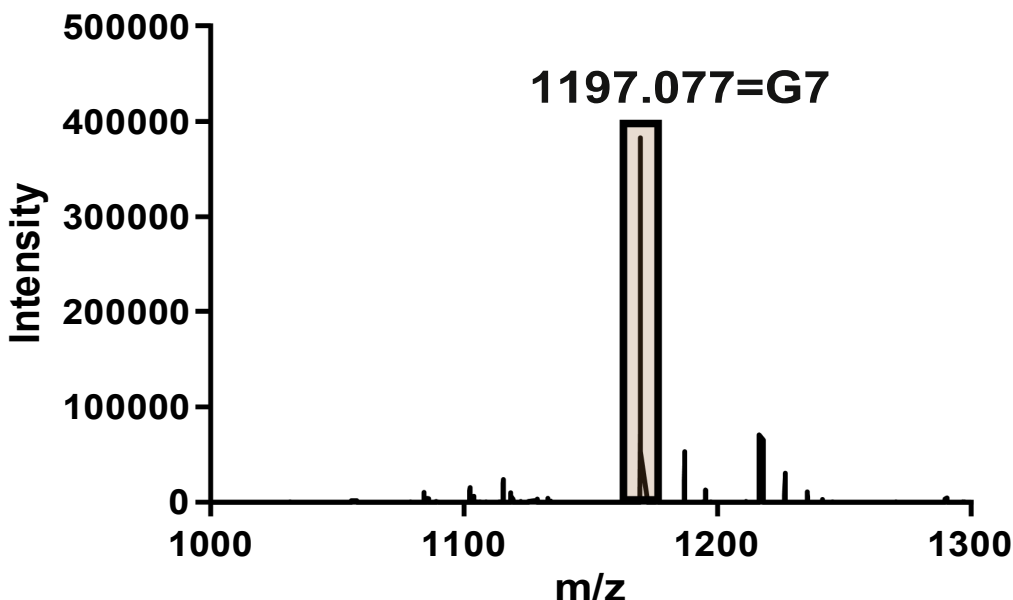
Figure 68. MS peak corresponding to the oligosaccharide purified from *Ba. cellulosyliticus* WH2 supernatant.

As it can be appreciated in the graphs from the LC/MS, the mass/charge relation (m/z) corresponding to two different peaks were obtained. The first peak (Figure 67) corresponding to glucobiose. On the other hand, the second peak showed a bigger m/z value, corresponding to glucoheptose (Figure 68). Even though the exact bond conformation and conformational structure are not provided, these results show the ability of both *Ba. thetaiotaomicron* VPI 5482 and *Ba. cellulosyliticus* WH2 to produce different oligosaccharides originated from the degradation of *Fusarium* β-glucan. The variation in the mass of the oligosaccharides is directly related to the type of enzymes involved in the degradation process. Although these bacteria were the only ones to be analysed by LC/MS, due to the lack of time and resources, it must be mentioned that other *Bacteroides* sp. or *Victivallis vadensis* may present variations in the m/z results of their peaks. This fact is due to differences in the Polysaccharide Utilization Loci (PULs) that are present in the bacteria genome. PULs encode a variety of proteins,

127

specially glycoside hydrolases which have different catalytic activities.

3.3.2 Identification of released SCFAs when *Bacteroides* sp. degrade *Fusarium* β-glucan

SCFAs are carboxylic acids with aliphatic tails of 1–6 carbons defined as "carbohydrate polymers with three or more monomeric units, which are neither digested nor absorbed in the small intestine of humans" by the Codex Alimentarius (also known as Food Code) Commission (CAC). The most abundant SCFAs produced by anaerobic fermentation of dietary fibers (DF) in the intestine are acetate (C2), propionate (C3), and butyrate (C4) (Parada Venegas et al., 2019).

Bacteroidota and Bacillota are the most abundant phyla in the intestine, with members of the Bacteroidota mainly producing acetate and propionate, while Bacillota mostly produce butyrate in the human gut. The production of other SCFAs is mediated by other species, for example, *Bifidobacterium* genus (belonging to the phylum Actinobacteria) that produce acetate and lactate during carbohydrate fermentation (Parada Venegas et al., 2019).

The supernatants from *Ba. cellulosyliticus* WH2, *Ba. thetaiotaomicron* VPI 5482 and *Ba. vulgatus* ATCC 8482 were injected into a GC/MS spectrometer using headspace analysis for aqueous solutions. The results are shown in the Table 13 below:

Bacterium	Acetate (A, mM)	Propionate (P, mM)	Ratio P/A
Ba. cellulosyliticus WH2	12.51 ± 1.18	219 ± 15.47	17.52 ± 1.06
Ba. thetaiotaomicron VPI 5482	2.45 ± 0.39	11 ± 1.42	4.58 ± 0.34
Ba. vulgatus ATCC 8482	9.00 ± 0.85	200 ± 17.59	22.22 ± 2.13

Table 13. SCFAs production by different *Bacteroides* sp. using *Fusarium* β-glucan.

This data reveals the production of beneficial SCFAs by *Bacteroides,* with a highly potential as antiinflamatory and immune regulator compounds. The data also underlines the fact that propionate production was higher than acetate production. Furthermore, to be noted is the fact that the maximum P/A ratio (propionate/acetate ratio) value was reached for *Ba. vulgatus* ATCC 8482*,* compared with *Ba. cellulosyliticus* WH2 and *Ba. thetaiotaomicron* VPI 5482, when *Fusarium* β-glucan is the only carbon source. The presence of other SCFAs in its anion forms such as formate, butyrate, isobutyrate, valerate, isovalerate and caproate was not detected within the experimental conditions.

3.3.3 Designing experiments in minimal media containing supernatants from *Bacteroides* sp. (main degraders or donors) as a carbon source to establish if *Bifidobacterium* sp. and *Lactiplantibacillus plantarum* WCFS1 (as secondary degraders or acceptors) can grow

Once it was proven the ability of *Bacteroides* sp. to degrade β-glucan, it was necessary to study how these primary polysaccharide degraders interacted with other members of the Human Gut Microbiota. For this purpose, the cultures of *Bacteroides* sp. were centrifugated and then the supernatants were filtered. These supernatants, which were produced previously during the digestion of *Fusarium* β-glucan by *Bacteroides* sp.,

contained the digestion products released during the process. For this reason, these digestion mixes obtained from *Ba. cellulosyliticus* WH2, *Ba. thetaiotaomicron* VPI 5482 and *Ba. vulgatus* ATCC 8482, once they were totally sterilized and filtered, were used as carbon sources for *Bifidobacterium* sp. (see Figure 69).
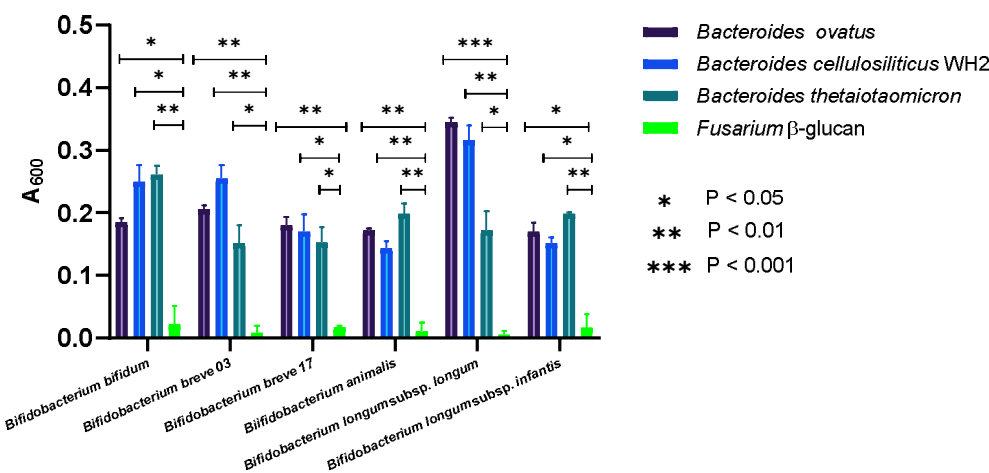
Figure 69. Growth during 24 hours of six *Bifidobacterium* sp. in *Bacteroides* sp. supernatants.

The results show how all the *Bifidobacterium* sp. were able to grow using these supernatants from *Bacteroides* sp., having the capacity to use the oligosaccharides as an energy source, although they were not able to use the intact polysaccharide.

The growth of these *Bifidobacterium* sp. with the three supernatants was also obtained when using a monitored plate reader for a period of 24 hours. Although the three different *Bacteroides* supernatants promoted bifidobacterial growth, the curves showed important differences between them. This seems logical due to the variations in the bifidobacterial genomes, which reflects in a diverse range of utilization systems for sugar metabolism. The bacterium *Lactiplantibacillus plantarum* WCFS1 was tested as well.

Firstly, in the case of *Ba. cellulosyliticus* WH2 supernatant, the best rates were found for *Bifidobacterium longum* subsp. *longum* and *Bifidobacterium longum* subsp. *infantis*, respectively. Nevertheless, the lowest was *Lactiplantibacillus plantarum* WCFS1 while *Bifidobacterium bifidum* PRL2010 showed no growth at all (see Figure 70).
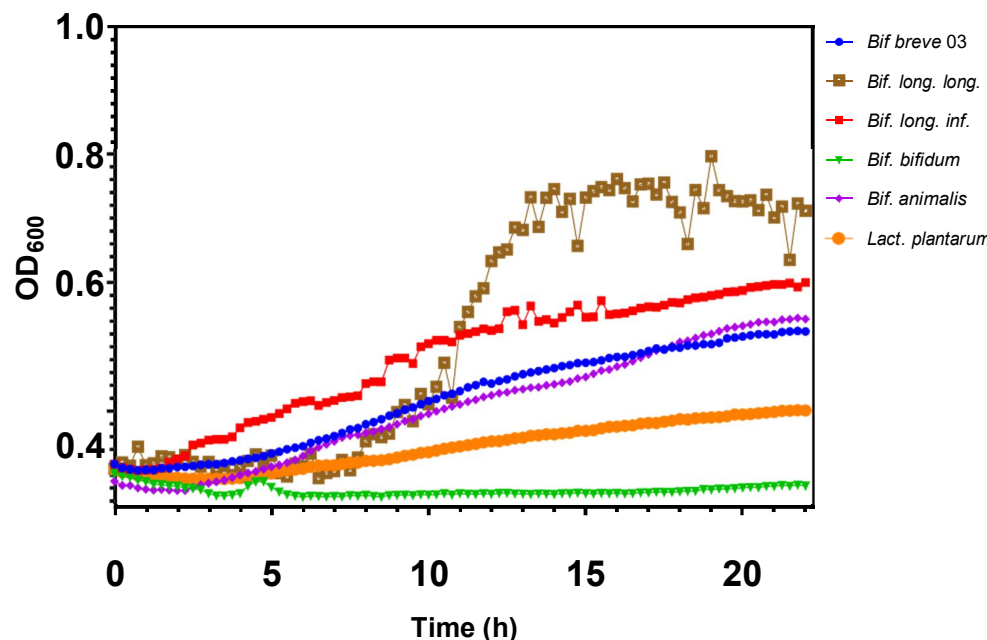
Figure 70. Growth curves of *Bifidobacterium* sp. and *Lactiplantibacillus plantarum* WCFS1 using supernatant of *Bacteroides cellulosyliticus* WH2 as carbon source.

131

The supernatant obtained from *Ba. thetaiotaomicron* VPI 5482 led to similar results, just with a significant increment in the growth of *Bifidobacterium longum* subsp. *infantis* (Figure 71). The last supernatant, from *Ba. vulgatus*, produced very interesting data because only *Bifidobacterium longum* subsp. *longum* NCIMB 8809 reached an important growth rate (Figure 72).
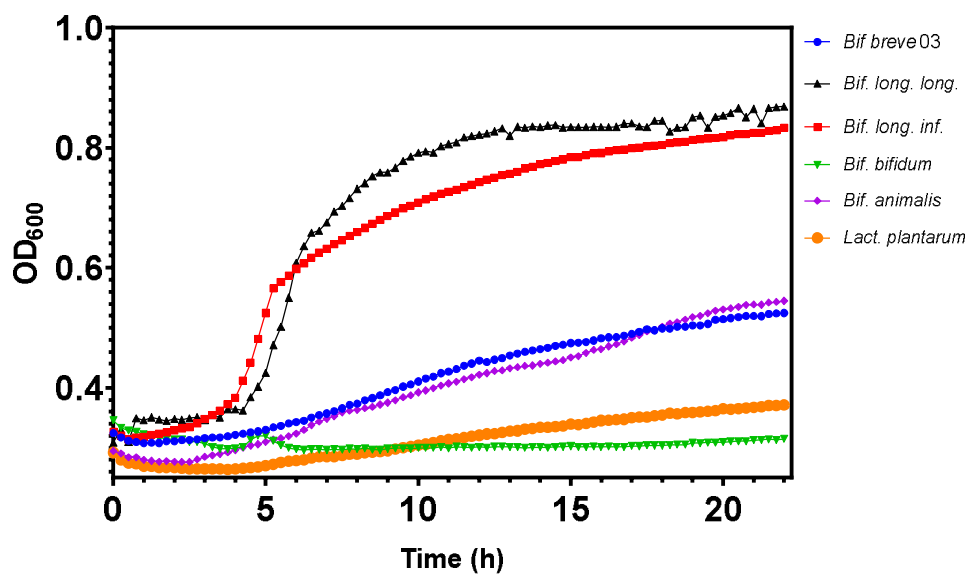
Figure 71. Growth curves of *Bifidobacterium* sp. and *Lactiplantibacillus plantarum* WCFS1 using a supernatant of *Bacteroides thetaiotaomicron* VPI 5482 as carbon source.
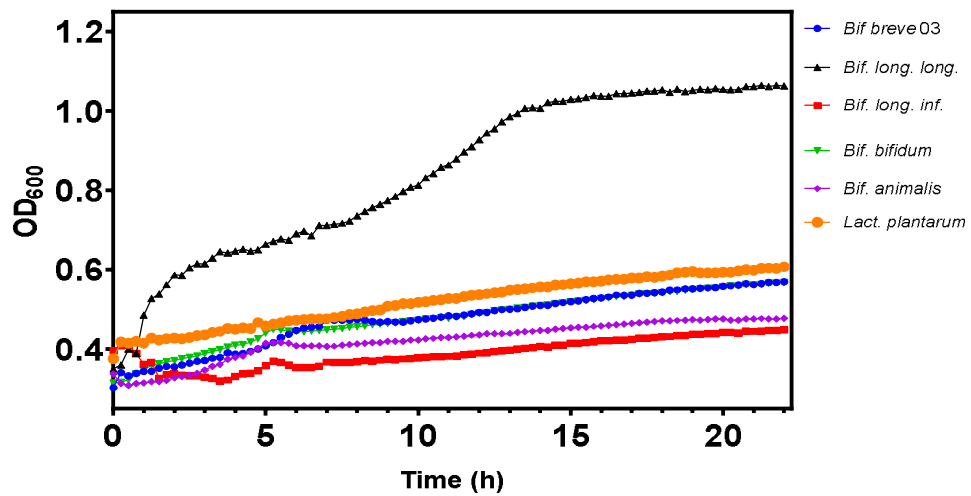
Figure 72. Growth curves of *Bifidobacterium* sp. and *Lactiplantibacillus plantarum* WCFS1 using a supernatant of *Bacteroides vulgatus* ATCC 8482 as carbon source.

The differences in the utilization of these supernatants by *Bifidobacterium* sp. suppose a proof that cross-feeding relationships are established specifically between different bacteria genera since the *Bacteroides* sp. digestion products are used differently by *Bifidobacterium* sp. Not all bifidobacteria are supported by all supernatants neither these supernatants promoted all bifidobacteria.

The chromatogram below (Figure 73) shows a comparison between the supernatant obtained from a culture of *Ba. cellulosyliticus* WH2 and the same supernatant after it was used as a carbon source for *Bifidobacterium longum* subsp. *longum*, which was the *Bifidobacterium* with the highest growth rate in the plater reader when using *Bacteroides* supernatants (see Figure 70). It is to be noted that the presence of the secondary degrader *Bifidobacterium longum* subsp. *longum* decreased the intensity of the oligosaccharides, causing the disappearance of some of them that appeared in the original supernatant (Figure 73, see square brackets).
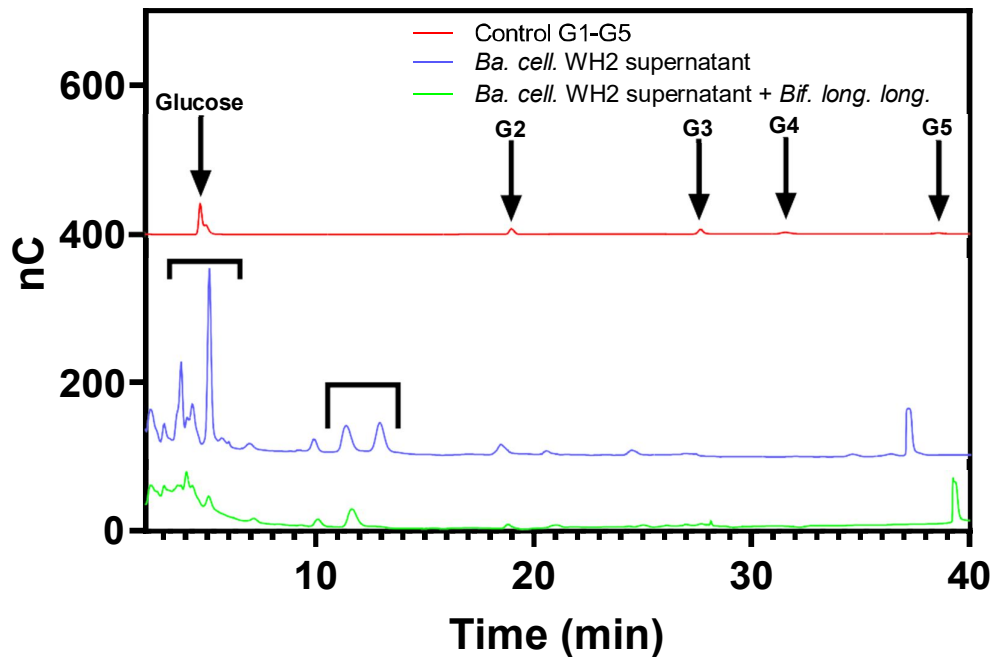
Figure 73. HPLC chromatogram of the supernatant obtained from a culture of *Ba. cellulosyliticus* WH2 and the same supernatant after inoculum of *Bifidobacterium longum* subsp. longum NCIMB 8809.

In the case of the supernatant obtained from *Ba. thetaiotaomicron* VPI 5482, the bacterium *Bifidobacterium longum* subsp. *longum* decreased the intensity of the oligosaccharides (Figure 74, see square brackets), even leading to the disappearance of some of them that appeared in the original supernatant.
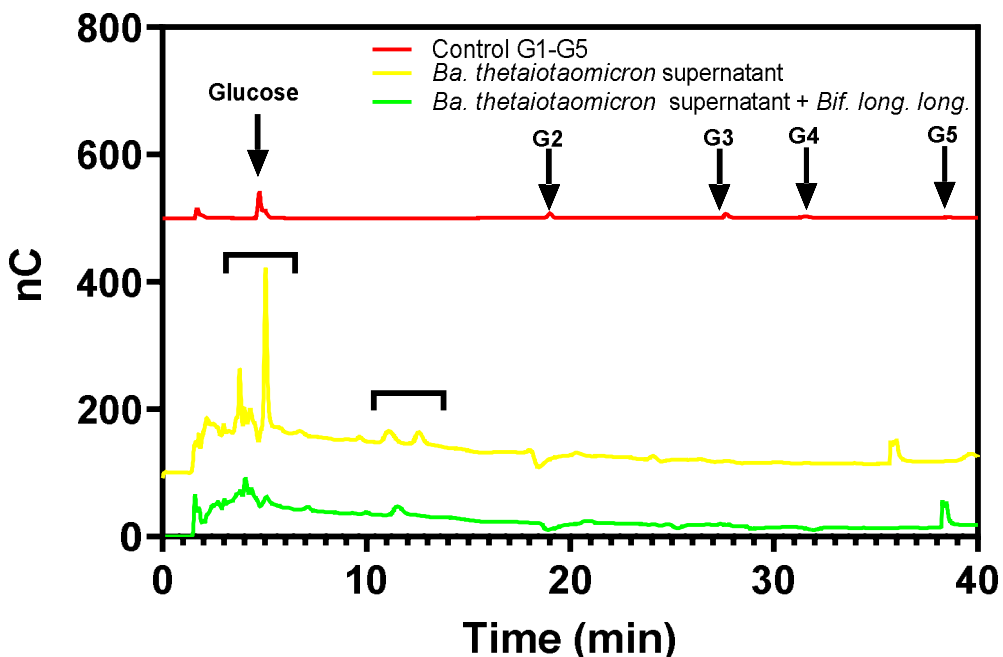
Figure 74. HPLC chromatogram of the supernatant obtained from a culture of *Ba. thetaiotaomicron* VPI 5482 and the same supernatant after inoculum of *Bifidobacterium longum* subsp. *longum* NCIMB 8809.

3.3.4 Designing experiments in minimal media containing supernatants from *Roseburia* sp. (main degraders or donors) as a carbon source to establish if *Bifidobacterium* sp. and *Lactiplantibacillus plantarum* WCFS1 (as secondary degraders or acceptors) can grow

Additionally, supernatants from *Roseburia intestinalis* and *Roseburia inulinovorans* were also filtered and given to bifidobacterial species as carbon source. The graph below reflects the growth of the bifidobacterial species with each supernatant. The supernatant from *Roseburia intestinalis* promoted intensely *Bifidobacterium breve* 17 and *Bifidobacterium adolescentis,* while *Bifidobacterium breve* 03 and *Bifidobacterium animalis* DSM 20104 showed soft growth (Figure 75).

In the case of *Roseburia inulinovorans,* the supernatant promoted all bifidobacterial species, with *Bifidobacterium adolescentis, Bifidobacterium breve* 17

and *Lactiplantibacillus plantarum* WCFS1 as the best users (Figure 75). *Roseburia inulinovorans* prevailed as a better donor than *Roseburia intestinalis*. However, both species showed a good ability to help the growth of secondary beneficial bacteria such as *Bifidobacterium* and *Lactiplantibacillus plantarum* WCFS1. The observed variations are due to the genomic differences, and it is necessary for a total clarification that explains deeply this behaviour, but the required studies and time largely exceed the resources of this research project.
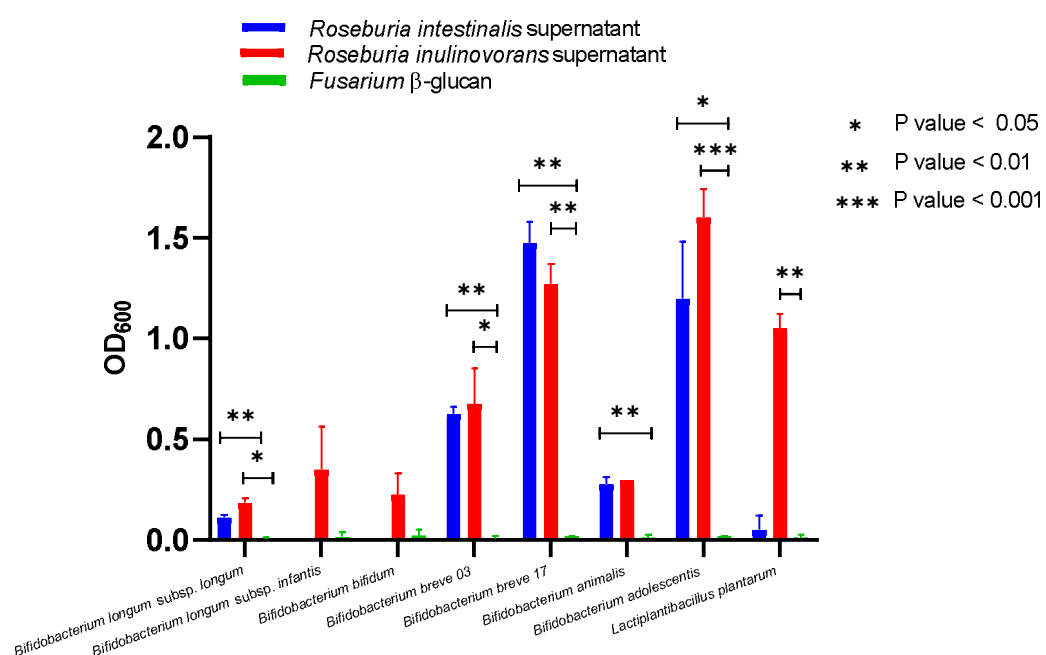
Figure 75. Growth of six *Bifidobacterium* sp. with supernatants obtained from *Roseburia intestinalis* and *Roseburia inulinovorans*.

3.3.5 Designing co-culture experiments in minimal media containing *Bacteroides* sp. as the main degrader and *Bifidobacterium* sp. and *Lactiplantibacillus plantarum* WCFS1 as a secondary degrader

Although the potential prebiotic effect of the β-glucan was detected previously once bifidobacterial species grew in supernatants of *Bacteroides*, the coexistence of both bacteria in the same culture media was also tested to have a better proof of the syntrophic relation between them. Since the human gut behaves as a dynamic environment where millions of different species live together, it was essential to have in situ both bacteria at the same time.

Using 50 mL cultures of minimal media with 1 mg/mL of β-glucan, different species of *Bacteroides* and *Bifidobacterium* were grown together at the same time. The growth and presence of both were detected in two different ways: firstly, using specific selection media for each, BHI supplemented with 20 μg/mL ampicillin, in the case of *Bacteroides,* and MRS supplemented with 10 μg/mL mupirocin, in the case of *Bifidobacterium*; secondly, via the detection of 16S rRNA of each bacterial specie using qPCR.

***Bacteroides cellulosyliticus* WH2-*Bifidobacterium longum* subsp. *longum* NCIMB 8809**

The choice of this pair of bacteria lies in the fact that *Bifidobacterium longum* subsp. *longum* NCIMB880 presented the best growth rate among all employed bifidobacterial species (see section 3.3.3, Figure 70). The Figure 76 below shows how, in a period of 30 hours, both species could grow in minimal media where *Fusarium* β-glucan was the unique carbon source. The total amount of both bacteria, measured by counting the colony forming units, increased in both species, showing a faster growth during the first 10 hours and a stabilization period until the end. The number of colonies for *Ba.*

cellulosyliticus WH2 remained higher than *Bifidobacterium* for the total duration of the experiment (see Figure 76).
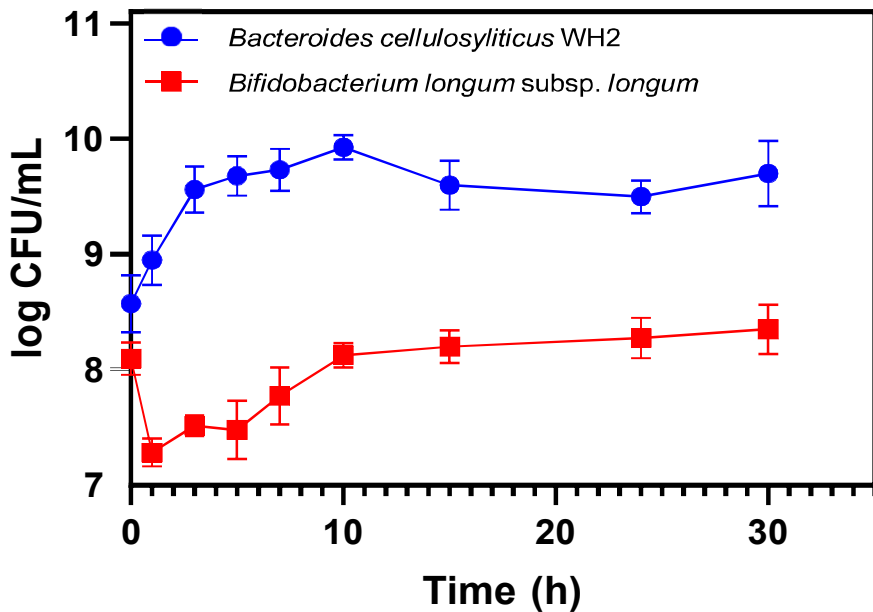
Figure 76. Colony forming units of *Ba. cellulosyliticus* WH2 and *Bi. longum* subsp. *longum* NCIMB 8809.

If we only consider the relative abundance (see Figure 77 below) obtained by qPCR, it could be observed that the relative amount of *Ba. cellulosyliticus* WH2 in the media decreased while the relative abundance of *Bifidobacterium longum* subsp. *longum* suffered a soft increase. This decrease does not mean necessarily that *Bacteroides* is dying in the culture, since the number of colonies showed an increase, but it must be taken as proof of the existence of a symbiotic relationship between bacteria that led to a bigger increase in the case of *Bifidobacterium*. The secondary degrader, in the end, needs the primary degradation by *Bacteroides* over the intact polymer chain of *Fusarium* β-glucan to have access to the digestion products that will be used as its carbon and energy source. Considering the data obtained in this experiment, together with the previous cultures in which the supernatants acted as carbon source, it can be

concluded that this pair of bacteria established a positive and symbiotic cross-feeding relation between them, with the final persistence of both in the media.
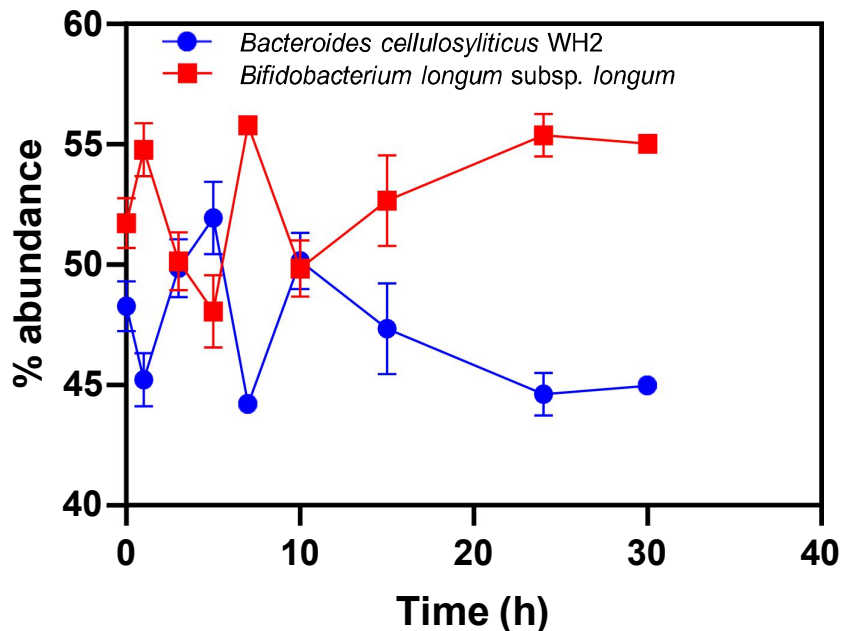
Figure 77. Percentage of *Ba. cellulosyliticus* WH2 and *Bi. longum* subsp. *longum* NCIMB 8809.

Bacteroides cellulosyliticus WH2-*Bifidobacterium longum* subsp. *infantis* ATCC 15697

Having in mind the growth obtained for *Bifidobacterium longum* subsp. *infantis* ATCC 15697 when using just the supernatant obtained from *Ba. cellulosyliticus* WH2 (see section 3.3.3), a similar cross-feeding experiment was carried out to compare both subspecies of bifidobacterial with *Ba. cellulosyliticus* WH2. In this case, it was observed an increase in the total number of colonies (see Figure 78 below), although the count of *Bacteroides* decreased during the first three hours, with the number of bifidobacterial increased more than *Bacteroides*. This fact supposes a significant difference from the previous experiment which reported more colonies of *Bacteroides* than *Bifidobacterium*.
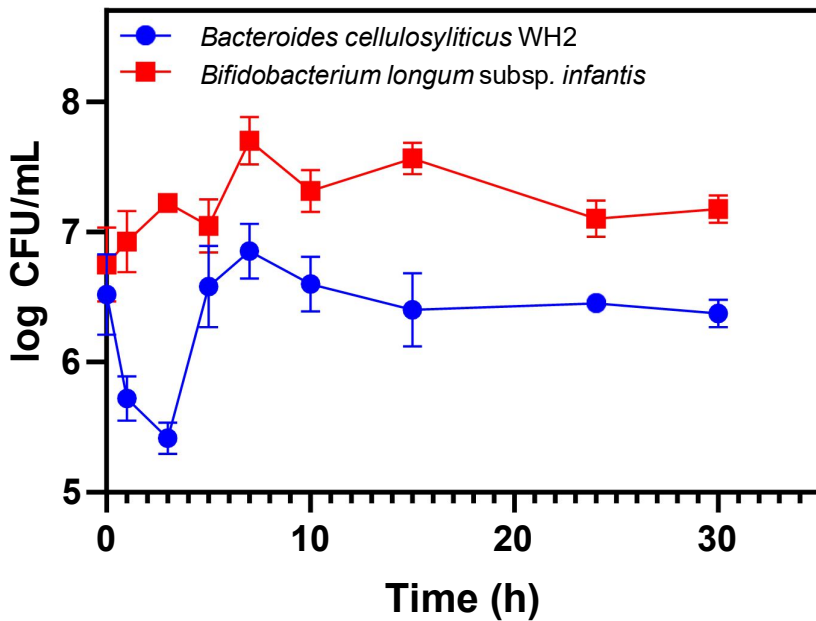
Figure 78. Colony forming units of *Ba. cellulosyliticus* WH2 and *Bi. longum* subsp. *infantis* ATCC 15697.

Focusing on the relative abundance provided by the qPCR, *Ba. cellulosyliticus* WH2 experienced a decrease in its relative abundance compared with *Bifidobacterium longum* subsp. *infantis*, which ended the culture with higher values. As it happened in the previous study, here the number of colonies for both bacteria increased while the qPCR assays reflected an increase in bifidobacterial abundance. *Bifidobacterium longum* subsp. *infantis* seems to be supported by the presence of *Ba. cellulosyiticus* WH2, but there is no growth inhibition between them. Both bacteria interact with each other in a cross-feeding relation, which allowed them to persist, taking advantage of the same substrate, *Fusarium* β-glucan (See Figure 79 below).
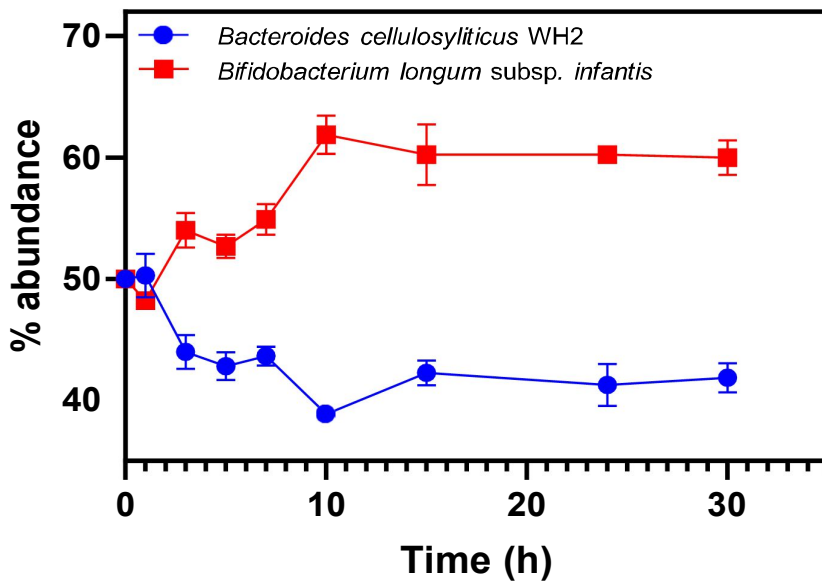
Figure 79. Percentage of *Ba. cellulosyliticus* WH2 and *Bi. longum* subsp. *infantis* ATCC 15697.

Both subspecies of *Bifidobacterium longum* seems to be supported by the presence of *Ba. cellulosyiticus* WH2. Nevertheless, the culture experiments using the supernatants underlined better values than *Bifidobacterium longum* subsp. *infantis*. Focusing on the number of colonies, *Bifidobacterium longum* subsp. *longum* showed better numbers than *Bifidobacterium longum* subsp. *infantis*. However, the relative abundance underlined a major increase for *Bifidobacterium longum* subsp. *infantis* when 16S RNA is measured.

For this reason, the results obtained for both pairs of bacteria, together with the data obtained for the previous experiment using the supernatants as carbon source (see section 3.3.3), highlighted *Bifidobacterium longum* subsp. *infantis* as a better user of the products released by *Ba. cellulosyliticus* WH2, compared to *Bifidobacterium longum* subsp. *longum*.

141

The combination of culture techniques, employing specific antibiotic resistance, and molecular biology techniques, gives a wide and fulfilled vision of the interactions between bacteria. Nevertheless, the mechanism(s) underneath this divergence among two *Bifidobacterium* sp. are beyond the scope of this thesis, but they suggest that the genomic differences between them may play an important role in this distinct feeding behaviour.

Bacteroides cellulosyliticus WH2-*Lactiplantibacillus plantarum* WCFS1

The last set of experiments for *Ba. cellulosyliticus* WH2 included *Lactiplantibacillus plantarum* WCFS1 as a secondary degrader bacterium belonging to the Bacillota phylum, and which differs considerably from the previous *Bifidobacterium* sp.

Firstly, the counting of the colony-forming units highlighted a major amount of *Bacteroides* than *Lactiplantibacillus*. Nevertheless, it must be considered that the range of values was bigger for both bacteria compared with the previous two sets of experiments (Figure 80).
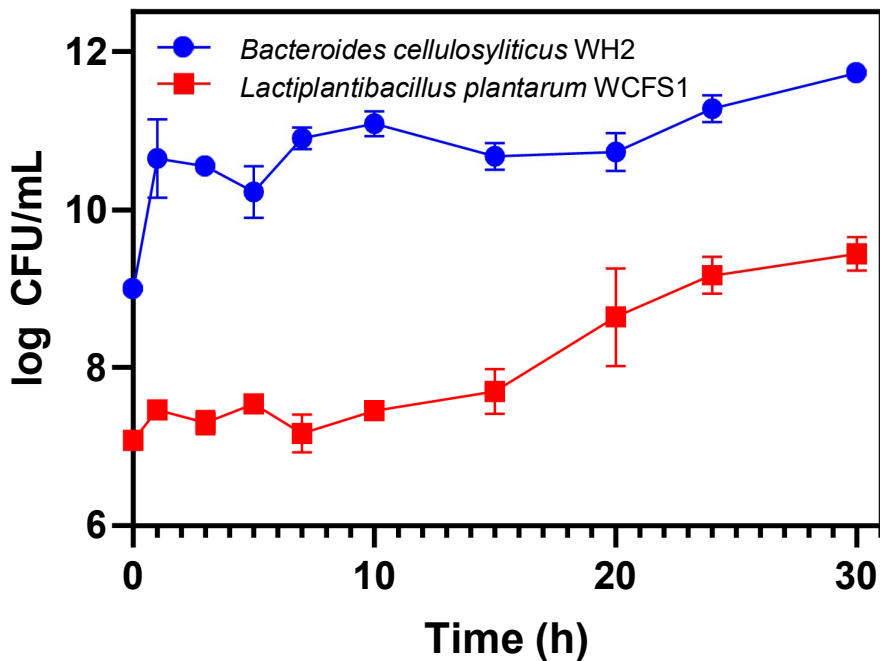
Figure 80. Colony forming units of *Ba. cellulosyliticus* WH2 and *Lactiplantibacillus plantarum* WCFS1.

Furthermore, the qPCR reflected a major value of relative abundance for *Lactiplantibacillus,* which showed a soft decrease in the last hours of co-culture. The graph below underlines good coordination between both bacteria during the first ten hours. Nevertheless, since that moment the main degrader, *Ba. cellulosyliticus* WH2 takes prevalence over *Lactiplantibacillus* (see Figure 81 below).
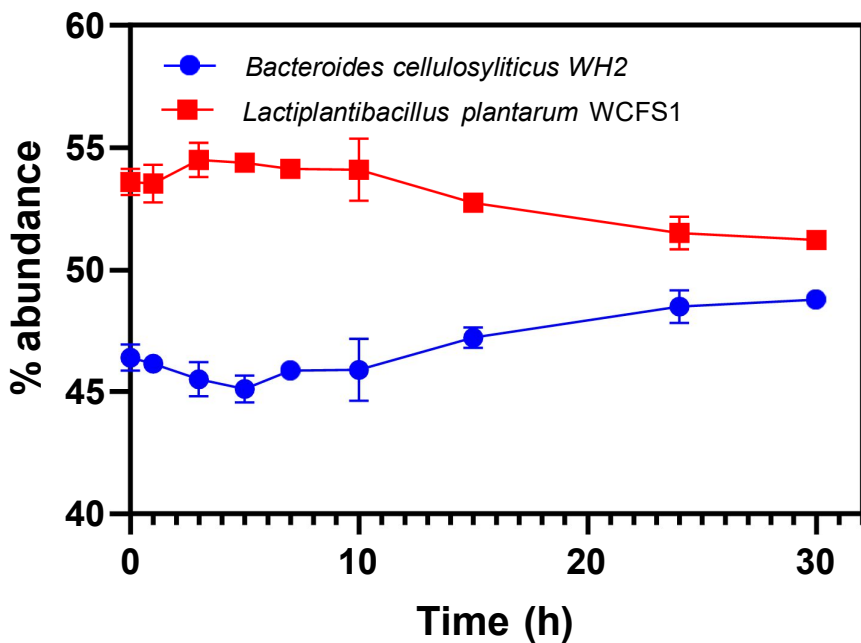
Figure 81. Percentage of *Ba. cellulosyliticus* WH2 and *Lactiplantibacillus plantarum* WCFS1.

Even though *Ba. cellulosyliticus* WH2 has more colony forming units, the abundance in qPCR experiments seems to be lower than *Lactiplantibacillus.* This fact may be related to an excessive use of the antibiotic vancomycin for the selection of *Lactiplantibacillus*, but the search of the exact solution would need more in-depth research.

To summarize, *Ba. cellulosyliticus* WH2 was proven as a good donor to three different bacteria, promoting the growth and persistence of all of them. Nevertheless, it is difficult to choose one over another since a combination of two different methods implies a deeper analysis.

Lactiplantibacillus plantarum WCFS1 reported higher values in the counting of colony-forming units. However, it was impossible to obtain the same initial number of colony-forming units, which makes it difficult the comparison among bacteria. Moreover, it must be exposed the fact that the genera *Bifidobacterium* and *Lactiplantibacillus* are composed of bacteria that differs both genetically and phenotypically. The capacity to be cultured in agar media from a taken aliquot is variable depending on the used bacteria. Even if each bacterium can form an individual colony on the agar plate, the mechanisms to avoid the antibiotic are different, and it is a mistake to think that bacteria belonging to different phyla will show the same ability to achieve their respective survival.

Therefore, *Ba. cellulosyliticus* WH2 is a donor of oligosaccharides to different bacteria from diverse genera and phyla, while the full description of its preferred secondary recipients remains still unclear and needs a deeper investigation. The huge diversity and variability within the Human Gut Microbiota make it a vast source of discoveries that can have applications in our way to understand bacterial behaviour and microorganism interactions.

Bacteroides thetaiotaomicron VPI 5482-*Bifidobacterium longum* subsp. *longum* NCIMB 8809

The second main degrader employed in these cross-feeding experiments was *Ba. thetaiotaomicron* VPI 5482. For the first secondary degrader, *Bifidobacterium longum* subsp. *longum* NCIMB 8809, the co-culture revealed a good ability for both bacteria to increase their colonies counting during the experiment (see Figure 82 below). The total increase for *Bifidobacterium* was bigger than *Bacteroides*, although the total number of colonies was much bigger for the main degrader.

Symbiosis was observed during a longer period than in the case of *Ba. cellulosyliticus* WH2, because the bifidobacteria rose constantly for 48 hours, instead of the previous 30 hours used in the experiment with *Ba. cellulosyliticus* WH2. This fact is in accordance with the previous data obtained in the section 3.3.3, since *Bifidobacterium longum* subsp. *longum* exhibited the best growth rate among all the studied bacteria in the monitored plate reader using the supernatant from *Ba. thetaiotaomicron* VPI 5482 (see section 3.3.3).

Compared with the previous set of experiments, which comprised *Ba. cellulosyliticus* WH2 and *Bifidobacterium longum* subsp. *longum,* the number of bifidobacterial colonies was higher when *Ba. thetaiotaomicron* VPI 5482 acted as the main polysaccharide degrader and *Bifidobacterium longum* subsp. *longum* as secondary degrader.
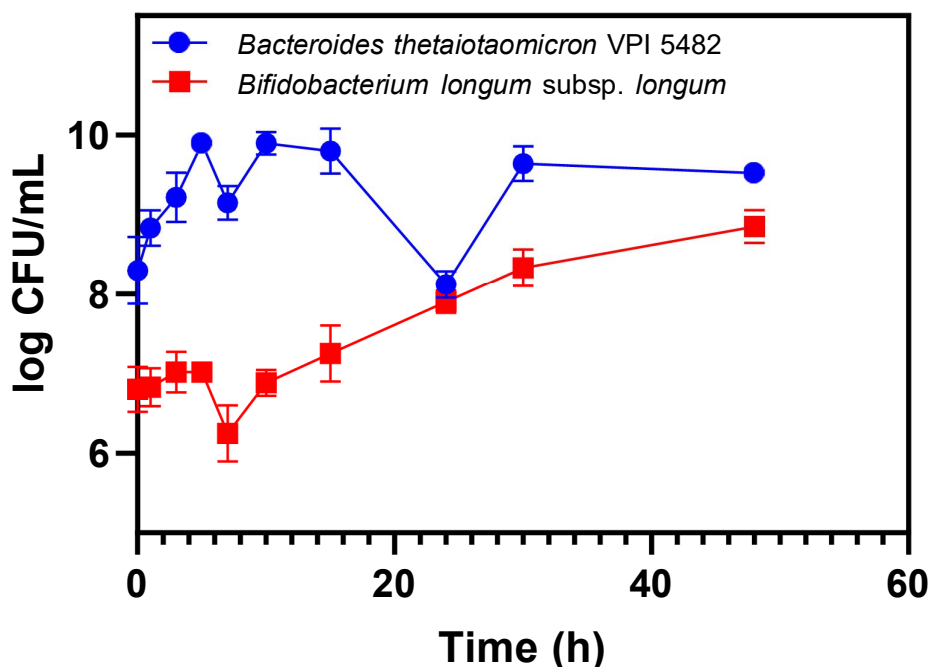
Figure 82. Colony forming units of *Ba. thetaiotaomicron* VPI 5482 and *Bi. longum* subsp. *longum* NCIMB 8809.

The qPCR data (see Figure 83 below) reflected initial variations in the relative abundance of both bacteria, with ups and downs during the first hours of study. After this, *Bacteroides* prevailed over the secondary degrader *Bifidobacterium.* This is in accordance with the data shown previously in the counting of colony-forming units.
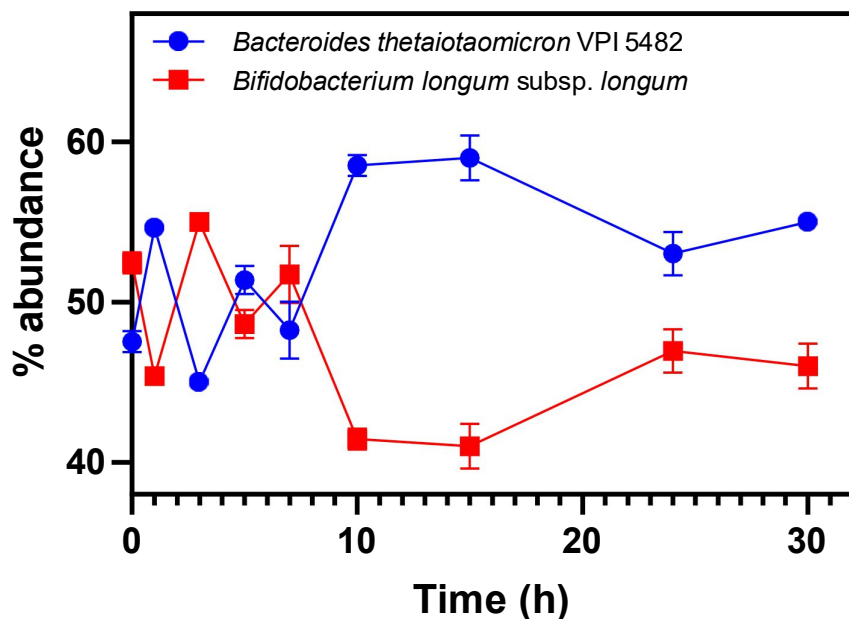
Figure 83. Percentage of *Ba. thetaiotaomicron* VPI 5482 and *Bi.longum* subsp. *longum* NCIMB 8809.

Bacteroides thetaiotaomicron VPI 5482-*Bifidobacterium longum* subsp. *infantis* ATCC 15697

In the case of *Bifidobacterium longum* subsp. *infantis* ATCC 15697 both bacteria grew together with good rates (see Figure 84 below) values, showing an increasing number of colonies with the past of the time, in a similar way to *Ba. cellulosyliticus* WH2. Nevertheless, in this case *Bacteroides* disposed of more colonies than *Bifidobacterium*, although it was previously reported that this *Bifidobacterium* had higher values of colony forming units counting than *Ba. cellulosyliticus* WH2 (see Figure 78).
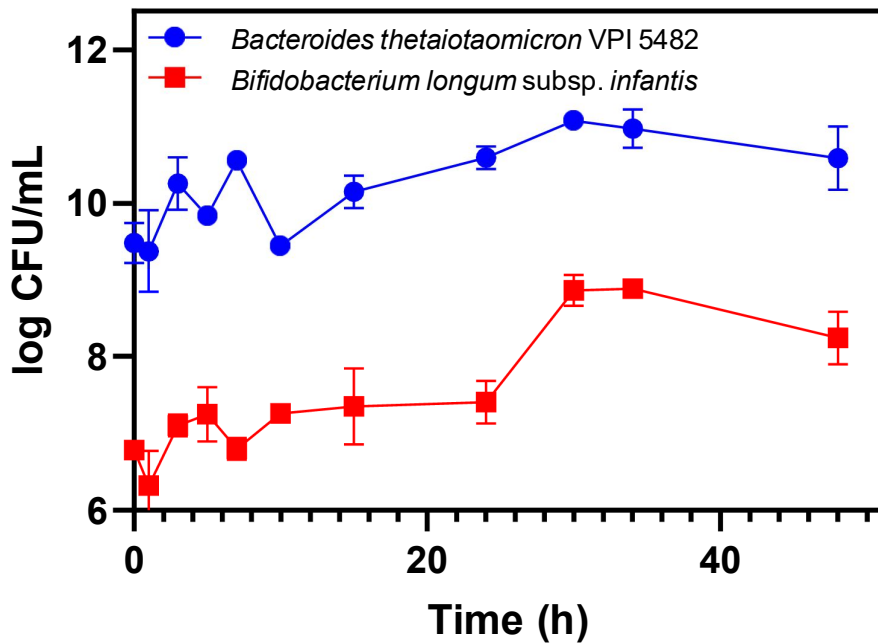
Figure 84. Colony forming units of *Ba. thetaiotaomicron* VPI 5482 and *Bi. longum* subsp. *infantis* ATCC 15697.

Furthermore, the relative abundance of *Bifidobacterium longum* subsp. *infantis* was reduced in the qPCR. On contrary, *Bacteroides thetaiotaomicron* was increased in abundance during the total duration of the experiment (see Figure 85 below).

In addition, *Ba. thetaiotaomicron* showed a similar behaviour when coculturing with both subspecies of *Bifidobacterium longum*. *Ba. thetaiotaomicron,* contributed to an increase in the number of colonies of bifidobacteria, the secondary degrader, but keeping bifidobacteria relative abundance under the quantity of the main degrader.
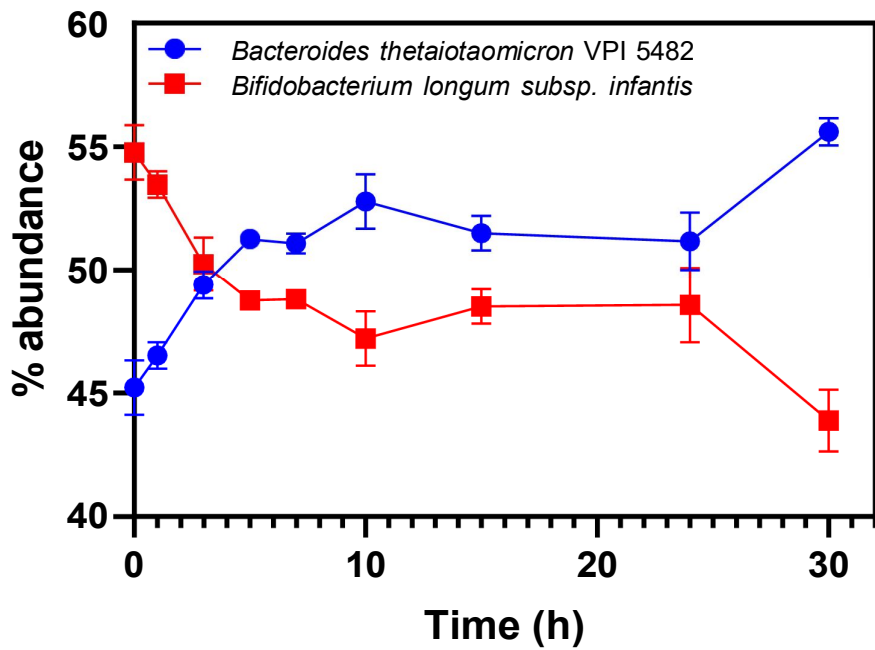
Figure 85. Percentage of *Ba. thetaiotaomicron* VPI 5482 and *Bi. longum* subsp. *infantis* ATCC 15697.

Bacteroides thetaiotaomicron-Lactiplantibacillus plantarum WCFS1

The last pair of bacteria employed was the combination of *Ba. thetaiotaomicron* VPI 5482 with *Lactiplantibacillus plantarum* WCFS1. The counting of colony-forming units revealed interesting results, with both bacteria growing similarly, although *Bacteroides* sp. finished with slightly higher values (see Figure 86 below).
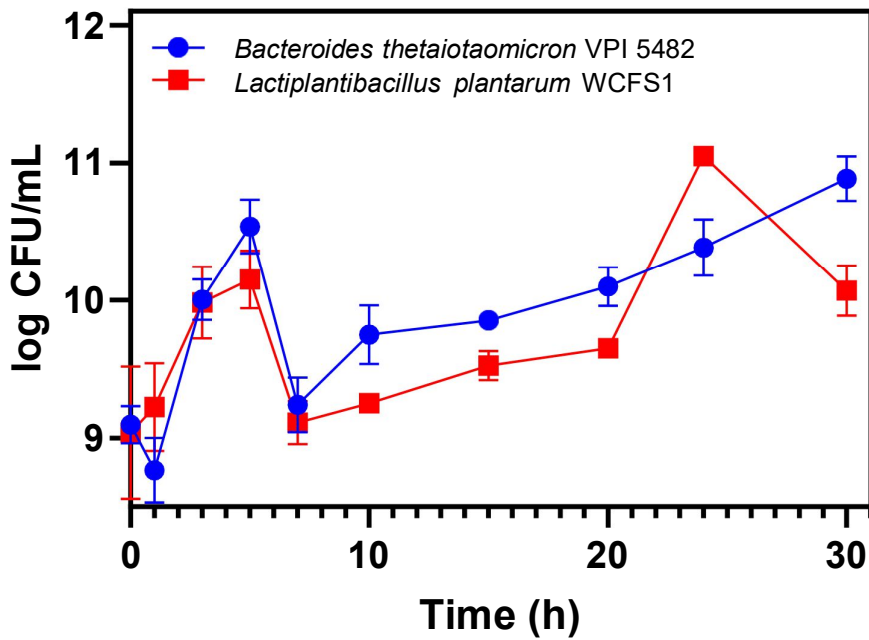
Figure 86. Colony forming units of *Ba. thetaiotaomicron* **VPI 5482 and** *Lactiplantibacillus plantarum* **WCFS1.**

The qPCR revealed that both bacteria abundances were kept practically constant, showing *Lactiplantibacillus plantarum* WCFS1 higher values than *Bacteroides* sp. (see Figure 87 below). The reason for this difference between the results shown in the counting of colony forming units and the qPCR data may lie in the different ability of each microorganism to be cultured in agar plates, and the different tolerance of each one to their selection antibiotic, although the clarification of this discrepancy would require further investigation.
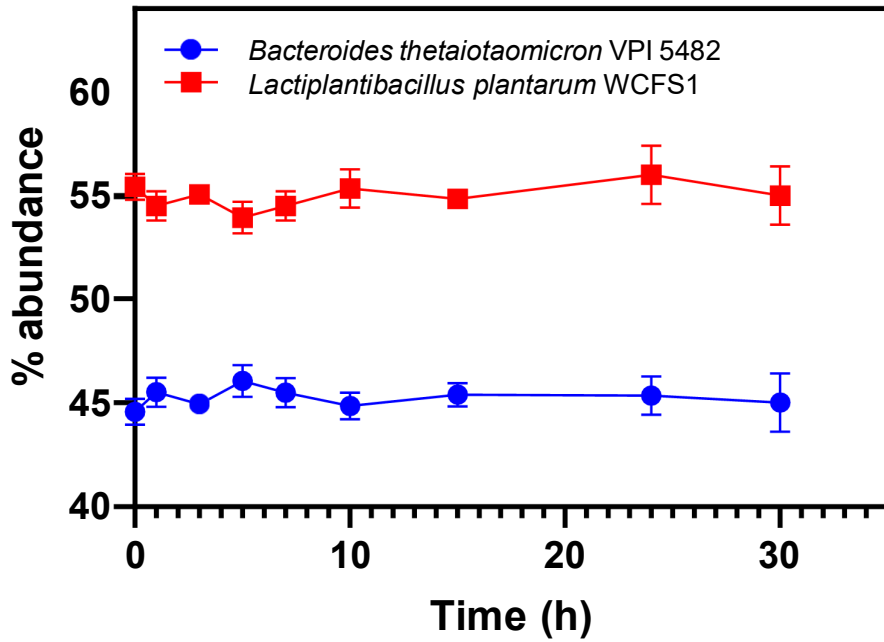
Figure 87. Percentage of *Ba. thetaiotaomicron* VPI 5482 and *Lactiplantibacillus plantarum* WCFS1.

An increase in the colony forming units was observed for *Lactiplantibacillus* when coculturing it with both *Bacteroides* sp. (see Figures 80 and 86). Nevertheless, the qPCR data did not reflect such increase in the abundance of *Lactiplantibacillus* in any of both *Bacteroides* sp. (see Figures 81 and 87).

Granted the difficulty of comparing different bacteria with the data revealed by colony counting and qPCR, it can be said that the different set of experiments with main and secondary degraders revealed the existence of cross-feeding relations with *Fusarium* β-glucan as carbon source. The determination of the best pair of bacteria for the cross-feeding supposes a complex task for which in-depth research is required.

4 Discussion

The HGM comprises a highly competitive and complex environment, where a multitude of diverse bacteria species coexist together. The variable nature of these interactions has been studied deeply, resulting in many beneficial effects correlated with these bacteria. Therefore, the microorganisms dwelling in the human gut constitute an important tool whose analysis and understanding may lead to healthy applications.

The aim of section 3.1 was the novel extraction and purification of *Fusarium* β-glucan, the main ingredient employed in Quorn® products whose chemical structure consists of a linear β-(1,3)-glucan backbone with β-(1,6)-glucan as side chains. This allowed the total isolation of it, separating the clean substrate from the rest of the components of mycoprotein before its use in further experiments. Subsequently, this novel polysaccharide, once isolated from the rest of the components, was employed as carbon source for the cell growth of different bacteria species belonging to the HGM. The culture of *Bacteroides* sp., which is a bacteria genus whose members have been widely described as polysaccharide degraders, revealed a broad ability for the utilization of this carbohydrate. Furthermore, the data accomplished in this thesis highlighted the variability within the genus *Bacteroides*, since differences were observed in their growth rates when using this substrate. The presence of PULs located within the genome of *Bacteroides* explains these variations, because the number of genes encoding enzymes involved in polysaccharide degradation, such as glycoside hydrolases and polysaccharide lyases, is different depending on which *Bacteroides* sp. is used.

It should be noted that not only members of genus *Bacteroides* were shown as degraders of *Fusarium* β-glucan. Other bacteria such as *Roseburia intestinalis* DSM 14610, *Roseburia inulinovorans* DSM 16841, *Akkermansia muciniphila* DSM 22959 or *Victivallis vadensis* ATCC BAA-548 also manifested the capacity to grow with this carbohydrate. The genus *Roseburia*, together with the mentioned *Akkermansia,* has been related to multiple beneficial effects, a fact that supports the potential as a prebiotic of mycoprotein. Moreover, *Victivallis vadensis* is a bacterium that has a high number of genes encoding glycoside hydrolases, although just a few publications have focused on it. Therefore, the acquired data provided further evidence that *Fusarium* β-glucan exhibited a prebiotic role, acting as a carbon and energy source for a wide spectrum of beneficial bacteria in the human gut which could use it.

Section 3.2 was focused on the determination of the differential gene regulation and protein expression triggered by *Fusarium* β-glucan. The proteomics assays, together with the study of the kinetic parameters associated with the glycoside hydrolases, supposes an essential tool to discover the mechanisms and metabolic pathways involved in the digestion of *Fusarium* β-glucan. Proteomics analysis was developed on *Ba. cellulosyliticus* WH2 and *Ba. vulgatus* ATCC 8482 grown on glucose (acting as reference) or *Fusarium* β-glucan as carbon sources, to identify proteins that exhibit increased expression when the strains were grown on the complex polymer. This analysis revealed that all proteins encoded by two PULs in *Ba. cellulosyliticus* WH2 (representing locus tags BcellWH2_01929-BcellWH2_01932 and BcellWH2_02537-BcellWH2_02542, respectively) exhibit increased expression when *Ba. cellulosyliticus* WH2 was grown on *Fusarium* β-glucan metabolism (when compared to growth on glucose). The first PUL was predicted to encode two GH3 enzymes (BcellWH2_01926 and BcellWH2_01927) and a GH157 member

153

(BcellWH2_01931), while the proteins encoded by locus tags BcellWH2_01928 and BcellWH2_01929 represent the SusC/D-like pair predicted to be involved in polysaccharide substrate binding and recognition at the bacterial cell surface. The second PUL encodes a GH30_3 (BcellWH2_02537, a predicted endo-β-1,6-glucanase according to the CAZY database), a GH2 (BcellWH2_02541) and a protein without known function (BcellWH2_02538). In addition to these proteins, BcellWH2_02539 and BcellWH2_02540 represent the predicted SusC/D pair in the second PUL.

In the case of *Ba. vulgatus* ATCC 8482, two PULs showed higher expression when grown on *Fusarium* β-glucan (representing locus tags BVU_0839-BVU_0844 and BVU_1150-BVU_1153, respectively). The first PUL was predicted to encode two GH30_4 enzymes (BVU_08043 and BVU_08044) and a protein without known function (BVU_08040). The proteins encoded by locus tags BVU_08041 and BVU_08042 represent the SusC/D-like. The second PUL encodes a GH2 (BVU_1151, a predicted endo-β-1,6-glucanase according to the CAZY database), while BVU_1152 and BVU_1153 represent the predicted SusC/D pair.

To confirm the proteomics data, *Ba. cellulosyliticus* WH2 was grown and performed RT-qPCR on selected SusC/D pairs identified in the above described PULs. Since differential expression was observed on RT-qPCR, it seems that their corresponding PULs are responsible for growth on fungal β-glucan.

The next set of experiments involved the cloning and protein expression for the GHs encoded in those genes of *Ba. cellulosyliticus* WH2. This unveiled a wide range of catalytic activities and specificities, with different enzymes working together, acting as parts of complex cascades, to digest and break the mentioned polysaccharide. As it was mentioned before, *Ba. cellulosyliticus* WH2 used two PULs to degrade this

Fusarium β-glucan, as revealed by proteomics. Within these PULs, *Ba. cellulosyliticus* WH2 encodes a novel GH157 (BcellWH2_01931) and a GH30_3 (BcellWH2_02537), both predicted to be located at the cell surface, to start the degradation of the complex glycan. These PULs were also shown to encode additional glycoside hydrolases required to fully degrade the oligosaccharides released by the outer membrane surface proteins and incorporated into the periplasm by the SusC/D-like pairs. These periplasmic proteins represent typical β-glucosidases belonging to GH families 3 and 2. Particularly interesting is the case of BcellWH2_02538, an unknown protein with a predicted location to be in the surface of *Ba. cellulosyliticus* WH2 and which was firstly assigned to a described catalytic activity in this thesis. This protein is in a perfect location to be a Surface Glycan Binding Protein (SGBP), which has been shown to help the SusC/D-like pair in the binding of oligosaccharides at the bacterial cell surface. The determination of its structure and biological function make it clear the fact that the employment of new types of substrates would amplify the number of families and subfamilies of enzymes harboured in CAZy. The reason for the presence of three different β-glucosidases (two GH3 and one GH2) encoded by these PULs to target fungal β-glucan remains unclear. *Ba. cellulosyliticus* WH2 could act on several types of β-glucans, not only fungal sources, with different chemical structures. For that reason, the bacterium use distinct β-glucosidases to hydrolyse different linkages in these oligosaccharides. However, these β-glucosidases might be redundant and the bacterium is evolving to remove some of these genes from its genome under the high selection pressure imposed by the gut environment. The presence of different catalytic activities involved in the metabolism of *Fusarium* β-glucan acts as proof of the metabolic machinery arranged by gut bacteria which allows the growth with this substrate. These complex molecular interactions, at a molecular level, make possible

the key and fundamental obtention of energy which, in the end, allows the survival of both our microbiota and us.

The aim of section 3.3 was to elucidate the digestion products released during the bacterial metabolism of *Fusarium* β-glucan and determine the cross-feeding relations established with it. This purpose was achieved via the purification and isolation of the supernatants obtained from the cultures of *Bacteroides* sp. and other bacteria. This allowed the further structural analysis and identification of the oligosaccharides released as digestion products. In addition, metabolomics analysis of the culture media to assess short chain fatty acid (SCFA) using the GC/MS showed the production of SCFAs, mainly propionate and acetate by *Bacteroides* sp. There are a lot of studies which emphasise the beneficial effects related to the SCFAs production, such as anti-inflammatory cytokine production and immune regulation, among others. Furthermore, it should be also noted the implications of SCFAs as neuromodulators, since they target the gut-brain axes and enhance serotonin production, which affects behaviour, memory and learning. Accordingly, the digestion products associated with *Fusarium* β-glucan may display several healthy effects. Given this fact we should delete the traditional concept of mycoprotein as a simple food product, changing to a microbial substrate whose employment might lead to multiple health outcomes.

The digestion products of *Bacteroides* sp., contained in the filtered supernatants, were then utilized in minimal media as a potential substrate for *Bifidobacterium* sp. and *Lactiplantibacillus plantarum* WCFS1, both bacteria species which lacked the intrinsic ability to use the polymer. The growth curves showed that these secondary degraders could then use those digested by-products. For this reason, the next set of experiments was designed to establish cooperative co-cultures where different bacteria

species, main and secondary degraders, would use *Fusarium* β-glucan at the same time. This would simulate, on a minor scale, the substrate competitiveness in the human gut. The results showed that *Ba. cellulosyliticus* WH2 and *Ba. thetaiotaomicron* VPI-5482 can share oligosaccharides with other members of the gut microbiota. *Ba. cellulosyliticus* WH2 was shown to allow cross-feeding interactions with *Bi. longum* subsp. *longum*, *Bi. longum* subsp. *infantis* and *Lactiplantibacillus plantarum* WCFS1. In addition, *Ba. thetaiotaomicron* VPI-5482 was shown to promote specific cross-feeding with *Bi. longum* subsp. *longum*, *Bi. longum* subsp. *infantis* and *Lactiplantibacillus plantarum* WCFS1, enabling growth of both bacteria in co-culture. Since the oligosaccharides released by *Ba. cellulosyliticus* WH2 and *Ba. thetaiotaomicron* VPI-5482 are different (glucobiose and glucoheptose, respectively), it will select for specific interactions in the gut. The observed interactions demonstrated a symbiotic behaviour among bacteria, with both types of *Bacteroides* sp. supporting the growth of the secondary degraders which were then able to use *Fusarium* β-glucan as a carbon source in the co-culture. There was no signal of mutual repression between the studied bacteria. Furthermore, it is important to note that neither all *Bacteroides* sp. nor *Bifidobacterium* sp. were analysed to see the existence of cross-feeding interactions. That would be an impossible task to achieve in a three-years thesis project. This also strengthens the importance of broadening these studies in the future, filling them out with an increasing number of new species and potential substrates, to have a more completed and defined model of polysaccharide degradation by HGM.

Some limitations affect the scale and scientific purpose of the thesis, since the mechanism of action corresponding to the huge number of bacteria that live together conforming our microbiota cannot be extrapolated from an experiment involving just

a pair of them. Therefore, the mentioned studies are just minor-scale models of the real and multicomplex bacterial gut environment. Nevertheless, these experiments constitute the first step to achieve a better understanding of how bacteria are modulated, which might play an important role in the prevention of nutritious disorders and health problems. They also contribute greatly to the knowledge of fungus polysaccharides, whose importance has risen in the last few years. *Fusarium* mycoprotein showed a large variety of interesting characteristics, due to its low-fat content and high amounts of protein and fibre. In addition, *Fusarium* β-glucan obtained from mycoprotein supposes a novel substrate, whose potential as a bacterial carbon source was described for the first time in this study and whose type of bonds and structure differs from similar fungus polysaccharides reported in the past. Although several enzymes of *Bacteroides* sp. showed catalytic activity on *Fusarium* β-glucan, the total disclosure of cell wall structure of *Fusarium venenatum* remains unknown. The whole bacteria spectrum capable of its degradation still needs wider expansion.

Today, there is a worryingly high incidence of disorders related to fat-based diets and the excessive consumption of meat in western diets. This fact points out the need for healthy and non-invasive alternatives which may counteract both ecological and health problems, making urgent the search for better prevention techniques and novel treatments.

For that purpose, the desired solution might be achieved by interpreting our microbiota not just as simple microscopic individuals which inhabit our body, but as a useful tool whose utilization and modulation in our favour can lead us to a more advantageous and sustainable world. This would be a better way to target the creation of better compositions in the food industry, changing to more sustainable and environment-friendly production models and making easier its degradation by beneficial gut

microorganisms, modifying our microbiota and reducing antibiotic overuse.

The data shown in this thesis contributes to this aim, serving as the first of many more steps to follow in the knowledge path. Even though its limitations, this thesis has established a core of techniques that have been revealed to be useful and productive in the study of the Human Gut Microbiota, specially in the case of the polysaccharide degraders *Bacteroides* sp. and the secondary degraders belonging to the genus *Bifidobacterium* and *Lactobacillus*.

The inclusion of new approaches and the revision of the previously used ones would contribute to a better, wider, and deeper understanding of these bacteria populations. Furthermore, the addition of more bacteria species to this initial quorum, together with new types of carbon sources obtained from either fungus sources or other ones is desirable to increase the credibility of the data and the feasible applications which may derive from it.

.

5 Future work

The data obtained in this thesis covers a range of techniques and experimental approaches which all together give us a better understanding of the Human Gut Microbiota. The potential of *Bacteroides* sp. as glycan degrader was widely tested and the ability to cross-feed with other members such as *Bifidobacterium* sp. and *Lactiplantibacillus plantarum* WCFS1 was proven as well.

Preliminary experiments carried out by me and other members of the research group are not shown in this thesis, but they revealed that other bacterial species apart from *Bacteroides* sp. and *Bifidobacterium* sp. might play an important role in *Fusarium* β-glucan metabolism and other similar polysaccharides, specially *Roseburia* sp. and *Victivallis vadensis*. These bacteria might show better growth rates and even they may produce important metabolites such as oligosaccharides or SCFAs with potential prebiotic effects in human health. Different studies support the fact that *Roseburia* sp. are good polysaccharide degraders, while that same potential in the case of *Victivallis* is derived from the genome analysis instead of the experimental procedure.

Because of the vast number of microbes which are present in our organism, it seems logical to think that other bacteria are taking part in the process, due to the complexity of the continuous interconnections within our microbiota. For this reason, the methodology established in this thesis should be enlarged in the future, diversifying the range of bacteria species studied as potential degraders, and using more experimental techniques to assure better and more definitive conclusions. Despite it would suppose the utilization of more resources, the derived applications for human health will surely be worth the effort.

6 References

Abdelazez, A., Abdelmotaal, H., Evivie, S. E., Melak, S., Jia, F. F., Khoso, M. H., Z., Z. T., Zhang, L. J., Sami, R., and Meng, X. C. (2018). Screening Potential Probiotic Characteristics of Lactobacillus brevis Strains In Vitro and Intervention Effect on TypeI Diabetes In Vivo. *Biomed. Res. Int.*, 7356173. https://doi.org/10.1155/2018/7356173.

Abete, I., Romaguera, D., Vieira, A. R., Lopez de Munain, A., and Norat, T. (2014). Association between total, processed, red and white meat consumption and all-cause, CVD and IHD mortality: a meta-analysis of cohort studies. *Br. J. Nutr.*, *112*(5), 762-775. https://doi.org/10.1017/s000711451400124x.

Abuqwider, J. N., Mauriello, G., and Altamimi, M. (2021). *Akkermansia muciniphila*, a New Generation of Beneficial Microbiota in Modulating Obesity: A Systematic Review. *Microorganisms*, *9*(5). https://doi.org/10.3390/microorganisms9051098.

Alessandri, G., Milani, C., Duranti, S., Mancabelli, L., Ranjanoro, T., Modica, S., Carnevali, L., Statello, R., Bottacini, F., Turroni, F., Ossiprandi, M., Sgoifo, A., van Sinderen, D., and Ventura, M. (2019). Ability of bifidobacteria to metabolize chitin-glucan and its impact on the gut microbiota. *Sci. Rep.*, *9(1)*. https://doi.org/doi:10.1038/s41598-019-42257-z.

Alexandratos, N., and, Bruinsma, J. (2012). *World agriculture towards 2030/2050: the 2012 revision*.

An, C., Kuda, T., Yazaki, T., Takahashi, H., and Kimura, B. (2013). FLX Pyrosequencing Analysis of the Effects of the Brown-Algal Fermentable Polysaccharides Alginate and Laminaran on Rat Cecal Microbiotas. *Appl. Environ. Microbiol.*, *79*, 860-876. https://doi.org/doi:10.1128/AEM.02354-12.

Ananthakrishnan, A. N., Luo, C., Yajnik, V., Khalili, H., Garber, J. J., Stevens, B. W., Cleland, T., and Xavier, R. J. (2017). Gut Microbiome Function Predicts Response to Anti-integrin Biologic Therapy in Inflammatory Bowel Diseases. *Cell Host Microbe*, *21*(5), 603-610. https://doi.org/10.1016/j.chom.2017.04.010.

Anderson, K. L., and, Salyers, A. A. (1989). Biochemical evidence that starch breakdown by *Bacteroides thetaiotaomicron* involves outer membrane starch-binding sites and periplasmic starch-degrading enzymes. *J. Bacteriol.*, *171*(6), 3192-3198. https://doi.org/10.1128/jb.171.6.3192-3198.1989.

Aoe, S., Nakamura, F., and Fujiwara, S. (2018). Effect of Wheat Bran on Fecal Butyrate-Producing Bacteria and Wheat Bran Combined with Barley on *Bacteroides* Abundance in Japanese Healthy Adults. *Nutrients*, *10(12)*. https://doi.org/doi:10.3390/nu10121980.

Arora, T., Loo, L., Anastasovska, J., Gibson, G., Tuohy, K., Sharma, R., Sharma, R., Swann, J., Deaville, E., Sleeth, M., Thomas, E., Holmes, E., Bell, J., and Frost, G. . (2012). Differential Effects of Two Fermentable Carbohydrates on Central Appetite Regulation and Body Composition. *PLoS One*, *7(8)*. https://doi.org/doi:10.1371/journal.pone.0043263.

Arpaia, N., Campbell, C., Fan, X., Dikiy, S., van der Veeken, J., deRoos, P., Liu, H., Cross, J. R., Pfeffer, K., Coffer, P. J., and Rudensky, A. Y. (2013). Metabolites produced by commensal bacteria promote peripheral regulatory T-cell generation. *Nature*, *504*(7480), 451-455. https://doi.org/10.1038/nature12726.

Arumugam, M., Raes, J., Pelletier, E., Le Paslier, D., Yamada, T., Mende, D., Fernandes, G., Tap, J., Bruls, T., Batto, J., Bertalan, M., Borruel, N., Casellas, F., Fernandez, L., Gautier, L., Hansen, T., Hattori, M., Hayashi, T., Kleerebezem, M., Kurokawa, K., Leclerc, M., Levenez, F., Manichanh, C., Nielsen, H., Nielsen, T., Pons, N., Poulain, J., Qin, J., Sicheritz-Ponten, T., Tims, S., Torrents, D., Ugarte, E., Zoetendal, E., Wang, J., Guarner, F., Pedersen, O., de Vos, W., Brunak, S., Doré, J., MetaHIT Consortium, Weissenbach, J., Ehrlich, S., and Bork, P. (2013). Enterotypes of the human gut microbiome. *Nature*, *473*, 7349-7359. https://doi.org/doi:10.1038/nature09944.

Barbeyron, T., Gerard, A., Potin, P., Henrissat, B., and Kloareg B. (1998). The kappa-carrageenase of the marine bacterium Cytophaga drobachiensis. Structural and

phylogenetic relationships within family-16 glycoside hydrolases. *Mol. Biol. Evol.*, *15,* 528-37. https://doi.org/10.1093/oxfordjournals.molbev.a025952.

Bautista, C. T., Wurapa, E., Sateren, W. B., Morris, S., Hollingsworth, B., and Sanchez, J. L. (2016). Bacterial vaginosis: a synthesis of the literature on etiology, prevalence, risk factors, and relationship with chlamydia and gonorrhea infections. *Mil. Med. Res.*, *3*, 4. https://doi.org/10.1186/s40779-016-0074-5.

Belzer, C., Chia, L. W., Aalvink, S., Chamlagain, B., Piironen, V., Knol, J., and de Vos, W. M. (2017). Microbial Metabolic Networks at the Mucus Layer Lead to Diet-Independent Butyrate and Vitamin B(12) Production by Intestinal Symbionts. *mBio*, *8*(5). https://doi.org/10.1128/mBio.00770-17.

Bengoa, A. A., Dardis, C., Gagliarini, N., Garrote, G. L., Abraham, A. G. (2020). Exopolysaccharides From *Lactobacillus paracasei* Isolated From Kefir as Potential Bioactive Compounds for Microbiota Modulation. *Front. Microbiol.*, *11*, 583254. https://doi.org/10.3389/fmicb.2020.583254.

Bennke, C., Krüger, K., Kappelmann, L., Huang, S., Gobet, A., Schüler, M., Barbe, V., Fuchs, B., Michel, G., Teeling, H., and Amann, R. (2016). Polysaccharide utilization loci of Bacteroidetes from two contrasting open ocean sites in the North Atlantic. *Environ. Microbiol.*, *12*, 4456-4470. https://doi.org/doi:10.1111/1462-2920.13429.

Berntsson, R. P., Smits, S. H., Schmitt, L., Slotboom, D. J., and Poolman, B. (2010). A structural classification of substrate-binding proteins. *FEBS Lett*, *584*(12), 2606-2617. https://doi.org/10.1016/j.febslet.2010.04.043.

Bottin, J. H., Swann, J. R., Cropp, E., Chambers, E. S., Ford, H. E., Ghatei, M. A., Frost, G. S. (2016). Mycoprotein reduces energy intake and postprandial insulin release without altering glucagon-like peptide-1 and peptide tyrosine-tyrosine concentrations in healthy overweight and obese adults: a randomised-controlled trial. *Br. J. Nutr.*, *116*(2), 360-374. https://doi.org/10.1017/s0007114516001872.

Briggs, J., Grondin, J., and Brumer, H. (2020). Communal living: glycan utilization by the human gut microbiota. *Environ. Microbiol.* https://doi.org/doi:10.1111/1462-2920.15317.

Brown, H., and, Koropatkin, N. (2020). Host glycan utilization within the Bacteroidetes Sus-like paradigm. *Glycobiology*, *cwaa054*. https://doi.org/doi:10.1093/glycob/cwaa054.

Burley, V. J., Paul, A. W., and Blundell, J. E. (1993). Influence of a high-fibre food (myco-protein) on appetite: effects on satiation (within meals) and satiety (following meals). *Eur. J. Clin. Nutr.*, *47*(6), 409-418.

Byun, R., Nadkarni, M. A., Chhour, K. L., Martin, F. E., Jacques, N. A., and Hunter, N. (2004). Quantitative analysis of diverse *Lactobacillus* species present in advanced dental caries. *J. Clin. Microbiol.*, *42*(7), 3128-3136. https://doi.org/10.1128/jcm.42.7.3128-3136.2004.

Bzducha-Wróbel, A., Błażejak, S., and Tkacz, K. (2012). Cell wall structure of selected yeast species as a factor of magnesium binding ability. *Eur. Food Res. Technol.*, *235*(2), 355-366. https://doi.org/https://doi.org/10.1007/s00217-012-1761-4.

Calatayud, M., Verstrepen, L., Ghyselinck, J., Van den Abbeele, P., Marzorati, M., Modica, S., Ranjanoro, T., and Maquet, V. (2021). Chitin Glucan Shifts Luminal and Mucosal Microbial Communities, Improve Epithelial Barrier and Modulates Cytokine Production In Vitro. *Nutrients*, *13*(9). https://doi.org/10.3390/nu13093249.

Cameron, E., Kwiatkowski, K., Lee, B., Hamaker, B., Koropatkin, N., and Martens, E. (2014). Multifunctional Nutrient-Binding Proteins Adapt Human Symbiotic Bacteria for Glycan Competition in the Gut by Separately Promoting Enhanced Sensing and Catalysis. *mBio*, *5(5):e01441-14*. https://doi.org/doi:10.1128/mBio.01441-14.

Cameron, E., Maynard, M., Smith, C., Smith, T., Koropatkin, N. a. M., E. (2012). Multidomain Carbohydrate-binding Proteins Involved in *Bacteroides thetaiotaomicron* Starch Metabolism. *J. Biol. Chem.*, *287(41)*, 34614-34625. https://doi.org/doi:10.1074/jbc.M112.397380.

Canani, R. B., Costanzo, M. D., Leone, L., Pedata, M., Meli, R., and Calignano, A. (2011). Potential beneficial effects of butyrate in intestinal and extraintestinal diseases. *World J Gastroenterol.*, *17*(12), 1519-1528. https://doi.org/10.3748/wjg.v17.i12.1519.

Cani, P., and, de Vos, M. (2017). Next-generation beneficial microbes: The case of *Akkermansia muciniphila*. *Front. Microbiol.*, *8:1765*. https://doi.org/doi:10.3389/fmicb.2017.01765.

Cantarel, B., Lombard, V., and Henrissat, B. (2012). Complex Carbohydrate Utilization by the Healthy Human Microbiome. *PLoS One*, *7(6):e28742* https://doi.org/doi:10.1371/journal.pone.0028742.

Carlson, J., Erickson, J., Hess, J., Gould, T., and Slavin, J. (2017). Prebiotic Dietary Fiber and Gut Health: Comparing the in Vitro Fermentations of Beta-Glucan, Inulin and Xylooligosaccharide. *Nutrients*, *9*, 1361-1377. https://doi.org/doi:10.3390/nu9121361.

Cherta-Murillo, A., Lett, A. M., Frampton, J., Chambers, E. S., Finnigan, T. J. A., and Frost, G. S. (2020). Effects of mycoprotein on glycaemic control and energy intake in humans: a systematic review. *Br. J. Nutr.*, *123*(12), 1321-1332. https://doi.org/10.1017/s0007114520000756.

Cho, K., and, Salyers, A. (2001). Biochemical Analysis of Interactions between Outer Membrane Proteins That Contribute to Starch Utilization by *Bacteroides thetaiotaomicron*. *J. Bacteriol.*, *183*, 7224-7230. https://doi.org/doi:10.1128/jb.183.24.7224-7230.2001.

Choromanska, A., Kulbacka, J., Rembialkowska, N., Pilat, J., Oledzki, R., Harasym, J., and Saczko, J. (2015). Anticancer properties of low molecular weight oat beta-glucan–An in vitro study. *Int. J. Biol. Macromol.*, *80*, 23-28. https://doi.org/doi:10.1016/j.ijbiomac.2015.05.035.

Coelho, M. O. C., Monteyne, A. J., Dunlop, M. V., Harris, H. C., Morrison, D. J., Stephens, F. B., and Wall, B. T. (2020). Mycoprotein as a possible alternative source of dietary protein to support muscle and metabolic health. *Nutr. Rev.*, *78*(6), 486-497. https://doi.org/10.1093/nutrit/nuz077.

Collado, M. C., Isolauri, E., Salminen, S., and Sanz, Y. (2009). The impact of probiotic on gut health. *Curr. Drug Metab.*, *10*(1), 68-78. https://doi.org/10.2174/138920009787048437.

Collins, K., Fitzgerald, G., Stanton, C., and Ross, R. (2016). Looking Beyond the Terrestrial: The Potential of Seaweed Derived Bioactives to Treat Non-Communicable Diseases. *Mar. Drugs*, *14(3):60*. https://doi.org/doi:10.3390/md14030060.

Colosimo, R., Mulet-Cabero, A. I., Warren, F. J., Edwards, C. H., Finnigan, T. J. A., and Wilde, P. J. (2020). Mycoprotein ingredient structure reduces lipolysis and binds bile salts during simulated gastrointestinal digestion. *Food Funct.*, *11*(12), 10896-10906. https://doi.org/10.1039/d0fo02002h.

Colov, E., Degett, T., Raskov, H., and Gögenur, I. (2020). The Impact of the Gut Microbiota on Prognosis After Surgery for Colorectal Cancer - A Systematic Review and Meta-Analysis. *APMIS*, *118*, 162-176. https://doi.org/doi:10.1111/apm.13032.

Consortium, T. C. (2018). Ten years of CAZypedia: a living encyclopedia of carbohydrate-active enzymes. *Glycobiology*, *28*, 3-8. https://doi.org/doi:10.1093/glycob/cwx089.

Cosola, C., De Angelis, M., Rocchetti M., Montemurno E., Maranzano V., D. G., Manno C., Zito A., Gesualdo M., Ciccone M., Gobbetti M. and Gesualdo, L. (2017). Beta-Glucans Supplementation Associates with Reduction in P-Cresyl Sulfate Levels and Improved Endothelial Vascular Reactivity in Healthy Individuals. *PLoS One*, *12(1)e0169635*. https://doi.org/doi:10.1371/journal.pone.0169635

Cui, Y., Wang, M., Zheng, Y., Miao, K., and Qu, X. (2021). The Carbohydrate Metabolism of Lactiplantibacillus plantarum. *Int. J. Mol. Sci.*, *22*(24). https://doi.org/10.3390/ijms222413452.

Dao, M. C., Everard, A., Aron-Wisnewsky, J., Sokolovska, N., Prifti, E., Verger, E. O., Kayser, B. D., Levenez, F., Chilloux, J., Hoyles, L., Dumas, M. E., Rizkalla, S. W., Doré, J., Cani, P. D., and Clément, K. (2016). *Akkermansia muciniphila* and improved

metabolic health during a dietary intervention in obesity: relationship with gut microbiome richness and ecology. *Gut*, *65*(3), 426-436. https://doi.org/10.1136/gutjnl-2014-308778.

De Angelis, M., Montemurno, E., Vannini, L., Cosola, C., Cavallo, N., Gozzi, G., Maranzano, V., Di Cagno, R., Gobbetti, M., and Gesualdo, L. (2015). Effect of Whole-Grain Barley on the Human Fecal Microbiota and Metabolome. *Appl. Environ. Microbiol.*, *81*, 7945-7956. https://doi.org/doi:10.1128/AEM.02507-15.

De Filippo, C., Cavalieria, D., Di Paola, M., Ramazzottic, M., Poullet, J., Massart, S., Collini, S., Pieraccini, G., and Lionetti, P. (2010). Impact of diet in shaping gut microbiota revealed by a comparative study in children from Europe and rural Africa. *Proc. Natl. Acad. Sci. U. S. A.*, *107*, 14691–14696. https://doi.org/doi:10.1073/pnas.1005963107.

De Paepe, K., Kerckhof, F., Verspreet, J., Courtin, C., and Van de Wiele, T. (2017). Inter-individual differences determine the outcome of wheat bran colonization by the human gut microbiome. *Environ. Microbiol.*, *8*, 3251-3326. https://doi.org/doi:10.1111/1462-2920.13819.

De Vadder, F., Kovatcheva-Datchary, P., Z., C., , Duchampt, A., Bäckhed, F., and Mithieux, G. (2016). Microbiota-produced succinate improves glucose homeostasis via intestinal gluconeogenesis. *Cell Metab.*, *24*, 151-157. https://doi.org/doi:10.1016/j.cmet.2016.06.013.

De Vadder, F., Kovatcheva-Datchary, P., Goncalves, D., Vinera, J., Zitoun, C., Duchampt, A., Bäckhed, F., and Mithieux, G. (2014). Microbiota-generated Metabolites Promote Metabolic Benefits via Gut-Brain Neural Circuits. *Cell*, *156*, 84-96. https://doi.org/doi:10.1016/j.cell.2013.12.016.

Déjean, G., Tamura, K., Cabrera, A., Jain, N., Pudlo, N. A., Pereira, G., Viborg, A. H., Van Petegem, F., Martens, E. C., and Brumer, H. (2020). Synergy between Cell Surface Glycosidases and Glycan-Binding Proteins Dictates the Utilization of Specific Beta(1,3)-Glucans by Human Gut *Bacteroides*. *mBio*, *11*(2), e00095-00020. https://doi.org/https://doi.org/10.1128/mbio.00095-20.

Del Cornò, M., G., S., and Conti, L. (2020). Shaping the Innate Immune Response by Dietary Glucans: Any Role in the Control of Cancer? *Cancers (Basel)*. *12*, 155-171. https://doi.org/doi:10.3390/cancers12010155.

Depommier, C., Everard, A., Druart, C., Maiter, D., Thissen, J. P., Loumaye, A., Hermans, M. P., Delzenne, N. M., de Vos, W. M., and Cani, P. D. (2021). Serum metabolite profiling yields insights into health promoting effect of *A. muciniphila* in human volunteers with a metabolic syndrome. *Gut Microbes*, *13*(1), 1994270. https://doi.org/10.1080/19490976.2021.1994270.

Depommier, C., Van Hul, M., Everard, A., Delzenne, N. M., De Vos, W. M., Cani, P. D. (2020). Pasteurized *Akkermansia muciniphila* increases whole-body energy expenditure and fecal energy excretion in diet-induced obese mice. *Gut Microbes*, *11*(5), 1231-1245. https://doi.org/10.1080/19490976.2020.1737307.

Derrien, M., Belzer, C., and de Vos, W. M. (2017). *Akkermansia muciniphila* and its role in regulating host functions. *Microb. Pathog.*, *106*, 171-181. https://doi.org/10.1016/j.micpath.2016.02.005.

Derrien, M., Vaughan, E. E., Plugge, C. M., and de Vos, W. M. (2004). *Akkermansia muciniphila* gen. nov., sp. nov., a human intestinal mucin-degrading bacterium. *Int J Syst Evol Microbiol*, *54*(Pt 5), 1469-1476. https://doi.org/10.1099/ijs.0.02873-0.

Dobrinčić, A., Balbino, S., Zorić, Z., Pedisić, S., Bursać Kovačević, D., Elez Garofulić, I., and Dragović-Uzelac, V. (2020). Advanced Technologies for the Extraction of Marine Brown Algal Polysaccharides. *Mar Drugs*, *18*(3). https://doi.org/doi:10.3390/md18030168.

Dong, J. L., Yu, X., Dong, L. E., and Shen, R. L. (2017). In vitro fermentation of oat β-glucan and hydrolysates by fecal microbiota and selected probiotic strains. *J. Sci. Food Agric.*, *97*(12), 4198-4203. https://doi.org/10.1002/jsfa.8292.

Du, B., Meenu, M., Liu, H., and Xu, B. (2019). A Concise Review on the Molecular Structure and Function Relationship of β-Glucan. *Int. J. Mol. Sci.*, *20*(16). https://doi.org/doi:10.3390/ijms20164032.

Duncan, S. H., Aminov, R. I., Scott, K. P., Louis, P., Stanton, T. B., and Flint, H. J. (2006). Proposal of *Roseburia faecis* sp. nov., *Roseburia hominis* sp. nov. and *Roseburia inulinivorans* sp. nov., based on isolates from human faeces. *Int. J. Syst. Evol. Microbiol.*, *56*(Pt 10), 2437-2441. https://doi.org/10.1099/ijs.0.64098-0.

Duncan, S. H., Hold, G. L., Barcenilla, A., Stewart, C. S., and Flint, H. J. (2002). *Roseburia intestinalis* sp. nov., a novel saccharolytic, butyrate-producing bacterium from human faeces. *Int. J. Syst. Evol. Microbiol.*, *52*(Pt 5), 1615-1620. https://doi.org/10.1099/00207713-52-5-1615.

Duranti, S., Milani, C., Lugli, G., Mancabelli, L., Turroni, F., Ferrario, C., Mangifesta, M., Viappiani, A., Sánchez, B., Margolles, A., van Sinderen, D., and Ventura, M. (2016). Evaluation of Genetic Diversity Among Strains of the Human Gut Commensal *Bifidobacterium Adolescentis*. *Sci. Rep.*, *6:23971*. https://doi.org/doi:10.1038/srep23971.

Egan, M., Motherway, M. O., Kilcoyne, M., Kane, M., Joshi, L., Ventura, M., and van Sinderen, D. (2014). Cross-feeding by *Bifidobacterium breve* UCC2003 during co-cultivation with *Bifidobacterium bifidum* PRL2010 in a mucin-based medium. *BMC Microbiol.*, *14*, 282. https://doi.org/https://doi.org/10.1186/s12866-014-0282-7.

Eilam, O., Zarecky, R., Oberhardt, M., Ursell, L., Kupiec, M., Knight, R., Gophna, U., and Ruppin, E. (2014). Glycan degradation (GlyDeR) analysis predicts mammalian gut microbiota abundance and host diet-specific adaptations. *mBio*, *5(4):e01526-14*. https://doi.org/doi:10.1128/mBio.01526-14.

Ejby, M., Fredslund, F., Andersen, J. M., Vujičić Žagar, A., Henriksen, J. R., Andersen, T. L., Svensson, B., Slotboom, D. J., Abou Hachem, M. (2016). An ATP Binding Cassette Transporter Mediates the Uptake of α-(1,6)-Linked Dietary Oligosaccharides in *Bifidobacterium* and Correlates with Competitive Growth on These Substrates. *J. Biol. Chem.*, *291*(38), 20220-20231. https://doi.org/10.1074/jbc.M116.746529.

Ejby, M., Fredslund, F., Vujicic-Zagar, A., Svensson, B., Slotboom, D. J., and Abou Hachem, M. (2013). Structural basis for arabinoxylo-oligosaccharide capture by the probiotic *Bifidobacterium animalis* subsp. *lactis* Bl-04. *Mol. Microbiol.*, *90*(5), 1100-1112. https://doi.org/10.1111/mmi.12419.

Ejby, M., Guskov, A., Pichler, M. J., Zanten, G. C., Schoof, E., Saburi, W., Slotboom, D. J., and Abou Hachem, M. (2019). Two binding proteins of the ABC transporter that confers growth of *Bifidobacterium animalis* subsp. *lactis* ATCC27673 on β-mannan possess distinct manno-oligosaccharide-binding profiles. *Mol. Microbiol.*, *112*(1), 114-130. https://doi.org/10.1111/mmi.14257.

El Kaoutari, A., Armougom, F., G., J., R., D., and Henrissat, B. (2013). The abundance and variety of carbohydrate-active enzymes in the human gut microbiota. *Nat. Rev. Microbiol.*, *7*, 497-504. doi: 410.1038/nrmicro3050.

Everard, A., Belzer, C., Geurts, L., Ouwerkerk, J. P., Druart, C., Bindels, L. B., Guiot, Y., Derrien, M., Muccioli, G. G., Delzenne, N. M., de Vos, W. M., and Cani, P. D. (2013). Cross-talk between *Akkermansia muciniphila* and intestinal epithelium controls diet-induced obesity. *Proc. Natl. Acad. Sci. U. S. A.*, *110*(22), 9066-9071. https://doi.org/10.1073/pnas.1219451110.

Falony, G., Verschaeren, A., De Bruycker, F., De Preter, V., Verbeke, K., Leroy, F., and De Vuyst, L. (2009). In vitro kinetics of prebiotic inulin-type fructan fermentation by butyrate-producing colon bacteria: implementation of online gas chromatography for quantitative analysis of carbon dioxide and hydrogen gas production. *Appl. Environ. Microbiol.*, *75*(18), 5884-5892. https://doi.org/10.1128/aem.00876-09.

Fernández-Veledo, S., and, Vendrell, J. (2019). Gut microbiota-derived succinate: Friend or foe in human metabolic diseases? *Rev. Endocr. Metab. Disord.*, *20*, 439–447. https://doi.org/doi:10.1007/s11154-019-09513-z.

Finnigan, T. J. A., Wall, B. T., Wilde, P. J., Stephens, F. B., Taylor, S. L., and Freedman, M. R. (2019). Mycoprotein: The Future of Nutritious Nonmeat Protein, a Symposium Review. *Curr. Dev. Nutr.*, *3*(6), nzz021. https://doi.org/10.1093/cdn/nzz021.

Fischbach, M. A., and, Sonnenburg, J. L. (2011). Eating for two: how metabolism establishes interspecies interactions in the gut. *Cell Host Microbe*, *10*(4), 336-347. https://doi.org/10.1016/j.chom.2011.10.002.

Flint, H. J., Scott, K. P., Duncan, S. H., Louis, P., and Forano, E. (2012). Microbial degradation of complex carbohydrates in the gut. *Gut Microbes*, *3*(4), 289-306. https://doi.org/10.4161/gmic.19897.

Foley, M. H., Cockburn, D. W., and, Koropatkin, N. M. (2016). The Sus operon: a model system for starch uptake by the human gut Bacteroidetes. *Cell Mol. Life Sci.*, *73*(14), 2603-2617. https://doi.org/doi:10.1007/s00018-016-2242-x.

Fu, X., Zhan, Y., Li, N., Yu, D., Gao, W., Gu, Z., Zhu, L., Li, R., and Zhu, C. (2021). Enzymatic Preparation of Low-Molecular-Weight *Laminaria japonica* Polysaccharides and Evaluation of Its Effect on Modulating Intestinal Microbiota in High-Fat-Diet-Fed Mice. *Front. Bioeng. Biotechnol.*, *9*, 820892. https://doi.org/10.3389/fbioe.2021.820892.

Gani, A., Shah, A., Ahmad, M., Ashwar, B., and Masoodi, F. (2018). β-d-glucan as an enteric delivery vehicle for probiotics. *Int J. Biol. Macromol.*, *106*, 864-869. https://doi.org/doi:10.1016/j.ijbiomac.2017.08.093.

Geerlings, S. Y., Kostopoulos, I., de Vos, W. M., and Belzer, C. (2018). *Akkermansia muciniphila* in the Human Gastrointestinal Tract: When, Where, and How? *Microorganisms*, *6*(3). https://doi.org/10.3390/microorganisms6030075.

Geller, A., Shrestha, R., and Yan, J. (2019). Yeast-Derived β-Glucan in Cancer: Novel Uses of a Traditional Therapeutic. *Int. J. Biol. Macromol.*, *20*, 3618-3637. https://doi.org/doi:10.3390/ijms20153618.

Gerritsen, J., Timmerman, H. M., Fuentes, S., van Minnen, L. P., Panneman, H., Konstantinov, S. R., Rombouts, F. M., Gooszen, H. G., Akkermans, L. M., Smidt, H. a. R., G. T. (2011). Correlation between protection against sepsis by probiotic therapy and stimulation of a novel bacterial phylotype. *Appl. Environ. Microbiol.*, *77*(21), 7749-7756. https://doi.org/10.1128/aem.05428-11.

Gibson, G. R., Hutkins, R., Sanders, M. E., Prescott, S. L., Reimer, R. A., Salminen, S. J., Scott, K., Stanton, C., Swanson, K. S., Cani, P. D., Verbeke, K., Reid, G. (2017). Expert consensus document: The International Scientific Association for Probiotics and Prebiotics (ISAPP) consensus statement on the definition and scope of prebiotics. *Nat. Rev. Gastroenterol. Hepatol.*, *14*(8), 491-502. https://doi.org/doi:10.1038/nrgastro.2017.75.

Glenwright, A., Pothula, K., Bhamidimarri, S., Chorev, D., Baslé, A., Firbank, S., Zheng, H., Robinson, C., Winterhalter, M., Kleinekathöfer, U., Bolam D., and van den Berg, B. (2017). Structural basis for nutrient acquisition by dominant members of the human gut microbiota. *Nature*, *541*, 407–411. https://doi.org/doi:10.1038/nature20828.

Gloster, T. M., Turkenburg, J. P., Potts, J. R., Henrissat, B., and Davies, G. J. (2008). Divergence of catalytic mechanism within a glycosidase family provides insight into evolution of carbohydrate metabolism by human gut flora. *Chem. Biol.*, *15*(10), 1058-1067. https://doi.org/10.1016/j.chembiol.2008.09.005.

Goldin, B. R., and, Gorbach, S. L. (2008). Clinical indications for probiotics: an overview. *Clin. Infect. Dis.*, *46 Suppl 2*, S96-100; discussion S144-151. https://doi.org/10.1086/523333.

Goldstein, E. J., Tyrrell, K. L., and, Citron, D. M. (2015). *Lactobacillus* species: taxonomic complexity and controversial susceptibilities. *Clin. Infect. Dis.*, *60 Suppl 2*, S98-107. https://doi.org/10.1093/cid/civ072.

Grander, C., Adolph, T. E., Wieser, V., Lowe, P., Wrzosek, L., Gyongyosi, B., Ward, D. V., Grabherr, F., Gerner, R. R., Pfister, A., Enrich, B., Ciocan, D., Macheiner, S., Mayr, L., Drach, M., Moser, P., Moschen, A. R., Perlemuter, G., Szabo, G., Cassard, A. M. a. T.,

H. (2018). Recovery of ethanol-induced *Akkermansia muciniphila* depletion ameliorates alcoholic liver disease. *Gut*, *67*(5), 891-901. https://doi.org/10.1136/gutjnl-2016-313432.

Grondin, J. M., Tamura, K., Déjean, G., Abbott, D. W. a. B., H. (2017). Polysaccharide Utilization Loci: Fueling Microbial Communities. *J. Bacteriol.*, *199*(15), e00860-00816. https://doi.org/https://doi.org/10.1128/jb.00860-16.

Gu, Y., Xiao, X., Pan, R., Zhang, J., Zhao, Y., Dong, Y. a. C., H. (2021). *Lactobacillus plantarum* dy-1 fermented barley extraction activates white adipocyte browning in high-fat diet-induced obese rats. *J. Food. Biochem.*, *45*(4), e13680. https://doi.org/10.1111/jfbc.13680.

Gudi, R., Suber, J., Brown, R., Johnson, B., and Vasu, C. (2020). Pretreatment with Yeast-Derived ComplexDietary Polysaccharides Suppresses Gut Inflammation, Alters the Microbiota Composition, and Increases ImmuneRegulatory Short-Chain Fatty Acid Production in C57BL/6 Mice. *J. Nutr.*, *150*, 1291-1302. https://doi.org/doi:10.1093/jn/nxz328.

Gupta, R. S., Nanda, A., and Khadka, B. (2017). Novel molecular, structural and evolutionary characteristics of the phosphoketolases from bifidobacteria and Coriobacteriales. *PLoS One*, *12*(2), e0172176. https://doi.org/10.1371/journal.pone.0172176.

Hamer, H. M., Jonkers, D., Venema, K., Vanhoutvin, S., Troost, F. J. a. B., R. J. (2008). Review article: the role of butyrate on colonic function. *Aliment. Pharmacol. Ther.*, *27*(2), 104-119. https://doi.org/10.1111/j.1365-2036.2007.03562.x.

Hansen, C. H., Krych, L., Nielsen, D. S., Vogensen, F. K., Hansen, L. H., Sørensen, S. J., Buschard, K. a. H., A. K. (2012). Early life treatment with vancomycin propagates Akkermansia muciniphila and reduces diabetes incidence in the NOD mouse. *Diabetologia*, *55*(8), 2285-2294. https://doi.org/10.1007/s00125-012-2564-7.

Hao, H., Zhang, X., Tong, L., Liu, Q., Liang, X., Bu, Y., Gong, P., Liu, T., Zhang, L., Xia, Y., Ai, L., and Yi, H. (2021). Effect of Extracellular Vesicles Derived From Lactobacillus plantarum Q7 on Gut Microbiota and Ulcerative Colitis in Mice. *Front. Immunol.*, *12*, 777147. https://doi.org/doi:10.3389/fimmu.2021.777147.

Harris, H. C., Edwards, C. A., and, Morrison, D. J. (2019). Short Chain Fatty Acid Production from Mycoprotein and Mycoprotein Fibre in an In Vitro Fermentation Model. *Nutrients*, *11*(4). https://doi.org/10.3390/nu11040800.

Hehemann, J., Kelly, A., Pudlo, N., Martens, E., and Borastona, A. (2012). Bacteria of the human gut microbiome catabolize red seaweed glycans with carbohydrate-active enzyme updates from extrinsic microbes. *Proc. Natl. Acad. Sci. U. S. A.*, *109*, 19786-19791. https://doi.org/doi:10.1073/pnas.1211002109.

Henrion, M., Francey, C., Lê, K. A. a. L., L. (2019). Cereal B-Glucans: The Impact of Processing and How It Affects Physiological Responses. *Nutrients*, *11*(8). https://doi.org/doi:10.3390/nu11081729.

Hillman, E. T., Kozik, A. J., Hooker, C. A., Burnett, J. L., Heo, Y., Kiesel, V. A., Nevins, C. J., Oshiro, J., Robins, M. M., Thakkar, R. D., Wu, S. T. a. L., S. R. (2020). Comparative genomics of the genus *Roseburia* reveals divergent biosynthetic pathways that may influence colonic competition among species. *Microb. Genom.*, *6*(7). https://doi.org/10.1099/mgen.0.000399.

Ho, J., Nicolucci, A. C., Virtanen, H., Schick, A., Meddings, J., Reimer, R. A. a. H., C. (2019). Effect of Prebiotic on Microbiota, Intestinal Permeability, and Glycemic Control in Children With Type 1 Diabetes. *J Clin. Endocrinol. Metab.*, *104*(10), 4427-4440. https://doi.org/10.1210/jc.2019-00481.

Hooda, S., Matte, J., Vasanthan, T., and, Zijlstra, T. (2010). Dietary Oat b-Glucan Reduces Peak Net Glucose Flux and Insulin Production and Modulates Plasma Incretin in Portal-Vein Catheterized Grower Pigs. *J. Nutr.*, *140*, 1564-1569. https://doi.org/doi:10.3945/jn.110.122721.

Hosseini, E., Grootaert, C., Verstraete, W., and Van de Wiele, T. (2011). Propionate as a health-promoting microbial metabolite in the human gut. *Nutr. Rev.*, *69*, 245-258. https://doi.org/doi:10.1111/j.1753-4887.2011.00388.x.

Hou, D., Zhao, Q., Yousaf, L., Chen, B., Xue, Y., and Shen, Q. (2020). A comparison between whole mung bean and decorticated mung bean: beneficial effects on the regulation of serum glucose and lipid disorders and the gut microbiota in high-fat diet and streptozotocin-induced prediabetic mice. *Food Funct.*, *11(6), 5525-5537*. https://doi.org/ doi: 10.1039/d0fo00379d.

Hu, F. B., Otis, B. O., and McCarthy, G. (2019). Can Plant-Based Meat Alternatives Be Part of a Healthy and Sustainable Diet? *Jama*, *322*(16), 1547-1548. https://doi.org/10.1001/jama.2019.13187.

Hughes, S. A., Shewry, P. R., Gibson, G. R., McCleary, B. V. a. R., R. A. (2008). In vitro fermentation of oat and barley derived beta-glucans by human faecal microbiota. *FEMS Microbiol. Ecol.*, *64*(3), 482-493. https://doi.org/10.1111/j.1574-6941.2008.00478.x.

Humpenöder, F., Bodirsky, B. L., Weindl, I., Lotze-Campen, H., Linder, T. a. P., A. (2022). Projected environmental benefits of replacing beef with microbial protein. *Nature*, *605*(7908), 90-96. https://doi.org/10.1038/s41586-022-04629-w.

Huo, J., Lei, M., Zhou, Y., Zhong, X., Liu, Y., Hou, J., Long, H., Zhang, Z., Tian, M., Xie, C., Wu, W. (2021). Structural characterization of two novel polysaccharides from Gastrodia elata and their effects on *Akkermansia muciniphila*. *Int. J. Biol. Macromol.*, *186*, 501-509. https://doi.org/10.1016/j.ijbiomac.2021.06.157.

Inan, M. S., Rasoulpour, R. J., Yin, L., Hubbard, A. K., Rosenberg, D. W. a. G., C. (2000). The luminal short-chain fatty acid butyrate modulates NF-kappaB activity in a human colonic epithelial cell line. *Gastroenterology*, *118*(4), 724-734. https://doi.org/10.1016/s0016-5085(00)70142-9.

James, K., Bottacini, F., Contreras, J. I. S., Vigoureux, M., Egan, M., Motherway, M. O., Holmes, E., and van Sinderen, D. (2019). Metabolism of the predominant human milk oligosaccharide fucosyllactose by an infant gut commensal. *Sci. Rep.*, *9*(1), 1542. https://doi.org/doi:10.1038/s41598-019-51901-7.

James, K., O'Connell Motherway, M., Penno, C., O'Brien, R. L., van Sinderen, D. (2018). *Bifidobacterium breve* UCC2003 Employs Multiple Transcriptional Regulators To Control Metabolism of Particular Human Milk Oligosaccharides. *Appl. Environ. Microbiol.*, *84*(9). https://doi.org/https://doi.org/10.1128/aem.02774-17

Jayachandran, M., Chen, J., Chung, S. S. M., and Xu, B. (2018). A critical review on the impacts of β-glucans on gut microbiota and human health. *J. Nutr. Biochem.*, *61*, 101-110. https://doi.org/doi:10.1016/j.jnutbio.2018.06.010.

Ji-lin, D., Xiao, Y., Lianger, D., and Rui-ling, S. (2017). In vitro fermentation of oat β-glucan and hydrolysates by fecal microbiota and selected probiotic strains. *J. Sci. Food Agric.*, *97*, 4198-4203. https://doi.org/doi:10.1002/jsfa.8292.

Jin, X., Liu, Y., Wang, J., Wang, X., Tang, B., Liu, M. a. L., X. (2022). β-Glucan-triggered *Akkermansia muciniphila* expansion facilitates the expulsion of intestinal helminth via TLR2 in mice. *Carbohydr. Polym.*, *275*, 118719. https://doi.org/10.1016/j.carbpol.2021.118719.

Kagimura, F. Y., da Cunha, M. A., Barbosa, A. M., Dekker, R. F., and Malfatti, C. R.,. (2015). Biological activities of derivatized D-glucans: a review. *Int. J. Biol. Macromol.*, *72*, 588-598. https://doi.org/doi:10.1016/j.ijbiomac.2014.09.008.

Kang, C.-H., Kim, Y., Han, S. H., Jeong, Y., Park, H. a. P., Nam-Soo. (2019). Probiotic Properties of Bifidobacteria Isolated from Feces of Infants. *Journal of Milk Science and Biotechnology*, *37*(1), 40-48. https://doi.org/10.22424/jmsb.2019.37.1.40.

Kazer, J., Orfanos, G., and Gallop, C. (2021). Quorn Footprint Comparison Report.

Kelsen, J., and, Wub, G. (2012). The gut microbiota, environment and diseases of modern society. *Gut Microbes*, *3*, 374-382. https://doi.org/doi:10.4161/gmic.21333.

Koropatkin, N., Cameron, E., and Martens, E. (2012). How glycan metabolism shapes the human gut microbiota. *Nat. Rev. Microbiol.*, *10*, 323-335. https://doi.org/doi:10.1038/nrmicro2746.

Koropatkin, N., and, Smith, T. (2010). SusG: A Unique Cell-Membrane-Associated a-Amylase from a Prominent Human Gut Symbiont Targets Complex Starch Molecules. *Structure*, *18(2)*, 200-215. https://doi.org/doi:10.1016/j.str.2009.12.010.

Kostopoulos, I., Elzinga, J., Ottman, N., Klievink, J. T., Blijenberg, B., Aalvink, S., Boeren, S., Mank, M., Knol, J., de Vos, W. M., Belzer, C. (2020). Akkermansia muciniphila uses human milk oligosaccharides to thrive in the early life conditions in vitro. *Sci Rep*, *10*(1), 14330. https://doi.org/10.1038/s41598-020-71113-8

Kumar, P., Chatli, M. K., Mehta, N., Singh, P., Malav, O. P. a. V., A. K. (2017). Meat analogues: Health promising sustainable meat substitutes. *Crit. Rev. Food Sci. Nutr.*, *57*(5), 923-932. https://doi.org/10.1080/10408398.2014.939739.

Labourel, A., Jam, M., Jeudy, A., Hehemann, J., Czjzek, M., and Michel, G. (2014). The b-Glucanase ZgLamA from *Zobellia galactanivorans* Evolved a Bent Active Site Adapted for Efficient Degradation of Algal Laminarin. *J. Biol. Chem.* , *289*, 2027-2042. https://doi.org/doi:10.1074/jbc.M113.538843.

Labourel, A., Jam, M., Legentil, L., Sylla, B., Hehemann, J., Ferrières, V., Czjzek, M., and Michel, G. (2015). Structural and biochemical characterization of the laminarinase ZgLamCGH16 from *Zobellia galactanivorans* suggests preferred recognition of branched laminarin. *Acta. Crystallogr. D. Biol. Crystallogr.*, *71*, 173-184. https://doi.org/doi:10.1107/S139900471402450X.

Lapébie, P., Lombard, V., Drula, E., Terrapon, N. a. H., B. (2019). Bacteroidetes use thousands of enzyme combinations to break down glycans. *Nat. Commun.*, *10*(1), 2043. https://doi.org/10.1038/s41467-019-10068-5.

Laserna-Mendieta, E., Clooney, A., Carretero-Gomez, J., Moran, C., Sheehan, D., and Nolan, J. (2018). Determinants of reduced genetic capacity for butyrate synthesis by the gut microbiome in Crohn's disease and ulcerative colitis. *J. Crohns Colitis*, *12(2)*, 204-216. https://doi.org/doi:10.1093/ecco-jcc/jjx13.

Lebeer, S., Vanderleyden, J., De Keersmaecker, S. C. (2008). Genes and molecules of lactobacilli supporting probiotic action. *Microbiol. Mol. Biol. Rev.*, *72*(4), 728-764. https://doi.org/10.1128/mmbr.00017-08.

Leccese-Terraf, M. C., Juárez Tomás, M. S., Rault, L., Le Loir, Y., Even, S., and Nader-Macías, M. E. (2016). Biofilms of vaginal *Lactobacillus reuteri* CRL 1324 and *Lactobacillus rhamnosus* CRL 1332: kinetics of formation and matrix characterization. *Arch. Microbiol.*, *198*(7), 689-700. https://doi.org/10.1007/s00203-016-1225-5.

Li, H., Fang, Q., Nie, Q., Hu, J., Yang, C., Huang, T., Li, H. a. N., S. (2020). Hypoglycemic and Hypolipidemic Mechanism of Tea Polysaccharides on Type 2 Diabetic Rats via Gut Microbiota and Metabolism Alteration. *J. Agric. Food. Chem.*, *68*(37), 10015-10028. https://doi.org/10.1021/acs.jafc.0c01968.

Li, J., Lin, S., Vanhoutte, P. M., Woo, C. W. a. X., A. (2016). *Akkermansia Muciniphila* Protects Against Atherosclerosis by Preventing Metabolic Endotoxemia-Induced Inflammation in Apoe-/- Mice. *Circulation*, *133*(24), 2434-2446. https://doi.org/10.1161/circulationaha.115.019645.

Li, N., Wang, X., Sun, C., Wu, X., Lu, M., Si, Y., Ye, X., Wang, T., Yu, X., Zhao, X., Wei, N. a. W., X. (2019). Change of intestinal microbiota in cerebral ischemic stroke patients. *BMC Microbiol.*, *19*(1), 191. https://doi.org/10.1186/s12866-019-1552-1.

Lin, X. H., Huang, K. H., Chuang, W. H., Luo, J. C., Lin, C. C., Ting, P. H., Young, S. H., Fang, W. L., Hou, M. C. a. L., F. Y. (2018). The long term effect of metabolic profile and microbiota status in early gastric cancer patients after subtotal gastrectomy. *PLoS One*, *13*(11), e0206930. https://doi.org/10.1371/journal.pone.0206930.

Liu, J., Tang, J., Li, X., Yan, Q., Ma, J., and Jiang, Z. (2019). Curdlan (*Alcaligenes faecalis*) (1→3)-β-d-Glucan Oligosaccharides Drive M1 Phenotype Polarization in Murine Bone

Marrow-Derived Macrophages via Activation of MAPKs and NF-κB Pathways. *Molecules*, *24*(23). https://doi.org/doi:10.3390/molecules24234251.

Liu, Y., Heath, A., Galland, B., Rehrer, N., Drummond, L., Wu, X., Bell, T. J., Lawley, T., Sims, I., and Tannock, G. (2020). Prioritization of substrate use by a co-culture of five species of gut bacteria fed mixtures of arabinoxylan, xyloglucan, □-glucan, and pectin. *Appl. Environ. Microbiol.*, *86(2):e01905-19*. https://doi.org/doi:10.1042/BJ20101185.

Lombard, V., Bernard, T., Rancurel, C., Brumer, H., Coutinho, P., and, Henrissat, B. (2010). A hierarchical classification of polysaccharide lyases for glycogenomics. *Biochem. J.*, *432(3):437-44*. https://doi.org/doi:10.1042/BJ20101185.

Lopera, T. J., Lujan, J. A., Zurek, E., Zapata, W., Hernandez, J. C., Toro, M. A., Alzate, J. F., Taborda, N. A., Rugeles, M. T. ana A.-J., W. (2021). A specific structure and high richness characterize intestinal microbiota of HIV-exposed seronegative individuals. *PLoS One*, *16*(12), e0260729. https://doi.org/10.1371/journal.pone.0260729.

Luna, E., Parkar, S. G., Kirmiz, N., Hartel, S., Hearn, E., Hossine, M., Kurdian, A., Mendoza, C., Orr, K., Padilla, L., Ramirez, K., Salcedo, P., Serrano, E., Choudhury, B., Paulchakrabarti, M., Parker, C. T., Huynh, S., Cooper, K. a. F., G. E. (2022). Utilization Efficiency of Human Milk Oligosaccharides by Human-Associated *Akkermansia* Is Strain Dependent. *Appl. Environ. Microbiol.*, *88*(1), e0148721. https://doi.org/10.1128/aem.01487-21.

Luo, S., Zhang, X., Huang, S., Feng, X., Zhang, X. a. X., D. (2022). A monomeric polysaccharide from *Polygonatum sibiricum* improves cognitive functions in a model of Alzheimer's disease by reshaping the gut microbiota. *Int. J. Biol. Macromol.*, *213*, 404-415. https://doi.org/10.1016/j.ijbiomac.2022.05.185.

Luo, Y., Zhang, L., Li, H., Smidt, H., Wright, A., Zhang, K., Ding, X., Zeng, Q., Bai, S., Wang, J., Li, J., Zheng, P., Tian, G., Cai, J., and Chen, D. (2017). Different Types of Dietary Fibers Trigger Specific Alterations in Composition and Predicted Functions ofColonic Bacterial Communities in BALB/c Mice. *Front. Microbiol.*, *8:966*. https://doi.org/doi:10.3389/fmicb.2017.00966.

Lynch, M., Sweeney, T., Callan, J., O'Sullivan, J., and O'Doherty, J. (2010). The effect of dietary Laminaria-derived laminarin and fucoidan on nutrient digestibility, nitrogen utilisation, intestinal microflora and volatile fatty acid concentration in pigs. *J. Sci. Food Agric.*, *90*, 430-437. https://doi.org/doi:10.1002/jsfa.3834.

Machiels, K., Joossens, M., Sabino, J., De Preter, V., Arijs, I., Eeckhaut, V., Ballet, V., Claes, K., Van Immerseel, F., Verbeke, K., Ferrante, M., Verhaegen, J., Rutgeerts, P., and Vermeire, S. (2014). A decrease of the butyrate-producing species *Roseburia hominis* and *Faecalibacterium prausnitzii* defines dysbiosis in patients with ulcerative colitis. *Gut*, *63*(8), 1275-1283. https://doi.org/10.1136/gutjnl-2013-304833.

Maraki, S., Mavromanolaki, V., Stafylaki, D., and Kasimati, A. (2020). Surveillance of Antimicrobial Resistance in Recent Clinical Isolates of Gram-negative Anaerobic Bacteria in a Greek University Hospital. *Anaerobe*, *62:102173*. https://doi.org/doi:10.1016/j.anaerobe.2020.102173.

Martens, E. C., Lowe, E. C., Chiang, H., Pudlo, N. A., Wu, M., McNulty, N. P., Abbott, D. W.,Henrissat, B., Gilbert, H. J., Bolam, D. N., and Gordon, J. I. (2011). Recognition and degradation of plant cell wall polysaccharides by two human gut symbionts. *PLoS Biol., 9,* e1001221. https://doi.org/10.1371/journal.pbio.1001221.

McNulty, N., Wu, M., Erickson, A., Pan, C., Erickson, B., Martens, E., Pudlo, N., Muegge, B., Henrissat, B., Hettich, R., and Gordon, J. (2013). Effects of diet on resource utilization by a model human gut microbiota containing *Bacteroides cellulosilyticus* WH2, a symbiont with an extensive glycobiome. *PLoS Biol.*, *11(8):e1001637*. https://doi.org/doi:10.1371/journal.pbio.1001637.

Menshova, R., Ermakova, S., Anastyuk, S., Isakov, V., Dubrovskaya, Y., Kusaykin, M., Umb, B., and Zvyagintseva, T. (2014). Structure, Enzymatic Transformation and Anticancer Activity of Branched High Molecular Weight Laminaran From Brown Alga *Eisenia*

Bicyclis. *Carbohydr. Polym.*, *99*, 101-109.
https://doi.org/doi:10.1016/j.carbpol.2013.08.037.

Metzler-Zebeli, B., Hooda, S., Pieper, R., Zijlstra, R., van Kessel, A., Mosenthin, R., and Gänzle, M. (2010). Nonstarch Polysaccharides Modulate Bacterial Microbiota, Pathways for Butyrate Production, and Abundance of Pathogenic *Escherichia coli* in the Pig Gastrointestinal Tract. *Appl. Environ. Microbiol.*, *76*, 3692-3701. https://doi.org/doi:10.1128/AEM.00257-10.

Mikkelsen, M., Jensen, M., and Nielsen, T. (2017). Barley beta-glucans varying in molecular mass and oligomer structure affect cecal fermentation and microbial composition but not blood lipid profiles in hypercholesterolemic rats. *Food Funct.*, *8*, 4723-4732. https://doi.org/doi:10.1039/c7fo01314k.

Milani, C., Lugli, G. A., Duranti, S., Turroni, F., Bottacini, F., Mangifesta, M., Sanchez, B., Viappiani, A., Mancabelli, L., Taminiau, B., Delcenserie, V., Barrangou, R., Margolles, A., van Sinderen, D., and Ventura, M. (2014). Genomic encyclopedia of type strains of the genus *Bifidobacterium*. *Appl. Environ. Microbiol.*, *80*(20), 6290-6302. https://doi.org/10.1128/aem.02308-14.

Milani, C., Lugli, G. A., Duranti, S., Turroni, F., Mancabelli, L., Ferrario, C., Mangifesta, M., Hevia, A., Viappiani, A., Scholz, M., Arioli, S., Sanchez, B., Lane, J., Ward, D. V., Hickey, R., Mora, D., Segata, N., Margolles, A., van Sinderen, D. a. V., M. (2015). Bifidobacteria exhibit social behavior through carbohydrate resource sharing in the gut. *Sci. Rep.*, *5*, 15782. https://doi.org/10.1038/srep15782.

Miyamoto, J., Watanabe, K., Taira, S., Kasubuchi, M., Li, X., Irie, J.,, Itoh, H., and Kimura, I. (2018). Barley β-glucan improves metabolic condition via short-chain fatty acids produced by gut microbial fermentation in high fat diet fed mice. *PLoS One*, *3(4):e0196579*. https://doi.org/doi:10.1371/journal.pone.0196579.

Morris, B. E., Henneberger, R., Huber, H., and Moissl-Eichinger, C. (2013). Microbial syntrophy: interaction for the common good. *FEMS Microbiol. Rev.*, *37*(3), 384-406. https://doi.org/10.1111/1574-6976.12019.

Munoz, J., James, K., Bottacini, F. a. V. S., D. (2020). Biochemical analysis of cross-feeding behaviour between two common gut commensals when cultivated on plant-derived arabinogalactan. *Microb. Biotechnol.*, *13*(6), 1733-1747. https://doi.org/doi:10.1111/1751-7915.13577.

Muthuramalingam, K., Singh, V., Choi, C., Choi, S. I., Kim, Y. M., Unno, T. a. C., M. (2020). Dietary intervention using (1,3)/(1,6)-β-glucan, a fungus-derived soluble prebiotic ameliorates high-fat diet-induced metabolic distress and alters beneficially the gut microbiota in mice model. *Eur. J. Nutr.*, *59*(6), 2617-2629. https://doi.org/10.1007/s00394-019-02110-5.

Neyrinck, A. M., Possemiers, S., Verstraete, W., De Backer, F., Cani, P. D. a., Delzenne, N. M. (2012). Dietary modulation of clostridial cluster XIVa gut bacteria (*Roseburia* spp.) by chitin-glucan fiber improves host metabolic alterations induced by high-fat diet in mice. *J. Nutr. Biochem.*, *23*(1), 51-59. https://doi.org/10.1016/j.jnutbio.2010.10.008.

Nguyen, S., Kim, J., Guevarra, R., Lee, J., and Unno, T. (2016). Laminarin favorably modulates gut microbiota in mice fed a high-fat diet. *Food Funct.*, *7*, 4193-4201. https://doi.org/doi:10.1039/c6fo00929h.

Nguyen, T. T., Nguyen, P. T., Nguyen, T. T., Nguyen, T. B., Bui, N. B., and Nguyen, H. T. (2022). Efficacy of the incorporation between self-encapsulation and cryoprotectants on improving the freeze-dried survival of probiotic bacteria. *J. Appl. Microbiol.*, *132*(4), 3217-3225. https://doi.org/10.1111/jam.15473.

Nie, K., Ma, K., Luo, W., Shen, Z., Yang, Z., Xiao, M., Tong, T., Yang, Y., and Wang, X. (2021). *Roseburia intestinalis*: A Beneficial Gut Organism From the Discoveries in Genus and Species. *Front. Cell Infect. Microbiol.*, *11*, 757718. https://doi.org/10.3389/fcimb.2021.757718.

Nilholm, C., Manoharan, L., Roth, B., D'Amato, M., and Ohlsson, B. (2022). A starch- and sucrose-reduced dietary intervention in irritable bowel syndrome patients produced a

shift in gut microbiota composition along with changes in phylum, genus, and amplicon sequence variant abundances, without affecting the micro-RNA levels. *United European Gastroenterol. J.*, *10*(4), 363-375. https://doi.org/10.1002/ueg2.12227.

Nishida, A., Inoue, I., Inatomi, O., Bamba, S., Naito, Y., and Andoh, A. (2018). GutMicrobiota in the Pathogenesis of Inflammatory Bowel Disease. *Clin. J. Gastroenterol.*,*11*, 1-10. https://doi.org/doi:10.1007/s12328-017-0813-5.

Nishijima, S., Suda, W., Oshima, K., Kim, S., Hirose, Y., Morita, H., and Hattori M. (2016). The gut microbiome of healthy Japanese and its microbial and functional uniqueness. *DNA Res.*, 1-9. https://doi.org/doi:10.1093/dnares/dsw002.

O'Callaghan, J., and, O'Toole, P. W. (2013). *Lactobacillus*: host-microbe relationships. *Curr. Top Microbiol. Immunol.*, *358*, 119-154. https://doi.org/10.1007/82_2011_187.

O'Morain, V. L., Chan, Y. H., Williams, J. O., Alotibi, R., Alahmadi, A., Rodrigues, N. P., Plummer, S. F., Hughes, T. R., Michael, D. R., and Ramji, D. P. (2021). The Lab4P Consortium of Probiotics Attenuates Atherosclerosis in LDL Receptor Deficient Mice Fed a High Fat Diet and Causes Plaque Stabilization by Inhibiting Inflammation and Several Pro-Atherogenic Processes. *Mol. Nutr. Food Res.*, *65*(17), e2100214. https://doi.org/10.1002/mnfr.202100214.

Pabois, O., Antoine-Michard, A., Zhao, X., Omar, J., Ahmed, F., Alexis, F., Harvey, R. D., Grillo, I., Gerelli, Y., Grundy, M. M., Bajka, B., Wilde, P. J., and Dreiss, C. A. (2020). Interactions of bile salts with a dietary fibre, methylcellulose, and impact on lipolysis. *Carbohydr. Polym.*, *231*, 115741. https://doi.org/10.1016/j.carbpol.2019.115741

Panpetch, W., Somboonna, N., Bulan, D., Issara-Amphorn, J., Finkelman, M., Worasilchai, N., Chindamporn, A., Palaga, T., Tumwasorn, S., and Leelahavanichkul, A. (2017). Oral administration of live- or heat-killed *Candida albicans* worsened cecal ligation and puncture sepsis in a murine model possibly due to an increased serum (1→3)-β-D-glucan. *PLoS One*, *2(7):e0181439.* https://doi.org/doi:10.1371/journal.pone.0181439.

Panpetch, W., Chancharoenthana, W., Bootdee, K., Nilgate, S., Finkelman, M., Tumwasorn, S., and Leelahavanichkul, A. (2018). *Lactobacillus rhamnosus* L34 Attenuates Gut Translocation-Induced Bacterial Sepsis in Murine Models of Leaky Gut. *Infect. Immun.*, *86*(1). https://doi.org/10.1128/iai.00700-17.

Panpetch, W., Kullapanich, C., Dang, C. P., Visitchanakun, P., Saisorn, W., Wongphoom, J., Wannigama, D. L., Thim-Uam, A., Patarakul, K., Somboonna, N., Tumwasorn, S., Leelahavanichkul, A. (2021). *Candida* Administration Worsens Uremia-Induced Gut Leakage in Bilateral Nephrectomy Mice, an Impact of Gut Fungi and Organismal Molecules in Uremia. *mSystems*, *6*(1). https://doi.org/10.1128/mSystems.01187-20.

Parada Venegas, D., De la Fuente, M. K., Landskron, G., González, M. J., Quera, R., Dijkstra, G., Harmsen, H. J. M., Faber, K. N. a., Hermoso, M. A. (2019). Short Chain Fatty Acids (SCFAs)-Mediated Gut Epithelial and Immune Regulation and Its Relevance for Inflammatory Bowel Diseases. *Front. Immunol.*, *10*, 277. https://doi.org/doi:10.3389/fimmu.2019.00277.

Patil, N., Le, V., Sligar, A., Mei, L., Chavarria, D., Yang, E., and Baker, A. (2018). Algal Polysaccharides as Therapeutic Agents for Atherosclerosis. *Front. Cardiovasc. Med.*, *5:153.* https://doi.org/doi:10.3389/fcvm.2018.00153.

Petrova, M. I., Lievens, E., Malik, S., Imholz, N., and Lebeer, S. (2015). *Lactobacillus* species as biomarkers and agents that can promote various aspects of vaginal health. *Front. Physiol.*, *6*, 81. https://doi.org/10.3389/fphys.2015.00081.

Plovier, H., Everard, A., Druart, C., Depommier, C., Van Hul, M., Geurts, L., Chilloux, J., Ottman, N., Duparc, T., Lichtenstein, L., Myridakis, A., Delzenne, N. M., Klievink, J., Bhattacharjee, A., van der Ark, K. C., Aalvink, S., Martinez, L. O., Dumas, M. E., Maiter, D., de Vos, W. M., and Cani, P. D. (2017). A purified membrane protein from *Akkermansia muciniphila* or the pasteurized bacterium improves metabolism in obese and diabetic mice. *Nat. Med.*, *23*(1), 107-113. https://doi.org/10.1038/nm.4236.

Pokusaeva, K., Fitzgerald, G., and van Sinderen, D. (2010). Carbohydrate metabolism in Bifidobacteria. *Genes Nutr.*, *6*, 285-306. https://doi.org/doi:10.1007/s12263-010-0206-6.

Pokusaeva, K., O'Connell-Motherway, M., Zomer, A., Macsharry, J., Fitzgerald, G. F., and van Sinderen, D. (2011). Cellodextrin utilization by *Bifidobacterium breve* UCC2003. *Appl. Environ. Microbiol.*, *77*(5), 1681-1690. https://doi.org/https://doi.org/10.1128/aem.01786-10.

Pruss, K. M., Marcobal, A., Southwick, A. M., Dahan, D., Smits, S. A., Ferreyra, J. A., Higginbottom, S. K., Sonnenburg, E. D., Kashyap, P. C., Choudhury, B., Bode, L., and Sonnenburg, J. L. (2021). Mucin-derived O-glycans supplemented to diet mitigate diverse microbiota perturbations. *Isme j.*, *15*(2), 577-591. https://doi.org/10.1038/s41396-020-00798-6.

Qin, J., Li, R., Raes, J., Arumugam, M., Burgdorf, K., Manichanh, C., Nielsen, T., Pons, N., Levenez, F., Yamada, T., Mende, D., Li, J., Xu, J., Li, S., Li, D., Cao, J., Wang, B., Liang, H., Zheng, H., Xie, Y., Tap, J., Lepage, P., Bertalan, M., Batto, J., Hansen, T., Paslier, D., Linneberg, A., Nielsen, H., Pelletier, E., Renault, P., Sicheritz-Ponten, T., Turner, K., Zhu, H., Yu, C., Li, S., Jian, M., Zhou, Y., Li, Y., Zhang, X., Li, S., Qin, N., Yang, H., Wang, J., Brunak, S., Doré, J., Guarner, F., Kristiansen, K., Pedersen, O., Parkhill, J., Weissenbach, J., MetaHIT Consortium; Bork, P., Ehrlich, S., and Wang, J. (2010). A Human Gut Microbial Gene Catalogue Established by Metagenomic Sequencing. *Nature*, *7285*, 59-65. https://doi.org/doi:10.1038/nature08821.

Quan, Y., Song, K., Zhang, Y., Zhu, C., Shen, Z., Wu, S., Luo, W., Tan, B., Yang, Z., and Wang, X. (2018). *Roseburia intestinalis*-derived flagellin is a negative regulator of intestinal inflammation. *Biochem. Biophys. Res. Commun.*, *501*(3), 791-799. https://doi.org/10.1016/j.bbrc.2018.05.075.

Quigley, E. (2017). Microbiota-Brain-Gut Axis and Neurodegenerative Diseases. *Curr. Neurol. Neurosci. Rep.*, *17(12):94*. https://doi.org/doi:10.1007/s11910-017-0802-6.

Rajilić-Stojanović, M., Shanahan, F., Guarner, F., and de Vos, W. M. (2013). Phylogenetic analysis of dysbiosis in ulcerative colitis during remission. *Inflamm. Bowel Dis.*, *19*(3), 481-488. https://doi.org/10.1097/MIB.0b013e31827fec6d.

Rakoff-Nahoum, S., Coyne, M. J., and, Comstock, L. E. (2014). An ecological network of polysaccharide utilization among human intestinal symbionts. *Curr. Biol.*, *24*(1), 40-49. https://doi.org/10.1016/j.cub.2013.10.077.

Rakoff-Nahoum, S., Foster, K. R., and, Comstock, L. E. (2016). The evolution of cooperation within the gut microbiota. *Nature*, *533*(7602), 255-259. https://doi.org/10.1038/nature17626.

Reunanen, J., Kainulainen, V., Huuskonen, L., Ottman, N., Belzer, C., Huhtinen, H., de Vos, W. M., Satokari, R. (2015). *Akkermansia muciniphila* Adheres to Enterocytes and Strengthens the Integrity of the Epithelial Cell Layer. *Appl. Environ. Microbiol.*, *81*(11), 3655-3662. https://doi.org/10.1128/aem.04050-14.

Rios-Covian, D., Arboleya, S., Hernandez-Barranco, A. M., Alvarez-Buylla, J. R., Ruas-Madiedo, P., Gueimonde, M., and de los Reyes-Gavilan, C. G. (2013). Interactions between *Bifidobacterium* and *Bacteroides* species in cofermentations are affected by carbon sources, including exopolysaccharides produced by bifidobacteria. *Appl. Environ. Microbiol.*, *79*(23), 7518-7524. https://doi.org/https://doi.org/10.1128/aem.02545-13.

Rivière, A., Selak, M., Lantin, D., Leroy, F., and De Vuyst, L. (2016). Bifidobacteria and Butyrate-Producing Colon Bacteria: Importance and Strategies for Their Stimulation in the Human Gut. *Front. Microbiol.*, *7*, 979. https://doi.org/10.3389/fmicb.2016.00979.

Rodriguez, J., Neyrinck, A. M., Zhang, Z., Seethaler, B., Nazare, J. A., Robles Sánchez, C., Roumain, M., Muccioli, G. G., Bindels, L. B., Cani, P. D., Maquet, V., Laville, M., Bischoff, S. C., Walter, J., and Delzenne, N. M. (2020). Metabolite profiling reveals the interaction of chitin-glucan with the gut microbiota. *Gut Microbes*, *12*(1), 1810530. https://doi.org/10.1080/19490976.2020.1810530.

Rogowski, A., Briggs, J. A., Mortimer, J. C., Tryfona, T., Terrapon, N., Lowe, E. C., Baslé, A., Morland, C., Day, A. M., Zheng, H., Rogers, T. E., Thompson, P., Hawkins, A. R., Yadav, M. P., Henrissat, B., Martens, E. C., Dupree, P., Gilbert, H. J., and Bolam, D. N. (2015). Glycan complexity dictates microbial resource allocation in the large intestine. *Nat. Commun.*, *6*, 7481. https://doi.org/https://doi.org/10.1038/ncomms8481.

Roos, S., Engstrand, L., and, Jonsson, H. (2005). *Lactobacillus gastricus* sp. nov., *Lactobacillus antri* sp. nov., *Lactobacillus kalixensis* sp. nov. and *Lactobacillus ultunensis* sp. nov., isolated from human stomach mucosa. *Int. J. Syst. Evol. Microbiol.*, *55*(Pt 1), 77-82. https://doi.org/10.1099/ijs.0.63083-0.

Rosburg, V., Boylston, T., and White, P. (2010). Viability of Bifidobacteria Strains in Yogurt with Added Oat Beta-Glucan and Corn Starch during Cold Storage. *J. Food Sci.*, *75*, 439-444. https://doi.org/doi:10.1111/j.1750-3841.2010.01620.x.

Rumberger, J., Arch, J., and, Green, A. (2014). Butyrate and other short-chain fatty acids increase the rate of lipolysis in 3T3-L1 adipocytes. *PeerJ*, *2:e611*. https://doi.org/doi:10.7717/peerj.611.eCollection2014.

Ryan, P. M., London, L. E., Bjorndahl, T. C., Mandal, R., Murphy, K., Fitzgerald, G. F., Shanahan, F., Ross, R. P., Wishart, D. S., Caplice, N. M., and Stanton, C. (2017). Microbiome and metabolome modifying effects of several cardiovascular disease interventions in apo-E(-/-) mice. *Microbiome*, *5*(1), 30. https://doi.org/10.1186/s40168-017-0246-x.

Salyers, A. A., Gherardini, F., and, O'Brien, M. (1981). Utilization of xylan by two species of human colonic *Bacteroides*. *Appl. Environ. Microbiol.*, *41*(4), 1065-1068. https://doi.org/10.1128/aem.41.4.1065-1068.1981.

Sanjiwani, M. I. D., Aryadi, I. P. H., and Semadi, I. M. S. (2022). Review of Literature on *Akkermansia muciniphila* and its Possible Role in the Etiopathogenesis and Therapy of Type 2 Diabetes Mellitus. *J. ASEAN Fed. Endocr. Soc.*, *37*(1), 69-74. https://doi.org/10.15605/jafes.037.01.13.

Schwalm, N. D., 3rd, , and, Groisman, E. A. (2017). Navigating the Gut Buffet: Control of Polysaccharide Utilization in *Bacteroides* spp. *Trends Microbiol.*, *25*(12), 1005-1015. https://doi.org/10.1016/j.tim.2017.06.009.

Schwartz, B., and, Hadar, Y. (2014). Possible mechanisms of action of mushroom-derived glucans on inflammatory bowel disease and associated cancer. *Ann. Transl. Med.*, *2(2):19*. https://doi.org/doi:10.3978/j.issn.2305-5839.2014.01.0.

Scillato, M., Spitale, A., Mongelli, G., Privitera, G. F., Mangano, K., Cianci, A., Stefani, S., and Santagati, M. (2021). Antimicrobial properties of *Lactobacillus* cell-free supernatants against multidrug-resistant urogenital pathogens. *Microbiologyopen*, *10*(2), e1173. https://doi.org/10.1002/mbo3.1173.

Scott, K. P., Martin, J. C., Chassard, C., Clerget, M., Potrykus, J., Campbell, G., Mayer, C. D., Young, P., Rucklidge, G., Ramsay, A. G., and Flint, H. J. (2011). Substrate-driven gene expression in *Roseburia inulinivorans*: importance of inducible enzymes in the utilization of inulin and starch. *Proc. Natl. Acad. Sci. U. S. A.*, *108 Suppl 1*(Suppl 1), 4672-4679. https://doi.org/doi:10.1073/pnas.1000091107.

Scott, K. P., Martin, J. C., Duncan, S. H., and Flint, H. J. (2014). Prebiotic stimulation of human colonic butyrate-producing bacteria and bifidobacteria, in vitro. *FEMS Microbiol. Ecol.*, *87*(1), 30-40. https://doi.org/10.1111/1574-6941.12186.

Sellimi, S., Maalej, H., Rekik, D., Benslima, A., Ksouda, G., Hamdi, M., Sahnoun, Z., Suming, L., Nasri, M., and Hajji, M. (2018). Antioxidant, antibacterial and in vivo wound healing properties of laminaran purified from *Cystoseira barbata* seaweed. *Int. J. Biol. Macromol.* , *19*, 633-644. https://doi.org/doi:10.1016/j.ijbiomac.2018.07.171.

Seo, B., Jeon, K., Moon, S., Lee, K., Kim, W. K., Jeong, H., Cha, K. H., Lim, M. Y., Kang, W., Kweon, M. N., Sung, J., Kim, W., Park, J. H., and Ko, G. (2020). *Roseburia* spp. Abundance Associates with Alcohol Consumption in Humans and Its Administration Ameliorates Alcoholic Fatty Liver in Mice. *Cell Host Microbe*, *27*(1), 25-40.e26. https://doi.org/10.1016/j.chom.2019.11.001.

Seth, E., and, Taga, M. (2014). Nutrient cross-feeding in the microbial world. *Front. Microbiol.*, *5:350. doi: 10.3389/fmicb.2014.00350.* .

Shen, J., Tong, X., Sud, N., Khound, R., Song, Y., Maldonado-Gomez, M. X., Walter, J., and Su, Q. (2016). Low-Density Lipoprotein Receptor Signaling Mediates the Triglyceride-Lowering Action of *Akkermansia muciniphila* in Genetic-Induced Hyperlipidemia. *Arterioscler Thromb. Vasc. Biol.*, *36*(7), 1448-1456. https://doi.org/10.1161/atvbaha.116.307597.

Shen, R., Cai, F., Dong, J., and Hu, X. (2011). Hypoglycemic Effects and Biochemical Mechanisms of Oat Products on Streptozotocin-Induced Diabetic Mice. *J. Agric. Food Chem.*, *59*, 8895-8900 https://doi.org/doi:10.1021/jf200678q.

Shen, R., Dang, D., Dong, J., and Hu, X. (2012). Effects of Oat β-Glucan and Barley β-Glucan on Fecal Characteristics, Intestinal Microflora, and Intestinal Bacterial Metabolites in Rats. *J. Agric. Food Chem.*, *60*, 11301-11308. https://doi.org/doi:10.1021/jf302824h.

Sheridan, P. O., J. C., Lawley, T. D., Browne, H. P., Harris, H. M. B., Bernalier-Donadille, A., Duncan, S. H., O'Toole, P. W., P. Scott K, and J. F. H. (2016). Polysaccharide utilization loci and nutritional specialization in a dominant group of butyrate-producing human colonic Firmicutes. *Microb. Genom.*, *2*(2), e000043. https://doi.org/10.1099/mgen.0.000043.

Shipman, J., Berleman, J., and, Salyers, A. (2020). Characterization of Four Outer Membrane Proteins Involved in Binding Starch to the Cell Surface of *Bacteroides thetaiotaomicron*. *J. Bacteriol.*, *182*, 5365-5372. https://doi.org/doi:10.1128/jb.182.19.5365-5372.2000.

Si, X., Shang, W., Zhou, Z., Strappe, P., Wang, B., Bird, A., and Blanchard, C. (2018). Gut Microbiome-Induced Shift of Acetate to Butyrate Positively Manages Dysbiosis in High Fat Diet. *Mol. Nutr. Food Res.*, *62*(3). https://doi.org/10.1002/mnfr.201700670.

Singh, R. P. (2019). Glycan utilisation system in Bacteroides and Bifidobacteria and their roles in gut stability and health. *Appl. Microbiol. Biotechnol.*, *103*(18), 7287-7315. https://doi.org/doi:10.1007/s00253-019-10012-z.

Smith, A., O'Doherty, J., Reilly, P., Ryan, M., Bahar, B., and Sweeney, T. (2011). The effects of laminarin derived from *Laminaria digitata* on measurements of gut health: selected bacterial populations, intestinal fermentation, mucin gene expression and cytokine gene expression in the pig. *Br. J. Nutr.*, *105*, 669-677. https://doi.org/doi:10.1017/S0007114510004277.

Smith, N. W., Shorten, P. R., Altermann, E., Roy, N. C., and McNabb, Warren C. (2019). The Classification and Evolution of Bacterial Cross-Feeding [Review]. *Frontiers in Ecology and Evolution*, *7*. https://doi.org/10.3389/fevo.2019.00153.

Sonnenburg, E., Smits, S., Tikhonov, M., Higginbottom, S., Wingreen, N., and Sonnenburg, J. (2016). Diet-induced extinctions in the gut microbiota compound over generations. *Nature*, *529(7585):212-5*. https://doi.org/doi:10.1038/nature16504.

Stier, H., Ebbeskotte, V., and Gruenwald, J. (2014). Immune-modulatory effects of dietary Yeast Beta-1,3/1,6-D-glucan. *Nutr. J.*, *13:38*. https://doi.org/doi:10.1186/1475-2891-13-38.

Sweeney, T., Collins, C., Reilly, P., Pierce, K., Ryan, M., and O'Doherty, J. (2012). Effect of purified b-glucans derived from *Laminaria digitata*, *Laminaria hyperborea* and *Saccharomyces cerevisiae* on piglet performance, selected bacterial populations, volatile fatty acids and pro-inflammatory cytokines in the gastrointestinal tract of pigs. *Br. J. Nutr.*, *108*, 1226-1234. https://doi.org/doi:10.1017/S0007114511006751.

Takei, M., Kuda, T., Taniguchi, M., Nakamura, S., Hajime, T., and Kimura, B. (2020). Detection and isolation of low molecular weight alginate- and laminaran-susceptible gut indigenous bacteria from ICR mice. *Carbohydr. Polym.*, *238:116205*. https://doi.org/doi:10.1016/j.carbpol.2020.116205.

Tamanai-Shacoori, Z., Smida, I., Bousarghin, L., Loreal, O., Meuric, V., Fong, S. B., Bonnaure-Mallet, M., and Jolivet-Gougeon, A. (2017). *Roseburia* spp.: a marker of health? *Future Microbiol.*, *12*, 157-170. https://doi.org/10.2217/fmb-2016-0130.

Tamura, K., Hemsworth, G., Dejean, G., Rogers, T., Pudlo, N., Urs, K., Jain, N., Davies, G., Martens, E., and Brumer, H. (2017). Molecular mechanism by which prominent human-gut Bacteroidetes utilize mixed-linkage beta-glucans, major health-promoting cereal polysaccharides. *Cell Rep.*, *21*, 417-430. https://doi.org/doi:10.1016/j.celrep.2017.09.049.

Tamura, K., Foley, M., Gardill, B., Dejean, G., Schnizlein, M., Bahr, C., Creagh, A., van Petegem, F., Koropatkin, N., and Brumer, H. (2019). Surface glycan-binding proteins are essential for cereal beta-glucan utilization by the human gut symbiont *Bacteroides ovatus*. *Cell. Mol. Life Sci.*, *76(21)*, 4319-4340. https://doi.org/doi:10.1007/s00018-019-03115-3.

Temple, M., Cuskin, F., Baslé, A., Hickey, N., Speciale, G., Williams, S., Gilbert, H., and Lowe, E. (2017). A Bacteroidetes locus dedicated to fungal 1,6-β-glucan degradation: Unique substrate conformation drives specificity of the key endo-1,6-β-glucanase. *J. Biol. Chem.*, *292(25):10639-10650*. https://doi.org/doi:10.1074/jbc.M117.787606.

Temuujin, U., Chi, W. J., Park, J. S., Chang, Y. K., Song, J. Y., and Hong, S. K. (2012). Identification and characterization of a novel β-galactosidase from *Victivallis vadensis* ATCC BAA-548, an anaerobic fecal bacterium. *J. Microbiol.*, *50*(6), 1034-1040. https://doi.org/10.1007/s12275-012-2478-6.

Terrapon, N., Lombard, V., Drula, E., Lapébie, P., Al-Masaudi, S., G., H., and Henrissat, B. (2018). PULDB: the expanded database of Polysaccharide Utilization Loci. *Nucleic Acids Res.*, *46(D1):D677-D683*. https://doi.org/doi:10.1093/nar/gkx1022.

Thomas, F., Bordron, P., Eveillard, D., and Michel, G. (2017). Gene Expression Analysis of *Zobellia galactanivorans* during the Degradation of Algal Polysaccharides Reveals both Substrate-Specific and Shared Transcriptome-Wide Responses. *Front. Microbiol.*, *8:1808*. https://doi.org/doi:10.3389/fmicb.2017.01808.

Thursby, E., and, Juge, N. (2017). Introduction to the human gut microbiota. *Biochem. J.*, *474*(11), 1823-1836. https://doi.org/10.1042/bcj20160510.

Tuomisto, H. L. (2022). Mycoprotein produced in cell culture has environmental benefits over beef. *Nature*, *605*(7908), 34-35. https://doi.org/10.1038/d41586-022-01125-z.

Turnbull, W. H., and, Ward, T. (1995). Mycoprotein reduces glycemia and insulinemia when taken with an oral-glucose-tolerance test. *Am. J. Clin. Nutr.*, *61*(1), 135-140. https://doi.org/10.1093/ajcn/61.1.135.

Turnbull, W. H., Walton, J., and, Leeds, A. R. (1993). Acute effects of mycoprotein on subsequent energy intake and appetite variables. *Am J. Clin. Nutr.*, *58*(4), 507-512. https://doi.org/10.1093/ajcn/58.4.507.

Turroni, F., Bottacini, F., Foroni, E., Mulder, I., Kim, J. H., Zomer, A., Sánchez, B., Bidossi, A., Ferrarini, A., Giubellini, V., Delledonne, M., Henrissat, B., Coutinho, P., Oggioni, M., Fitzgerald, G. F., Mills, D., Margolles, A., Kelly, D., van Sinderen, D., and Ventura, M. (2010). Genome analysis of *Bifidobacterium bifidum* PRL2010 reveals metabolic pathways for host-derived glycan foraging. *Proc Natl. Acad. Sci. U. S. A.*, *107*(45), 19514-19519. https://doi.org/10.1073/pnas.1011100107.

Turroni, F., van Sinderen, D., and Ventura, M. (2011). Genomics and ecological overview of the genus *Bifidobacterium*. *Int. J. Food Microbiol.*, *149*, 37-44. https://doi.org/doi:10.1016/j.ijfoodmicro.2010.12.010.

Turroni, F., Peano, C., Pass, D., Foroni, E., S., M., Claesson, M., Kerr, C., Hourihane, J., Murray, D., Fuligni, F., Gueimonde, M., Margolles, A., De Bellis, G., O'Toole, P., van Sinderen, D., Marchesi, J., and Ventura, M. (2012). Diversity of Bifidobacteria within the Infant Gut Microbiota. *PLoS One*, *(5):e36957*. https://doi.org/doi:10.1371/journal.pone.0036957.

Turroni, F., Özcan, E., Milani, C., Mancabelli, L., Viappiani, A., van Sinderen, D., Sela, D. A., and Ventura, M. (2015). Glycan cross-feeding activities between bifidobacteria under in vitro conditions. *Front. Microbiol.*, *6*, 1030. https://doi.org/doi:10.3389/fmicb.2015.01030.

Turroni, F., Duranti, S., Milani, C., Lugli, G., van Sinderen, D., and Ventura, M. (2019). *Bifidobacterium bifidum*: A Key Member of the Early Human Gut Microbiot. *Microorganisms*, 7(11):544. . https://doi.org/doi:10.3390/microorganisms7110544.

Turunen, K., Tsouvelakidou, E., Nomikos, T., Mountzouris, K., Karamanolis, D., Triantafillidis, J., and Kyriacou, A. (2011). Impact of beta-glucan on the faecal microbiota of polypectomized patients: A pilot study. *Anaerobe*, *17*, 403-406. https://doi.org/doi:10.1016/j.anaerobe.2011.03.025.

Ugalde, U. O., and, Castrillo, J. I. (2002). Single cell proteins from fungi and yeasts. *Appl. Mycol. Biotechnol.*, *2*, 123-149. https://doi.org/https://doi.org/10.1016/S1874-5334(02)80008-9.

Valguarnera, E., Scott N.E., Azimzadeh, P., Feldman, M. (2018). Surface Exposure and Packing of Lipoproteins into Outer Membrane Vesicles Are Coupled Processes in *Bacteroides*. mSphere, 3(6):e00559-18 https://doi.org/10.1128/mSphere.00559-18.

Van den Abbeele, P., Gérard, P., Rabot, S., Bruneau, A., El Aidy, S., Derrien, M., Kleerebezem, M., Zoetendal, E. G., Smidt, H., Verstraete, W., Van de Wiele, T., and Possemiers, S. (2011). Arabinoxylans and inulin differentially modulate the mucosal and luminal gut microbiota and mucin-degradation in humanized rats. *Environ. Microbiol.*, *13*(10), 2667-2680. https://doi.org/10.1111/j.1462-2920.2011.02533.x.

van Passel, M. W., Kant, R., Palva, A., Lucas, S., Copeland, A., Lapidus, A., Glavina del Rio, T., Dalin, E., Tice, H., Bruce, D., Goodwin, L., Pitluck, S., Davenport, K. W., Sims, D., Brettin, T. S., Detter, J. C., Han, S., Larimer, F. W., Land, M. L., Hauser, L., Kyrpides, N., Ovchinnikova, G., Richardson, P. P., de Vos, W. M., Smidt, H., and Zoetendal, E. G. (2011). Genome sequence of *Victivallis vadensis* ATCC BAA-548, an anaerobic bacterium from the phylum Lentisphaerae, isolated from the human gastrointestinal tract. *J Bacteriol*, *193*(9), 2373-2374. https://doi.org/10.1128/jb.00271-11.

Varela-Pérez, A., Romero-Chapol, O. O., Castillo-Olmos, A. G., García, H. S., Suárez-Quiroz, M. L., Singh, J., Figueroa-Hernández, C. Y., Viveros-Contreras, R., and Cano-Sarmiento, C. (2022). Encapsulation of *Lactobacillus gasseri*: Characterization, Probiotic Survival, In Vitro Evaluation and Viability in Apple Juice. *Foods*, *11*(5). https://doi.org/10.3390/foods11050740.

Vega, K., and, Kalkum, M. (2012). Chitin, chitinase responses, and invasive fungal infections. *Int. J. Microbiol.*, *2012*, 920459. https://doi.org/10.1155/2012/920459.

Venardou, B., O'Doherty, J. V., McDonnell, M. J., Mukhopadhya, A., Kiely, C., Ryan, M. T. a. S., T. (2021). Evaluation of the in vitro effects of the increasing inclusion levels of yeast β-glucan, a casein hydrolysate and its 5 kDa retentate on selected bacterial populations and strains commonly found in the gastrointestinal tract of pigs. *Food Funct.*, *12*(5), 2189-2200. https://doi.org/10.1039/d0fo02269a.

Vetvicka, V., Vannucci, L., and Sima, P. (2020). β-glucan as a new tool in vaccine development. *Scand. J. Inmunol.*, *91:e12833*. . https://doi.org/doi:10.1111/sji.12833.

Viborg, A., Terrapon, N., Lombard, V., Michel, G., Czjzek, M., Henrissat, B., and Brumer, H. (2019). A subfamily roadmap of the evolutionarily diverse glycoside hydrolase family 16 (GH16). *J. Biol. Chem.*, *294(44):15973-15986*. https://doi.org/doi:10.1074/jbc.RA119.010619.

Vitaglione, P., Mennella, I., Ferracane, R., Rivellese, A., Giacco, R., Ercolini, D., Gibbons, S., La Storia, A., Gilbert, J., Jonnalagadda, S., Thielecke, F., Gallo, M., Scalfi, L., and Fogliano, V. (2015). Whole-grain wheat consumption reduces inflammation in a randomized controlled trial on overweight and obese subjects with unhealthy dietary and lifestyle behaviors: role of polyphenols bound to cereal dietary fiber. *Am. J. Clin. Nutr.*, *101(2):251-61*. https://doi.org/doi:10.3945/ajcn.114.088120.

Viborg, A. H., Terrapon, N., Lombard, V., Michel, G.,Czjzek, M., Henrissat, B., and Brumer, H. (2019). A subfamily roadmap of the evolutionarily diverse glycoside hydrolase family 16 (GH16). *J. Biol. Chem.*, *294*, 15973-15986. https://doi.org/10.1074/jbc.RA119.010619.

von Schantz, L., Håkansson, M., Logan, D., Walse, B., Österlin, J., Nordberg-Karlsson, E., and Ohlin, M. (2012). Structural basis for carbohydrate-binding specificity—A comparative assessment of two engineered carbohydrate-binding modules. *Glycobiology*, *22, 948–961*. https://doi.org/https://doi.org/10.1093/glycob/cws063.

Vu, V., Muthuramalingam, K., Singh, V., Hyun, C., Kim, Y. M., Unno, T. a. C., M. (2022). Effects of β-glucan, probiotics, and synbiotics on obesity-associated colitis and hepatic manifestations in C57BL/6J mice. *Eur. J. Nutr.*, *61*(2), 793-807. https://doi.org/10.1007/s00394-021-02668-z.

Walker, A. W., Ince, J., Duncan, S. H., Webster, L. M., Holtrop, G., Ze, X., Brown, D., Stares, M. D., Scott, P., Bergerat, A., Louis, P., McIntosh, F., Johnstone, A. M., Lobley, G. E., Parkhill, J. and F., H. J. (2011). Dominant and diet-responsive groups of bacteria within the human colonic microbiota. *Isme j*, *5*(2), 220-230. https://doi.org/10.1038/ismej.2010.118.

Wang, M., Wang, X., Zhang, L., Yang, R., Fei, C., Zhang, K., Wang, C., Liu, Y., and Xue, F. (2019). Effect of sulfated yeast beta-glucan on cyclophosphamide-induced immunosuppression in chickens. *Int. Inmunopharmacol.*, *74:105690*. https://doi.org/doi:10.1016/j.intimp.2019.105690.

Wang, C., Qiao, W., Chen, H., Xu, X., and Zhu, L. (2019). A short-term stimulation of ethanol enhances the effect of magnetite on anaerobic digestion. *Appl. Microbiol. Biotechnol.*, *103*(3), 1511-1522. https://doi.org/doi:10.1007/s00253-018-9531-2

Wang, J., Zhang, W., Wang, S., Wang, Y., Chu, X., and Ji, H. (2021). *Lactobacillus plantarum* Exhibits Antioxidant and Cytoprotective Activities in Porcine Intestinal Epithelial Cells Exposed to Hydrogen Peroxide. *Oxid, Med, Cell Longev,*, *2021*, 8936907. https://doi.org/https://doi.org/10.1155/2021/8936907.

Wang, Q., Sheng, X., Shi, A., Hu, H., Yang, Y., Liu, L., Fei, L., and Liu, H. (2017). β-Glucans: Relationships between Modification, Conformation and Functional Activities. *Molecules*, *22*(2). https://doi.org/https://doi.org/10.3390/molecules22020257.

Wang, Y., Ames, N., Tun, H., Tosh, S., Jones, P., and Khafipour, E. (2016). High Molecular Weight Barley β-Glucan Alters Gut Microbiota Toward Reduced Cardiovascular Disease Risk. *Front. Microbiol.*, *7:129*. https://doi.org/doi:10.3389/fmicb.2016.00129.

Wegh, C. A. M., Geerlings, S. Y., Knol, J., Roeselers, G. a., Belzer, C. (2019). Postbiotics and Their Potential Applications in Early Life Nutrition and Beyond. *Int. J. Mol. Sci.*, *20*(19). https://doi.org/https://doi.org/10.3390/ijms20194673.

Wexler, A., and, Goodman, A. (2017). An insider's perspective: *Bacteroides* as a window into the microbiome. *Nat. Microbiol.*, *2:17026*. https://doi.org/https://doi.org/10.1038/nmicrobiol.2017.26.

WHO/FAO. (2007). Food and Agricultural Organization of the United Nations and World Health Organization. Health and nutritional properties of probiotics in food including powder milk with live lactic acid bacteria. . https://doi.org/http://www.who.int/foodsafety/publications/.

Wilson, F. M., and, Harrison, R. J. (2021). CRISPR/Cas9 mediated editing of the Quorn fungus Fusarium venenatum A3/5 by transient expression of Cas9 and sgRNAs targeting endogenous marker gene PKS12. *Fungal Biol. Biotechnol.*, *8*(1), 15. https://doi.org/https://doi.org/10.1186/s40694-021-00121-8.

Wong, C. B., Odamaki, T., and Xiao, J. (2019). Beneficial effects of *Bifidobacterium longum* subsp. *longum* BB536 on human health: Modulation of gut microbiome as the principal action. *J. Funct. Foods*, *54*, 506-519. https://doi.org/https://doi.org/10.1016/j.jff.2019.02.002.

Wu, X., Chen, D., Yu, B., Luo, Y., Zheng, P., Mao, X., Yu, J., and He, J. (2018). Effect of different dietary non-starch fiber fractions on growth performance, nutrient digestibility, and intestinal development in weaned pigs. *Nutrition*, *51-52*, 20-28. https://doi.org/doi:10.1016/j.nut.2018.01.011.

Wu, Z., Xu, Q., Gu, S., Chen, Y., Lv, L., Zheng, B., Wang, Q., Wang, K., Wang, S., Xia, J., Yang, L., Bian, X., Jiang, X., Zheng, L., and Li, L. (2022). *Akkermansia muciniphila*

Ameliorates Clostridioides difficile Infection in Mice by Modulating the Intestinal Microbiome and Metabolites. *Front. Microbiol.*, *13*, 841920. https://doi.org/10.3389/fmicb.2022.841920.

Xia, S., Gao, B., Li, A., Xiong, J., Ao, Z., and Zhang, C. (2014). Preliminary Characterization, Antioxidant Properties and Production of Chrysolaminarin from Marine Diatom *Odontella aurita*. *Mar. Drugs*, *12*, 4883-4897. https://doi.org/doi:10.3390/md12094883.

Xu, M., Mo, X., Huang, H., Chen, X., Liu, H., Peng, Z., Chen, L., Rong, S., Yang, W., Xu, S., and Liu, L. (2020). Yeast β-glucan alleviates cognitive deficit by regulating gut microbiota and metabolites in Aβ1–42-induced AD-like mice. *Int. J. Biol. Macromol.*, *161*, 258-270. https://doi.org/doi:10.1016/j.ijbiomac.2020.05.180.

Yang, F., Wang, J., Zhang, H., Xie, Y., Jin, J., Liu, H., Pang, X., and Hao, H. (2021). Hypoglycemic effects of space-induced Lactobacillus plantarum SS18-5 on type 2 diabetes in a rat model. *J Food Biochem.*, *45*(9), e13899. https://doi.org/10.1111/jfbc.13899.

Yang, J., Martínez, I., Walter, J., Keshavarzian, A., and Rose, D. (2013). In vitro characterization of the impact of selected dietary fibers on fecal microbiota composition and short-chain fatty acid production. *Anaerobe*, *23*, 74-81 https://doi.org/doi:10.1016/j.anaerobe.2013.06.012.

Yang, X., Xie, L., Li, Y., and Wei, C. (2009). More than 9,000,000 Unique Genes in Human Gut Bacterial Community: Estimating Gene Numbers Inside a Human Body *PLoS One*, *4(6):e6074*. https://doi.org/doi:10.1371/journal.pone.0006074.

Yau, Y. F., El-Nezami, H., Galano, J. M., Kundi, Z. M., Durand, T., and Lee, J. C. (2020). *Lactobacillus rhamnosus* GG and Oat Beta-Glucan Regulated Fatty Acid Profiles along the Gut-Liver-Brain Axis of Mice Fed with High Fat Diet and Demonstrated Antioxidant and Anti-Inflammatory Potentials. *Mol. Nutr. Food Res.*, *64*(18), e2000566. https://doi.org/10.1002/mnfr.202000566.

Yoshitake, R., Hirose, Y., Murosaki, S., and Matsuzaki, G. (2021). Heat-killed *Lactobacillus plantarum* L-137 attenuates obesity and associated metabolic abnormalities in C57BL/6 J mice on a high-fat diet. *Biosci. Microbiota Food Health*, *40*(2), 84-91. https://doi.org/10.12938/bmfh.2020-040.

Zeybek, N., Rastall, R. A., and Buyukkileci, A. O. (2020). Utilization of xylan-type polysaccharides in co-culture fermentations of *Bifidobacterium* and *Bacteroides* species. *Carbohydr. Polym.*, *236*, 116076. https://doi.org/10.1016/j.carbpol.2020.116076.

Zhai, Q., Feng, S., Arjan, N., and Chen, W. (2019). A next generation probiotic, *Akkermansia muciniphila*. *Crit. Rev. Food Sci. Nutr.*, *59*(19), 3227-3236. https://doi.org/10.1080/10408398.2018.1517725.

Zhang, L., Ouyang, Y., Li, H., Shen, L., Ni, Y., Fang, Q., Wu, G., Qian, L., Xiao, Y., Zhang, J., Yin, P., Panagiotou, G., Xu, G., Ye, J., and Jia, W. (2019). Metabolic phenotypes and the gut microbiota in response to dietary resistant starch type 2 in normal-weight subjects: a randomized crossover trial. *Sci. Rep.*, *9*(1), 4736. https://doi.org/10.1038/s41598-018-38216-9.

Zhang, L., Wang, Y., Wu, F., Wang, X., Feng, Y., and Wang, Y. (2022). MDG, an *Ophiopogon japonicus* polysaccharide, inhibits non-alcoholic fatty liver disease by regulating the abundance of *Akkermansia muciniphila*. *Int. J. Biol. Macromol.*, *196*, 23- 34. https://doi.org/10.1016/j.ijbiomac.2021.12.036.

Zhang, J., Wang, P., Tan, C., Zhao, Y., Zhu, Y., Bai, J., and, Xiao, X. (2022). Integrated transcriptomics and metabolomics unravel the metabolic pathway variations for barley β-glucan before and after fermentation with *L. plantarum* DY-1. *Food Funct.*, *13*(8), 4302-4314. https://doi.org/10.1039/d1fo02450g.

Zhang, M., Chekand, J., Dodda, D., Hong, P., Radlinski, L., Revindran, V., Nairb, S., Mackie R., and Cann, I. (2014). Xylan utilization in human gut commensal bacteria is orchestrated by unique modular organization of polysaccharide-degrading enzymes.

Proc. Natl. Acad. Sci., *111(35):E3708-17*. https://doi.org/doi:10.1073/pnas.1406156111.

Zhang, M., Kim, J., and Huang, A. (2018). Optimizing Tumor Microenvironment for Cancer immunotherapy: β-Glucan-Based Nanoparticles. *Front. Inmunol.*, *9*, 341-353. https://doi.org/doi:10.3389/fimmu.2018.00341.

Zhang, P., Hu, X., Zhen, H., Xu, C., and Fan, M. (2012). Oat β-Glucan Increased ATPases Activity and Energy Charge in Small Intestine of Rats *J. Agric. Food Chem.*, *60*, 9822-9827. https://doi.org/doi:10.1021/jf3017496.

Zhang, X., Shen, D., Fang, Z., Jie, Z., Qiu, X., Zhang, C., Chen, Y., and Ji, L. (2013). Human gut microbiota changes reveal the progression of glucose intolerance. *PLoS One*, *8*(8), e71108. https://doi.org/10.1371/journal.pone.0071108.

Zhao, J., and Cheung, P. (2013). Comparative proteome analysis of *Bifidobacterium longum* subsp. *infantis* grown on β-glucans from different sources and a model for their utilization. *J. Agric Food Chem.*, *70*, 4360-4370. https://doi.org/doi:10.1021/jf400792j.

Zhao, W., Peng, C., Sakandar, H. A., Kwok, L. Y., and Zhang, W. (2021). Meta-Analysis: Randomized Trials of *Lactobacillus plantarum* on Immune Regulation Over the Last Decades. *Front. Immunol.*, *12*, 643420. https://doi.org/10.3389/fimmu.2021.643420.

Zhao, Y., Wu, C., Bai, J., Li, J., Cheng, K., Zhou, X., Dong, Y., Xiao, X. (2020). Fermented barley extracts with *Lactobacillus plantarum* dy-1 decreased fat accumulation of *Caenorhabditis elegans* in a daf-2-dependent mechanism. *J. Food Biochem.*, *44*(11), e13459. https://doi.org/10.1111/jfbc.13459.

Zhen, W., Liu, Y., Shao, Y., Ma, Y., Wu, Y., Guo, F., Abbas, W., Guo, Y., and Wang, Z. (2021). Yeast β-Glucan Altered Intestinal Microbiome and Metabolome in Older Hens. *Front. Microbiol.*, *12*, 766878. https://doi.org/10.3389/fmicb.2021.766878.

Zhong, Y., Marungruang, N., Fak, F., and Nyman, M. (2015). Effects of two whole-grain barley varieties on caecal SCFA, gut microbiota and plasma inflammatory markers in rats consuming low- and high-fat diets. *Br. J. Nutr.*, *10*, 1558-1570. https://doi.org/doi:10.1017/S0007114515000793.

Zhou, X., Lu, J., Wei, K., Wei, J., Tian, P., Yue, M., Wang, Y., Hong, D., Li, F., Wang, B., Chen, T., and Fang, X. (2021). Neuroprotective Effect of Ceftriaxone on MPTP-Induced Parkinson's Disease Mouse Model by Regulating Inflammation and Intestinal Microbiota. *Oxid. Med. Cell Longev.*, 9424582. https://doi.org/10.1155/2021/9424582.

Zhu, F., Du, B., and, Xu, B. (2016). A critical review on production and industrial applications of beta-glucans. *Food Hydrocoll.*, *52*, 275-288. https://doi.org/https://doi.org/10.1016/j.foodhyd.2015.07.003.

Zoetendal, E. G., Plugge, C. M., Akkermans, A. D. L., and de Vos, W. M. (2003). *Victivallis vadensis* gen. nov., sp. nov., a sugar-fermenting anaerobe from human faeces. *Int. J. Syst. Evol. Microbiol.*, *53*(Pt 1), 211-215. https://doi.org/10.1099/ijs.0.02362-0.

7 Publications

The publications included in this thesis were developed during my PhD in Northumbria University. They are included as part of this thesis, and they are shown in chronological order of publication.

Review

A comprehensive review on the impact of β-glucan metabolism by *Bacteroides* and *Bifidobacterium* species as members of the gut microbiota

Pedro J. Fernandez-Julia [a], Jose Munoz-Munoz [a,*], Douwe van Sinderen [b,*]

[a] *Department of Applied Sciences, Northumbria University, Newcastle Upon Tyne NE1 8ST, Tyne & Wear, England, United Kingdom*
[b] *School of Microbiology & APC Microbiome Ireland, University College Cork, Ireland University College Cork, Cork, Ireland*

ARTICLE INFO

ABSTRACT

β-glucans are polysaccharides which can be obtained from different sources, and which have been described as potential prebiotics. The beneficial effects associated with β-glucan intake are that they reduce energy intake, lower cholesterol levels and support the immune system. Nevertheless, the mechanism(s) of action underpinning these health effects related to β-glucans are still unclear, and the precise impact of β-glucans on the gut microbiota has been subject to debate and revision. In this review, we summarize the most recent advances involving structurally different types of β-glucans as fermentable substrates for Bacteroidetes (mainly *Bacteroides*) and *Bifidobacterium* species as glycan degraders. *Bacteroides* is one of the most abundant bacterial components of the human gut microbiota, while bifidobacteria are widely employed as a probiotic ingredient. Both are generalist glycan degraders capable of using a wide range of substrates: *Bacteroides* spp. are specialized as primary degraders in the metabolism of complex carbohydrates, whereas *Bifidobacterium* spp. more commonly metabolize smaller glycans, in particular oligosaccharides, sometimes through syntrophic interactions with *Bacteroides spp.*, in which they act as secondary degraders.

© 2018 Elsevier B.V. All rights reserved.

Contents

1. Introduction

β-Glucans are complex polysaccharides composed of D-glucopyranosyl residues that are linked through β-bonds. These ubiquitous polymers are present in cells walls of yeast, fungi, seaweed, bacteria and cereals, such as wheat, oat and barley [1,2]. The macromolecular

* Corresponding authors.
    E-mail addresses: jose.munoz@northumbria.ac.uk (J. Munoz-Munoz),
d.vansinderen@ucc.ie (D. van Sinderen).

structure of β-glucans is different according to the extraction source. For instance, cereal β-glucans have a backbone of single β(1,3)-bonds separating short sections of β(1,4)-bonds, while seaweed β-glucans typically consist of a β(1,3)-linkage backbone with single β(1,6) branching points, in which the resulting side chain contains β(1,3)-linkages (Fig. 1). Additionally, mushroom-derived β-glucans typically represent polymers composed of β(1,6)-linked branches from a β(1,3) backbone, while bacterial β-glucans simply consist of a linear β(1,3) backbone (Fig. 1) [3–6].

β-glucans can be modified by physical, chemical and biological methods, which affect their primary structure, spatial conformations and bioactivity. In fact, modification and transformation of β-glucans may not only improve their biological functionalities in the human gut, but also their applications as a prebiotic [7–9]). Such processed β-glucans have been reported to (*i*) reduce glucose and cholesterol blood levels, (*ii*) promote production of short chain fatty acids (SCFAs), which may act as important modulators of host immune function, (*iii*) decrease energy intake, and (*iv*) lower obesity, diabetes and cardiovascular risk [10–16]. Moreover, several studies have underlined a wide range of interesting properties of β-glucans, such as anticancer effects [17–20], immunomodulatory abilities [21], anti-inflammatory activities [22], or their role as potential adjuvants for vaccine delivery and efficacy [23] or as delivery vehicles for probiotics [24].

The focus of this review is on outlining various metabolic routes described for structurally different dietary β-glucans by human gut *Bacteroides* and *Bifidobacterium* spp. in order to clarify the various effects these polysaccharides may have on the abundance and metabolic activity of mentioned gut commensals. Understanding glycan metabolism is fundamental to determine how polysaccharides shape the microbial gut communities, as well as its associated health effects. In addition, this understanding will facilitate the development of nutraceutical-based strategies to increase the content of specific beneficial bacteria.

The gut and its associated Human Gut Microbiota (HGM) together form a recently considered novel organ of the human body that impacts on human health in a variety of ways [25,26]. The HGM in Western populations represents a complex microcosm of trillions of microorganisms, with Bacteroidetes and Firmicutes being the most dominant phyla, and Actinobacteria, Proteobacteria and Verrucomicrobia being less abundant components (Fig. 2) [27,28]. Nonetheless, such minor components may still represent important ecological players in the complexity of

HGM, especially for the metabolic interactions they offer to members of the Bacteroidetes and Firmicutes phyla. For example, *Akkermansia muciniphila* (which belongs to the Verrucomicrobia phylum) has recently been shown to represent a human gut commensal that supports host health [29,30]. The relative abundance of *Akkermansia muciniphila* has been inversely correlated with obesity, diabetes, cardiometabolic diseases and low-grade inflammation, highlighting its potential as a probiotic to support human health and well-being [29,30].

Bacteroides is the main genus within the Bacteroidetes phylum, though recent metagenome studies have indicated that four distinct *Prevotella* clades in this phylum have been underrepresented in Western populations [31]. Most *Bacteroides* members are common gut commensals, though they can act as opportunistic pathogens under certain conditions, an example of this being *Bacteroides fragilis* [32,33]. *Bacteroides* are widespread in different natural niches and human populations and possess a wide range of mechanisms to adapt to and persist in various competitive environments [31,34–37]. *Bacteroides* species are widely known for their role as primary glycan degraders since their genomes contain a relatively high number of genes (when compared to other members of the gut microbiota) encoding carbohydrate active enzymes, such as glycoside hydrolases (GHs) and polysaccharide lyases (PLs) [38,39]. For this reason, they are able to access a broad range of complex carbohydrate substrates [40]. Some members, such as *Bacteroides thetaiotaomicron* (289 GHs and 23 PLs) or *Bacteroides cellulosilyticus* (431 GHs and 30 PLs), dedicate around 18% of their genome content to carbohydrate metabolism, thereby reflecting their huge metabolic capacity and versatility to use this type of carbon and energy source [41,42]. Carbohydrate active enzymes or CAZYmes are classified into different families according to protein sequence similarities, which means that they commonly elicit related activities. Therefore, enzymes belonging to the same family have a similar protein sequence, a conserved catalytic apparatus and similar quaternary structure [42–44].

Bacteroides genomes harbour polysaccharide utilization loci (PULs), which are clusters of genes involved in the detection and digestion of a specific polysaccharide. To date, all sequenced *Bacteroides* genomes contain PULs, which typically encode surface glycan binding proteins (SGBPs), enzymes for carbohydrate degradation (GHs and PLs), TonB-dependent transporters (TBDT) and sensors/regulators [43].
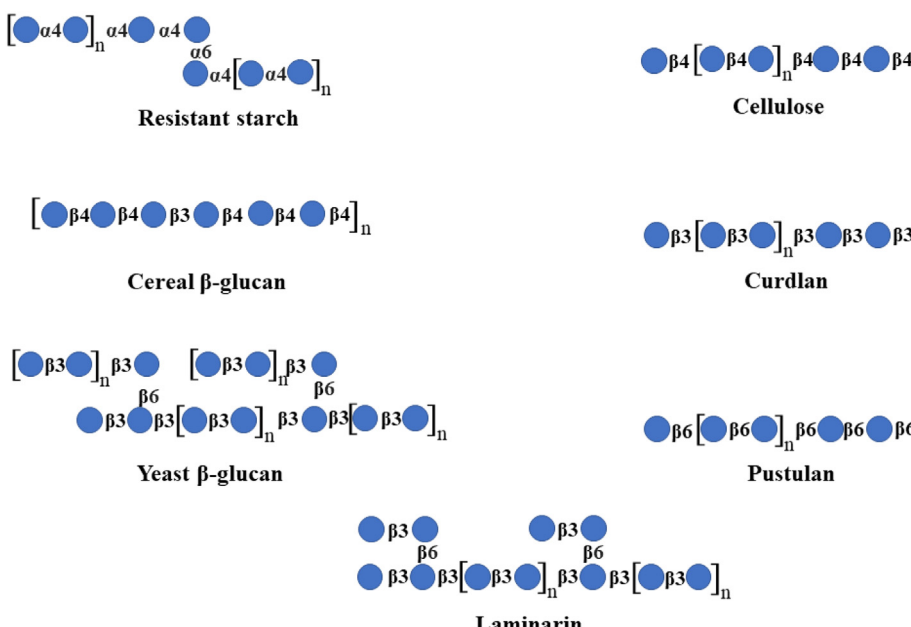
Fig. 1. Structure of different types of alpha- (resistant starch) and β-glucans. The sources of β-glucans are varied: cereals, brown algae (Laminarin), *Saccharomyces cerevisiae* (yeast), Fungi *Lasallia pustulata* (Pustulan), bacteria, e.g. *Alcaligenes faecalis* (Curdlan), and plants (cellulose) [5].
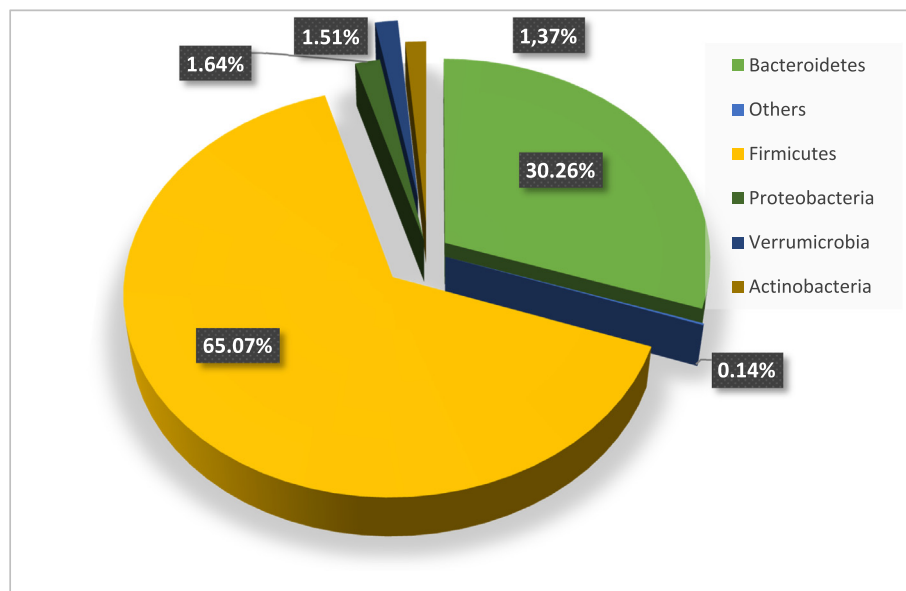
Fig. 2. Distribution of major bacterial phyla population according to their relative abundance in the human gut [28].

Polysaccharide breakdown usually begins at the cell surface by a GH or PL, which degrades the complex intact polysaccharide into oligosaccharides. These released oligosaccharides are then transported by the *Bacteroides* species into the periplasm by SusC-like TBDT proteins [45], although they may also be utilized by other bacteria as substrates through *cross-feeding*, a common phenomenon observed for complex polysaccharides or cofactors [38,39,46–48]. In the periplasm, several *exo-* and *endo*-glycosidases are responsible for further hydrolysis of the internalized oligosaccharides, and this degradation commonly releases a signal molecule (typically a di—/tri—/tetrasaccharide), which binds to the sensor/regulator, thereby triggering transcriptional induction of the corresponding PUL. The final step of this degradative process involves the incorporation of monosaccharides into the cytoplasm where they are channelled into central carbon catabolism. This general PUL model was first described for starch metabolism by *Bacteroides*

thetaiotaomicron [49,50] and was the first to describe how *Bacteroides* species carried out starch degradation [51–53]. The corresponding PUL, designated *sus*, is composed of eight genes, *sus*RABCDEFG, whose encoded proteins constitute a complex and cell envelope-associated apparatus highly specialized in starch catabolism [51–53]. The SusC/D complex is predominantly responsible for starch binding with SusE and SusF being involved in increasing the efficiency of the binding process [51–53]. SusG generates internal hydrolytic cuts in the bound starch, releasing oligosaccharides that are transported into the periplasmic compartment by SusC [51–53]. Here, SusA and SusB, both glycoside hydrolases, degrade these malto-oligosaccharides to glucose, which is then transported into the cytosol [51–53]. Transcriptional regulation of the whole process is accomplished by SusR in response to starch availability [51–53]. A schematic representation of this starch degradation process is shown in Fig. 3.
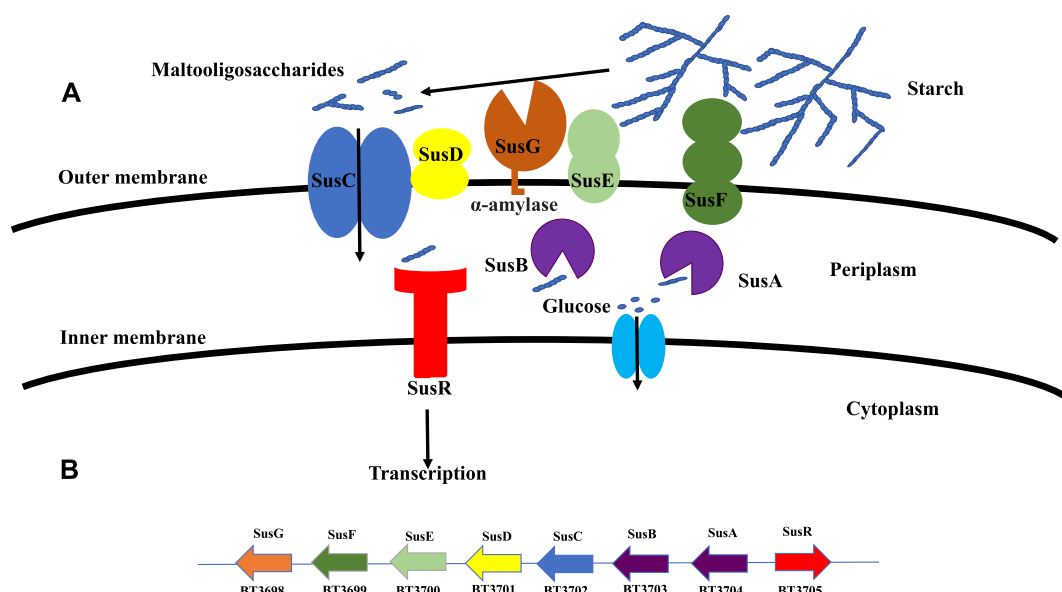
Fig. 3. A. Cartoon representation of starch utilization system model in *Bacteroides thetaiotaomicron VPI-5482* [51,54]. The hydrolytic degradation of complex intact polysaccharide is initiated at the outside surface of the cell by SusG (alpha-amylase), thereby generating oligosaccharides. These oligosaccharides are incorporated into the periplasm by binding and import proteins (facilitated by the SusC/SusD pair), which allows further degradation to glucose by other glycoside hydrolases (SusA and SusB) and which generates a signal molecule for the regulator (SusR), causing transcriptional activation of the entire PUL. **B.** Genomic content of the PUL for starch metabolism in *Bacteroides thetaiotaomicron VPI-5482* [51,54].

Bifidobacterium is a genus belonging to the Actinobacteria phylum whose species occupy several ecological niches, since they may be isolated from waste water, the oral cavity and the gastrointestinal tract of humans and other mammals [55,56]. Some species are commonly identified in adults, such as *Bifidobacterium adolescentis* and *Bifidobacterium pseudocatenulatum*, while *Bifidobacterium bifidum*, *Bifidobacterium breve*, and *Bifidobacterium longum* subsp. *infantis*, are typically isolated from faecal samples of breast-fed infants [57,58]. Various studies have demonstrated the positive health impact or probiotic effect of certain bifidobacterial species/strains, such as those belonging to *Bifidobacterium breve*, *Bifidobacterium longum* or *Bifidobacterium bifidum* [24,59]. In the context of this review, it should be noted that certain bifidobacteria have been reported to ferment laminarin, curdlan or oat β-glucan [60].

Also bifidobacteria contain gene clusters, each of which being dedicated to the metabolism of a specific poly/oligosaccharide [61]. These clusters encode ABC transporters (most frequently observed), permeases or proton symporters to facilitate transport of mono−/oligo-saccharides, such as fucosyllactose, fucose or galactooligosaccharides, into the cytoplasm. Once internalized, intracellular glycoside hydrolases degrade these oligosaccharides into monosaccharides and/or channel these hexoses or pentoses into the central carbohydrate metabolic pathway for energy generation (Fig. 4) [62].

Bifidobacterium is unique in using a specialized central metabolic carbohydrate route, called the "bifid shunt", which employs a number of key enzymes, such as fructose-6-phosphoketolase, being considered a key taxonomic marker for the Bifidobacteriaceae family [61,63,64]. The bifid shunt is used by *Bifidobacterium* for the metabolism of hexoses and pentoses, and theoretically can produce more ATP molecules per molecule of glucose than alternative carbohydrate fermentation strategies used by lactic acid bacteria or *Bacteroides* species [65]. This unique bifidobacterial pathway lacks the enzymes aldolase, which is characteristic of glycolysis, and glucose-6-phosphate dehydrogenase, typical of hexosemonophosphate pathways [61,63,64]. However, monosaccharide fermentation in bifidobacteria is characterized by fructose-6-phosphate phosphoketolase, from which the pathway obtained its name as the phosphoketolase route or "bifid shunt" [61,63,64].

2. Cereal β-glucans

Cereals are the most common and widespread source of β-glucan in the human diet and their chemical structures are usually described as homoglucopolysaccharides with a backbone of single β(1,3)-bonds separating short sections of β(1,4)bonds [1,2]. Due to the large variety of existing cereals, we will focus our review on β-glucans isolated from oat, barley and wheat.

One particular utilization locus was identified in *Bacteroides ovatus* ATCC 8483 (Bovatus_02740-Bovatus_02745) when this strain metabolizes barley-derived, mixed-linkage β-glucans (MLG, Fig. 5) [66,67]. This locus encodes a GH16 *endo*-β-glucanase (BoGH16$_{MLG}$) which hydrolyses β(1,4)-linkages that are preceded by a β(1,3)-linked glucosyl residue, and a GH3 *exo*-β-glucosidase that digests the oligosaccharides released by BoGH16$_{MLG}$ to glucose. This PUL also encodes two Surface Glycan Binding Proteins (SGBPs), a SusD$_{MLG}$-like homolog and BoSGBP$_{MLG}$. The SusD$_{MLG}$-like homolog is essential for growth of *Bacteroides ovatus* ATCC8483 on barley β-glucan because it incorporates the oligosaccharides originated by BoGH16$_{MLG}$ into the periplasm. In contrast, BoSGBP$_{MLG}$ is not essential for growth though it may assist in oligosaccharide scavenging. PULs homologous to the Bovatus_02740-Bovatus_02745 PUL of *Bacteroides ovatus* are present in the genomes of *Bacteroides xylanosolvens* XB1A and *Bacteroides uniformis* ATCC 8492, which highlights the apparent prevalence of PULs dedicated to β-glucan metabolism among *Bacteroides* species [66,67].

2.1. Oat β-glucans

The effect of oat β-glucan ingestion has been shown to be associated with a modest increase in bacterial richness (yet decreasing the *Bacteroides* population) in both ileal effluent and faecal samples when compared with intake of cellulose or carboxymethylcellulose (Table 1) [68]. Also, the effect was viscosity-dependent, since low-viscosity oat β-glucan reduces the relative abundance of *Bacteroides* to a higher degree when compared to high-viscosity oat β-glucan. Moreover, the same decreasing effect was observed in a similar study where oat β-glucan was compared with pectin, inulin and arabinoxylan (Table 1) [69].

However, in a subsequent study in BALB/c mice, oat β-glucan ingestion decreased bacterial biodiversity yet caused an increase in the relative abundance of the phylum Bacteroidetes compared with the control and with a mixture oat β-glucan-cellulose. In addition, *Bacteroides* was found as the dominant genus in the colon and it was associated with a higher concentration of beneficial short chain fatty acids (SCFAs), such as propionate and acetate (Table 1) [70]. The increase in *Bacteroides*

Fig. 4. Schematic representation of the fucose and fucosyllactose utilization system in *Bifidobacterium kashiwanohense* [62]. Fucosyllactose is incorporated into the cytoplasm by an ABC transporter permease with a sugar binding domain (SBD), transmembrane domain (TMD) and an ATP-hydrolysing cytosolic domain (CBD). Once in the cytoplasm, a fucosidase (GH95 or GH29) and a β-galactosidase break the oligosaccharide into fucose, galactose and glucose, which are then further channelled into the central carbohydrate metabolic pathways, i.e. the bifid shunt, or in the case of fucose into a separate metabolic pathway. The monomer fucose is imported into the cytoplasm by means of a fucose permease after which it enters the fucose metabolic pathway [62].

Fig. 5. A. Example of the mixed-linkage glycan (MLG) utilization locus in *Bacteroides ovatus* ATCC 8483 [67]. In a similar way to starch metabolism, mixed linkage β-glucan is first degraded outside the cell by a cell surface-associated GH16 (BoGH16$_{MLG}$), which generates oligosaccharides. The SusC/SusD-like pair incorporates these oligosaccharides into the periplasm, where a GH3 (β-glucosidase, BoGH3$_{MLG}$) degrades these internalized oligosaccharides into glucose monomers, which are then internalized into the cytoplasm. **B.** Genomic content of the MLG PUL in *Bacteroides ovatus* ATCC 8483 [66,67].

Table 1
Carbohydrate intake and intervention parameters for the intervention trials with *Bacteroides* genus influences.

Reference	Type of β-glucan	Duration	Organism	Analized parameters	Main Outcomes
[68]	Oat β-glucan	17 days	8 cross-bred Duroc-Landrace pigs	Bacterial populations, SCFAs levels	Oat β-glucan ingestion was associated with a reduction in *Bacteroides*
[69]	Oat β-glucan	12 h of incubation	15 healthy humans	Bacterial populations, BCFAs and SCFAs fermentation	Oat β-glucan ingestion was associated with a reduction in *Bacteroides* and *Bifidobacterium*
[70]	Oat β-glucan	8 weeks	28 health male BALB/c mice,	Bacterial populations, SCFAs production, feed intake, body weight gain	Oat β-glucan decreased the bacterial biodiversity yet increased the relative abundance of the phylum Bacteroidetes. *Bacteroides* was found as the predominant genus in the colon and it was associated with a higher concentration of beneficial short chain fatty acids (SCFAs), such as propionate and acetate
[71]	Oatwell (28% oat β-glucan)	24 h of incubation	3 healthy humans	Bacterial populations, SCFAs production	Oatwell was related to higher *Bacteroides* abundance and propionate concentration
[76]	Barley β-glucan	25 days	8 groups of 7 male Wistar rats	Bacterial populations, SCFAs production, feed intake, body gain, amino acid production, cholesterol levels	Barley β-glucan increased the production of SCFAs, reduced inflammation and cholesterol levels, and lowered the abundance of *Bacteroides fragilis* in the caecum
[77]	Barley β-glucan (125 g/day of bread with 3 g of barley β-glucan)	3 months	20 policemized human patients	Bacterial populations, SCFAs concentration	No significance difference during the intervention. Nevertheless, two weeks after cessation of the treatment, *Bacteroides* genus was found significantly decreased
[78]	Low and medium molecular weight barley β-glucan	39 days	48 male Wistar rats	Bacterial populations, SCFAs concentration, Feed intake, body gain, plasma lipid levels	The ratio *Bacteroides/Prevotella* was reduced by low and medium molecular weight barley β-glucan
[79]	Low and high molecular weight barley β-glucan	35 days	30 human subjects	Bacterial populations, CVD risk factors	High molecular weight barley β-glucan can significantly increase *Bacteroides* and reduce CVD risk
[80]	Barley β-glucan extracted from Glucagel™ and arabinoxylan, xyloglucan, glucan, and pectin.	48 h of incubation	*Bacteroides ovatus* ATCC 8483 T310, *Bifidobacterium longum* subspecies *longum* ATCC 15707 T, *Megasphaera elsdenii* DSM 20460 T311, *Ruminococcus gnavus* ATCC 29149 T, and *Veillonella parvula* DSM 2008 T	Bacterial growth	*Bacteroides ovatus* ATCC 8483 T310 prioritizes the use of barley β-glucan before the other substrates, with higher growth rates than the other studies species except *Veillonella parvula.*
[83]	Whole wheat grains	8 weeks	68 human subjects	Bacterial populations, pHenolic compounds levels glycaemia, plasma lipids, inflammatory markers and	Wheat β-glucan was correlated with an increase in Bacteroidetes phylum and *Bacteroides* genus. *Bacteroides* could reduce inflammatory markers TNF-α and IL-6 and plays a role in reducing pathologies associated with inflammation
[84]	Whole wheat grains	48 h of incubation	10 health humans	Bacterial populations,	*Bacteroides cellulosilyticus*, *Bacteroides ovatus* and *Bacteroides stercoris* were described as predominantly

(continued on next page)

Table 1 (*continued*)

Reference	Type of β-glucan	Duration	Organism	Analized parameters	Main Outcomes
					wheat-bran β-glucan degraders, while *Bacteroides uniformis, Bacteroides dorei* and *Bacteroides eggertii* were enriched in the β-glucans from wheat-lumen, so not all *Bacteroides* present the same feed-responsive behaviour
[85]	durum wheat flour and whole-grain barley pasta	2 months	26 healthy humans	Bacterial populations, blood cholesterol, amino acid concentration, SCFAs levels	No clear change in the microbiota composition. Increase in 2-methyl-propanoic acid, acetic acid, butanoic (butyric) acid, and propanoic (propionic) acid
[86]	wheat bran and BarleyMax	4 weeks	60 healthy humans	Dietary Intake, Biochemical Analysis, Microbiota Composition, SCFA levels	Increase in *Bacteroides* genus, Higher SCFAs concentrations, especially butyric acid
[104]	Laminaran	2 weeks	18 male Wistar rats	Microbiota composition, body weight, carbohydrate levels, organic acids levels	Reduction in Bacteroidetes abundance. Laminaran also can reduce the levels of cecal putrefaction substances levels
[105]	Laminaran	6 weeks	18 female BALB/c mice	Bacterial population, carbohydrate active enzymes activity, body weight	Increase in relative abundance of Bacteroidetes phylum, especially the genus *Bacteroides*, and a decrease in the Firmicutes phylum. Laminarin ingestion shifted the microbiota at the species level towards a higher energy metabolism, and therefore increasing the number of carbohydrate active enzymes. Laminarin also slowed weight gain in mice and decreased the bacterial species diversity.
[106]	Laminaran	11–13 days	18 male ICR mice	Bacterial populations	*Bacteroides intestinalis* and *Bacteroides acidifaciens*, producing succinate and acetate, which are precursors of beneficial propionate and butyrate

populations was also reported by Carlson et al. using Oatwell (oat-bran containing 28% oat β-glucan, Table 1) [71].

Additionally, different studies have demonstrated the effect of oat β-glucans in *Bifidobacterium* (Table 2). Wu et al. found that *Bifidobacterium* content was decreased by the dietary supplementation with oat β-glucans [72]. Nevertheless, an in vitro fermentation study by Ji-lin et al. showed *Bifidobacterium longum* BB536 as a good degrader of raw and hydrolysed oat β-glucans hydrolysates, with preference for the hydrolysed fractions (Table 2) [73]. Another study concluded that the addition of β-glucan to yogurt increased survival of *Bifidobacterium longum* R0175 (Table 2) [74]. Furthermore, *Bifidobacterium* abundance

was demonstrated to increase significantly in rats fed with oat whole meal or oat β-glucan compared with a control group, with rats exhibiting a higher growth rate when fed on pure oat β-glucan (Table 2) [75].

2.2. Barley β-glucans

Supplementation with barley β-glucan in rats with low or high-fat diet increased the production of SCFAs, reduced inflammation and cholesterol levels, and lowered the abundance of *Bacteroides fragilis* NCTC 9343 in the caecum (Table 1) [76]. Additionally, in a study with

Table 2
Carbohydrate intake and intervention parameters for the intervention trials with *Bifidobacterium* genus influences.

Reference	Type of β-glucan	Duration	Organism	Analized parameters	Main Outcomes
[72]	Oat β-glucan	25 days	32 weaned pigs	Bacterial populations, body weight, serum parameters	Oat β-glucan supplementation decreased *Bifidobacterium*
[73]	Oat β-glucan and its hydrolysates	1 week	3 male Sprague-Dawley rats	SCFA production, bacterial growth of different faecal microbiota	No significant differences with intact oat β-glucan However, the oat β-glucan hydrolysates OGH treatment evidently promoted the growth of *Bifidobacterium longum* BB536. The hydrolysates of oat β-glucan produced greater amounts of SCFA (mainly acetate, propionate and butyrate) with no significant difference in SCFA pattern when compared with oat β-glucan.
[74]	Oat β-glucan	35 days	Pure strains of *Bifidobacterium breve* R0070, *Bifidobacterium longum* R0175	Bacterial growth	These data indicate that the addition of beta-glucan to yogurt increased survival of *Bifidobacterium longum* R0175
[75]	Oat β-glucan	4 weeks	30 male SD rats	Food Intake, body Weight, ATPase activity, bacterial population	Oat β-glucan decreased glycaemia and insulin response while it increased ATPase activity and *Bifidobacterium* relative abundance
[81]	Glucagel™ (80% barley derived β-glucan)	8 weeks	36 C57BL/6 male mice	Body weight, food intake, tissue weights and adiposity Data, Gut microflora composition and SCFAs	Barley β-glucan attenuate weight gain and increase relative abundance of *Bifidobacterium* both in faeces and caecal contents over the 8 weeks of dietary intervention
[76]	Barley β-glucan	25 days	56 male Wistar rats	Cecal microbiota, SCFAs levels, cholesterol, TAG and inflammatory levels, feed intake, weight gain, caecal content, pH, tissue weight	Barley β-glucan was related with an increase in the abundance of *Bifidobacterium* and SCFA levels and a reduction in cholesterol levels and inflammatory markers
[82]	Barley β-glucan	8–12 weeks	male C57BL/6 J mice (amount not given)	Bacterial populations, SCFAs production	Barley β-glucan suppressed appetite and improved insulin sensitivity. Furthermore, barley β-glucan increased the relative abundance of the genus *Bifidobacterium* and SCFA production

polypectomyced patients (patients having colorectal polyps), no significance difference was observed during a 90-day feeding intervention using 3 g/day of barley β-glucan. Nevertheless, two weeks after cessation of the treatment, the abundance of the genus *Bacteroides* was found to be significantly decreased (Table 1) [77]. A similar negative correlation was observed in hypercholesterolemic rats fed with a medium molecular weight (530 kDa) barley β-glucan diet (Table 1) [78]. However, the application of 3 g/day of this medium molecular weight barley β-glucan in hypercholesterolemic human patients increased the relative abundance of Bacteroidetes, while that of Firmicutes was decreased. Interestingly, no significant differences were observed when patients received 3 g/d or 5 g/d of low molecular weight barley β-glucan. These findings therefore suggest that the promoting effect of Bacteroidetes abundance by barley β-glucan is molecular weight-dependent (Table 1) [79]. In addition, *Bacteroides ovatus* ATCC 8483 prioritizes the use of barley β-glucan in a mixture with pectin, xyloglucan and arabinoxylan, being able to use this substrate when it was the only carbon source in the medium, with higher growth rates than *Bifidobacterium longum* subsp. *longum, Megasphaera elsdenii*, and *Ruminococcus gnavus*, but lower than *Veillonella parvula* (Table 1) [80].

In *Bifidobacterium*, the bifidogenic effect of barley β-glucan supplementation in food/feed has been described in various publications. For instance, Arora et al. discovered that C57BL/6 mice, when maintained on a high fat diet containing 10% barley β-glucan during 8 weeks, showed a lower body weight gain and also an increase in relative abundance of *Bifidobacterium* in both faecal and caecal samples (Table 2) [81]. Similar results were found in rats fed on a low fat diet supplemented with barley β-glucan for 25 days [76] and, in a similar way, in other murine trials (Table 2) [82].

2.3. Wheat β-glucans

In obese subjects with an unhealthy dietary behaviour, wheat β-glucan was correlated with a relative abundance increase in members belonging to the Bacteroidetes phylum and *Bacteroides* genus. It was also suggested that *Bacteroides* reduces the levels of inflammatory markers TNF-α and IL-6, and that it plays a role in reducing pathologies associated with inflammation (Table 1) [83]. In a similar study, *Bacteroides cellulosilyticus, Bacteroides ovatus* and *Bacteroides stercoris* were described as predominantly wheat-bran β-glucan degraders, while *Bacteroides uniformis, Bacteroides dorei* and *Bacteroides eggertii* were enriched in β-glucans derived from wheat-lumen, so apparently not all *Bacteroides* species exhibit the same glycan utilization behaviour (Table 1) [84]. The authors showed differences in the structure and composition of wheat bran

and lumen, suggesting that these differences explain the different metabolic capabilities [84]. Nevertheless, the use of whole grains instead of extracted β-glucan requires further studies for wheat.

2.4. Mix of different cereals

A dietary intervention using 3 g/d of durum wheat flour and whole-grain barley pasta for 2 months did not reveal any significant differences in the microbiota composition of the subjects (Table 1) [85]. However, in another trial with wheat bran and barley in Japanese adults, a positive interaction was observed when both cereals were combined, causing an increase in relative abundance of the genus *Bacteroides* and other butyrate-producing species (Table 1) [86]. Differences in the microbiota composition of distinct human populations as a result of varying diets and life styles may explain these apparently conflicting findings [87–89].

Regarding *Bifidobacterium,* Shen et al. carried out a comparative study of the prebiotic efficacy of oat and barley β-glucan in rats. The study resulted in an increase in *Bifidobacterium* abundance using either of these cereals, with a more pronounced effect for oat β-glucan [90].

3. Seaweed β-glucans

Seaweeds are potential prebiotics rich in three polysaccharides depending on the seaweed source, being either brown, green or red algae. In brown algae, fucoidan, alginate and laminarin have been shown to act as antioxidant, cognitive protective, anti-inflammatory, anti-angiogenic, anti-cancer, anti-viral, and anti-hyperglycemic agents, thus having very promising potential as a food additive and prebiotic [91,92]. Laminarin (Fig. 1) is a glucose-based homopolysaccharide with a β(1,3) backbone and β(1,6) branches at a 3:1 ratio, being isolated from the brown algae species *Laminaria* and *Alaria*, representing almost a 50% of algal dry matter. Laminarin is a type of β-glucan with special interest because of its proposed anticancer, antioxidant and immunomodulatory activities [93–95]. For instance, in a recent study, both native laminarin and its enzymatic digestion products inhibited cell transformation on SK-MEL-28 human melanoma and DLD-1 human colon cancer cells, where the maximum anticancer effect was shown to be correlated with a high level of branching [95].

Recently, a paper on β(1,3)-glucan metabolism by *Bacteroides* species, showed that *Bacteroides uniformis* ATCC 8492, *Bacteroides thetaiotaomicron* NLAE-zl-H207 and *Bacteroides fluxus* YIT 12057 have the ability to metabolize laminarin as a carbon source because of the defined PUL architecture where a GH158 is key in the release of oligosaccharides [96]. These authors described a putative β(1,3)-glucan
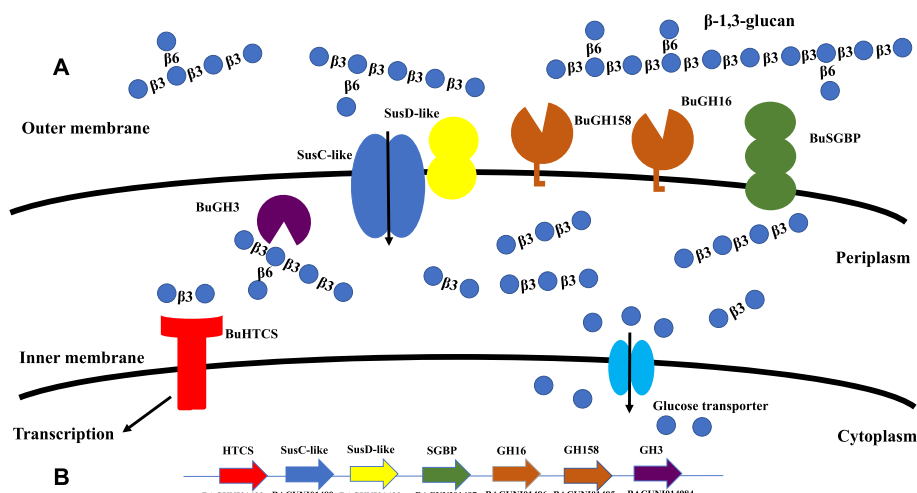
Fig. 6. A. Schematic representation of β(1,3)-glucan degradation by *Bacteroides uniformis* ATCC 8492 based in analogy with the starch utilization system [96]. **B.** Genomic content of the β(1,3)-glucan PUL in *Bacteroides uniformis* ATCC 8492 [96].

utilization locus in *Bacteroides uniformis* ATCC 8492 (Fig. 6A and B, BACUNI_01484-BACUNI_01490) that encodes a TonB-dependent transporter (TBDT, SusC-like), two cell surface glycan-binding proteins (SusD-like and BuSGBP), three glycoside hydrolases (BuGH16, BuGH158 and BuGH3) and a hybrid two-component regulatory system (BuHTCS) (Fig. 6B). BuGH158 was described as a specific laminarinase, while BuGH16 was shown to be a broad-specificity *endo*-β(1,3)-glucanase with activity towards yeast β-glucan and mixed-linkage glucan from cereals. For its part, BuGH3 was described as a specific β(1,3) glucosidase which handles the hydrolysis products of BuGH158 and BuGH16. However, only BuSGBP was able to bind β-(1,3)-glucans (Fig. 6A). Despite the fact that homologous PULs active on β(1,3)-glucans have been detected in some species of *Bacteroides thetaiotaomicron* NLAE-zl-H207 and *Bacteroides fluxus* YIT 12057, the one described in *Bacteroides uniformis* ATCC 8492 was shown to be highly prevalent in the microbiome of humans, and unique with an ability to utilize three different types of β(1,3)-glucan, i.e. that from laminarin, curdlan and yeast.

Although the main purpose of this review is the effect of β-glucans on selected elements of the HGM, laminarin has also been widely studied as a growth substrate for various marine *Bacteroides* species. An analysis of Bacteroidetes-fosmids from ocean regions showed that 4 out of 14 identified PULs were laminarin-specific, and were co-located with predicted β-glucosidase-encoding genes, thereby underscoring the role of laminarin as a common metabolic substrate for ocean-derived Bacteroidetes species [97].

At species level, the degradation of laminarin in the marine bacterium *Zobellia galactanivorans* has been described in different studies. Thomas et al. studied gene transcription in *Zobellia galactanivorans* Dsij[T] when it grows on laminarin as its sole carbon source (Fig. 7) [98]. The authors determined that this marine polysaccharide induced the expression of the cluster ZOBELLIA_209 to ZOBELLIA_214, which is predicted to encode two TonB-dependent receptors (ZOBELLIA_212 and ZOBELLIA _214) and their associated surface glycan-binding proteins (ZOBELLIA_211 and ZOBELLIA_213), respectively. These gene pairs are characteristic features of PUL clusters present in Bacteroidetes genomes [43]. In addition, this cluster encodes a predicted carbohydrate binding module family 4 (CBM4, ZOBELLIA_209), whose family has been characterized to bind to β(1,3)-glucan, β(1,3-1,4)-glucan, β(1,6)-glucan, xylan, and amorphous cellulose (CAZY database, http://www.cazy.org/; [99–102]). Therefore, this cluster is involved in the recognition, binding and incorporation of laminarin at the cellular surface of *Zobellia galactanivorans,* which has been used as a bacterial model to understand the algal carbon metabolism showing several adaptive treats
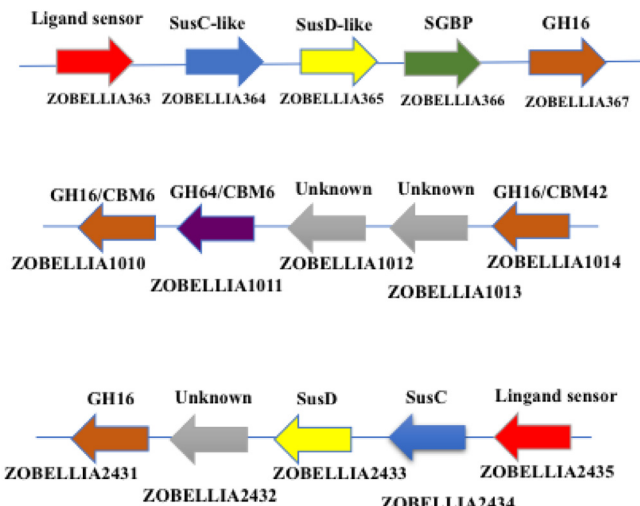
to algal-associated life [103], representing a clear example for a genomic cluster dedicated to laminarin, Fig. 7.

Another study showed that the incorporation of 2% of brown algae laminarin in feed for a rat trial decreased the relative abundance of the Bacteroidetes phylum in caecal microbiota populations. Specifically, the ratio of identified clones, based on 16S rRNA gene sequencing, of *Bacteroides capillosus* fell around 27% compared to the control (Table 1) [104]. By contrast, in a study with mice fed with a high fat diet as control and comparing with a high fat + laminarin diet, the authors found that the diet without laminarin led to an increase in Actinobacteria, whereas dietary supplementation with laminarin witnessed an increase in the relative abundance of Bacteroidetes, especially the genus *Bacteroides*, and a decrease in Firmicutes. Laminarin ingestion shifted the microbiota at species level towards a higher energy metabolism, increasing the *Bacteroides* species, and therefore increasing the number of carbohydrate active enzymes. Laminarin also slowed weight gain in mice and decreased the bacterial species diversity (Table 1) [105]. The same increase in Bacteroidetes/Firmicutes ratio was observed in a recent study with albino mice (Table 1) [106] in which laminarin was shown to be metabolized by *Bacteroides intestinalis* and *Bacteroides acidifaciens*, producing succinate and acetate as end-products, which are precursors of the beneficial short chain fatty acids (SCFAs) propionate and butyrate, respectively [107–109].

In contrast, several feeding studies have concluded that laminarin from *Laminaria digitata* and *Laminaria hyperborea* does not affect the relative abundance of *Bifidobacterium* in the gut microbiota [110,111]. Nevertheless, Lynch et al. reported a linear decrease in caecal *Bifidobacterium* in boars as a result of the addition of laminarin from *Laminaria hyperborea* [112]. The above reports do highlight the need for further in depth studies to thoroughly analyse the effect of laminarin on the HGM.

4. Fungal β-glucans

Fungal β-glucans are polymers composed of a β(1,6) or β(1,3) backbone, with a variable branching degree (Fig. 1). *Bacteroides* species have been reported as degraders of different types of fungal β-glucan. For example, when β-glucan from *Saccharomyces cerevisiae* (β-1,3-glucan with β-1,6-linked side chains) was administered to C57BL/6 mice, it was shown to cause a reduction in bacterial diversity, yet an increase in relative abundance of the phylum Bacteroidetes. This effect was accompanied with higher levels of SCFAs such as acetic, propionic and butyric acids [113]. Also, the positive correlation between an increase in Bacteroidetes and SCFA production was observed when mice with colorectal polyps were fed with a complex β-glucan-chitin complex (KytoZyme SA) [114].

As we stated in the seaweed β-glucan section, Dejean et al. showed the ability of certain *Bacteroides* species to metabolize β(1,3)-glucan from laminarin, yet also from yeast [96]. They showed that the same PUL was involved in the degradation of both of these β-glucan substrates (Fig. 6). In another study, β(1,3)-glucan from *Candida albicans* was shown to increase the relative abundance of the *Bacteroides* genus when mice were administered live or heat killed-*Candida* [115]. In addition, one particular PUL (BT3309-BT3314) from *Bacteroides thetaiotaomicron* VPI-5182 has been associated with the degradation of fungal β(1,6)-glucan (pustulan, Fig. 8A and B), a common component of fungal cell walls of mushrooms and yeast [116]. BT3312 (GH30_3) represents an *endo*-β(1,6)-glucanase located at the cell surface accompanied by a SGBP (BT3313), a SusC-like (BT3310), a SusD-like (BT3311) and a β-glucosidase (GH3, BT3314). *Bacteroides thetaiotaomicron* employs a very efficient mechanism to fully metabolize pustulan as a carbon and energy source (Fig. 8A). The SGBP BT3313 binding protein starts the degradation process by recognising and binding the intact polysaccharide at the cell surface of *Bacteroides thetaiotaomicron*. Following this, the BT3312 (GH30_3) enzyme cleaves the intact glycan into smaller glucooligosaccharides, which will then be internalized into the periplasm

Fig. 7. Genomic composition of the laminarin PUL in *Zobellia galactinovorans* Dsij[T] [103].
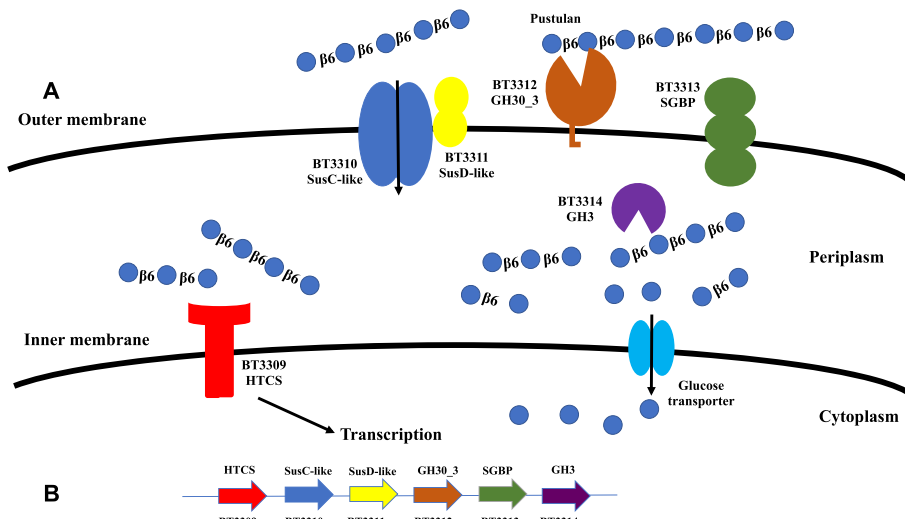
Fig. 8. A. Schematic of β-(1,6)-glucan (pustulan) degradation by *Bacteroides thetaiotaomicron* VPI-5482 [116]. This linear β-glucan is degraded by a GH30_3 in the surface of *Bacteroides thetaiotaomicron* and the resulted oligosaccharides are incorporated into the periplasm, where another GH3 (β-glucosidase) hydrolyses the smaller oligosaccharides into single glucose monomers. **B.** Genomic content of the pustulan PUL in *Bacteroides thetaiotaomicron* VPI-5482 [116].

by the permease pair BT3310/BT3311 (SusC-like/SusD-like). In the periplasm, a GH3 enzyme (BT3314) will continue metabolism by degrading the internalized 1,6-glucooligosaccharides (Fig. 8A). BT3314 has been shown to exhibit a 30-fold higher activity for 1,6-glucobiose than for 1,3- or 1,4-glucobiose, and probably possesses two subsites into the active site, because of its similar activity on 1,6-glucobiose and 1,6-glucotriose [116]. The latter report postulated that the observed slow metabolism of 1,6-glucooligosaccharides in the periplasm of *Bacteroides thetaiotaomicron* may allow the persistence of a higher concentration of the "induced ligand" for BT3309 (HTCS or regulator of the PUL), enabling the locus to be up-regulated for an extended period of time for the use of pustulan as a carbon source by *Bacteroides thetaiotaomicron*. Comparative genome analysis with other species revealed that homologous PULs are located in the genomes of *Bacteroides uniformis* ATCC 8492, *Bacteroides ovatus* ATCC 8483 and *Bacteroides xylanosolvens* XB1A [116].

Recent studies have addressed the role of fungal β-glucans in *Bifidobacterium*. For instance, Wang et al. studied the correlation between sulphated β-glucan from *Saccharomyces cerevisiae* and immune response [117]. Using immuno-suppressed chickens as a result of cyclophosphamide treatment, the addition of 0.4 g of yeast β-glucans per kilogram of chicken was shown to alleviate the immuno-suppression, affecting the concentration of cytokines and promoting the proliferation of *Bifidobacterium* [117]. Furthermore, supplementation with yeast β-glucans in Alzheimer-induced mice has been shown to cause an increase in the relative abundance of the genus *Bifidobacterium*, which was similar to that found in control mice [118]. Recently, in a macro study by Alessandri et al., the authors evaluated the growth ability of hundred bifidobacterial strains using glucan-chitin complex from *Aspergillus niger* as the only carbon source. All strains were shown to exhibit some, though mostly modest growth with *Bifidobacterium breve* and *Bifidobacterium bifidum* strains eliciting the highest levels of growth [119].

Zhao and Cheung showed that mushroom β-glucans elicit a prebiotic effect by enhancing growth of *Bifidobacterium longum* subsp. *infantis* [59]. These authors studied the proteomic profile of this catabolic process, showing that this bifidobacterial species expresses 17 proteins that may be linked to mushroom β-glucan degradation. These proteins include ABC transporters of sugars, enolase and a phosphoenol phosphotransferase system. Among the 17 proteins, a predicted intracellular glucanase is highly expressed. The authors proposed a metabolic model for this degradation where (some parts of) the autoclaved polysaccharide (which is likely to cause hydrolysis of this glycan) is incorporated into the cytoplasm by ABC transport system and PTS

(phosphotransferase system) proteins. After this incorporation, the intracellular glucanase breaks down the polysaccharide into glucose monomers, which are subsequently incorporated into the central fermentative pathway or "bifid shunt" [59].

Several papers have addressed the impact and metabolism of dietary plant glucosides, such as flavonoids and gingenosides, on bifidobacterial and *Bacteroides* metabolism [120–123]. However, very few studies have identified bifidobacterial β-glucosidases active on β-glucan. Pokusaeva et al. identified the *cldC* gene in *Bifidobacterium breve* UCC2003 to be involved in the metabolism of cellodextrins, which are β(1,4)-glucose hydrolysis products from cellulose (Fig. 1) [124]. The authors showed the ability of this bacterium to use cellobiose, cellotriose, cellotetraose and cellopentaose through the *cldEFGC* gene cluster with a higher preference for cellobiose. Disruption of the *cldC* gene resulted in the inability of *Bifidobacterium breve* UCC2003 to use these cellodextrins as a carbon source, confirming that this gene cluster is uniquely required for cellodextrin metabolism by this bacterium. It is reasonable to assume that these enzymes would be able to degrade MLG oligosaccharides in a similar way to cellodextrin oligosaccharides, though this hypothesis awaits experimental validation. Indeed, more studies are required to fully understand the impact of β-glucan oligosaccharide metabolism on proliferation of bifidobacterial species in the gut.

5. Conclusions

In this review we discussed recent publications that have studied the effect of β-glucans from different sources on microbiota changes pertaining to Bacteroidetes (mainly *Bacteroides* species) and *Bifidobacterium*. As previously reported, *Bacteroides* species possess an extensive ability for glycan degradation, due to the presence of PULs in their genomes [38,39], allowing them to use different types of substrates and to occupy different niches and environments [31,35,36]. We have focussed our review on the most predominant types of β-glucans, clarifying the role of these polysaccharides as potential substrates for Bacteroidetes and *Bifidobacterium*, as important bacterial representatives of the adult gut microbiota [34]. Of a total of 16 studies involving fungal, seaweed and cereal β-glucans, 8 concluded that dietary inclusion of β-glucans causes an increase in the relative abundance of members of the Bacteroidetes phylum or *Bacteroides* genus, where some studies also highlight beneficial effects elicited by specific species (Table 1) [84,106]. Nevertheless, 7 studies (6 with β-glucans from cereals and 1 from seaweed) revealed the opposite results, a negative effect on the relative abundance of Bacteroidetes or *Bacteroides*, and

only one reported a 'no effect' conclusion (Table 1). The most significant disparity was found for cereal β-glucans [86]. In oat β-glucans, we found a similar number of studies with positive or negative correlations on the Bacteroidetes increase. In addition, for barley β-glucans, the number of studies published showing negative conclusions was higher than the published with positive correlations.

One would imagine that the same substrate should have equal consequences for a specific bacterial genus, so the variation in the results may be due to the utilization of different models, substrates and/or methodologies (Table 1) [79]. The results may differ in a molecular weight-dependent manner even when using the same substrate. Furthermore, the utilization of different model systems (pigs, rats, mice or humans) is likely to play an important role in this variation, because of the distinct microbiota composition in each of these mammalian species (Table 1) [77–79,82]. While it seems that the positive effects are very clear for fungal and seaweed β-glucans [88,101,102], the differences observed between the three types of β-glucans must be tested in more detail and further studies should be done for the three sources in order to clarify if the observed disparity in the experimental results is caused by the application of non-unique procedures, or, by contrast, if these correlations between the substrates and the degraders remain stable [77–79,99–102]. Due to the increasing interest in β-glucans as potential prebiotics and their effect on human health, this work provides further avenues to understand the behaviour of β-glucan-fed HGM.

Very little is currently known about the molecular mechanism how *Bifidobacterium* degrade different β-glucan types. Only a small number of papers have established the prebiotic effect of cereal and fungal β-glucans, both through in vitro fermentations and by means of human trials. Strains from *Bifidobacterium breve*, *Bifidobacterium bifidum* and *Bifidobacterium longum* have been shown to be able to at least partially degrade fungal β-glucan-chitin complex [119]. These authors showed the transcriptional profile of *Bifidobacterium breve* 2 L when using this complex substrate as a unique carbon source. Due to the complexity of β-glucan-chitin, the authors expect that other bacterial members of the gut microbiota community are involved in the complete metabolism of β-glucan-chitin through syntrophic interactions [119].

More mechanistic studies are needed to understand the size of oligosaccharides incorporated by bifidobacterial transporters. In addition, detailed structural mechanistic insights and substrate specificity studies of glucosidases and glucanases in *Bifidobacterium* species, when they act on several types of β-glucan, are required to expand our knowledge on the direct or indirect (through cross-feeding) use of these glycans as prebiotics. Finally, there is a clear knowledge gap regarding the cross-feeding process between different members of *Bacteroides* and *Bifidobacterium* and further studies are needed to shed light on the molecular details of such syntrophic interactions, a good example of this being the cross-feeding interactions involving dietary arabinogalactan [46]. Such studies will allow the rational design of nutraceutical strategies with the help of particular β-glucans as functional food ingredients, perhaps in combination with certain bifidobacterial species in so-called synbiotic formulations.

CRediT authorship contribution statement

P.F.-J.: writing – original draft preparation. D.v.S. and J.M.-M.: writing – review, editing, and conceptualization. All authors contributed to the article and approved the submitted version.

Declaration of competing interest

The authors declare no conflict of interests.

Acknowledgements

Availability of data and materials

Not applicable.

Author agreements

All authors agree to publish this article.

Consent for publication

Not applicable.

Ethics approval and consent to participate

Not applicable.

References

[1] B. Du, M. Meenu, H. Liu, B. Xu, A concise review on the molecular structure and function relationship of β-glucan, Int. J. Mol. Sci. 20 (2019) 4032–4049, https://doi.org/10.3390/ijms20164032.

[2] M. Henrion, C. Francey, A. Lê, L. Lamothe, Cereal B-glucans: the impact of processing and how it affects physiological responses, Nutrients 11 (2019) 1729–1742, https://doi.org/10.3390/nu11081729.

[3] Jayachandran, M., Cheng, J., Chung, S., and Xu, B., A critical review on the impacts of β-glucans on gut microbiota and human health, J. Nutr. Biochem. 61 (2018) 101–110. doi: https://doi.org/10.1016/j.jnutbio.2018.06.010.

[4] J. Liu, J. Tang, X. Li, Q. Yan, J. Ma, Z. Jiang, Curdlan (Alcaligenes faecalis) (1→3)-β-d-glucan oligosaccharides drive M1 phenotype polarization in murine bone marrow-derived macrophages via activation of MAPKs and NF-κB pathways, Molecules 24 (2019) 4251–4266, https://doi.org/10.3390/molecules24234251.

[5] R. Singh, Glycan utilisation systemin Bacteroides and Bifidobacteria and their roles in gut stability and health, Appl. Microbiol. Biotechnol. (18) (2019) 7287–7315, https://doi.org/10.1007/s00253-019-10012-z.

[6] Dobrincic, A., Balbino, S., Zoric, Z., Pedisic, S., Bursac-Kovacevic, D., Elez-Garofulic, I., and Dragovic-Uzelac, V., Advanced technologies for the extraction of marine brown algal polysaccharides, mar. Drugs 28 (2020) 168–196. doi: https://doi.org/10.3390/md18030168.

[7] Q. Wang, X. Sheng, A. Shi, H. Hu, Y. Yang, L. Liu, L. Fei, H. Liu, β-Glucans: relationships between modification, conformation and functional activities, Molecules 22 (2017) 257–269, https://doi.org/10.3390/molecules22020257.

[8] Kagimura, F., da Cunhaa, M., Barbosa, A., Dekkerc, R., and Malfatti, C., Biological activities of derivatized d-glucans: a review, Int. J. Biol. Macromol.. 72 (2015) 588–598. doi: https://doi.org/10.1016/j.ijbiomac.2014.09.008.

[9] Gibson, G., Hutkins, R., Sanders, M., Prescott, S., Reimer, R., Salminen, S., Scott, K., Stanton, C., Swanson, K., Cani, P., Verbeke, K., and Reid, G., The International Scientific Association for Probiotics and Prebiotics (ISAPP) consensus statement on the definition and scope of prebiotics, Nat. Rev. Gastroenterol. Hepatol. 8 (2017) 491–502. doi: https://doi.org/10.1038/nrgastro.2017.75.

[10] F. Zhu, B. Du, B. Xu, A critical review on production and industrial applications of beta-glucans, Food Hydrocoll. 52 (2016) 275–288, https://doi.org/10.1016/j.foodhyd.2015.07.003.

[11] C. Cosola, M. De Angelis, M. Rocchetti, E. Montemurno, V. Maranzano, G. Dalfino, C. Manno, A. Zito, M. Gesualdo, M. Ciccone, M. Gobbetti, L. Gesualdo, Beta-glucans supplementation associates with reduction in P-Cresyl sulfate levels and improved endothelial vascular reactivity in healthy individuals, PLoS One 12 (1) (2017) e0169635, https://doi.org/10.1371/journal.pone.0169635.

[12] R. Shen, F. Cai, J. Dong, X. Hu, Hypoglycemic effects and biochemical mechanisms of oat products on streptozotocin-induced diabetic mice, J. Agric. Food Chem. 59 (2011) 8895–8900, https://doi.org/10.1021/jf200678q.

[13] S. Hooda, J. Matte, T. Vasanthan, T. Zijlstra, Dietary oat b-glucan reduces peak net glucose flux and insulin production and modulates plasma incretin in portal-vein catheterized grower pigs, J. Nutr. 140 (2010) 1564–1569, https://doi.org/10.3945/jn.110.122721.

[14] J. Rumberger, J. Arch, A. Green, Butyrate and other short-chain fatty acids increase the rate of lipolysis in 3T3-L1 adipocytes, PeerJ 2 (2014) e611, https://doi.org/10.7717/peerj.611. eCollection 2014.

[15] Hosseini, E., Grootaert, C., Verstraete, W., and Van de Wiele, T., Propionate as a health-promoting microbial metabolite in the human gut, Nutr. Rev. 69 (2011) 245–258. doi: https://doi.org/10.1111/j.1753-4887.2011.00388.x.

[16] De Vadder, F., Kovatcheva-Datchary, P., Goncalves, D., Vinera, J., Zitoun, C., Duchampt, A., Bäckhed, F., and Mithieux, G., Microbiota-generated metabolites promote metabolic benefits via gut-brain neural circuits, Cell 156 (2014) 84–96. doi: https://doi.org/10.1016/j.cell.2013.12.016.

[17] A. Choromanska, J. Kulbacka, N. Rembialkowska, J. Pilat, R. Oledzki, J. Harasym, J. Saczko, Anticancer properties of low molecular weight oat beta-glucan–An

in vitro study, Int. J. Biol. Macromol. 80 (2015) 23–28, https://doi.org/10.1016/j.ijbiomac.2015.05.035.

[18] M. Del Cornò, S. Gessani, L. Conti, Shaping the innate immune response by dietary glucans: any role in the control of Cancer? Cancers (Basel) 12 (2020) 155–171, https://doi.org/10.3390/cancers12010155.

[19] Zhang, M., Kim, J., and Huang, A., Optimizing tumor microenvironment for cancer immunotherapy: β-glucan-based nanoparticles, front. Inmunol. 9 (2018) 341–353. doi: https://doi.org/10.3389/fimmu.2018.00341.

[20] A. Geller, R. Shrestha, J. Yan, Yeast-derived β-glucan in cancer: novel uses of a traditional therapeutic, Int. J. Biol. Macromol. 20 (2019) 3618–3637, https://doi.org/10.3390/ijms20153618.

[21] H. Stier, V. Ebbeskotte, J. Gruenwald, Immune-modulatory effects of dietary yeast Beta-1,3/1,6-D-glucan, Nutr. J. 13 (2014) 38, https://doi.org/10.1186/1475-2891-13-38.

[22] B. Schwartz, Y. Hadar, Possible mechanisms of action of mushroom-derived glucans on inflammatory bowel disease and associated cancer, Ann. Transl. Med. 2 (2) (2014) 19, https://doi.org/10.3978/j.issn.2305-5839.2014.01.03.

[23] Vetvicka, V., Vannucci, L. and Sima, P., β-Glucan as a new tool in vaccine development, Scand. J. Inmunol. 91 (2020) e12833. doi: https://doi.org/10.1111/sji.12833.

[24] Gani, A., Shah, A., Ahmad, M., Ahmad, B., and Masoodi, F., β-D-glucan as an enteric delivery vehicle for probiotics, Int. J. Biol. Macrol. 106 (2018) 864–869. doi: https://doi.org/10.1016/j.ijbiomac.2017.08.093.

[25] E. Quigley, Microbiota-brain-gut axis and neurodegenerative diseases, Curr. Neurol. Neurosci. Rep. 17 (12) (2017), 94, https://doi.org/10.1007/s11910-017-0802-6.

[26] Nishida, A., Inoue, I., Inatomi, O., Bamba, S., Naito, Y., and Andoh, A., Gut microbiota in the pathogenesis of inflammatory bowel disease, Clin. J. Gastroenterol. 11 (2018) 1–10. doi: https://doi.org/10.1007/s12328-017-0813-5.

[27] Qin, J., Li, R., Raes, J., Arumugam, M., Burgdorf, K., Manichanh, C., Nielsen, T., Pons, N., Levenez, F., Yamada, T., Mende, D., Li, J., Xu, J., Li, S., Li, D., Cao, J., Wang, B., Liang, H., Zheng, H., Xie, Y., Tap, J., Lepage, P., Bertalan, M., Batto, J., Hansen, T., Paslier, D., Linneberg, A., Nielsen, H., Pelletier, E., Renault, P., Sicheritz-Ponten, T., Turner, K., Zhu, H., Yu, C., Li, S., Jian, M., Zhou, Y., Li, Y., Zhang, X., Li, S., Qin, N., Yang, H., Wang, S., Brunak, S., Doré, J., Guarner, F., Kristiansen, K., Pedersen, O., Parkhill, J., Weissenbach, J., MetaHIT Consortium; Bork, P., Ehrlich, S., and Wang, J., A human gut microbial gene catalogue established by metagenomic sequencing, Nature 7285 (2010) 59–65. doi: https://doi.org/10.1038/nature08821.

[28] X. Yang, L. Xie, Y. Li, C. Wei, More than 9,000,000 unique genes in human gut bacterial community: estimating gene numbers inside a human body, PLoS One 4 (6) (2009), e6074, https://doi.org/10.1371/journal.pone.0006074.

[29] D. Hou, Q. Zhao, L. Yousaf, B. Chen, Y. Xue, Q. Shen, A comparison between whole mung bean and decorticated mung bean: beneficial effects on the regulation of serum glucose and lipid disorders and the gut microbiota in high-fat diet and streptozotocin-induced prediabetic mice, Food Funct. 11 (6) (2020) 5525–5537, https://doi.org/10.1039/d0fo00379d.

[30] Cani, P., and de Vos, M., Next-generation beneficial microbes: the case of *Akkermansia muciniphila*, Front. Microbiol. 8 (2017) 1765. doi: https://doi.org/10.3389/fmicb.2017.01765.

[31] Wexler, A., and Goodman, A., An insider's perspective: Bacteroides as a window into the microbiome, Nat. Microbiol. 2 (2017) 17026. doi: https://doi.org/10.1038/nmicrobiol.2017.26.

[32] S. Maraki, V. Mavromanolaki, D. Stafylaki, A. Kasimati, Surveillance of antimicrobial resistance in recent clinical isolates of gram-negative anaerobic bacteria in a Greek university hospital, Anaerobe 62 (2020), 102173, https://doi.org/10.1016/j.anaerobe.2020.102173.

[33] Colov, E., Degett, T., Raskov, H., and Gögenur, I., The impact of the gut microbiota on prognosis after surgery for colorectal cancer - a systematic review and meta-analysis, APMIS 118 (2020) 162–176. doi: https://doi.org/10.1111/apm.13032.

[34] Arumugam, M., Raes, J., Pelletier, E., Le Paslier, D., Yamada, T., Mende, D., Fernandes, G., Tap, J., Bruls, T., Batto, J., Bertalan, M., Borruel, N., Casellas, F., Fernandez, L., Gautier, L., Hansen, T., Hattori, M., Hayashi, T., Kleerebezem, M., Kurokawa, K., Leclerc, M., Levenez, F., Manichanh, C., Nielsen, H., Nielsen, T., Pons, N., Poulain, J., Qin, J., Sicheritz-Ponten, T., Tims, S., Torrents, D., Ugarte, E., Zoetendal, E., Wang, J., Guarner, F., Pedersen, O., de Vos, W., Brunak, S., Doré, J., MetaHIT Consortium, Weissenbach, J., Ehrlich, S., and Bork, P., Enterotypes of the human gut microbiome, Nature 473 (2013) 7349–7359. doi: https://doi.org/10.1038/nature09944.

[35] De Filippo, C., Cavalieria, D., Di Paola, M., Ramazzottic, M., Poullet, J., Massart, S., Collini, S., Pieraccini, G., and Lionetti, P., Impact of diet in shaping gut microbiota revealed by a comparative study in children from Europe and rural Africa, Proc. Natl. Acad. Sci. U. S. A. 107 (2010) 14691–14696. doi: https://doi.org/10.1073/pnas.1005963107.

[36] Kelsen, J., and Wub, G., The gut microbiota, environment and diseases of modern society, Gut Microbes 3 (2012) 374–382. doi: https://doi.org/10.4161/gmic.21333.

[37] N. Koropatkin, E. Cameron, E. Martens, How glycan metabolism shapes the human gut microbiota, Nat. Rev. Microbiol. 10 (2012) 323–335, https://doi.org/10.1038/nrmicro2746.

[38] El Kaoutari, A., Armougom, F., Gordon, J., Raoult, D., and Henrissat, B., The abundance and variety of carbohydrate-active enzymes in the human gut microbiota, Nat. Rev. Microbiol.. 7 (2013) 497–504. doi: https://doi.org/10.1038/nrmicro3050.

[39] B. Cantarel, V. Lombard, B. Henrissat, Complex carbohydrate utilization by the healthy human microbiome, PLoS One 7 (6) (2012), e28742, https://doi.org/10.1371/journal.pone.0028742.

[40] Eilam, O., Zarecky, R., Oberhardt, M., Ursell, L., Kupiec, M., Knight, R., Gophna, U., and Ruppin, E., Glycan degradation (GlyDeR) analysis predicts mammalian gut microbiota abundance and host diet-specific adaptations, mBio 5(4): (2014) e01526-14. doi: https://doi.org/10.1128/mBio.01526-14.

[41] N. Porter, E. Martens, The critical roles of polysaccharides in gut microbial ecology and physiology, Annu. Rev. Microbiol. 71 (2017) 349–369, https://doi.org/10.1146/annurev-micro-102215-095316.

[42] N. McNulty, M. Wu, A. Erickson, C. Pan, B. Erickson, E. Martens, N. Pudlo, B. Muegge, B. Henrissat, R. Hettich, J. Gordon, Effects of diet on resource utilization by a model human gut microbiota containing *Bacteroides cellulosilyticus* WH2, a symbiont with an extensive glycobiome, PLoS Biol. 11 (8) (2013), e1001637, https://doi.org/10.1371/journal.pbio.1001637.

[43] Grondin, J., Tamura, K., Déjean, G., Abbott, D., and Brumer, H., Polysaccharide utilization loci: fueling microbial communities, J. Bacteriol. 199 (15) (2017) e00860-16. doi: https://doi.org/10.1128/JB.00860-16.

[44] N. Terrapon, V. Lombard, E. Drula, P. Lapébie, S. Al-Masaudi, H. Gilbert, B. Henrissat, PULDB: the expanded database of polysaccharide utilization loci, Nucleic Acids Res. 46 (D1) (2018) D677–D683, https://doi.org/10.1093/nar/gkx1022.

[45] A. Glenwright, K. Pothula, S. Bhamidimarri, D. Chorev, A. Baslé, S. Firbank, H. Zheng, C. Robinson, M. Winterhalter, U. Kleinekathöfer, D. Bolam, B. van den Berg, Structural basis for nutrient acquisition by dominant members of the human gut microbiota, Nature 541 (2017) 407–411, https://doi.org/10.1038/nature20828.

[46] J. Munoz, K. James, F. Bottacini, D. Van Sinderen, Biochemical analysis of cross-feeding behaviour between two common gut commensals when cultivated on plant-derived arabinogalactan, Microb. Biotechnol. 13 (6) (2020) 1733–1747, https://doi.org/10.1111/1751-7915.13577.

[47] E. Seth, M. Taga, Nutrient cross-feeding in the microbial world, Front. Microbiol. 5 (2014) 350, https://doi.org/10.3389/fmicb.2014.00350.

[48] J. Briggs, J. Grondin, H. Brumer, Communal living: glycan utilization by the human gut microbiota, Environ. Microbiol. 23 (1) (2021) 15–35, https://doi.org/10.1111/1462-2920.15317.

[49] Shipman, J., Berleman, J., and Salyers, A., Characterization of four outer membrane proteins involved in binding starch to the cell surface of *Bacteroides thetaiotaomicron*, J. Bacteriol.. 182 (2020) 5365–5372. doi: https://doi.org/10.1128/jb.182.19.5365-5372.2000.

[50] K. Cho, A. Salyers, Biochemical analysis of interactions between outer membrane proteins that contribute to starch utilization by *Bacteroides thetaiotaomicron*, J. Bacteriol. 183 (2001) 7224–7230, https://doi.org/10.1128/jb.183.24.7224-7230.2001.

[51] M. Foley, D. Cockburn, N. Koropatkin, The Sus operon: a model system for starch uptake by the human gut Bacteroidetes, Cell. Mol. Life Sci. 73 (2016) 2603–2617, https://doi.org/10.1007/s00018-016-2242-x.

[52] Cameron, E., Maynard, M., Smith, C., Smith, T., Koropatkin, N. and Martens, E., Multidomain carbohydrate-binding proteins involved in *Bacteroides thetaiotaomicron* starch metabolism, J. Biol. Chem. 287(41) (2012) 34614–34625. doi: https://doi.org/10.1074/jbc.M112.397380.

[53] Cameron, E., Kwiatkowski, K., Lee, B., Hamaker, B., Koropatkin, N., and Martens, E., Multifunctional nutrient-binding proteins adapt human symbiotic bacteria for glycan competition in the gut by separately promoting enhanced sensing and catalysis, mBio 5(5) (2014) e01441-14. doi: https://doi.org/10.1128/mBio.01441-14.

[54] H. Brown, N. Koropatkin, Host glycan utilization within the Bacteroidetes Sus-like paradigm, Glycobiology (2020) https://doi.org/10.1093/glycob/cwaa054.

[55] Turroni, F., Duranti, S., Milani, C., Lugli, G., van Sinderen, D., and Ventura, M. , *Bifidobacterium bifidum*: a key member of the early human gut Microbiot, Microorganisms 7(11) (2019) 544. doi: https://doi.org/10.3390/microorganisms7110544.

[56] F. Turroni, D. van Sinderen, M. Ventura, Genomics and ecological overview of the genus *Bifidobacterium*, Int. J. Food Microbiol. 149 (2011) 37–44, https://doi.org/10.1016/j.ijfoodmicro.2010.12.010.

[57] F. Turroni, C. Peano, D. Pass, E. Foroni, M. Severgnini, M. Claesson, C. Kerr, J. Hourihane, D. Murray, F. Fuligni, M. Gueimonde, A. Margolles, G. De Bellis, P. O'Toole, D. van Sinderen, J. Marchesi, M. Ventura, Diversity of Bifidobacteria within the infant gut microbiota, PLoS One (5) (2012), e36957, https://doi.org/10.1371/journal.pone.0036957.

[58] S. Duranti, C. Milani, G. Lugli, L. Mancabelli, F. Turroni, C. Ferrario, M. Mangifesta, A. Viappiani, B. Sánchez, A. Margolles, D. van Sinderen, M. Ventura, Evaluation of genetic diversity among strains of the human gut commensal *Bifidobacterium Adolescentis*, Sci. Rep. 6 (2016) 23971, https://doi.org/10.1038/srep23971.

[59] Zhao, J., and Cheung, P., Comparative proteome analysis of *Bifidobacterium longum subsp. infantis* grown on β-glucans from different sources and a model for their utilization, J. Agric. Food Chem.. 70 (2013) 4360–4370. doi: https://doi.org/10.1021/jf400792j.

[60] J. Zhao, P. Cheung, Fermentation of β-glucans derived from different sources by Bifidobacteria: evaluation of their bifidogenic effect, J. Agric. Food Chem. 59 (11) (2011) 5986–5992, https://doi.org/10.1021/jf200621y.

[61] K. Pokusaeva, G. Fitzgerald, D. van Sinderen, Carbohydrate metabolism in Bifidobacteria, Genes Nutr. 6 (2010) 285–306, https://doi.org/10.1007/s12263-010-0206-6.

[62] K. James, F. Bottacini, J. Contreras, M. Vigoureux, M. Egan, M. Motherway, E. Holmes, D. van Sinderen, Metabolism of the predominant human milk oligosaccharide fucosyllactose by an infant gut commensal, Sci. Rep. 9 (1) (2019) 15427, https://doi.org/10.1038/s41598-019-51901-7.

[63] W. de Vries, A. Stouthamer, Pathway of glucose fermentation in relation to the taxonomy of bifidobacteria, J. Bacteriol. 93 (2) (1967) 574–576, https://doi.org/10.1128/JB.93.2.574-576.1967.

[64] G. Felis, F. Dellaglio, Taxonomy of lactobacilli and Bifidobacteria, Curr. Issues Intest. Microbiol. 8 (2) (2007) 44–61 (PMID: 17542335).

[65] Palframan, R., Gibson, G., and Rastall, R., Carbohydrate preferences of Bifidobacterium species isolated from the human gut, Curr. Issues Intest. Microbiol. 4(2) (2003) 71–75.

[66] K. Tamura, G. Hemsworth, G. Dejean, T. Rogers, N. Pudlo, K. Urs, N. Jain, G. Davies, E. Martens, H. Brumer, Molecular mechanism by which prominent human-gut Bacteroidetes utilize mixed-linkage beta-glucans, major health-promoting cereal polysaccharides, Cell Rep. 21 (2017) 417–430, https://doi.org/10.1016/j.celrep.2017.09.049.

[67] Tamura, K., Foley, M., Gardill, B., Dejean, G., Schnizlein, M., Bahr, C., Creagh, A., van Petegem, F., Koropatkin, N., and Brumer, H., Surface glycan-binding proteins are essential for cereal beta-glucan utilization by the human gut symbiont Bacteroides ovatus, Cell. Mol. Life Sci. 76(21) (2019) 4319–4340. doi: https://doi.org/10.1007/s00018-019-03115-3.

[68] Metzler-Zebeli, B., Hooda, S., Pieper, R., Zijlstra, R., van Kessel, A., Mosenthin, R., and Gänzle, M., Nonstarch polysaccharides modulate bacterial microbiota, pathways for butyrate production, and abundance of pathogenic Escherichia coli in the pig gastrointestinal tract, Appl. Environ. Microbiol. 76 (2010) 3692–3701. doi: https://doi.org/10.1128/AEM.00257-10.

[69] Yang, J., Martínez, I., Walter, J., Keshavarzian, A., and Rose, D., In vitro characterization of the impact of selected dietary fibers on fecal microbiota composition and short chain fatty acid production, Anaerobe 23 (2013) 74–81. doi: https://doi.org/10.1016/j.anaerobe.2013.06.012.

[70] Luo, Y., Zhang, L., Li, H., Smidt, H., Wright, A., Zhang, K., Ding, X., Zeng, Q., Bai, S., Wang, J., Li, J., Zheng, P., Tian, G., Cai, J., and Chen, D., Different types of dietary fibers trigger specific alterations in composition and predicted functions of colonic bacterial communities in BALB/c mice, Front. Microbiol. 8 (2017) 966. doi: https://doi.org/10.3389/fmicb.2017.00966.

[71] J. Carlson, J. Erickson, J. Hess, T. Gould, J. Slavin, Prebiotic dietary fiber and gut health: comparing the in vitro fermentations of Beta-glucan, inulin and Xylooligosaccharide, Nutrients 9 (2017) 1361–1377, https://doi.org/10.3390/nu9121361.

[72] X. Wu, D. Chen, B. Yu, Y. Luo, P. Zheng, X. Mao, J. Yu, J. He, Effect of different dietary non-starch fiber fractions on growth performance, nutrient digestibility, and intestinal development in weaned pigs, Nutrition 51-52 (2018) 20–28, https://doi.org/10.1016/j.nut.2018.01.011.

[73] Ji-lin, D., Xiao, Y., Lianger, D., and Rui-ling, S., In vitro fermentation of oat β-glucan and hydrolysates by fecal microbiota and selected probiotic strains, J. Sci. Food Agric. 97 (2017) 4198–4203. doi: https://doi.org/10.1002/jsfa.8292.

[74] Rosburg, V., Boylston, T., and White, P., Viability of Bifidobacteria strains in yogurt with added oat Beta-glucan and corn starch during cold storage, J. Food Sci. 75 (2010) 439–444. doi: https://doi.org/10.1111/j.1750-3841.2010.01620.x.

[75] P. Zhang, X. Hu, H. Zhen, C. Xu, M. Fan, Oat β-glucan increased ATPases activity and energy charge in small intestine of rats, J. Agric. Food Chem. 60 (2012) 9822–9827, https://doi.org/10.1021/jf3017496.

[76] Zhong, Y., Marungruang, N., Fak, K., and Nyman, M., Effects of two whole-grain barley varieties on caecal SCFA, gut microbiota and plasma inflammatory markers in rats consuming low- and high-fat diets, Br. J. Nutr. 113 (2015) 1158–1570. doi: https://doi.org/10.1017/S0007114515000793.

[77] K. Turunen, E. Tsouvelakidou, T. Nomikos, K. Mountzouris, D. Karamanolis, J. Triantafillidis, A. Kyriacou, Impact of beta-glucan on the faecal microbiota of polypectomized patients: a pilot study, Anaerobe 17 (2011) 403–406, https://doi.org/10.1016/j.anaerobe.2011.03.025.

[78] M. Mikkelsen, M. Jensen, T. Nielsen, Barley beta-glucans varying in molecular mass and oligomer structure affect cecal fermentation and microbial composition but not blood lipid profiles in hypercholesterolemic rats, Food Funct. 8 (2017) 4723–4732, https://doi.org/10.1039/c7fo01314k.

[79] Wang, Y., Ames, N., Tun, H., Tosh, S., Jones, P., and Khafipour, E., High molecular weight barley β-glucan alters gut microbiota toward reduced cardiovascular disease risk, front. Microbiol. 7 (2016) 129. doi: https://doi.org/10.3389/fmicb.2016.00129.

[80] Liu, Y., Heath, A., Galland, B., Rehrer, N., Drummond, L., Wu, X., Bell, T., Lawley, T., Sims, I., and Tannock, G., Prioritization of substrate use by a co-culture of five species of gut bacteria fed mixtures of arabinoxylan, xyloglucan, β-glucan, and pectin, Appl. Environ. Microbiol. 86(2) (2020) e01905–19. doi: https://doi.org/10.1128/AEM.01905-19.

[81] T. Arora, L. Loo, J. Anastasovska, G. Gibson, K. Tuohy, R. Sharma, R. Sharma, J. Swann, E. Deaville, M. Sleeth, E. Thomas, E. Holmes, J. Bell, G. Frost, Differential effects of two fermentable carbohydrates on central appetite regulation and body composition, PLoS One 7 (8) (2012), e43263, https://doi.org/10.1371/journal.pone.0043263.

[82] J. Miyamoto, K. Watanabe, S. Taira, M. Kasubuchi, X. Li, J. Irie, H. Itoh, I. Kimura, Barley β-glucan improves metabolic condition via short-chain fatty acids produced by gut microbial fermentation in high fat diet fed mice, PLoS One 3 (4) (2018) e0196579, https://doi.org/10.1371/journal.pone.0196579.

[83] P. Vitaglione, I. Mennella, R. Ferracane, A. Rivellese, R. Giacco, D. Ercolini, S. Gibbons, A. La Storia, J. Gilbert, S. Jonnalagadda, F. Thielecke, M. Gallo, L. Scalfi, V. Fogliano, Whole-grain wheat consumption reduces inflammation in a randomized controlled trial on overweight and obese subjects with unhealthy dietary and lifestyle behaviors: role of polyphenols bound to cereal dietary fiber, Am. J. Clin. Nutr. 101 (2) (2015) 251–261, https://doi.org/10.3945/ajcn.114.088120.

[84] De Paepe, K., Kerckhof, F., Verspreet, J., Courtin, C., and Van de Wiele, T., Interindividual differences determine the outcome of wheat bran colonization by the human gut microbiome, Environ. Microbiol. 8 (2017) 3251–3267. doi: https://doi.org/10.1111/1462-2920.13819.

[85] De Angelis, M., Montemurno, E., Vannini, L., Cosola, C., Cavallo, N., Gozzi, G., Maranzano, V., Di Cagno, R., Gobbetti, M., and Gesualdo, L., Effect of whole-grain barley on the human fecal microbiota and metabolome, Appl. Environ. Microbiol. 81 (2015) 7945–7956. doi: https://doi.org/10.1128/AEM.02507-15.

[86] S. Aoe, F. Nakamura, S. Fujiwara, Effect of wheat bran on fecal butyrate-producing Bacteria and wheat bran combined with barley on Bacteroides abundance in Japanese healthy adults, Nutrients 10 (12) (2018) 1980, https://doi.org/10.3390/nu10121980.

[87] Nishijima, S., Suda, W., Oshima, K., Kim, S., Hirose, Y., Morita, H., and Hattori M., The gut microbiome of healthy Japanese and its microbial and functional uniqueness, DNA Res. (2016) 1–9. doi: https://doi.org/10.1093/dnares/dsw002.

[88] Hehemann, J., Kelly, A., Pudlo, N., Martens, E., and Borastona, A., Bacteria of the human gut microbiome catabolize red seaweed glycans with carbohydrate-active enzyme updates from extrinsic microbes, Proc. Natl. Acad. Sci. U. S. A. 109 (2012) 19786–19791. doi: https://doi.org/10.1073/pnas.1211002109.

[89] E. Sonnenburg, S. Smits, M. Tikhonov, S. Higginbottom, N. Wingreen, J. Sonnenburg, Diet-induced extinctions in the gut microbiota compound over generations, Nature 529 (7585) (2016) 212–215, https://doi.org/10.1038/nature16504.

[90] Shen, R., Dang, D., Dong, J., and Hu, X., Effects of oat β-glucan and barley β-glucan on fecal characteristics, intestinal microflora, and intestinal bacterial metabolites in rats, J. Agric. Food Chem. 60 (2012) 11301–11308. doi: https://doi.org/10.1021/jf302824h.

[91] K. Collins, G. Fitzgerald, C. Stanton, R. Ross, Looking beyond the terrestrial: the potential of seaweed derived bioactives to treat non-communicable diseases, Mar. Drugs 14 (3) (2016) 60, https://doi.org/10.3390/md14030060.

[92] Patil, N., Le, V., Sligar, A., Mei, L., Chavarria, D., Yang, E., and Baker, A., Algal polysaccharides as therapeutic agents for atherosclerosis, Front. Cardiovasc. Med. 5 (2018) 153. doi: https://doi.org/10.3389/fcvm.2018.00153.

[93] S. Xia, B. Gao, A. Li, X. Xiong, Z. Ao, C. Zhang, Preliminary characterization, antioxidant properties and production of Chrysolaminarin from marine diatom Odontella aurita, Mar. Drugs 12 (2014) 4883–4897, https://doi.org/10.3390/md12094883.

[94] Sellimi, S., Maalej, H., Rekik, D., Benslima, A., Ksouda, G., Hamdi, M., Sahnoun, Z., Suming, L., Nasri, M., and Hajji, M., Antioxidant, antibacterial and in vivo wound healing properties of laminaran purified from Cystoseira barbata seaweed, Int. J. Biol. Macromol. 19 (2018) 633–644. doi: https://doi.org/10.1016/j.ijbiomac.2018.07.171.

[95] Menshova, R., Ermakova, S., Anastyuk, S., Isakov, V, Dubrovskaya, Y., Kusaykin, M., Umb, B., and Zvyagintseva, T., Structure, enzymatic transformation and anticancer activity of branched high molecular weight Laminaran from Brown alga Eisenia Bicyclis, Carbohydr. Polym. 99 (2014) 101–109. doi: https://doi.org/10.1016/j.carbpol.2013.08.037.

[96] Déjean, G., Tamura, K., Cabrera, A., Jain, N., Pudlo, N., Pereira, G., Viborg, A., Van Petegem, F., Martens, E. and Brumer, H., Synergy between cell surface Glycosidases and glycan-binding proteins dictates the utilization of specific Beta(1,3)-glucans by human gut Bacteroides, mBio 11(2) (2020) e00095-20. doi: https://doi.org/10.1128/mBio.00095-20.

[97] C. Bennke, K. Krüger, L. Kappelmann, S. Huang, A. Gobet, M. Schüler, V. Barbe, B. Fuchs, G. Michel, H. Teeling, R. Amann, Polysaccharide utilisation loci of Bacteroidetes from two contrasting open ocean sites in the North Atlantic, Environ. Microbiol. (12) (2016) 4456–4470, https://doi.org/10.1111/1462-2920.13429.

[98] Thomas, F., Bordron, P., Eveillard, D., and Michel, G., Gene expression analysis of Zobellia galactanivorans during the degradation of algal polysaccharides reveals both substrate-specific and shared transcriptome-wide responses, Front. Microbiol. 8 (2017) 1808. doi: https://doi.org/10.3389/fmicb.2017.01808.

[99] T.C. Consortium, Ten years of CAZypedia: a living encyclopedia of carbohydrate-active enzymes, Glycobiology 28 (2018) 3–8, https://doi.org/10.1093/glycob/cwx089.

[100] M. Zhang, J. Chekand, D. Dodda, P. Hong, L. Radlinski, V. Revindran, S. Nairb, R. Mackie, I. Cann, Xylan utilization in human gut commensal bacteria is orchestrated by unique modular organization of polysaccharide-degrading enzymes, Proc. Natl. Acad. Sci. 111 (35) (2014) E3708–E3717, https://doi.org/10.1073/pnas.1406156111.

[101] L von Schantz, M. Håkansson, D. Logan, B. Walse, J. Österlin, E. Nordberg-Karlsson, M. Ohlin, Structural basis for carbohydrate-binding specificity—a comparative assessment of two engineered carbohydrate-binding modules, Glycobiology 22 (2012) 948–961, https://doi.org/10.1093/glycob/cws063.

[102] V. Lombard, T. Bernard, C. Rancurel, H. Brumer, P. Coutinho, B. Henrissat, A hierarchical classification of polysaccharide lyases for glycogenomics, Biochem. J. 432 (3) (2010) 437–444, https://doi.org/10.1042/BJ20101185.

[103] T. Barbeyron, F. Thomas, V. Barbe, H. Teeling, C. Schenowitz, C. Dossat, A. Goesmann, C. Leblanc, F. Glöckner, M. Czjzek, R. Amann, G. Michel, Habitat and taxon as driving forces of carbohydrate catabolism in marine heterotrophic bacteria: example of the model algae-associated bacterium Zobellia galactanivorans DsijT, Environ. Microbiol. 18 (12) (2016) 4610–4627, https://doi.org/10.1111/1462-2920.13584.

[104] C. An, T. Kuda, T. Yazaki, H. Takahashi, B. Kimura, FLX pyrosequencing analysis of the effects of the Brown-algal fermentable polysaccharides alginate and Laminaran on rat Cecal microbiotas, Appl. Environ. Microbiol. 79 (2013) 860–876, https://doi.org/10.1128/AEM.02354-12.

[105] S. Nguyen, J. Kim, R. Guevarra, J. Lee, T. Unno, Laminarin favorably modulates gut microbiota in mice fed a high-fat diet, Food Funct. 7 (2016) 4193–4201, https://doi.org/10.1039/c6fo00929h.

[106] M. Takei, T. Kuda, M. Taniguchi, S. Nakamura, T. Hajime, B. Kimura, Detection and isolation of low molecular weight alginate- and laminaran-susceptible gut indigenous bacteria from ICR mice, Carbohydr. Polym. 238 (2020) 116205, https://doi.org/10.1016/j.carbpol.2020.116205.

[107] De Vadder, F., Kovatcheva-Datchary, P., Zitoun, C., Duchampt, A., Bäckhed, F., and Mithieux, G. , Microbiota-produced succinate improves glucose homeostasis via

intestinal gluconeogenesis, Cell Metab.. 24 (2016) 151–157. doi: https://doi.org/10.1016/j.cmet.2016.06.013.

[108] S. Fernández-Veledo, J. Vendrell, Gut microbiota-derived succinate: friend or foe in human metabolic diseases? Rev. Endocr. Metab. Disord. 20 (2019) 439–447, https://doi.org/10.1007/s11154-019-09513-z.

[109] Laserna-Mendieta, E., Clooney, A., Carretero-Gomez, J., Moran, C., Sheehan, D., and Nolan, J., Determinants of reduced genetic capacity for butyrate synthesis by the gut microbiome in Crohn's disease and ulcerative colitis, J. Crohns Colitis 12 (2) (2018) 204–216. doi: https://doi.org/10.1093/ecco-jcc/jjx13.

[110] A. Smith, J. O'Doherty, P. Reilly, M. Ryan, B. Bahar, T. Sweeney, The effects of laminarin derived from Laminaria digitata on measurements of gut health: selected bacterial populations, intestinal fermentation, mucin gene expression and cytokine gene expression in the pig, Br. J. Nutr. 105 (2011) 669–677, https://doi.org/10.1017/S0007114510004277.

[111] T. Sweeney, C. Collins, P. Reilly, K. Pierce, M. Ryan, J. O'Doherty, Effect of purified b-glucans derived from *Laminaria digitata*, *Laminaria hyperborea* and *Saccharomyces cerevisiae* on piglet performance, selected bacterial populations, volatile fatty acids and pro-inflammatory cytokines in the gastrointestinal tract of pigs, Br. J. Nutr. 108 (2012) 1226–1234, https://doi.org/10.1017/S0007114511006751.

[112] Lynch, M., Sweeney, T., Callan, J., O'Sullivan, J., and O'Doherty, J., The effect of dietary Laminaria-derived laminarin and fucoidan on nutrient digestibility, nitrogen utilisation, intestinal microflora and volatile fatty acid concentration in pigs, J. Sci. Food Agric. 90 (2010) 430–437. doi: https://doi.org/10.1002/jsfa.3834.

[113] R. Gudi, J. Suber, R. Brown, B. Johnson, C. Vasu, Pretreatment with yeast-derived complex dietary polysaccharides suppresses gut inflammation, alters the microbiota composition, and increases ImmuneRegulatory short-chain fatty acid production in C57BL/6 mice, J. Nutr. 150 (2020) 1291–1302, https://doi.org/10.1093/jn/nxz328.

[114] Bishehsari, F., Engen, P., Preite, N., Tuncil, Y., Naqib, A., Shaikh, M., Rossi, M., Wilber, S., Green, S., Hamaker, B., Khazaie, K., Voigt, R., Forsyth, C., and Keshavarzian, A., Dietary Fiber treatment corrects the composition of gut microbiota, promotes SCFA production, and suppresses colon carcinogenesis, Genes (Basel) 9(2) (2018) 102. doi: https://doi.org/10.3390/genes9020102.

[115] Panpetch, W., Somboonna, N., Bulan, D., Issara-Amphorn, J., Finkelman, M., Worasilchai, N., Chindamporn, A., Palaga, T., Tumwasorn, S., and Leelahavanichkul, A., Oral administration of live- or heat-killed *Candida albicans* worsened cecal ligation and puncture sepsis in a murine model possibly due to an increased serum $(1\rightarrow3)$-β-D-glucan, PLoS One 2(7) (2017) e0181439. doi: https://doi.org/10.1371/journal.pone.0181439.

[116] M. Temple, F. Cuskin, A. Baslé, N. Hickey, G. Speciale, S. Williams, H. Gilbert, E. Lowe, A Bacteroidetes locus dedicated to fungal 1,6-β-glucan degradation: unique substrate conformation drives specificity of the key endo-1,6-β-glucanase, J. Biol. Chem. 292 (25) (2017) 10639–10650, https://doi.org/10.1074/jbc.M117.787606.

[117] M. Wang, X. Wang, L. Zhang, R. Yang, C. Fei, K. Zhang, C. Wang, Y. Liu, F. Xue, Effect of sulfated yeast beta-glucan on cyclophosphamide-induced immunosuppression in chickens, Int. Inmunopharmacol. 74 (2017) 105690, https://doi.org/10.1016/j.intimp.2019.105690.

[118] M. Xu, X. Mo, H. Huang, X. Chen, H. Liu, Z. Peng, L. Chen, S. Rong, W. Yang, S. Xu, L. Liu, Yeast β-glucan alleviates cognitive deficit by regulating gut microbiota and metabolites in Aβ1–42-induced AD-like mice, Int. J. Biol. Macromol. 161 (2020) 258–270, https://doi.org/10.1016/j.ijbiomac.2020.05.180.

[119] G. Alessandri, C. Milani, S. Duranti, L. Mancabelli, T. Ranjanoro, S. Modica, L. Carnevali, R. Statello, F. Bottacini, F. Turroni, M. Ossiprandi, A. Sgoifo, D. van Sinderen, M. Ventura, Ability of bifidobacteria to metabolize chitin-glucan and its impact on the gut microbiota, Sci. Rep. 9 (1) (2019) 5755, https://doi.org/10.1038/s41598-019-42257-z.

[120] N. Modrackova, E. Vlkova, V. Tejnecky, C. Schwab, V. Neuzil-Bunesova, *Bifidobacterium* β-glucosidase activity and fermentation of dietary plant glucosides is species and strain specific, Microorganisms 8 (6) (2020) 839, https://doi.org/10.3390/microorganisms8060839.

[121] R. Zhang, X. Huang, H. Yan, X. Liu, Q. Zhou, Z. Luo, X. Tan, B. Zhang, Highly selective production of compound K from Ginsenoside Rd by hydrolyzing glucose at C-3 glycoside using β-glucosidase of *Bifidobacterium breve* ATCC 15700, J. Microbiol. Biotechnol. 29 (3) (2019) 410–418, https://doi.org/10.4014/jmb.1808.08059.

[122] S. Yan, P. Wei, Q. Chen, X. Chen, S. Wang, J. Li, C. Gao, Functional and structural characterization of a β-glucosidase involved in saponin metabolism from intestinal bacteria, Biochem. Biophys. Res. Commun. 496 (4) (2018) 1349–1356, https://doi.org/10.1016/j.bbrc.2018.02.018.

[123] Guadamuro, L., Flórez, A., Alegría, A., Vázquez, L., and Mayo, B., Characterization of four β-glucosidases acting on isoflavone-glycosides from *Bifidobacterium pseudocatenulatum* IPLA 36007, Food Res. Int. 100(Pt 1) (2017) 522–528. doi: https://doi.org/10.1016/j.foodres.2017.07.024.

[124] K. Pokusaeva, M. O'Connell-Motherway, A. Zomer, J. Macsharry, G. Fitzgerald, D. van Sinderen, Cellodextrin utilization by *bifidobacterium breve* UCC2003, App. Environ. Microbiol. 77 (5) (2011) 1681–1690, https://doi.org/10.1128/AEM.01786-10.

AMERICAN
SOCIETY FOR
MICROBIOLOGY | mBio®

Sulfation of Arabinogalactan Proteins Confers Privileged Nutrient Status to *Bacteroides plebeius*

Jose Munoz-Munoz,[a,b] Didier Ndeh,[a] Pedro Fernandez-Julia,[b] Gemma Walton,[c] Bernard Henrissat,[d,e] Harry J. Gilbert[a]

[a]Biosciences Institute, The Medical School, Newcastle University, Newcastle upon Tyne, United Kingdom
[b]Microbial Enzymology Group, Department of Applied Sciences, Northumbria University, Newcastle upon Tyne, United Kingdom
[c]Department of Food and Nutritional Sciences, Whiteknights, University of Reading, Reading, United Kingdom
[d]DTU Bioengineering, Technical University of Denmark, Lyngby, Denmark
[e]King Abdulaziz University, Department of Biological Sciences, Jeddah, Saudi Arabia

ABSTRACT The human gut microbiota (HGM) contributes to the physiology and health of its host. The health benefits provided by dietary manipulation of the HGM require knowledge of how glycans, the major nutrients available to this ecosystem, are metabolized. Arabinogalactan proteins (AGPs) are a ubiquitous feature of plant polysaccharides available to the HGM. Although the galactan backbone and galactooligosaccharide side chains of AGPs are conserved, the decorations of these structures are highly variable. Here, we tested the hypothesis that these variations in arabinogalactan decoration provide a selection mechanism for specific *Bacteroides* species within the HGM. The data showed that only a single bacterium, *B. plebeius*, grew on red wine AGP (Wi-AGP) and seaweed AGP (SW-AGP) in mono- or mixed culture. Wi-AGP thus acts as a privileged nutrient for a *Bacteroides* species within the HGM that utilizes marine and terrestrial plant glycans. The *B. plebeius* polysaccharide utilization loci (PULs) upregulated by AGPs encoded a polysaccharide lyase, located in the enzyme family GH145, which hydrolyzed Rha-Glc linkages in Wi-AGP. Further analysis of GH145 identified an enzyme with two active sites that displayed glycoside hydrolase and lyase activities, respectively, which conferred substrate flexibility for different AGPs. The AGP-degrading apparatus of *B. plebeius* also contained a sulfatase, BpS1_8, active on SW-AGP and Wi-AGP, which played a pivotal role in the utilization of these glycans by the bacterium. BpS1_8 enabled other *Bacteroides* species to access the sulfated AGPs, providing a route to introducing privileged nutrient utilization into probiotic and commensal organisms that could improve human health.

IMPORTANCE Dietary manipulation of the HGM requires knowledge of how glycans available to this ecosystem are metabolized. The variable structures that decorate the core component of plant AGPs may influence their utilization by specific organisms within the HGM. Here, we evaluated the ability of *Bacteroides* species to utilize a marine and terrestrial AGP. The data showed that a single bacterium, *B. plebeius*, grew on Wi-AGP and SW-AGP in mono- or mixed culture. Wi-AGP is thus a privileged nutrient for a *Bacteroides* species that utilizes marine and terrestrial plant glycans. A key component of the AGP-degrading apparatus of *B. plebeius* is a sulfatase that conferred the ability of the bacterium to utilize these glycans. The enzyme enabled other *Bacteroides* species to access the sulfated AGPs, providing a route to introducing privileged nutrient utilization into probiotic and commensal organisms that could improve human health.

KEYWORDS *Bacteroides*, human microbiota, arabinogalactan, glycan-degrading enzymes, microbial ecology, privileged nutrient, sulfatases

The human large bowel is resident to trillions of bacteria that play a pivotal role in the health and nutrition of their host (1, 2). The major nutrients available to this microbial community, defined as the human gut microbiota (HGM), are dietary polysaccharides,

which are not degraded by endogenous intestinal enzymes, and host glycans (3, 4). Reflecting their dependence on complex carbohydrates bacteria within the HGM, particularly those belonging to the *Bacteroidetes* phylum, express large numbers of carbohydrate-active enzymes, or CAZymes (5, 6). Manipulating the HGM through dietary or nutraceutical strategies offers opportunities for maximizing the health benefits of this microbial community. Given the importance of polysaccharides as a major nutrient for the HGM, understanding complex glycan utilization by this ecosystem is an essential prerequisite to successful dietary intervention. Consequently, there have been numerous studies exploring the mechanisms by which specific members of the HGM utilize selected glycans (7–12) (for reviews, see references 13 and 14). The *Bacteroides* spp., in general, produce surface endo-acting glycoside hydrolases or polysaccharide lyases that initiate the degradation of specific polysaccharides. The resultant oligosaccharides, imported into the periplasm, are degraded by an extended repertoire of CAZymes, leading to the generation of the monosaccharide components of these glycans. The genes encoding specific glycan-degrading systems are coregulated by the target polysaccharide and are organized into genomic regions termed polysaccharide utilization loci, or PULs (15). In addition to orchestrating the synthesis of the requisite CAZymes, PULs also encode the outer member transport protein, termed SusC, and surface binding proteins, such as SusD homologs (16) and the glycan sensor/regulator (17).

Arabinogalactan proteins (AGPs) are a ubiquitous feature of plant polysaccharides available to the HGM. In highly processed plant-derived components of the diet, such as red wine, the levels of complex plant-derived carbohydrates, such as AGPs and rhamnogalacturonan II (RGII), are particularly elevated (18). This is because during fermentation, yeast is able to utilize simple carbohydrates but not complex glycans such as AGPs and RGII. The glycan component of AGPs (comprising 90% of these glycoproteins) comprises a backbone of β-1,3-galactose units that are decorated with β-1,6-galactooligosacchrides and arabinofuranose units. The β-1,6-galactan side chains are often decorated with a range of sugars such as rhamnose, glucuronic acid, and additional arabinose units (19). Previous studies have shown that the utilization of arabinogalactans between organisms is dependent on the degree of polymerization (DP) of the glycan (20). Indeed, the capacity to grow on complex arabinogalactans with a high DP is restricted to a very small number of *Bacteroides* spp. These keystone organisms generated oligosaccharides that were utilized by bacteria capable of growing only on simple small arabinogalactans (20). Based on these observations, we hypothesize that the variable structures of arabinogalactans provide a selection mechanism for specific *Bacteroides* spp. within the HGM.

To test the hypothesis proposed above, we evaluated the capacity of our collection of *Bacteroides* spp. isolated from the HGM to grow on an AGP isolated from wine (Wi-AGP). The data showed that only a single bacterium, *B. plebeius*, was capable of growing on the glycan in mono- or mixed culture. Wi-AGP can thus act as a privileged nutrient for a *Bacteroides* spp. that has acquired the capacity to utilize marine and terrestrial plant glycans. Analysis of the enzymes required to depolymerize Wi-AGP demonstrated that a sulfatase was critical to the utilization of this glycan, consistent with the observed sulfation of this glycan. Furthermore, the substrate flexibility of an AGP-specific CAZyme was mediated through two distinct active sites, displaying glycoside hydrolase and polysaccharide lyase activities, respectively, which, uniquely, are located in a single catalytic module.

RESULTS AND DISCUSSION

Wi-AGP is utilized exclusively by *B. plebeius*. Wi-AGP was purified from red wine by gel filtration chromatography, and its capacity to act as a growth substrate for our collection of HGM *Bacteroides* spp. was evaluated. The data showed that only *B. plebeius* grew on Wi-AGP (Table 1). To further explore Wi-AGP bacterial utilization, the ability of the glycan to act as a growth substrate in batch cultures mimicking the distal colon inoculated with a fecal sample (comprises the HGM) was assessed (Fig. 1). The proportion of bacteria in the original HGM and the ecosystem cultured on inulin or Wi-AGP was evaluated by sequencing the V4 of 16S rRNA molecules. V4 is one of the highly

TABLE 1 HGM-derived *Bacteroides* species cultured on LA-, GA-, SW- and Wi-AGP[a]

Bacteroides species	LA-AGP	GA-AGP	SW-AGP	Wi-AGP
Bacteroides thetaiotaomicron ATCC29418	red			
Bacteroides cellulosilyticus DSM 14838	red	green	red	red
Bacteroides caccae ATCC 43185	red	green	red	red
Bacteroides ovatus ATCC 8483	red	red	red	red
Bacteroides vulgatus ATCC 8482	red	red	red	red
Bacteroides uniformis ATCC 8492	red	red	red	red
Bacteroides plebeius DSM 17135	red	red	green	green
Bacteroides xylanisolvens DSM18836	red	red	red	red
B. fragilis ATCC 25285	red	red	red	red
Bacteroides nordii ATCC BAA-998	red	red	red	red
Bacteroides finegoldii DSM 17565	red	red	red	red
Bacteroides intestinalis DSM 17393	red	red	red	red
Bacteroides stercoris ATCC 43183	red	red	red	red
Bacteroides massiliensis DSM 17679	red	red	red	red
Bacteroides dorei DSM 17855	red	red	red	red
Parabacteroides gordonii DSM 23371	red	red	red	red
Parabacteroides johnsonii DSM 23371	red	red	red	red
Parabacteroides merdae ATCC 43184	red	red	red	red
Dysgonomonas mossii DSM 22836	red	red	red	red
Dysgonomonas gadei ATCC BAA-286	green	green	red	red

[a]Cells colored green and red indicate, respectively, growth or no growth of the bacteria. The data for larchwood (LA-AGP) and gum arabic AGP (GA-AGP) were published previously (20).

variable regions of rRNA, and its sequence provides information on the genus and species of its bacterial origin (21). In the uncultured HGM *B. plebeius*, rRNA was not detected among the 162,000 V4 sequences obtained, in which 40% of the sequences were from the *Bacteroides* genus. This demonstrates that *B. plebeius*, if present, comprises an extremely small proportion of the HGM. When the HGM was cultured on inulin, there was an increase in the proportion of the *Bacteroides* and *Verrucomicrobia* genera; however, *B. plebeius* was again not detected among the 204,000 sequences analyzed. In the HGM grown on Wi-AGP, 64% of the 540,000 sequences obtained were from *Bacteroides* species. Significantly, ~80% of the *Bacteroides* sequences encoded *B. plebeius* rRNA molecules, which equates to 50% of the total HGM. The data showed that Wi-AGP strongly selects for the growth of *B. plebeius* within the *Bacteroides* genus and in models of the HGM, and thus, this glycan is a privileged nutrient for the bacterium.

B. plebeius utilizes a sulfated AGP. *B. plebeius* is an unusual member of the HGM in that it has acquired the capacity to utilize a marine polysaccharide, porphyran, which is a major carbohydrate in the seaweed (red algae) *Porphyra yezoensis* (22). Marine algal polysaccharides ae often highly sulfated, exemplified by porphyran and AGP from the green alga *Codium fragile* (SW-AGP) (23). To assess whether the capacity of *B. plebeius* to utilize Wi-AGP reflects its ability to desulfate glycans, growth of our collection of HGM-derived *Bacteroides* species on SW-AGP was assessed. The data (Table 1) showed that only *B. plebeius* was able to utilize SW-AGP. The structure of SW-AGP (Fig. 2) comprises a simple glycan in which the β-1,3-galactan backbone, the β-1,6-galactooligosaccharides, and the arabinose side chains are all sulfated (24). We propose that the unique capacity of *B. plebeius* to utilize SW-AGP and Wi-AGP reflects the ability of the bacterium to desulfate these polysaccharides.

To test the sulfatase hypothesis, PULs in the *B. plebeius* genome that are likely to orchestrate AGP degradation were identified using the PUL database (www.cazy.org/PULDB_new/) (25) and knowledge of the predicted activities of the CAZymes encoded by these loci. Within the CAZy database, glycoside hydrolases and polysaccharide lyases are grouped into sequence-based families and subfamilies (5). In many instances, the substrate specificity of these enzymes can be predicted by their assignment to a CAZy family. Inspection of the 42 PULs within the genome of *B. plebeius* revealed three loci, PUL5, PUL7, and PUL13, that contain genes encoding enzymes likely to contribute to AGP degradation. Examples include enzymes in glycoside hydrolase family 2 (GH2), GH27, GH43, and GH145, which contain a range of arabinofuranosidases, arabinopyranosidases, galactosidases, glucuronidases, and rhamnosidases (5). To evaluate
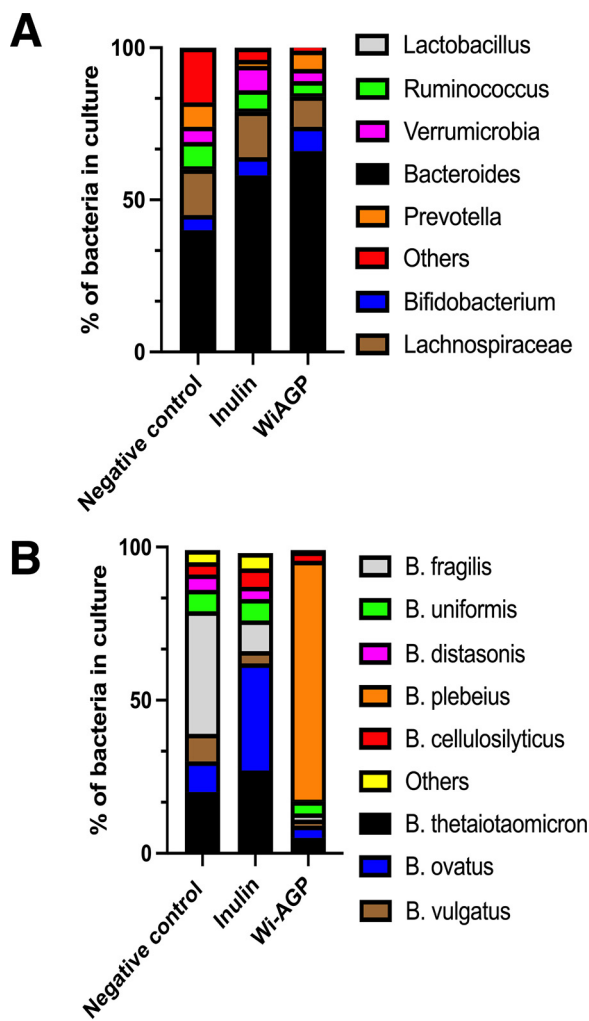
FIG 1 Proportion of bacterial genera and species in models of the HGM grown on different carbon sources. The HGM in a model colon was cultured in minimal media containing no carbon source (negative control), inulin, or red wine AGP (Wi-AGP). After 24 h, DNA was extracted from these cultures and subjected to metagenomics sequencing to determine the proportion of bacteria present. (A) Proportion of the major genera found in the HGM; (B) percentage of *Bacteroides* species from this microbial community. The numerical percentages of organisms in panels A and B are given in Table S1 in the supplemental material.

whether Wi-AGP and SW-AGP activate transcription of the three PULs, *B. plebeius* was cultured on the two glycans, and the mRNA levels of the cognate SusC genes, encoding outer membrane glycan transporters, were determined. These genes were selected, as they are expressed at high levels compared to other sequences within PULs. Furthermore, as they are always upregulated in an actively transcribed PUL, they are excellent indicators of loci that are switched on by a specific nutrient (26). The data (Fig. 3) showed that *bacple00403*, the *susC* gene of PUL7, was not activated by either AGP, indicating that this locus does not contribute to the observed growth on the two glycans. Significant transcription of *susC* from PUL5 and PUL13 was observed, demonstrating that both loci contribute to AGP degradation. The expression of *susC* from PUL13, however, was higher in response to SW-AGP than Wi-AGP. In contrast, transcripts of the equivalent gene in PUL5 were elevated in Wi-AGP cultures compared to when SW-AGP was the growth substrate, where upregulation of the locus was very modest. The observed differential transcription of the two AGP PULs by SW-AGP and Wi-AGP suggests that PUL5 is essential for the degradation of the wine glycan, while PUL13 contributes to the deconstruction of both polysaccharides. PUL5 encodes
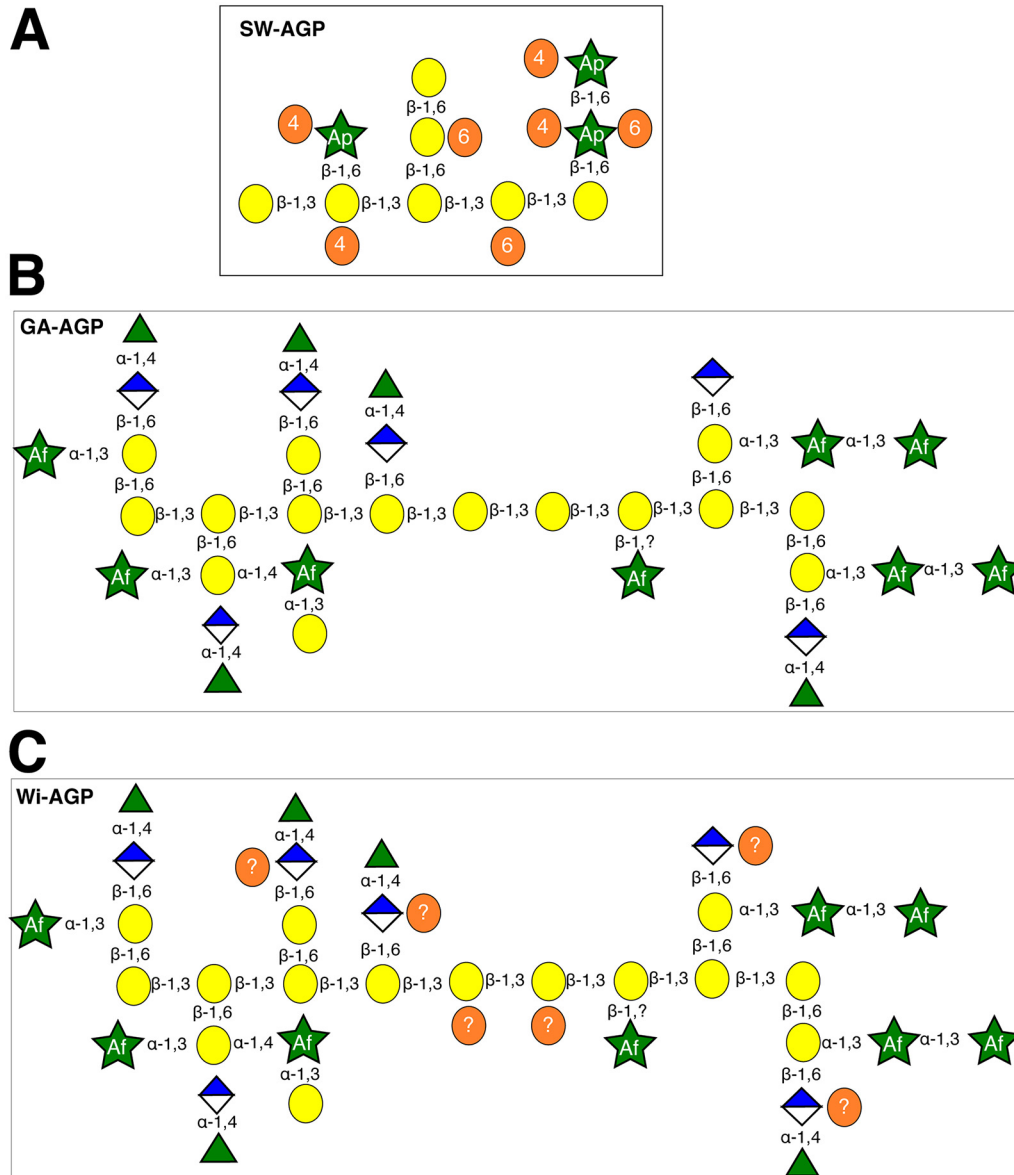
FIG 2 Structures of selected arabinogalactans. Structures of SW-AGP (A), GA-AGP (B), and Wi-AGP (C). The proposed structure of Wi-AGP is based on the observed activities of the GH145 polysaccharide lyase, the observation that BpS1_8 releases sulfate from Wi-AGP and that desulfation is required for cleavage of the β-1,3-galactan backbone by the GH43_24 exo-β-1,3-galactanase BpGH43_24. The precise position of the sulfates is unknown, hence the insertion of a question mark.

GH43_24 (Fig. 3), a subfamily that contains exclusively exo-β-1,3-galactanases (20). Of more significance, however, is the presence of the genes encoding GH145 and GH105 enzymes that are required to remove L-rhamnose-α-1,4-D-glucuronic acid (Rha-GlcA) disaccharides that cap some of the side chains in Wi-AG (see below); these structures are not present in SW-AGP. It is not clear why the expression of the locus is more pronounced in SW-AGP cultures but may reflect the concentration of the inducing ligands generated from the marine glycan.

A highly unusual feature of PUL13 is the presence of two genes (Fig. 3) encoding putative sulfatases BACPEL00986 and BACPEL00990, defined as BpS1-8 and BpS1-14, respectively. This led us to hypothesize that one or more of these sulfatases contribute to the capacity of *B. plebius* to deconstruct sulfated AGPs, explaining why the bacterium is the only known *Bacteroides* species within the HGM that can utilize SW-AGP and Wi-AGP as
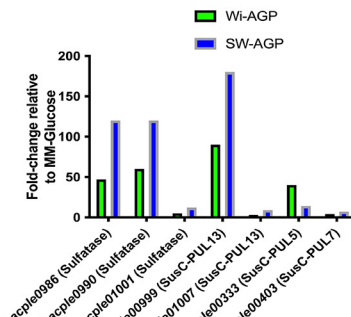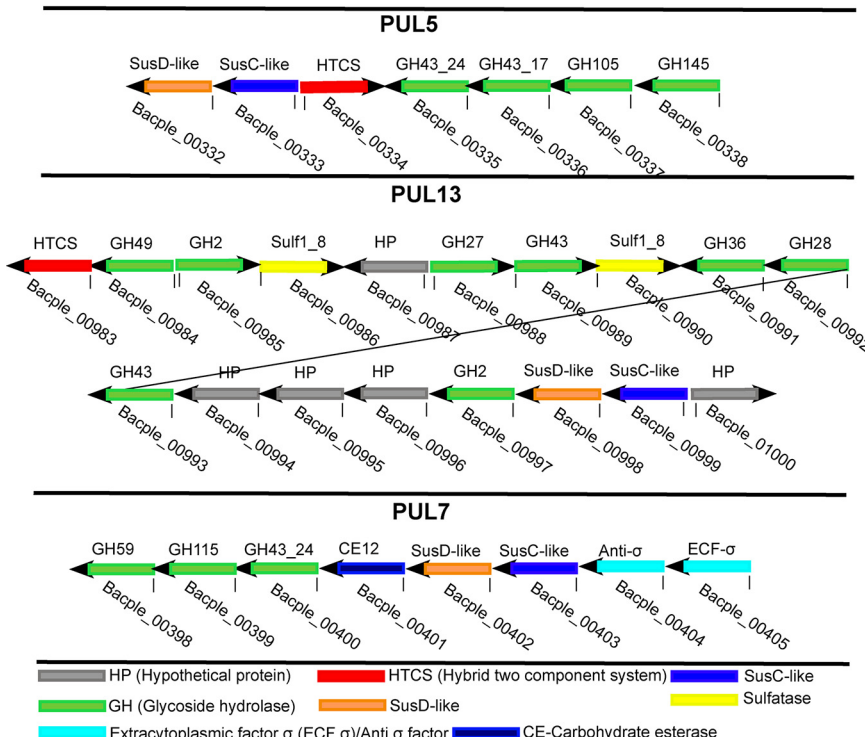
FIG 3 PULs upregulated by Wi-AGP and SW-AGP. (A) Cultures of *B. plebeius* were grown on SW-AGP (green bars) and Wi-AGP (blue bars) to mid-logarithmic phase, at which point RNA was extracted and subjected to quantitative reverse transcription-PCR (RT-PCR) using primers to amplify the genes shown. (B) Schematic of *B. plebeius* PULs upregulated by growth on the AGPs.

growth substrates. To evaluate this proposal, we expressed BpS1-8 in its active form and purified the N-terminal His-tagged enzyme by nickel ion affinity chromatography. The importance of sulfatase activity in the degradation of sulfated AGPs was demonstrated by exploring the activity of the GH43_24 exo-β-1,3-galactanase BpGH43_24 (BACPLE00335), which, by analogy with other enzymes in this subfamily (20), is predicted to target the backbone of AGPs, generating a series of decorated β-1,6-galactooligosaccharide side chains. The enzyme did not act on Wi-AGP; however, when the glycan was incubated with the putative exogalactanase in the presence of the predicted sulfatase BpS1_8, oligosaccharides were generated, showing that BpGH43_24 is likely active only on the desulfated polysaccharide (Fig. 4). To confirm this hypothesis, the activity of BpS1_8 was determined. The data (Table 2) showed that the enzyme released sulfate from 4-nitrophenyl-sulfate and Wi-AGP, demonstrating that BpS1_8 is a functional sulfatase, and the glycan, like SW-AGP, is sulfated. Microbial growth experiments provided further evidence for the importance of desulfation of Wi-AGP and SW-AGP when these glycans were used to culture *Bacteroides* species. The sulfatase BpS1_8 was incubated with Wi-AGP, and the treated
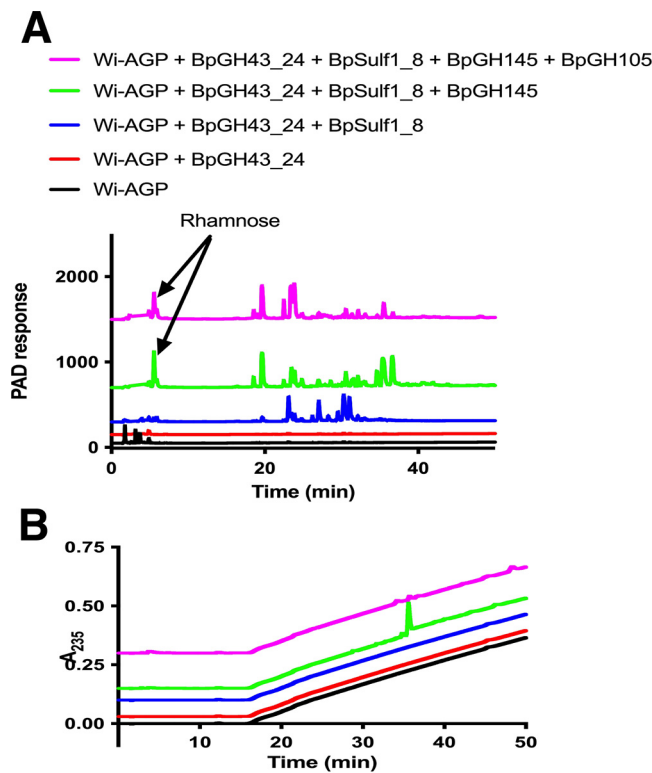
FIG 4 HPAEC analysis of the activity of selected enzymes encoded by PUL5 and PUL13. Wi-AGP was at 5 mg/ml for all reactions. Enzyme concentration was 1 μM. Reaction mixtures were incubated for 16 h in 20 mM sodium phosphate buffer, pH 7.0, containing 150 mM NaCl buffer. The data shown are representative of three independent replicates. Oligosaccharides generated were monitored by pulsed amperometric detection (PAD) (A) or UV absorbance at 235 nm (B).

glycan was assessed as a growth substrate for *B. cellulosilyticus*. The data, presented in Fig. 5, showed that the bacterium grew on the AGP only when pretreated with the sulfatase. These biochemical and microbial growth data demonstrate that desulfation of Wi-AGP is a prerequisite for its subsequent utilization by *B. cellulosilyticus*. Thus, the absence of sulfatase genes in the AGP PULs of *Bacteroides* species, other than *B. plebeius*, explains why these prokaryotes were unable to utilize the sulfated plant glycan. In a previous study, *B. cellulosilyticus* was shown to be a keystone organism that supports growth of other *Bacteroides* species on gum arabic AGP (GA-AGP) through the action of a surface endo-β-1,3-galactanase. The enzyme generated oligosaccharides from the AGP that could be

TABLE 2 Kinetics of GH145 enzymes and sulfatases

Enzyme or sulfatase	Substrate	K_{cat}/K_m
GH145 enzymes		
BT3686 WT[a]	Wi-AGP	$1.80 \times 10^2 \pm 5.6 \times 10^{1b}$
BT3686 R333A	Wi-AGP	Inactive
BT3686 H90A	Wi-AGP	Inactive
BT3686 Y143F	Wi-AGP	Inactive
BACPLE00338 WT[a]	Wi-AGP	$3.57 \times 10^3 \pm 1.05 \times 10^{2b}$
BACCELL00856 WT	Wi-AGP	$1.18 \times 10^3 \pm 6.90 \times 10^{1b}$
BACCELL00856 H90Q	Wi-AGP	Inactive
Sulfatases		
BACPLE00986 S76C	Wi-AGP	0.35 ± 0.04^b
BACPLE00986 S76C	SW-AGP	1.38 ± 0.14^b
BACPLE00986 S76C	4NP-sulfate[a]	0.1447 ± 0.004^c

[a]WT, wild-type enzyme; 4NP-sulfate, 4-nitrophenyl sulfate.
[b]Units are ml/mg^{-1} min^{-1}.
[c]Unit is mM^{-1} min^{-1}.
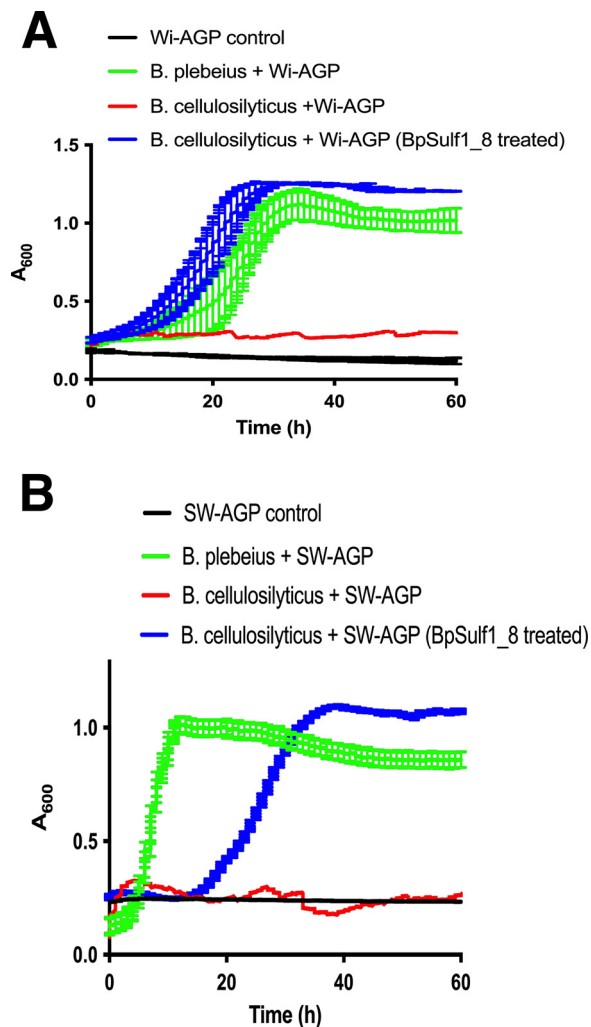
FIG 5 Growth of *Bacteroides* species on sulfated AGPs. Bacterial growth was assessed on SW-AGP and Wi-AGP. The *Bacteroides* species were cultured under anaerobic conditions at 37°C using an anaerobic cabinet on minimal medium containing an appropriate carbon source. The growth of the cultures was monitored by OD_{600} using a Gen5 v2.0 microplate reader. In blue, growth curves show the two AGPs had been treated with the sulfatase BpS1_8.

imported and thus utilized by the recipient organisms (20). To explore whether *B. plebeius* could support the growth of other *Bacteroides* on sulfated AGPs, *B. cellulosilyticus* was cocultured with *B. cellulosilyticus* on Wi-AGP and SW-AGP, and the different organisms were quantified by quantitative PCR (qPCR) of genomic specific sequences of these bacteria. The data (Fig. 6) showed that the proportion of *B. cellulosilyticus* sharply declined over time on both AGPs, and, indeed, there was only a modest increase in the CFU of the bacterium. Thus, *B. plebeius* did not support the growth of *B. cellulosilyticus* on Wi-AGP or SW-AGP and, hence, did not fulfill a keystone role in the utilization of sulfated AGPs. This indicates that desulfation of Wi-AGP and SW-AGP is an intracellular event. Indeed, BpS1_8 contains a canonical type I signal peptide, which is entirely consistent with its predicted periplasmic location. Thus, the desulfation of Wi-AGP and SW-AGP occurred after transport into the bacterium, explaining why the desulfated glycans were not accessible to other *Bacteroides* species.

From a broader perspective, within the *Bacteroides* of the HGM, there are no examples, other than PUL13 in *B. plebeius*, of sulfatase genes in PULs that encode enzyme systems that degrade terrestrial plant polysaccharides. Sulfatase genes, however, are common in loci that orchestrate the utilization of human (e.g., mucins and glycosaminoglycans) and
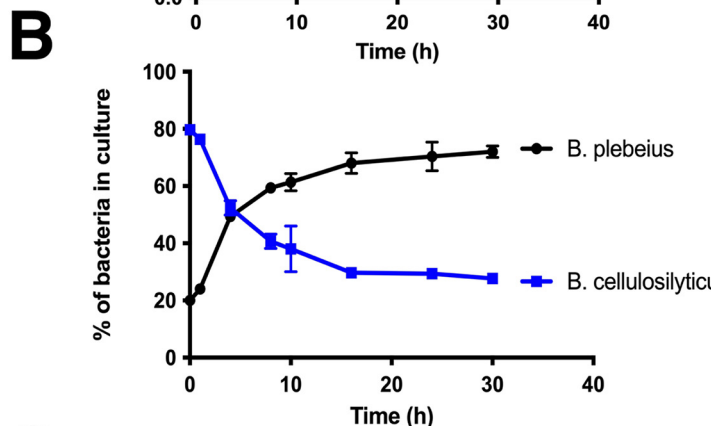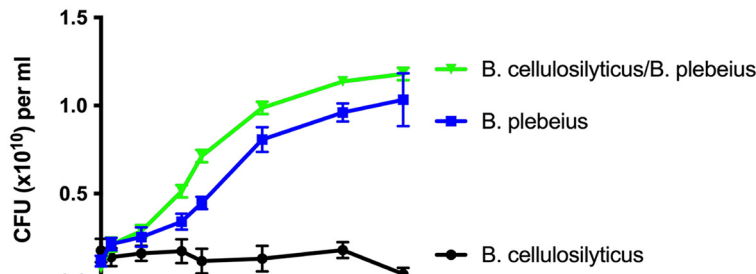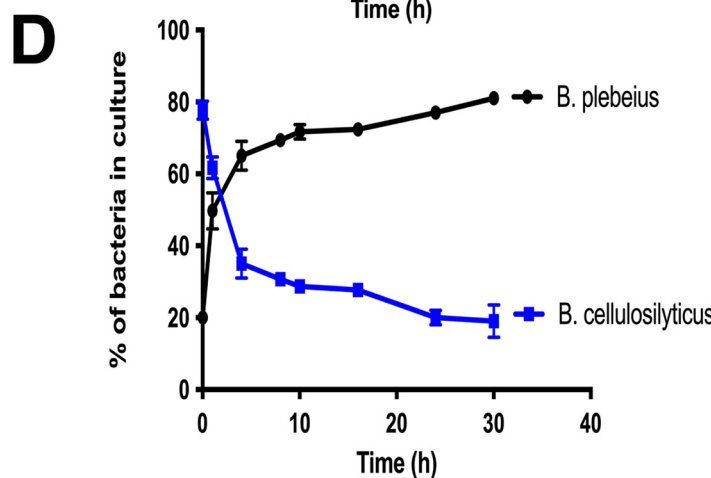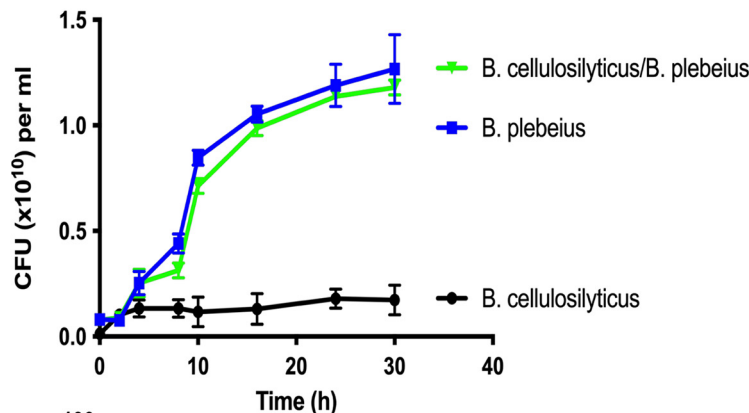
FIG 6 Growth profile of cocultures of *Bacteroides* species on sulfated AGPs. *B. plebeius* and *B. cellulosilyticus* strain DSM14838 were cultured on nutrient-rich (TYG) media overnight. The organisms

(Continued on next page)

marine (e.g., porphyran) glycans. Thus, this ecosystem is tailored to utilize terrestrial plant glycans that are often acetylated but are not known to be sulfated. This report, showing that sulfatases are required to enable growth of *Bacteroides* species on Wi-AGP, provides evidence for terrestrial plant glycan sulfation. The precise nature of the sulfation of Wi-AGP is unknown and clearly requires further analysis. In addition to PUL1 and PUL13 in *B. plebeius*, which encode porphyran (27), and SW-AGP/Wi-AGP utilization systems, respectively, there are three further PULs that contain sulfatase genes, hinting that additional sulfated polysaccharides may be targeted by *B. plebeius*. Two of these loci, PUL14 and PUL15, encode glycoside hydrolases from the fucosidase families GH29 and GH95, which may suggest that *B. plebeius* can utilize the marine polysaccharide fucoidan, comprising sulfated fucose residues, which is abundant in brown algae (28). It should also be emphasized that human glucans, such as 6-sulfo-sialyl Lewis X and A, also contain sulfated fucose residues, and thus, PUL14 and/or PUL15 may target these glycans rather than marine polysaccharides. Nevertheless, the sulfatase genes in the *B. plebeius* PULs suggest that the bacterium is adapted to utilize at least some abundant marine glycans. The marine origin of the sulfatase encoding PULs is interesting. Porphyran is a major component of red algal species used to prepare culinary nori, an important component of sushi. It is believed that porphyran utilization, orchestrated by PUL1, was the result of horizontal transfer of the requisite genes from an ancestral porphyranolytic marine bacterium, related to the extant marine *Bacteroidetes Zobellia galactanivorans* in the HGM of the Japanese population, where sushi is an integral component of the diet (29). While it is tempting to speculate that the AGP and, possibly, sulfated fucose glycan-utilizing PULs are also derived from a marine *Bacteroidetes*, no obvious orthologous loci are present in *Zobellia galactanivorans* or any other sequenced marine bacterium. The evolutionary mechanisms by which *B. plebeius* acquired the ability to degrade sulfated AGP are currently unclear.

The catalytic domain of GH145 rhamnosidases can contain two distinct and functional active sites. The *B. thetaiotaomicron* GH145 rhamnosidase BtGH145 (BT3686), is encoded by PUL_AGPS (20). The crystal structure of the enzyme in complex with the reaction product, glucuronic acid, together with biochemical analysis of appropriate mutants, showed that the posterior surface houses an active site of the seven-bladed β-propeller enzyme (30). This was surprising, as the catalytic center of all other β-propeller enzymes, including several CAZymes, is located on the anterior surface (31). In addition, the central catalytic residue in the posterior active site, His48 in BtGH145, is not invariant in GH145 (Table S2 in the supplemental material), and those enzymes lacking the histidine were shown not to display rhamnosidase activity against GA-AGP. Sequence comparison of *Bacteroides* GH145 enzymes, including BpGH145 (BACPEL00338) encoded by *B. plebeius* PUL5, reveals that highest amino acid conservation is on the anterior surface of the enzyme (Table S2). This led to the proposal that the anterior surface also comprises a functional catalytic center at least in progenitors of GH145 and possibly in members of the current GH145 family, particularly those that do not display rhamnosidase activity against GA-AGP (20). This hypothesis is strengthened further by the high degree of structural conservation between the polysaccharide lyase belonging to PL25 and the GH145 enzymes (Fig. 7). The root mean square deviation (RMSD) between the *B. thetaiotaomicron* GH145 enzyme BtGH145 (PDB ID 5MUK) and the PL25 enzyme (PDB ID 5UAM) is 2.33 Å. Furthermore, the catalytic apparatus of the PL25 lyase, comprising a triad of His, Tyr, and Arg (32), is completely conserved in GH145 *Bacteroides* enzymes and is structurally equivalent in the three-dimensional structures available (Fig. 7).

FIG 6 Legend (Continued)

were then inoculated at ~10^8 CFU per ml into minimal medium containing Wi-AGP (A and B) or SW-AGP (C and D) at 0.5% (wt/vol), either as a monoculture or in coculture. The cultures were incubated in anaerobic conditions, and at regular intervals, aliquots were removed and plated onto rich (brain heart infusion [BHI]) agar plates to determine the CFU. The ratios of the strains in the cocultures were determined by quantitative PCR with primers that amplify genomic sequences unique to each strain (see Materials and Methods for further details). (A and C) CFU for bacterial strains; (B and D) ratios of the organisms in the cocultures. Error bars represent the SEM of biological replicates ($n = 3$).
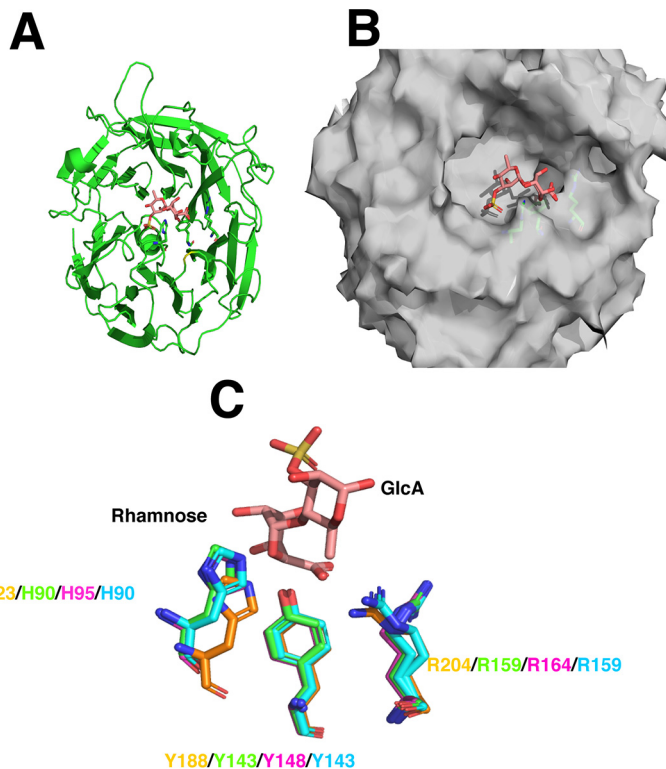
FIG 7 Structural conservation of the anterior active site of GH145 and PL25 polysaccharide lyases. (A) Cartoon (β-sheets depicted as broad arrows) of the β-propeller fold of the GH145 enzyme from *B. cellulosilyticus* (PDB ID 5MVH) viewed from the anterior surface. The ligand 3-sulfate-ʟ-rhamnose-α-1,4-ᴅ-glucuronic acid (RhaSO₃-GlcA) bound at the anterior catalytic center of a PL25 polysaccharide lyase (PDB ID 5UAS) is shown in stick format in salmon pink. (B) Surface representation of the broad active site pocket of the GH145 enzyme shown in panel A and the RhaSO₃-GlcA ligand. (C) Overlay of the catalytic triad of the PL25 *Pseudoalteromonas* sp. ulvan lyase (PDB ID 5UAM; yellow) and the GH145 enzymes from *B. cellulosilyticus* (green), *B. intestinalis* (PDB ID 5MUM; magenta), and *B. ovatus* (PDB ID 4IRT; yellow and cyan). The ligand bound to the active site of the ulvan lyase is again shown in salmon pink.

Based on the structural and sequence analysis of GH145, we propose that members of this family display polysaccharide lyase activity which is mediated by an active site located on the anterior surface of these enzymes. To test this hypothesis, we explored the activity of BtGH145 against Wi-AGP. The data (Fig. 8) showed that the enzyme released rhamnose, indicating it cleaves the Rha-α-1,4-GlcA linkage known to be present in this glycan (33). Significantly, rhamnose release was evident in the H48A mutant of BtGH145, which inactivates the posterior rhamnosidase (glycoside hydrolase) catalytic center that releases rhamnose from GA-AGP (30). Thus, the posterior active site that confers rhamnosidase activity does not act on Wi-AGP. This suggests that an active site in the anterior surface of the enzyme catalyzed the release of rhamnose from Wi-AGP. To evaluate this proposal, we substituted with Ala the three residues in BtGH145 (His90, Tyr143, and Arg333) located on the anterior surface that comprise the equivalent catalytic triad present in the PL25 polysaccharide lyase. The data (Table 2) showed that the three mutants were inactive against Wi-AGP, demonstrating that the release of rhamnose from this glycan was mediated by an active site on the anterior surface of the enzyme.

To evaluate further the conservation of lyase activity in GH145 enzymes, we assessed the activity of two other GH145 enzymes, BpGH145 (BACPLE00338) and BcGH145 (BACCELL00856) from *B. cellulosilyticus*. The two enzymes both lacked the catalytic histidine in posterior activity site (equivalent to His48 in BtGH145) and displayed no rhamnosidase activity against GA-AGP. BpGH145, and BcGH145, however, released rhamnose from Wi-AGP (Fig. 4 and Table 2). Mutation of the conserved His (His90) in the anterior surface of BcGH145 (equivalent to His90 in BtGH145) rendered the enzyme inactive against Wi-AGP

A

Legend:
- 300 μM rhamnose (black)
- Wi-AGP control (blue)
- Wi-AGP +BtGH145 (red)
- Wi-AGP +BtGH145H48A (green)
- Wi-AGP +BtGH145R333A (magenta)

B

Wi-AGP (10 mg/ml) + BtGH145 (1 μM)

C
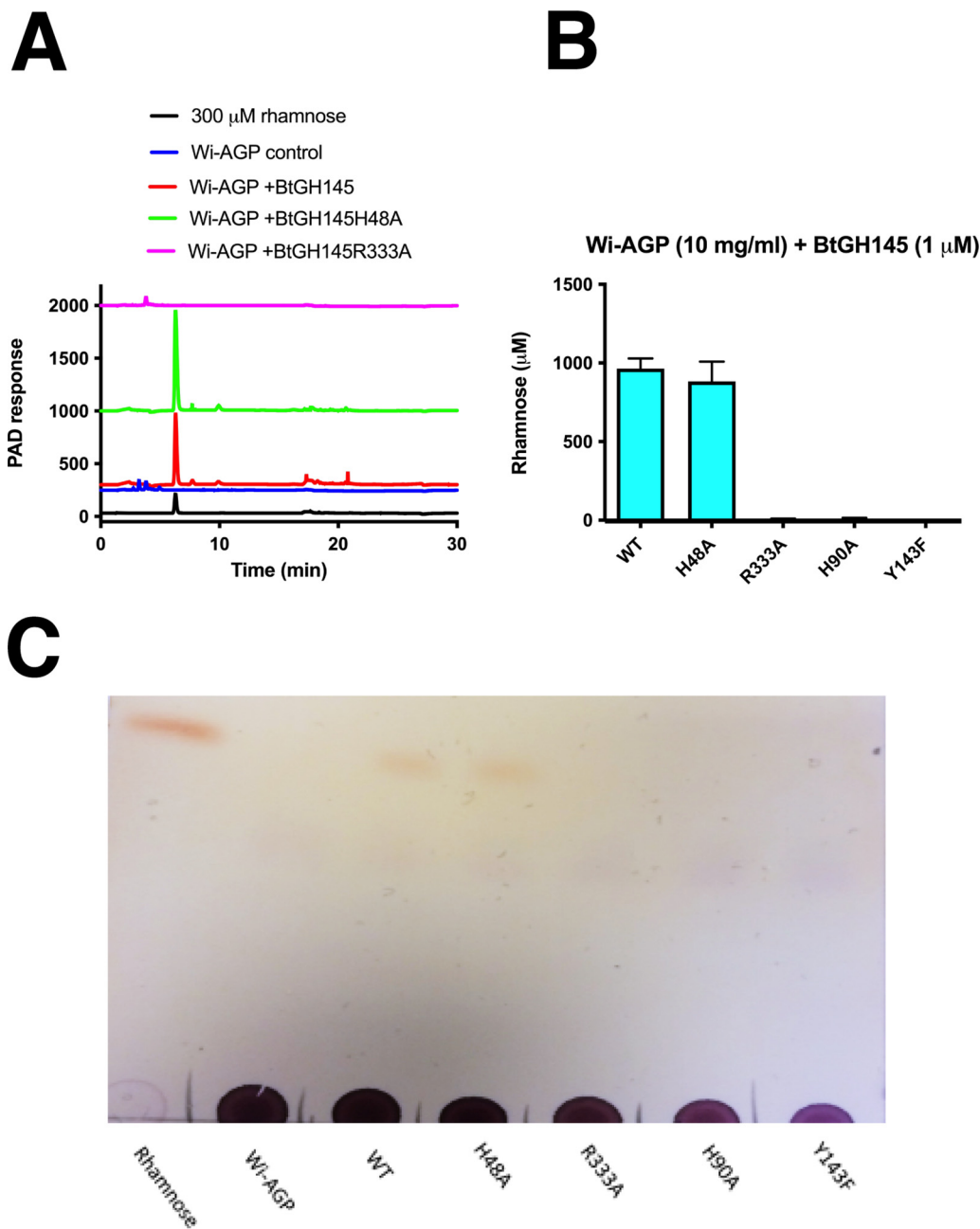
FIG 8 Exploring the activity of the GH145 enzyme BtGH145 against Wi-AGP. (A) Wild-type BtGH145 and mutants in which the catalytic residue in the posterior active site (H48A) and a conserved amino acid in the anterior catalytic center (R333A) were substituted with alanine and were incubated with Wi-AGP using standard conditions. After incubation for 16 h, the reaction mixtures were subjected to HPAEC using PAD to detect the reaction products. The release of rhamnose from Wi-AGP by wild type and mutants of BtGH145 were analyzed by direct biochemical quantification of the hexose sugar (B) and by TLC (C).

(Table 2). These data, in conjunction with the conservation of the catalytic apparatus with the PL25 ulvan lyase, indicated that cleavage of rhamnose from Wi-AGP is highly likely the result of polysaccharide lyase activity. This was confirmed by further analysis of the products generated by BpGH145. The GH145 enzyme generated rhamnose and an unsaturated product, evidenced by a signal at 235 nm typical of polysaccharide lyases. The unsaturated product was sensitive to BpGH105 (BACPLE00337), a member of GH105 that contains exclusively Δ-4,5-unsaturated β-glucuronyl hydrolases and Δ-4,5-unsaturated β-galacturonyl hydrolases (34) (Fig. 4). These data show that the anterior surface of GH145 enzymes houses a

catalytic center that displays polysaccharide lyase activity, irrespective of whether the posterior active site is functional.

An interesting feature of the polysaccharide lyase activity displayed by BpGH145, BcGH145, and the BtGH145 mutant H48A is that they cleave the Rha-GlcA linkage in Wi-AGP but not in GA-AGP. Although the precise nature of the Rha-GlcA targeted by the anterior lyase active site of the two GH145 enzymes is not clear, it does not comprise the simple terminal Rha-α-1,4-GlcA linkage in GA-AGP. It is probable that the anterior active site targets a sulfated substrate, likely GlcA or a sugar bound to the distal regions of the active site. It should be noted that close structural homologs of GH145 enzymes are the ulvan lyases in PL25, which catalyze Rha-GlcA linkages where the rhamnose is sulfated at O_3 (32). As unmodified rhamnose was released from Wi-AGP by BpGH145 and BtGH145, the terminal sugar did not appear to be sulfated. The retention of the catalytic triad within the *Bacteroides* GH145 enzymes indicates that the lyase activity is a conserved feature of the family. The evolutionary rationale for retaining the lyase activity in BtGH145 is unclear, as *B. thetaiotaomicron* does not utilize extensively sulfated AGPs, exemplified by wine and seaweed sources of these glycans. It is formerly possible that the bacterium is able to access growth substrates that are also targeted by the lyase activity of BtGH145. Although such glycans were not evaluated here, the BtGH145 lyase activity may target AGPs where only the GlcA in the terminal Rha-GlcA capping structures is sulfated. Such glycans would be degraded by *B. thetaiotaomicron* and other *Bacteroides* species in the HGM. In contrast to the extensive conservation of the anterior catalytic center in GH145 enzymes, the essential catalytic histidine in the posterior active site is present in only 70% of these proteins (20) (Table S2). Indeed, in GH145 members that are not derived from the organisms in the HGM, the retention of this histidine, and thus rhamnosidase activity, is rare. This phylogenetic analysis suggests that the lyase activity is a highly conserved feature of the family and is thus a primitive feature of these enzymes, while the rhamnosidase function reflects a recent selection pressure exerted by the human diet, exemplified by GA-AGP. It would seem unlikely that the lyase activity in all the GH145 enzymes targets exclusively sulfated AGPs; however, other potential substrates for these enzymes remain to be identified.

The presence of two discrete functional active sites in a single catalytic domain is a unique feature of GH145 enzymes. Several CAZymes containing two or more catalytic modules, joined by flexible linker sequences, have been described (35). The inherent mobility between these catalytic modules allows the active sites to access different regions of a common polysaccharide substrate, enabling synergistic interactions between the different activities. This is exemplified by the degradation of acetylated xylans by enzymes displaying endo-xylanase and acetyl esterase activities (36). In GH145 enzymes, the two active sites target different AGPs, and thus, there is no obvious requirement for synergy to operate between the posterior and anterior catalytic centers.

Conclusions. This report shows that Wi-AGP and SW-AGP are privileged nutrients for *B. plebeius* within the HGM and that sulfate decorations of the glycans are responsible for their restricted use as growth substrates. The manipulation of the HGM has the potential to have significant health benefits (37, 38). The fate of exogenous commensal and probiotic strains applied to an established HGM is variable, largely unpredictable, and greatly influenced by the background microbiota (39). Studies have shown that it is possible to establish an exogenous bacterium in the HGM when porphyran, a privileged nutrient for the organism, is supplied to the ecosystem. Furthermore, transfer of the large porphyran locus (21 to 34 genes) to other organisms also conferred a substantial competitive advantage in the presence of the marine polysaccharide (40). Here, we have shown that a second sulfated polysaccharide can also act as a privileged nutrient within the HGM. We propose that the sulfation of marine polysaccharides makes these glycans excellent privileged nutrient candidates in terrestrial ecosystems, where the deployment of sulfated plant polysaccharides as growth substrates is very limited. Although engineering porphyran utilization into health-promoting organisms is an attractive strategy, transferring a 21- to 34-gene locus into these bacteria is a

significant challenge. In contrast, transferring genes encoding a sulfatase, and possibly an appropriate SusC/SusD outer membrane sulfated AGP transporter, into the organism of choice may offer technical advantages that could increase the range of bacteria that can be engineered to utilize sulfated glycans such as Wi-AGP and SW-AGP.

MATERIALS AND METHODS

Purification of Wi-AGP. Wi-AGP was isolated from one liter of red wine (vino d'Itialia [12% alcohol]) by gel filtration chromatography. The wine (3 liters) was concentrated by rotary evaporation and precipitated with ethanol (80% [vol/vol]). The mixture was kept at 4°C for 12 h and the resulting precipitate collected by centrifugation at 4,000 × g for 10 min. The precipitate was dissolved in 200 ml water, reprecipitated with 80% (vol/vol) ethanol, and the process repeated. The final mixture in water was freeze-dried, and 400 mg of the resulting powder dissolved in 50 mM sodium acetate (NaOAC), pH 5. The sample was resolved using 300 ml of Sephadex G-75 resin (Sigma; catalog no. G75120) with 50 mM NaOAC (pH 5.0) as mobile phase at a flow rate of 1 ml/min. Eluted fractions (8 ml each) were collected and analyzed by thin-layer chromatography, acid hydrolysis, and high-performance anion-exchange chromatography (HPAEC). Fractions containing Wi-AGP were pooled, dialyzed (using a VWR Visking dialysis tubing [3,500 molecular weight cutoff]), and freeze-dried.

Cloning, expression, and purification of recombinant proteins. DNAs encoding enzymes lacking their signal peptides were amplified by PCR using appropriate primers. The amplified DNAs were cloned into pET28a with an N-terminal His$_6$ tag using NheI and XhoI restriction sites. To express an active form of the sulfatase BpS1_8, the S76C variant of the enzyme was generated. The *Escherichia coli* sulfatase-maturing enzyme is able to convert cysteine but not serine into the essential formylglycine residue. To express the recombinant genes encoding the AGP-degrading enzymes, *Escherichia coli* strains BL21(DE3) and Tuner, harboring appropriate recombinant plasmids, were cultured to mid-exponential phase in Luria-Bertani broth at 37°C. This was followed by the addition of 1 mM [strain BL21(DE3)] or 0.2 mM (Tuner) isopropyl-β-D-thiogalactopyranoside (IPTG) to induce recombinant gene expression, and the culture was incubated for a further 5 h at 37°C or 16 h at 16°C, respectively. The recombinant proteins were purified to >90% electrophoretic purity by immobilized metal ion affinity chromatography using Talon, a cobalt-based matrix, and eluted with 100 mM imidazole, as described previously (20).

Mutagenesis. Site-directed mutagenesis was conducted using the PCR-based QuikChange site-directed mutagenesis kit (Strategene) according to the manufacturer's instructions, using the appropriate plasmid encoding BtGH145, BpGH145, BcGH145, or BpS1_8 as the template and appropriate primer pairs.

CAZyme and sulfatase assays. Spectrophotometric quantitative assays for α-L-rhamnosidase activity were monitored by the continuous formation of NADH at $A_{340\ nm}$ using an extinction coefficient of 6,230 M^{-1} cm^{-1}, with an appropriately linked enzyme assay system. The assays were adapted from the Megazyme International assay kit (product code K-rhamnose). The standard reaction conditions were supplemented with 1 mM NAD+ and an excess of L-rhamnose dehydrogenase. The dehydrogenase oxidases released rhamnose to L-rhamnose-1,4-lactone with the concomitant reduction of NAD+ to NADH. The concentrations of Wi-AGP and SW-AGP ranged from 0 to 10 mg ml^{-1}. As the assays gave a linear relationship between rate and substrate concentration, only k_{cat}/K_m could be determined and not the individual kinetic parameters.

Spectrophotometric quantitative assays were deployed to measure the sulfatase activity of Bacple_00986 (BpSulf1_8) acting on SW-AGP, Wi-AGP, and 4-nitrophenyl sulfate (PNP-sulfate). For PNP-sulfate, the enzymatic assays were done in a continuous assay, monitoring the release of PNP by the enzyme and quantifying the activity at a wavelength of 400 nm. The product was quantified using a molar extinction coefficient of 10,500 M^{-1} cm^{-1}. When the polysaccharides were used as the substrates for the enzyme, we used the sulfate assay kit from Bioassay Systems (product code DSFT-200). The kit quantifies the formation of insoluble barium sulfate from barium chloride and the sulfate released by the substrate in polyethylene glycol. The turbidity measured at 600 nm is directly proportional to sulfate levels in the sample. This kit employed a stopped assay where different polysaccharide concentrations were incubated with the enzyme, aliquots were taken at different times, and the reaction was stopped by incubation at 100°C for 10 min. The aliquots were incubated with the working reagent prepared as the manufacturer indicated in the kit for 10 min, and absorbance at 600 nm was determined. To calculate the concentration of sulfate released in milligrams per milliliter, we performed a calibration curve with the same kit to ensure that the sulfate groups released fall within the curve range. We varied the polysaccharide concentrations from 0 to 10 mg/ml. As the assays gave a linear relationship between rate and substrate concentration, only k_{cat}/K_m could be determined and not the individual kinetic parameters.

The mode of action of enzymes was determined using HPAEC or thin-layer chromatography (TLC), as appropriate. In brief, aliquots of the enzyme reactions were removed at regular intervals and, after boiling for 10 min to inactivate the enzyme and centrifugation at 13,000 × g, the amount of substrate remaining or product produced was quantified by HPAEC using standard methodology. The reaction substrates and products were bound to a Dionex CarboPac PA100 column and glycans eluted with an initial isocratic flow of 100 mM NaOH and then a 0- to 200-mM sodium acetate gradient in 100 mM NaOH at a flow rate of 1.0 ml min^{-1}, using pulsed amperometric detection or absorbance at 235 nm. In TLC assays of enzyme activity, 5 μl of each sample was spotted onto silica plates and resolved in butanol/acetic acid/water at a concentration of 2:1:1 and carbohydrate products detected by spraying with 0.5% orcinol in 10% sulfuric acid and heating to 100°C for 10 min. All reactions were carried out in 20 mM sodium phosphate buffer, pH 7.0, with 150 mM NaCl at 37°C (defined as standard conditions) and performed in at least technical triplicates.

Growth of *Bacteroides*. *Bacteroides* spp. were routinely cultured under anaerobic conditions at 37°C using an anaerobic cabinet (Whitley A35 workstation; Don Whitley) in culture volumes of 0.2, 2, or 5 ml of TYG (tryptone-yeast extract-glucose medium) or minimal medium (MM) (31) containing 0.5 to 1% of an appropriate carbon source and 1.2 mg ml^{-1} porcine hematin (Sigma-Aldrich) as previously described (10). The growth of the cultures was monitored by optical density at 600 nm (OD$_{600}$) using a Gen5 v2.0 microplate reader (Biotek).

For batch fermentation of the HGM, sterile stirred batch culture fermentation vessels (300 ml working volume) were aseptically filled with 135 ml of sterile basal nutrient medium (2 g/liter peptone water, 2 g/liter yeast extract, 0.1 g/liter NaCl, 0.04 g/liter K$_2$HPO$_4$, 0.04 g/liter KH$_2$PO$_4$, 0.01 g/liter MgSO$_4$·7H$_2$O, 0.01 g/liter CaCl$_2$·6H$_2$O, 2 g/liter NaHCO$_3$, 0.5 g/liter L-cysteine HCl, 0.5 g/liter bile salts, 0.05 g/liter hemin [dissolved in a few drops of 1 M NaOH], 2 ml/liter Tween 80, 0.01 ml/liter vitamin K, and 4 ml/liter resazurin solution [0.025/100 ml]). Once in the fermentation vessels, sterile medium was maintained under anaerobic conditions by sparging the vessels with O$_2$-free N$_2$ overnight (15 ml/min). The temperature was held at 37°C using a circulating water bath and pH values controlled between 6.7 and 6.9 using an automated pH controller (Fermac 260; Electrolab, Tewkesbury, UK), which added acid or alkali as required (0.5 M HCl and 0.5 M NaOH). After the equilibration, all vessels were inoculated with 15 ml fecal slurry. Fecal slurry was prepared using stool from three anonymous healthy donors, which was then diluted in 1× phosphate-buffered saline (PBS) (pH 7.4) with 10% (wt/vol) dilution and mixed in a stomacher for 2 min. Batch culture vessels were set up in triplicate containing no carbon source, 5 g inulin, and 5 g Wi-AGP, respectively. Fecal slurries from stool samples were then added to the vessels. The fermentations occurred for 24 h, after which bacteria were recovered and subjected to rRNA profiling as described below.

16S rRNA profiling of the HGM cultured *in vitro*. Bacterial profiling of the variable region 4 (V4) of the 16S rRNA gene was carried out by NU-OMICS (Northumbria University). Briefly, PCR was performed carried out using 1× AccuPrime Pfx SuperMix, 0.5 μM each primer (515F, GTGCCAGCMGCCGCGGTAA, and 806R, GGACTACHVGGGTWTCTAAT) and 1 μl of template DNA under the following conditions: 95°C for 2 min; 30 cycles 95°C for 20 s, 55°C for 15 s, and 72°C for 5 min with a final extension at 72°C for 10 min. One positive- and one negative-control sample were included in each 96-well plate and carried through to sequencing. PCR products were normalized using SequalPrep normalization kit (Invitrogen). The DNA was then denatured using 0.2 M NaOH for 5 min and diluted to a final concentration of 5 pM, supplemented with 15% PhiX, and loaded onto a MiSeq V2 500-cycle cartridge (Illumina). The sequences obtained were run through the GALAXY server (Mothur program; https://training.galaxyproject.org/ training-material/topics/metagenomics/tutorials/mothur-miseq-sop/tutorial.html) to compare their similarity to the V4 region of rRNA of 10,000 curated sequenced bacteria, derived from the human Gut Microbiome and Earth Microbiome projects.

SUPPLEMENTAL MATERIAL

Supplemental material is available online only.

TABLE S1, DOCX file, 0.01 MB.

TABLE S2, DOCX file, 0.03 MB.

ACKNOWLEDGMENTS

REFERENCES

1. Clemente JC, Ursell LK, Parfrey LW, Knight R. 2012. The impact of the gut microbiota on human health: an integrative view. Cell 148:1258–1270. https://doi.org/10.1016/j.cell.2012.01.035.

2. Thursby E, Juge N. 2017. Introduction to the human gut microbiota. Biochem J 474:1823–1836. https://doi.org/10.1042/BCJ20160510.

3. El Kaoutari A, Armougom F, Gordon JI, Raoult D, Henrissat B. 2013. The abundance and variety of carbohydrate-active enzymes in the human gut microbiota. Nat Rev Microbiol 11:497–504. https://doi.org/10.1038/nrmicro3050.

4. Porter NT, Martens EC. 2017. The critical roles of polysaccharides in gut microbial ecology and physiology. Annu Rev Microbiol 71:349–369. https://doi.org/10.1146/annurev-micro-102215-095316.

5. Lombard V, Golaconda Ramulu H, Drula E, Coutinho PM, Henrissat B. 2014. The carbohydrate-active enzymes database (CAZy) in 2013. Nucleic Acids Res 42:D490–495. https://doi.org/10.1093/nar/gkt1178.

6. Ndeh D, Gilbert HJ. 2018. Biochemistry of complex glycan depolymerisation by the human gut microbiota. FEMS Microbiol Rev 42:146–164. https://doi.org/10.1093/femsre/fuy002.

7. Cuskin F, Lowe EC, Temple MJ, Zhu Y, Cameron EA, Pudlo NA, Porter NT, Urs K, Thompson AJ, Cartmell A, Rogowski A, Hamilton BS, Chen R, Tolbert TJ, Piens K, Bracke D, Vervecken W, Hakki Z, Speciale G, Munōz-Munōz JL, Day A, Peña MJ, McLean R, Suits MD, Boraston AB, Atherly T, Ziemer CJ, Williams SJ, Davies GJ, Abbott DW, Martens EC, Gilbert HJ. 2015. Corrigendum: human gut Bacteroidetes can utilize yeast mannan through a selfish mechanism. Nature 520:388. https://doi.org/10.1038/nature14334.

8. Larsbrink J, Rogers TE, Hemsworth GR, McKee LS, Tauzin AS, Spadiut O, Klinter S, Pudlo NA, Urs K, Koropatkin NM, Creagh AL, Haynes CA, Kelly AG, Cederholm SN, Davies GJ, Martens EC, Brumer H. 2014. A discrete genetic locus confers xyloglucan metabolism in select human gut Bacteroidetes. Nature 506:498–502. https://doi.org/10.1038/nature12907.

9. Ndeh D, Rogowski A, Cartmell A, Luis AS, Basle A, Gray J, Venditto I, Briggs J, Zhang X, Labourel A, Terrapon N, Buffetto F, Nepogodiev S, Xiao Y, Field RA, Zhu Y, O'Neil MA, Urbanowicz BR, York WS, Davies GJ, Abbott DW, Ralet MC, Martens EC, Henrissat B, Gilbert HJ. 2017. Complex pectin metabolism by gut bacteria reveals novel catalytic functions. Nature 544:65–70. https://doi.org/10.1038/nature21725.

10. Rogowski A, Briggs JA, Mortimer JC, Tryfona T, Terrapon N, Lowe EC, Basle A, Morland C, Day AM, Zheng H, Rogers TE, Thompson P, Hawkins AR, Yadav MP, Henrissat B, Martens EC, Dupree P, Gilbert HJ, Bolam DN. 2015. Glycan complexity dictates microbial resource allocation in the large intestine. Nat Commun 6:7481. https://doi.org/10.1038/ncomms8481.

11. Rakoff-Nahoum S, Coyne MJ, Comstock LE. 2014. An ecological network of polysaccharide utilization among human intestinal symbionts. Curr Biol 24:40–49. https://doi.org/10.1016/j.cub.2013.10.077.

12. Rakoff-Nahoum S, Foster KR, Comstock LE. 2016. The evolution of cooperation within the gut microbiota. Nature 533:255–259. https://doi.org/10.1038/nature17626.

13. Grondin JM, Tamura K, Dejean G, Abbott DW, Brumer H. 2017. Polysaccharide utilization loci: fueling microbial communities. J Bacteriol 199:e00860-16. https://doi.org/10.1128/JB.00860-16.

14. Koropatkin NM, Cameron EA, Martens EC. 2012. How glycan metabolism shapes the human gut microbiota. Nat Rev Microbiol 10:323–335. https://doi.org/10.1038/nrmicro2746.

15. Lapebie P, Lombard V, Drula E, Terrapon N, Henrissat B. 2019. Bacteroidetes use thousands of enzyme combinations to break down glycans. Nat Commun 10:2043. https://doi.org/10.1038/s41467-019-10068-5.

16. Bolam DN, Koropatkin NM. 2012. Glycan recognition by the Bacteroidetes Sus-like systems. Curr Opin Struct Biol 22:563–569. https://doi.org/10.1016/j.sbi.2012.06.006.

17. Sonnenburg ED, Sonnenburg JL, Manchester JK, Hansen EE, Chiang HC, Gordon JI. 2006. A hybrid two-component system protein of a prominent human gut symbiont couples glycan sensing in vivo to carbohydrate metabolism. Proc Natl Acad Sci U S A 103:8834–8839. https://doi.org/10.1073/pnas.0603249103.

18. Guadalupe Z, Ayestaran B. 2007. Polysaccharide profile and content during the vinification and aging of Tempranillo red wines. J Agric Food Chem 55:10720–10728. https://doi.org/10.1021/jf0716782.

19. Fincher GB, Stone BA, Clarke AE. 1983. Arabinogalactan proteins-structure, biosynthesis, and function. Annu Rev Plant Physiol 34:47–70. https://doi.org/10.1146/annurev.pp.34.060183.000403.

20. Cartmell A, Munoz-Munoz J, Briggs JA, Ndeh DA, Lowe EC, Basle A, Terrapon N, Stott K, Heunis T, Gray J, Yu L, Dupree P, Fernandes PZ, Shah S, Williams SJ, Labourel A, Trost M, Henrissat B, Gilbert HJ. 2018. A surface endogalactanase in Bacteroides thetaiotaomicron confers keystone status for arabinogalactan degradation. Nat Microbiol 3:1314–1326. https://doi.org/10.1038/s41564-018-0258-8.

21. Caporaso JG, Lauber CL, Walters WA, Berg-Lyons D, Lozupone CA, Turnbaugh PJ, Fierer N, Knight R. 2011. Global patterns of 16S rRNA diversity at a depth of millions of sequences per sample. Proc Natl Acad Sci U S A 108 (Suppl 1):4516–4522. https://doi.org/10.1073/pnas.1000080107.

22. Rees DA, Conway E. 1962. The structure and biosynthesis of porphyran: a comparison of some samples. Biochem J 84:411–416. https://doi.org/10.1042/bj0840411.

23. Kloareg B, Quatrano RS. 1988. Structure of the cell-walls of marine-algae and ecophysiological functions of the matrix polysaccharides. Oceanogr Mar Biol 26:259–315.

24. Estevez JM, Fernandez PV, Kasulin L, Dupree P, Ciancia M. 2009. Chemical and in situ characterization of macromolecular components of the cell walls from the green seaweed Codium fragile. Glycobiology 19:212–228. https://doi.org/10.1093/glycob/cwn101.

25. Terrapon N, Lombard V, Drula E, Lapebie P, Al-Masaudi S, Gilbert HJ, Henrissat B. 2018. PULDB: the expanded database of polysaccharide utilization loci. Nucleic Acids Res 46:D677–D683. https://doi.org/10.1093/nar/gkx1022.

26. Martens EC, Lowe EC, Chiang H, Pudlo NA, Wu M, McNulty NP, Abbott DW, Henrissat B, Gilbert HJ, Bolam DN, Gordon JI. 2011. Recognition and degradation of plant cell wall polysaccharides by two human gut symbionts. PLoS Biol 9:e1001221. https://doi.org/10.1371/journal.pbio.1001221.

27. Hehemann JH, Correc G, Barbeyron T, Helbert W, Czjzek M, Michel G. 2010. Transfer of carbohydrate-active enzymes from marine bacteria to Japanese gut microbiota. Nature 464:908–912. https://doi.org/10.1038/nature08937.

28. Larsen B, Haug A, Painter T. 1970. Sulphated polysaccharides in brown algae. III. Native state of fucoidan in Ascophyllum-nodosum and Fucus vesiculosus. Acta Chem Scand 24:3339–3352. & https://doi.org/10.3891/acta.chem.scand.24-3339.

29. Nisizawa K, Noda H, Kikuchi R, Watanabe T. 1987. The main seaweed foods in Japan. Hydrobiologia 151–152:5–29. https://doi.org/10.1007/BF00046102.

30. Munoz-Munoz J, Cartmell A, Terrapon N, Henrissat B, Gilbert HJ. 2017. Unusual active site location and catalytic apparatus in a glycoside hydrolase family. Proc Natl Acad Sci U S A 114:4936–4941. https://doi.org/10.1073/pnas.1701130114.

31. Czjzek M, Michel G. 2017. Innovating glycoside hydrolase activity on a same structural scaffold. Proc Natl Acad Sci U S A 114:4857–4859. https://doi.org/10.1073/pnas.1704802114.

32. Ulaganathan T, Boniecki MT, Foran E, Buravenkov V, Mizrachi N, Banin E, Helbert W, Cygler M. 2017. New ulvan-degrading polysaccharide lyase family: structure and catalytic mechanism suggests convergent evolution of active site architecture. ACS Chem Biol 12:1269–1280. https://doi.org/10.1021/acschembio.7b00126.

33. Pellerin P, Vidal S, Williams P, Brillouet JM. 1995. Characterization of five type II arabinogalactan-protein fractions from red wine of increasing uronic acid content. Carbohydr Res 277:135–143. https://doi.org/10.1016/0008-6215(95)00206-9.

34. Itoh T, Ochiai A, Mikami B, Hashimoto W, Murata K. 2006. A novel glycoside hydrolase family 105: the structure of family 105 unsaturated rhamnogalacturonyl hydrolase complexed with a disaccharide in comparison with family 88 enzyme complexed with the disaccharide. J Mol Biol 360:573–585. https://doi.org/10.1016/j.jmb.2006.04.047.

35. Montanier C, Money VA, Pires VM, Flint JE, Pinheiro BA, Goyal A, Prates JA, Izumi A, Stalbrand H, Morland C, Cartmell A, Kolenova K, Topakas E, Dodson EJ, Bolam DN, Davies GJ, Fontes CM, Gilbert HJ. 2009. The active site of a carbohydrate esterase displays divergent catalytic and noncatalytic binding functions. PLoS Biol 7:e71. https://doi.org/10.1371/journal.pbio.1000071.

36. Krska D, Larsbrink J. 2020. Investigation of a thermostable multi-domain xylanase-glucuronoyl esterase enzyme from Caldicellulosiruptor kristjanssonii incorporating multiple carbohydrate-binding modules. Biotechnol Biofuels 13:68. https://doi.org/10.1186/s13068-020-01709-9.

37. Arpaia N, Campbell C, Fan X, Dikiy S, van der Veeken J, deRoos P, Liu H, Cross JR, Pfeffer K, Coffer PJ, Rudensky AY. 2013. Metabolites produced by commensal bacteria promote peripheral regulatory T-cell generation. Nature 504:451–455. https://doi.org/10.1038/nature12726.

38. Round JL, Mazmanian SK. 2009. The gut microbiota shapes intestinal immune responses during health and disease. Nat Rev Immunol 9:313–323. https://doi.org/10.1038/nri2515.

39. Maldonado-Gomez MX, Martinez I, Bottacini F, O'Callaghan A, Ventura M, van Sinderen D, Hillmann B, Vangay P, Knights D, Hutkins RW, Walter J. 2016. Stable engraftment of Bifidobacterium longum AH1206 in the human gut depends on individualized features of the resident microbiome. Cell Host Microbe 20:515–526. https://doi.org/10.1016/j.chom.2016.09.001.

40. Shepherd ES, DeLoache WC, Pruss KM, Whitaker WR, Sonnenburg JL. 2018. An exclusive metabolic niche enables strain engraftment in the gut microbiota. Nature 557:434–438. https://doi.org/10.1038/s41586-018-0092-4.

Review

Cross-feeding interactions between human gut commensals belonging to the *Bacteroides* and *Bifidobacterium* genera when grown on dietary glycans

Pedro Fernandez-Julia[1], Daniel M. Commane[1], Douwe van Sinderen[2], Jose Munoz-Munoz[1]

[1]Microbial Enzymology Group, Department of Applied Sciences, Ellison Building A, University of Northumbria, Newcastle Upon Tyne NE1 8ST, UK.
[2]APC Microbiome Ireland and School of Microbiology, University College Cork, Western Road, Cork T12 YT20, Ireland.

Correspondence to: Prof. Douwe van Sinderen, APC Microbiome Ireland and School of Microbiology, University College Cork, Western Road, Cork T12 YT20, Ireland. E-mail: d.vansinderen@ucc.ie; Dr. Jose Munoz-Munoz, Microbial Enzymology Group, Department of Applied Sciences, Ellison Building A, University of Northumbria, Ellison Building A, Newcastle Upon Tyne, NE1 8ST, UK. E-mail: Jose.Munoz@northumbria.ac.uk

Abstract

Elements of the human gut microbiota metabolise many host- and diet-derived, non-digestible carbohydrates (NDCs). Intestinal fermentation of NDCs salvages energy and resources for the host and generates beneficial metabolites, such as short chain fatty acids, which contribute to host health. The development of functional NDCs that support the growth and/or metabolic activity of specific beneficial gut bacteria, is desirable, but dependent on an in-depth understanding of the pathways of carbohydrate fermentation. The purpose of this review is to provide an appraisal of what is known about the roles of, and interactions between, *Bacteroides* and *Bifidobacterium* as key members involved in NDC utilisation. *Bacteroides* is considered an important primary degrader of complex NDCs, thereby generating oligosaccharides, which in turn can be fermented by secondary degraders. In this review, we will therefore focus on *Bacteroides* as an NDC-degrading specialist and *Bifidobacterium* as an important and purported probiotic representative of secondary degraders. We will describe cross-feeding interactions between members of these two genera. We note that there are limited studies exploring the interactions between *Bacteroides* and *Bifidobacterium*, specifically concerning β-glucan and arabinoxylan metabolism. This review

therefore summarises the roles of these organisms in the breakdown of dietary fibre and the molecular mechanisms and interactions involved. Finally, it also highlights the need for further research into the phenomenon of cross-feeding between these organisms for an improved understanding of these cross-feeding mechanisms to guide the rational development of prebiotics to support host health or to prevent or combat disease associated with microbial dysbiosis.

Keywords: Cross-feeding, plant fibre, *Bacteroides*, *Bifidobacterium*, gut microbiota, prebiotic

INTRODUCTION

The diverse community of microorganisms that inhabit the human gastrointestinal tract make up the human gut microbiota (HGM)[1]. The HGM consists of protozoa, archaea, eukaryotes, viruses and bacteria, and these organisms have evolved to exist symbiotically within the host, exerting various beneficial roles, including but not limited to, energy retrieval, protection from invading pathogens, maintaining gut homeostasis, and modulating the immune system. The HGM is made up of three main phyla: Firmicutes, Bacteroidetes and Actinobacteria [Figure 1][2].

Changes in the composition of the gut microbiota can be influenced by various factors, such as type of diet, stress or environment, and may result in a so-called state of dysbiosis, an imbalance in the levels of members of the HGM that has been linked to various diseases. Depletion or overabundance of certain bacterial species throughout (part of) an individual's lifetime may contribute to gut disorders such as inflammatory bowel disease, which includes Crohn's disease and ulcerative colitis[3]. In this sense, it has been shown that a gut microbiota imbalance during infancy can provoke the development of diseases (e.g., auto-immune diseases) at a later life stage[4]. Moreover, metabolic products of the gut microbiota may promote diseases such as colorectal cancer and obesity and can affect signalling pathways within the host.

The complex structural variation of dietary polysaccharides, such as arabinoxylan, arabinogalactan or pectin, is determined by the monosaccharide composition, type of glycosidic linkage, side chains and substitutions[5]. Due to the high degree of structural diversity found among non-digestible carbohydrates (NDCs) that are part of the human diet, efficient metabolism of dietary and host-derived polysaccharides requires an array of highly specific enzymes, that all belong to the so-called Carbohydrate active enzymes (CAZymes)[6]. Host-derived polysaccharides such as mucins or glycosaminoglycans, and diet-derived polysaccharides, which include glucans, xylans, fructans, mannans and galactans, are mostly resistant to degradation by human enzymes and therefore they form fermentable substrates for members of the gut microbiota, especially in the colon[7]. Fermentation of dietary fibre by the gut microbiota typically produces short-chain fatty acids (SCFAs), such as acetate, propionate and butyrate, which are taken up by the host and used primarily as an energy source, thereby benefitting host health[8,9]. In addition, *Bifidobacterium* species produce lactate, as a major metabolic end-product, while some species generate 1,2-propanediol from fucose metabolism, and both of these metabolites can in turn be converted into SCFAs by other gut microbiota members. These metabolites affect various biological processes; in the intestinal lumen SCFAs lower the intestinal pH, which may inhibit the growth of pathogens, while this is also believed to influence the composition of the wider microbial community[10]. In intestinal epithelial cells, butyrate regulates cell proliferation, differentiation and gene expression in a manner associated with antineoplastic transformation. Systemically, propionate and acetate activate the free fatty acid receptors GPR41 and GPR43, which are expressed by enteroendocrine cells lining the gut and are present in other tissues, including adipocytes; these receptors may help to activate anti-inflammatory signalling pathways, control metabolism, and influence appetite and mood[11]. The ability of the resident bacteria in the gut to efficiently metabolize these otherwise indigestible glycans means that they share a symbiotic relationship with the host

PHYLUM	CLASS	ORDER	FAMILY	SPECIES
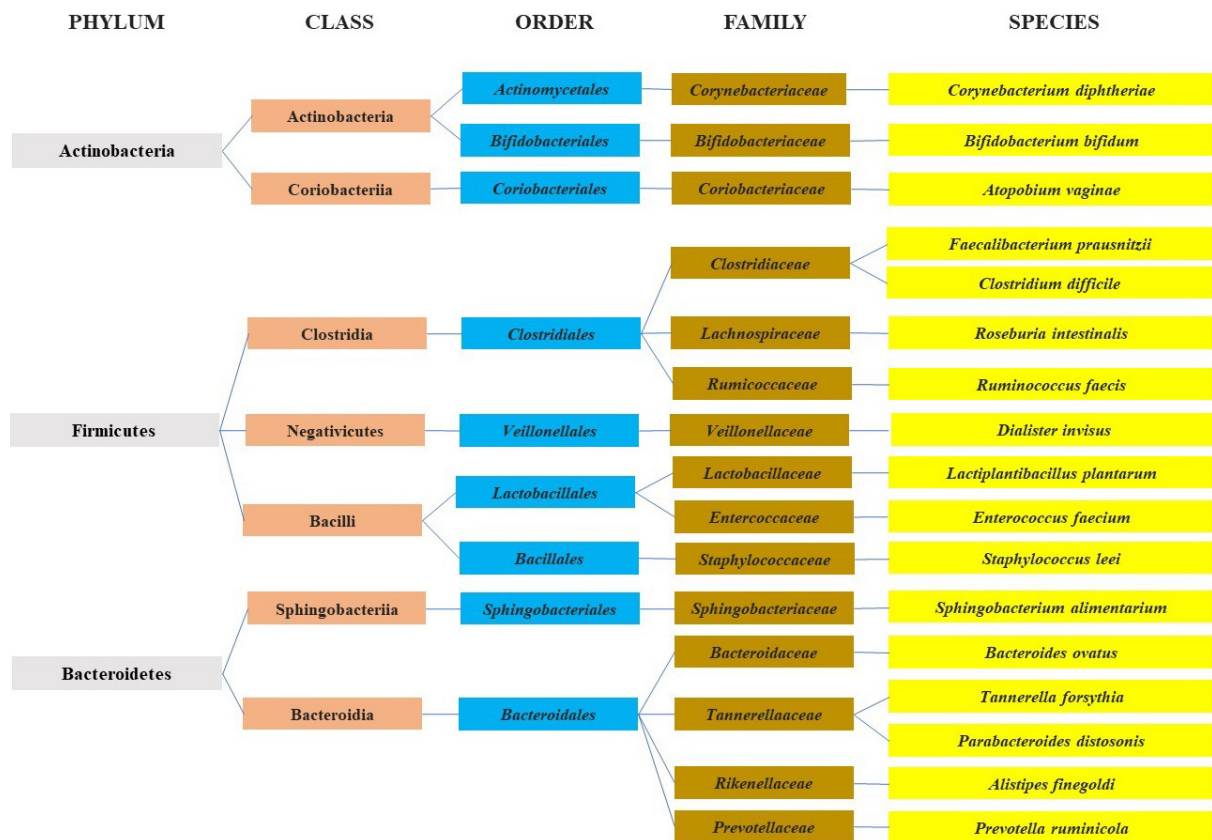
Figure 1. A diagram representing the most abundant microbial components of the human microbiota in the colonic section of the gut.

and with one another as these bacteria must effectively compete for carbohydrate nutrition and so have co-evolved efficient glycan-harvesting strategies.

The Gram-negative Bacteroidetes is one of the main phyla that make up the HGM. A large proportion of the genome of these organisms is dedicated to the metabolism of complex glycans, making them primary glycan degraders in the HGM[12]. Although several *Bacteroides* species are known to degrade a variety of distinct polysaccharides, there is not a single known species capable of metabolising all main dietary, complex glycans, such as starch, pectin, xylan or beta-glucan. The degradation of such complex carbohydrates is performed by CAZymes, whose encoding genes are arranged into clusters known as polysaccharide utilisation loci (PULs). These PULs encode, in addition to the above mentioned CAZymes [represented by glycoside hydrolases (GHs), polysaccharide lyases and carbohydrate esterases], various other proteins involved in glycan degradation, including cell surface glycan-binding proteins, TonB-dependent transporters, and sensors, which regulate PUL transcription[13]. For example, the first described PUL was the starch utilisation system (Sus-system) of *Bacteroides thetaiotaomicron* VPI-5182, which has been extensively studied. The cell surface-associated proteins SusE and SusF bind the polysaccharide substrate, thereby facilitating the initial starch degradation by SusG - an amylase enzyme, which is also located at the bacterial cell surface, and which hydrolyses the large polymeric substrate into smaller oligosaccharides. These oligosaccharides are then transported into the periplasmic compartment by the SusC/SusD complex (a TonB-dependent transporter), where they are further degraded into monosaccharides by SusA and SusB glycosidases [Figure 2].
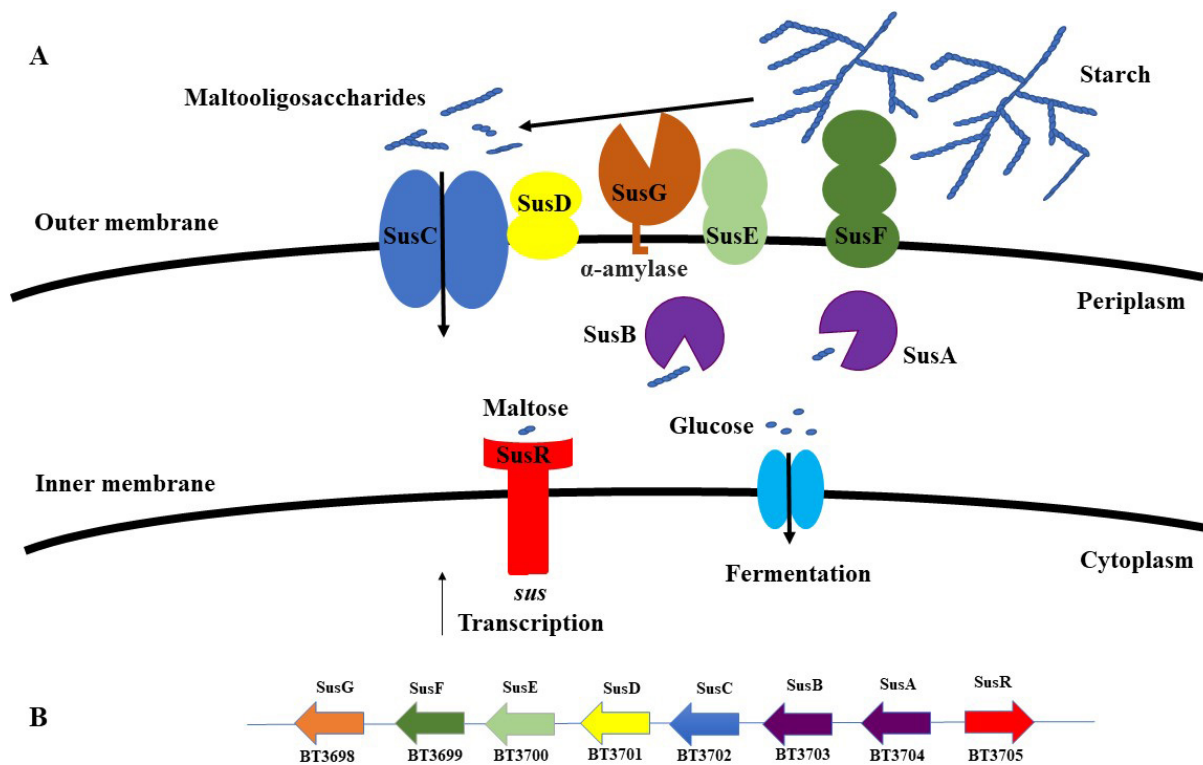
Figure 2. (A) A schematic overview of the PUL required for starch utilisation (Sus) in *B. thetaiotaomicron* VPI-5182. The substrate is bound by lipoproteins at the cell surface, where it is initially degraded to oligosaccharides and then transported to the periplasm, where it is further hydrolysed to monosaccharides which can then be transported into the cytoplasm of the cell. (B) Genomic content of *B. thetaiotaomicron* VPI-5182 PUL in its action on starch. PUL: Polysaccharide utilisation loci.

Firmicutes and Actinobacteria are the other two main phyla that are resident in the human gut. These phyla represent Gram-positive bacteria that possess different mechanisms for glycan degradation[14]. Gram-positive PULs (gpPULs) have a similar gene content to the PUL systems present in Bacteroidetes. However, gpPULs are devoid of the SusC/D-encoding gene pair that characterises an archetypical PUL[15]. The gpPULs encode proteins such as transporters (commonly ABC-type transporters), regulatory proteins (typically LacI-type regulators) and glycan-degrading enzymes (mostly GHs), and large glycans (i.e., those that have a DP of > 6-7 monosaccharidic moieties) must be degraded by extracellular (or cell envelope-bound) glycoside hydrolases. The resulting oligosaccharides are then typically bound by solute binding proteins associated with an ABC uptake system which internalizes them to be further degraded into monosaccharides.

In the HGM, the phylum Actinobacteria is largely represented by the *Bifidobacterium* genus. Members of this genus mainly produce lactate, acetate and formate (and sometimes 1,2-propanediol) as products of sugar fermentation in the gut[16]. Analysis of the genomes of *Bifidobacterium longum* subspecies *infantis* and *Bifidobacterium bifidum* show that they encode glycosyl hydrolases that are utilised in the degradation of human milk oligosaccharides[17]. *Bifidobacterium* species, however, typically degrade glycans with a lower degree of polymerisation than those utilized by Bacteroidetes members.

As mentioned above, *Bifidobacterium* species are generally able to metabolize a range of oligomeric and rather simple carbohydrates, commonly being unable to metabolise more complex polysaccharides that require extracellular GHs. Studies have reported evidence of cross-feeding behaviour between members of

the *Bifidobacterium* genus with other organisms, thereby allowing the complete metabolism of certain complex glycans[18]. An example of this is the interspecies cross-feeding relationship between *Bifidobacterium bifidum* and *Bifidobacterium breve* when co-cultured on sialyllactose[19]. This study showed how *Bi. breve* was able to cross feed on sialic acid, the product of 3'-sialyllactose degradation by *Bi. bifidum*. *Bifidobacterium* species have also been shown to produce metabolites, such as 1,2-propanediol, that can be used by other HGM members, e.g., *Lactobacillus spp.* or *Eubacterium hallii*, for cross-feeding purposes[20,21].

This review will focus on the molecular mechanisms underpinning cross-feeding interactions between members of *Bacteroides* and *Bifidobacterium* pertinent to the metabolism of dietary glycans, such as arabinoxylans. We selected these two genera because they are extensively studied as primary and secondary degraders of these glycans. Members of the genus *Bacteroides* have been shown to be glycan generalists that metabolize complex polysaccharides, generating extracellular oligosaccharides, which may be shared with other microbial members in the gut, such as particular *Bifidobacterium* species. The latter bacteria have been shown to generally act as specialists in the metabolism of oligosaccharides rather than complex intact polysaccharides. In addition, as we stated above, bifidobacteria are considered to represent beneficial microbes supporting human health. Arabinoxylans are present in commonly consumed cereals, like wheat or corn, and the cross-feeding behaviour between these two groups of bacteria demonstrates how they have co-evolved to utilise a varied range of diet and host-derived carbohydrate sources. We will explore both intra- and inter-genus interactions among members of these two genera. Although other metabolites have been shown to be involved in the cooperation or inhibition of different members of gut microbiota, such as 1,2-propanediol or methane, this review will focus on carbohydrates and their metabolic end products.

MICROBIAL INTERACTIONS FOR THE UTILISATION OF POLYSACCHARIDES

Microbial communities have evolved a balanced and dynamic network of metabolic interactions, which enable them to adapt and thrive within the human gastrointestinal tract (GIT). The competition for nutrients between members of the HGM has resulted in the evolution of ecological feeding strategies that increase the efficiency of glycan utilisation[22]. Although there are various distinct definitions describing such interactions in literature, Smith *et al.*[22] have defined bacterial metabolic cross-feeding as "an interaction between bacterial strains in which molecules resulting from the metabolism of one strain are further metabolised by another strain". The term "microbial syntrophy" is a closely related term to cross-feeding, which describes the obligately mutualistic metabolism of microorganisms whereby processes are carried out through metabolic interactions between organisms that are mutually dependent upon one another[23]. These syntrophic interactions can result in the metabolism of complex molecules, which would otherwise be unable to be degraded by the action of just one organism.

Bacteroides-Bacteroides interactions

The ability of various *Bacteroides* species to utilise polysaccharides has been well documented[24]. Initial *Bacteroides* processing of complex NDCs typically results in the extracellular release of polysaccharide breakdown products (PBPs) which then become available to other organisms that are unable to directly metabolise the complex NDC. Rakoff-Nahoum *et al.*[25] proposed this notion in 2014 and found that various *Bacteroides* species are able to degrade different plant-derived polysaccharides to varying degrees, thus producing varying amounts of PBPs. Interestingly, they observed that *B. ovatus* ATCC 8483 and *B. vulgatus* ATCC 8482 released only oligosaccharide PBPs from xylan breakdown, which contradicts the findings of Salyers *et al.*[26] in 1981, who previously described the production of xylose on the breakdown of xylan by these organisms. They then performed growth experiments showing that these PBPs were not universally utilised by the non-polysaccharide-utilising organisms meaning that the use is dependent upon the producer strain as well as the PBPs produced. The ability of the non-utilising strains to grow on these PBPs

suggests that they possess PULs that encode CAZymes required to metabolise the breakdown products. The observation of amylopectin breakdown in extracellular zones suggests that, as a consequence of releasing PBPs by the utilising strains, GH and PL CAZymes are also secreted. Communication between Gram-negative bacteria via outer membrane vesicles (OMVs) allows for the secretion of enzymes to extracellular regions where polysaccharide degradation can take place. This was demonstrated in[26] using western immunoblot analysis, which revealed that GH and PL enzymes were present in OMVs from *B. ovatus* ATCC 8483 and that their release supported the growth of *B. vulgatus* ATCC 8482 on inulin. This evidence is supported by a further study by Rakoff-Nahoum *et al.*[27] in 2016, which found that there is a co-operation between *B. ovatus* ATCC 8483, as primary degrader, in the breakdown of inulin releasing two GH enzymes (BACOVA_04502 and BACOVA_04503) that are not necessary for its metabolism. It is thought that *B. ovatus* ATCC 8483 expresses these enzymes for the purpose of feeding other organisms in its microbial community and that this process was beneficial for *B. vulgatus* ATCC 8482, which cannot digest inulin. In co-culture, *B. vulgatus* ATCC 8482 was shown to grow with increased fitness and in return, increased the fitness of *B. ovatus* ATCC 8483 possibly due to the production of molecules, PBP or other metabolites, that support the growth of *B. ovatus* ATCC 8483 or by the detoxification of substances that inhibit its growth. These studies highlight the interactions between members of the *Bacteroides* genus that allow the growth of organisms that do not possess the necessary degradative enzymes for the direct utilisation of certain carbohydrates. These interactions may be key in the establishment of a metabolically dynamic functional community of microorganisms in the human GIT.

Bifidobacterium-Bifidobacterium interactions

Bifidobacterium species have also been known to interact with one another to cooperatively break down carbohydrates[28]. The differing abilities of strains to utilise glycans have been thought to result in the evolution of cross-feeding activities between bifidobacterial strains. Studies have shown that *Bifidobacterium* species are able to secrete GH enzymes[29]. It is predicted that 10.9% of the GH enzymes encoded by *Bifidobacterium* are extracellular, of which 24% are predicted to be of the GH43 family, which act as β-xylosidases and α-L-arabinofuranosidases. Extracellular GH enzymes were identified in 43 bifidobacterial species, with the most prevalent being *Bifidobacterium biavatii* which was identified to secrete 17 GHs, while *Bifidobacterium scardovii* and *Bi. bifidum* each secreting 11 GHs[29]. This provides a strong indication for the existence of glycan sharing abilities among bifidobacterial strains. For example, co-cultivation of *Bi. bifidum* PRL2010 with *Bi. breve* 12L, *Bifidobacterium adolescentis* 22L and *Bifidobacterium thermophilum* JCM1207 supports the growth of *Bi. bifidum* PRL2010[28]. Furthermore, metabolic activity of *Bi. bifidum* PRL2010 was enhanced when co-cultivated with these other bifidobacterial strains, and transcription of genes involved in carbohydrate metabolism was enhanced. When grown in monoculture, *Bi. bifidum* PRL2010 was unable to utilise starch or xylan; however, the growth of PRL2010 was observed when this strain was cultivated together with *Bi. breve* 12L or *Bi. adolescentis* 22L. Conversely, a decrease in the growth of *Bi. breve* 12L and *Bi. thermophilum* JCM1207 was noted, suggesting that the utilisation of starch or xylan by *Bi. bifidum* PRL2010, respectively, did not benefit these strains and in fact imposed competitive pressure on these strains. The reduction in lactate and acetate production by *Bi. breve* 12L when grown in co-culture as opposed to monoculture supports the idea that the growth of this strain is hindered by the presence of another *Bifidobacterium* species. Transcriptomic analysis showed that the genes encoding an ABC-transporter and an MFS transporter in *Bi. bifidum* PRL2010 was upregulated when grown in co-culture. It was suggested that this upregulation was due to the production of simple carbohydrates by *Bi. breve* 12L and *Bi. adolescentis* 22L, which act as PBPs that can be utilised by *Bi. bifidum* PRL2010. Interestingly, upregulation of 21 genes of *Bi. breve* 12L was observed when co-cultures with *Bi. bifidum* PRL2010 on starch, and 42 genes when grown on xylan. This upregulation provides evidence for a mutualistic relationship between these two strains[28].

In addition to cross feeding on plant-derived glycans, certain members of the *Bifidobacterium* genus are involved in the metabolism of host-derived glycans and human milk oligosaccharides (HMOs)[19,30] (Egan *et al.*[30], 2014). *Bi. breve* UCC2003 is a known utiliser of sialic acid, which is a monosaccharide present in mucin and certain HMOs, and which is released by *Bi. Bifidum* PRL2010 when grown on such carbohydrate substrates due to the particular extracellular GH enzymes[30,31]. The production of sialic acid from the degradation of the HMO 3' sialyllactose by *Bi. bifidum* PRL2010 was shown to support the growth of *Bi. breve* UCC2003[19].

Bacteroides-Bifidobacterium interactions

Research has shown that *Bacteroides* and *Bifidobacterium* have a cross-feeding relationship in the utilisation of certain dietary and host-derived carbohydrates[18]. The sharing of partially degraded oligosaccharides, intermediary molecules, and genes by lateral gene transfer, contributes to the metabolic flexibility of the HGM. In 2010, Hehemann *et al.*[32], proposed that *Bacteroides plebeius*, a gut bacterium mainly present in the Japanese population, acquired genes from the marine bacterium *Zobellia galactanivorans* needed for the degradation of an algal polysaccharide, porphyran. This gene transfer was explained because seaweed is a common component of the Japanese diet, and bacteria associated with this nutrient may have been the route by which the novel CAZymes were acquired by *Bacteroides plebeius*. *Bacteroides* species often act as primary degraders of complex carbohydrates in the gut, releasing oligosaccharides that then become available for secondary degrader organisms[33]. Such cross-feeding activities are believed to allow less dominant organisms such as *Bifidobacterium* to utilise glycans as a source of nutrition without becoming completely out-competed by bacterial strains that are present in the gut in much higher numbers.

An investigation into the interactions between members of the *Bacteroides* and *Bifidobacterium* genera in the utilisation of different carbon sources was carried out by Rios-Covian *et al.*[34]. They cultured different combinations of two strains of *Bacteroides* and two strains of *Bifidobacterium* using exopolysaccharide, inulin or glucose as the sole carbon source. They found that *Bi. longum* NB677 and *Bi. breve* IPLA2004 are able to utilise glucose as a carbon source; however, neither grew on more complex polysaccharides. Conversely, *B. thetaiotaomicron* DSM 2079 and *B. fragilis* DSM 2151 were able to utilise all tested carbon sources. The authors found that the growth of *B. thetaiotaomicron* DSM 2079 on glucose was inhibited by the presence of *Bi. breve* IPLA2004, suggesting that the interaction between these organisms, when grown on this simple sugar, is not mutualistic. *B. fragilis* DSM 2151, on the other hand, was shown to increase the fitness of *Bi. longum* NB677. These results emphasized that the behaviour of co-cultures of different species is not universal and very much depends on the specific bacterial strain/species combination and particular carbon source.

Elsewhere Rogowski *et al.*[35], 2015 showed that bifidobacterial growth on xylooligosaccharides (XOS) may be supported by *Bacteroides* species. Notably, *Bi. adolescentis* ATCC 15703 was unable to utilise xylans, although it can degrade simple XOS such as linear arabino-xylooligosaccharides. These authors showed that xylans can be divided into complex xylan, such as corn bran (CX), which contains several different linkages and distinct monosaccharides, or simple xylan, such as wheat arabinoxylan (WAX), which consists of a smaller number of different monosaccharides and linkages[35]. WAX was degraded by *B. ovatus* ATCC 8483 using two PULs [Figure 3A and B], and some of the resulting breakdown products were then further metabolised by *Bi. adolescentis* ATCC 15703. However, this glycan sharing was not observed with CX. The authors of this study suggested that *Bi. adolescentis* ATCC 15703 lacked the machinery to degrade the PBPs released by *B. ovatus* ATCC 8483 from CX due to the complexity of these oligosaccharides. Specifically, *B. ovatus* ATCC 8483 was shown to encode a GH98, which is located at the bacterial cell surface to start degradation of the CX backbone. The authors hypothesized that if the efficient machinery is introduced into *Bi. adolescentis* ATCC 15703, this bacterium will be able to cross-feed with *B. ovatus* ATCC 8483, even with
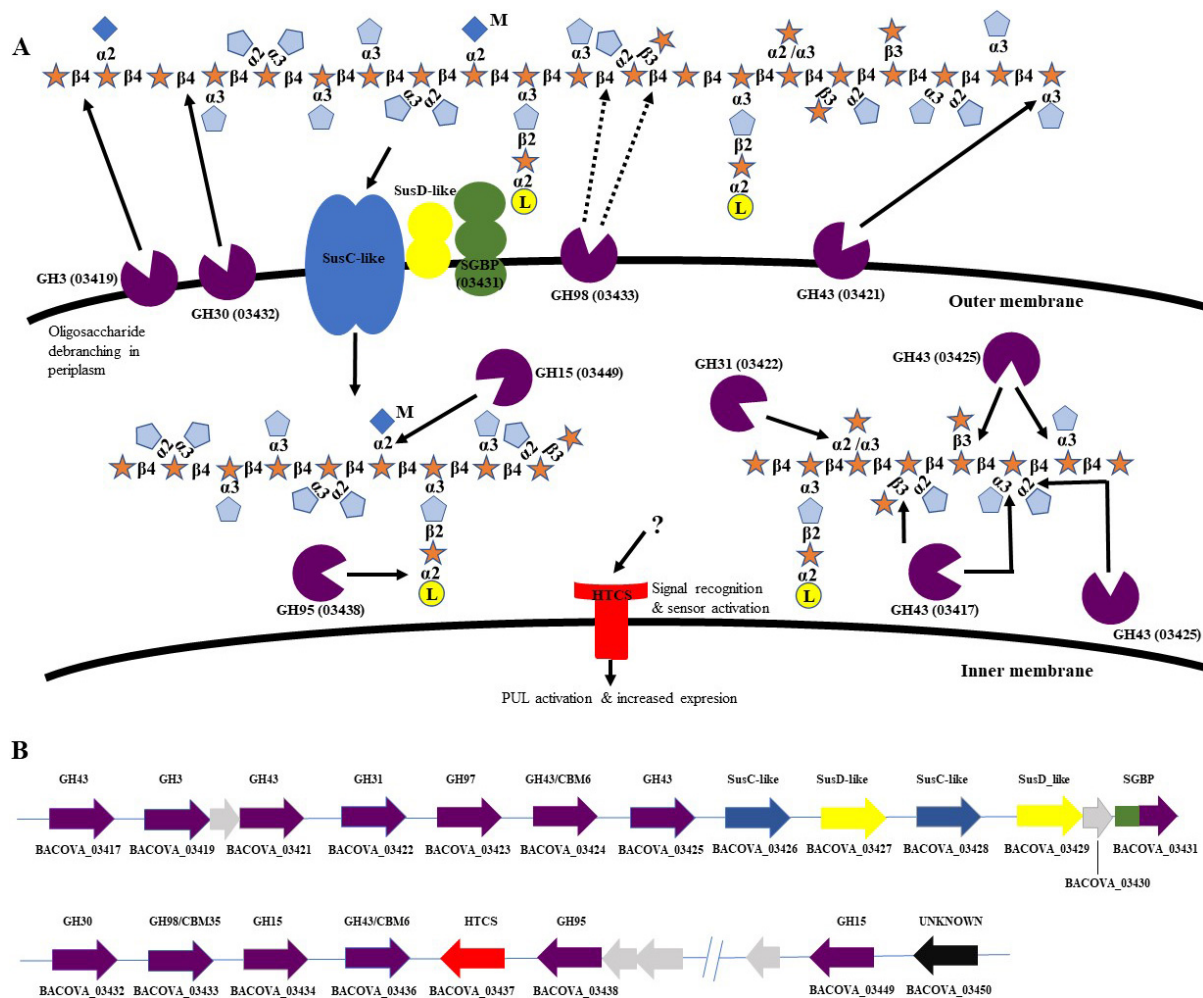
Figure 3. (A) A schematic representation of the glucoronoarabinoxylan utilisation system in *B. ovatus* ATCC 8483. The substrate is bound by lipoproteins at the cell surface where it is primarily degraded to oligosaccharides and then transported to the periplasm where it is further hydrolysed to monosaccharides which can then be transported to the cytoplasm of the cell. (B) Genomic content of *B. ovatus* ATCC 8483 PUL in its action on corn arabinoxylan.

complex xylans. To investigate this, they created a mutant strain of *B. ovatus* ATCC 8483 that lacked a functioning GH98 xylanase CAZyme (ΔGH98), thus preventing the cleavage of the backbone of CX and inhibiting its growth. When the ΔGH98 mutant was co-cultured with wild-type *B. ovatus* ATCC 8483 on CX media, growth of both strains was observed, which provides evidence that the wild-type strain releases PBPs from the breakdown of CX, which are then utilised by the mutant.

Further study into the utilisation of XOS by *Bacteroides* and *Bifidobacterium* strains in co-culture supported the findings of the previous study by Zeybek *et al.*[36]. Mono and co-culture fermentation experiments were carried out with various xylans as substrate; *Bi. bifidum*, *Bi. breve*, *Bi. longum* subspecies *infantis* and *Bi. longum* subspecies *longum* were unable to utilise XOS in monoculture; however, *Bifidobacterium animalis* subsp. *lactis* was able to grow on XOS but no other xylans. In monoculture, two *Bacteroides* strains, *B. ovatus* ATCC 8483 and *B. xylanisolvens* XB1A, showed good growth on xylose, XOS, beechwood xylan and corncob xylan. In co-culture, in the presence of the *Bacteroides* strains, *Bi. animalis* subsp. *lactis,* showed growth on beechwood and corncob xylans. *Bi. bifidum*, *Bi. breve*, *Bi. longum* subspecies *infantis* and *Bi. longum* subspecies *longum* showed no growth on any of the substrates in co-culture. These results highlight

the differences in xylan-type polysaccharide fermentation abilities of different bifidobacterial species as is the case in the degradation of inulin-type fructans observed by Falony *et al.*[37]. The observed growth of *Bi. animalis* subsp. *lactis,* in co-culture, provides evidence for a cross feeding relationship between this species and the *Bacteroides.* This is likely due to the release of XOS as a PBP on the extracellular hydrolysis of xylan by the *Bacteroides* species. This released XOS is subsequently utilised by *Bi. animalis* subsp. *lactis.* This also provides an explanation for the lack of growth of other *Bifidobacterium* species in co-culture as they are unable to utilise XOS.

Cross-feeding behaviour between *B. cellulosilyticus* DSM 14838 and certain bifidobacterial strains was analysed previously[38], where interactions between the assessed strains were observed during cultivation on plant-derived Larch Wood arabinogalactan (LW-AG, Figure 4). This study demonstrated how *B. cellulosilyticus* DSM 14838 primarily degrades LW-AG to release rhamnose and β-1,3-galactooligosaccharides, the latter being further metabolised by certain bifidobacterial strains. *Bi. breve* UCC 2003 grown in co-culture with *B. cellulosilyticus* DSM 14838 was shown to grow on LW-AG as a carbon source, whereas no growth was detected in monoculture, thus revealing a cross-feeding activity between these two organisms. Further investigation showed that the carbohydrates β-1,3-galactobiose and β-1,3-galactotriose are utilised by *Bi. breve* UCC 2003. In addition to *Bi. breve* UCC 2003, also *Bi. longum* subsp. *infantis* ATCC 15697 was shown to utilise AG-derived oligosaccharides released by *B. cellulosilyticus* DSM 14838. The *bgaA* gene was identified in the genome of *Bi. breve* UCC 2003 and was predicted to encode a GH2 enzyme which is involved in the degradation of β-1,3-galactooligosaccharides. The active site of the BgaA enzyme was identified as being specific to β-1,3-galactobiose and β-1,3-galactotriose. Interestingly, this gene was not identified in other bifidobacterial species examined, including *Bi. breve* JCM 7017, *Bi. bifidum* LMG13195, and *Bi. longum* subsp. *longum* NCIMB8809, this being consistent with their inability to cross-feed with *B. cellulosilyticus* DSM14838.

Although no cross-feeding interactions were observed, a study by Liu *et al.*[39] showed how certain *Bacteroides* and *Bifidobacterium* species are involved in the breakdown of polysaccharides in co-culture. Three polysaccharide mixtures, made up of different combinations of AX, xyloglucan, β-glucan and pectin, were used as the sole carbon source to perform co-cultivation experiments involving five different bacterial species, including *B. ovatus* ATCC 8483 and *Bi. longum* subsp. *longum* ATCC 15707. Size-exclusion chromatography showed that the observed degradation of the polysaccharides was carried out by *B. ovatus* ATCC 8483 and *Bi. longum* subsp. *longum* ATCC 15707, and the other bacterial species did not utilise these carbohydrates. Further analysis identified the release of oligosaccharides by *B. ovatus* ATCC 8483 on the hydrolysis of β-glucan; however, these glucooligosaccharides were not utilised by any of the other species in the co-culture. It was found that *B. ovatus* ATCC 8483 played a key role in the production of the SCFA succinate, which was utilised in the formation of propionate by other members of the co-culture, supporting the claim that *Bacteroides* species act as primary degraders of polysaccharides. This was also the case in the production of lactate by both *B. ovatus* ATCC 8483 and *Bi. longum* subsp. *longum* ATCC 15707, which was utilised by the other organisms. This study, along with previous studies discussed, highlights how the microorganisms in the human GIT can cooperatively interact in the breakdown of polysaccharides and benefit one another through PBPs and SCFA production as well as providing benefit to the human host.

CONCLUSION AND FUTURE PERSPECTIVES

The abilities of various *Bacteroides* and *Bifidobacterium* species to utilise different polysaccharides have been highlighted in this review. The identification of polysaccharide utilisation loci in the dominant gut phyla, *Bacteroides*, has helped to increase knowledge of the complex system in which glycan molecules are broken down. It has also allowed for further research into these utilisation mechanisms as well as the
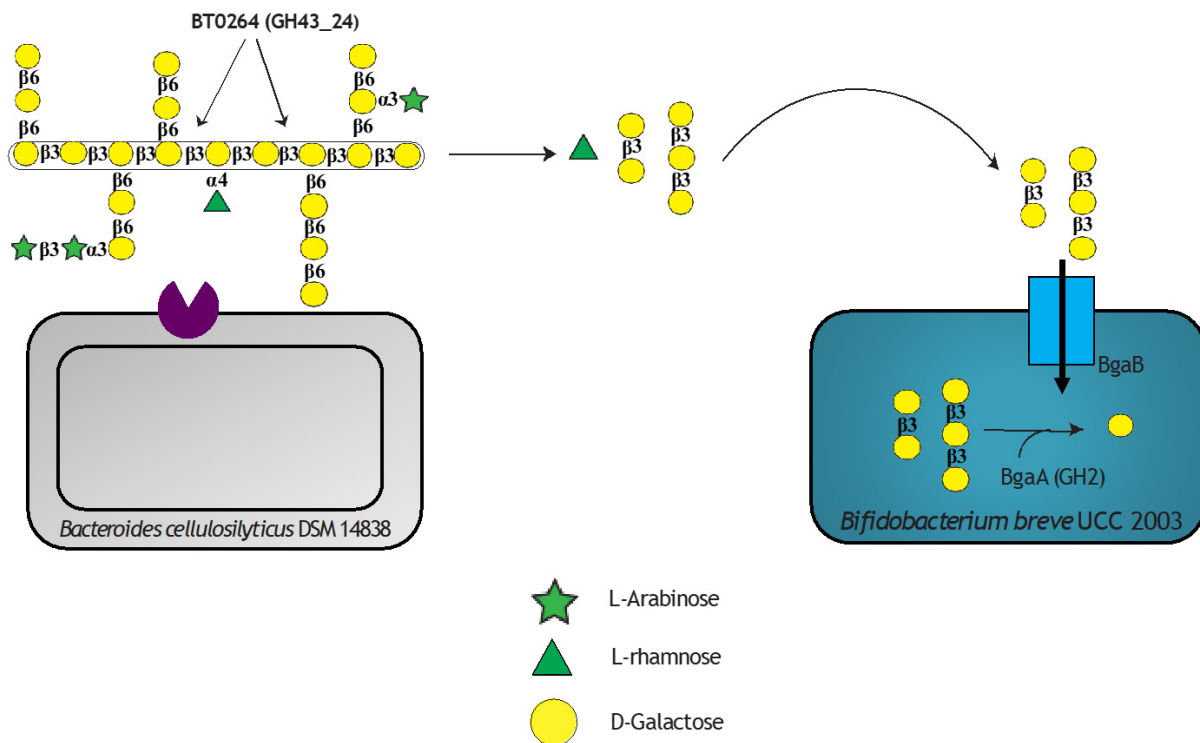
Figure 4. Molecular interactions between *B. cellulosilyticus* DSM 14838 PRL 2010 and *Bi. breve* UCC2003 when act on larch wood arabinogalactan. *B. cellulosilyticus* employs a GH43_24 on its surface to break down the complex polymer into smaller oligosaccharides releasing beta-1,3-galactobiose and beta-1,3-galactotriose and rhamnose into the medium. *Bi. breve* can use these galactooligosaccharides as carbon source degrading them to galactose using a specific GH2 in its cytoplasm. Galactose is later incorporated into the central catabolism of the cell.

ongoing characterisation of carbohydrate-active enzymes that are produced by all glycan-degrading bacteria, including *Bifidobacterium*. Understanding of enzyme function is essential to fully understand NDC utilisation and may help us predict the production of postbiotics, either SCFA or other bioactive compounds such as vitamins, from a given substrate. Enzymology also contributes to our understanding of the interactions between bacteria in the context of the complex community that is the human gut microbiota.

In the case of *Bacteroides* and *Bifidobacterium*, there is evidence for glycan-sharing and cross feeding activities between certain members of these two genera, particularly during the breakdown of dietary fibre. As has been discussed in this review, interactions between these two genera have previously been studied. However, it is likely that many other cross-feeding activities exist that have yet to be discovered. Interaction between *Bacteroides* and *Bifidobacterium* in the breakdown of arabinoxylan has been observed in a small number of studies; however, there is little to no literature available on possible cross-feeding activities on other dietary glycans, such as β-glucan, arabinogalactan, arabinan. Future research should investigate the interaction, if any, between *Bacteroides* and *Bifidobacterium* in the metabolism of dietary β-glucan and its effect on the human host. In addition, there are numerous other gut commensals, less dominant in the human large intestine such as *Lactobacillus reuteri*, which can be studied for their cross-feeding activities with *Bifidobacterium* (either involving dietary fibres or released mon-/oligo-saccharides), but also for the conversion of metabolic end products of one species (e.g., 1,2-propanediol, lactate) into other metabolites (propionate, butyrate). The experimental proof of the conservation of polysaccharide utilisation loci involved in β-glucan degradation specifically, amongst the *Bacteroides* would allow us to identify the

enzymes involved in the metabolism of these molecules, which would then provide a starting point to investigate whether *Bifidobacterium* has a role in the breakdown of this polysaccharide. Due to the extremely complex nature of the human gut microbiota as well as the complexity and variation in carbohydrate structure, much more research is required for us to fully understand the roles of each of the members of the human gut microbiota.

DECLARATIONS

Author contributions
Writing - original draft preparation: Fernandez-Julia P
Writing - review, editing, and conceptualization: Commane DM, van Sinderen D, Munoz-Munoz J
All authors contributed to the article and approved the submitted version.

Availability of data and materials
Not applicable.

Financial support and sponsorship
Munoz J received financial support from an internal grant in Northumbria University. van Sinderen D is a member of APC Microbiome Ireland which received financial support from Science Foundation Ireland, through the Irish Government's National Development Plan (SFI/12/RC/2273-P1 and SFI/12/RC/2273-P2).

Conflicts of interest
All authors declared that there are no conflicts of interest.

Ethical approval and consent to participate
Not applicable.

Consent for publication
Not applicable.

Copyright
© The Author(s) 2022.

REFERENCES

1. Thursby E, Juge N. Introduction to the human gut microbiota. *Biochem J* 2017;474:1823-36. DOI PubMed PMC
2. Belizário JE, Napolitano M. Human microbiomes and their roles in dysbiosis, common diseases, and novel therapeutic approaches. *Front Microbiol* 2015;6:1050. DOI PubMed PMC
3. Mar JS, LaMere BJ, Lin DL, et al. Disease severity and immune activity relate to distinct interkingdom gut microbiome states in ethnically distinct ulcerative colitis patients. *mBio* 2016;7:e01072-16. DOI PubMed PMC
4. Stewart CJ, Ajami NJ, O'Brien JL, et al. Temporal development of the gut microbiome in early childhood from the TEDDY study. *Nature* 2018;562:583-8. DOI PubMed PMC
5. Hamaker BR, Tuncil YE. A perspective on the complexity of dietary fiber structures and their potential effect on the gut microbiota. *J Mol Biol* 2014;426:3838-50. DOI PubMed
6. Grondin JM, Tamura K, Déjean G, Abbott DW, Brumer H. Polysaccharide utilization loci: fueling microbial communities. *J Bacteriol* 2017;199:e00860-16. DOI PubMed PMC
7. McNeil NI. The contribution of the large intestine to energy supplies in man. *Am J Clin Nutr* 1984;39:338-42. DOI PubMed
8. Le Poul E, Loison C, Struyf S, et al. Functional characterization of human receptors for short chain fatty acids and their role in polymorphonuclear cell activation. *J Biol Chem* 2003;278:25481-9. DOI PubMed
9. Parada Venegas D, De la Fuente MK, Landskron G, et al. Short chain fatty acids (SCFAs)-mediated gut epithelial and immune regulation and its relevance for inflammatory bowel diseases. *Front Immunol* 2019;10:277. DOI PubMed PMC
10. Besten G, van Eunen K, Groen AK, Venema K, Reijngoud DJ, Bakker BM. The role of short-chain fatty acids in the interplay between diet, gut microbiota, and host energy metabolism. *J Lipid Res* 2013;54:2325-40. DOI PubMed PMC
11. Ang Z, Ding JL. GPR41 and GPR43 in obesity and inflammation - protective or causative? *Front Immunol* 2016;7:28. DOI PubMed PMC

12. Lapébie P, Lombard V, Drula E, Terrapon N, Henrissat B. Bacteroidetes use thousands of enzyme combinations to break down glycans. *Nat Commun* 2019;10:2043. DOI PubMed PMC

13. Larsbrink L, McKee LS, Bacteroidetes bacteria in the soil: Glycan acquisition, enzyme secretion and gliding motility. *Adv Appl Microbiol* 2020;110:63-98. DOI

14. Koropatkin NM, Cameron EA, Martens EC. How glycan metabolism shapes the human gut microbiota. *Nat Rev Microbiol* 2012;10:323-35. DOI PubMed PMC

15. O Sheridan P, Martin JC, Lawley TD, et al. Polysaccharide utilization loci and nutritional specialization in a dominant group of butyrate-producing human colonic Firmicutes. *Microb Genom* 2016;2:e000043. DOI PubMed PMC

16. Van der Meulen R, Adriany T, Verbrugghe K, De Vuyst L. Kinetic analysis of bifidobacterial metabolism reveals a minor role for succinic acid in the regeneration of NAD+ through its growth-associated production. *Appl Environ Microbiol* 2006;72:5204-10. DOI PubMed PMC

17. Turroni F, Milani C, Duranti S, Mahony J, van Sinderen D, Ventura M. Glycan utilization and cross-feeding activities by Bifidobacteria. *Trends Microbiol* 2018;26:339-50. DOI PubMed

18. Singh RP. Glycan utilisation system in Bacteroides and Bifidobacteria and their roles in gut stability and health. *Appl Microbiol Biotechnol* 2019;103:7287-315. DOI PubMed

19. Egan M, O'Connell Motherway M, Ventura M, van Sinderen D. Metabolism of sialic acid by Bifidobacterium breve UCC2003. *Appl Environ Microbiol* 2014;80:4414-26. DOI PubMed PMC

20. Turroni F, Özcan E, Milani C, et al. Glycan cross-feeding activities between bifidobacteria under in vitro conditions. *Front Microbiol* 2015;6:1030. DOI PubMed PMC

21. Cheng CC, Duar RM, Lin X, et al. Ecological importance of cross-feeding of the intermediate metabolite 1,2-propanediol between bacterial gut symbionts. *Appl Environ Microbiol* 2020;86:e00190-20. DOI PubMed PMC

22. Smith NW, Shorten PR, Altermann E, Roy NC, Mcnabb WC. The classification and evolution of bacterial cross-feeding. *Front Ecol Evol* 2019;7:153. DOI

23. Morris BE, Henneberger R, Huber H, Moissl-Eichinger C. Microbial syntrophy: interaction for the common good. *FEMS Microbiol Rev* 2013;37:384-406. DOI PubMed

24. Schwalm ND 3rd, Groisman EA. Navigating the gut buffet: control of polysaccharide utilization in Bacteroides spp. *Trends Microbiol* 2017;25:1005-15. DOI PubMed

25. Rakoff-Nahoum S, Coyne MJ, Comstock LE. An ecological network of polysaccharide utilization among human intestinal symbionts. *Curr Biol* 2014;24:40-9. DOI PubMed PMC

26. Salyers AA, Gherardini F, O'Brien M. Utilization of xylan by two species of human colonic Bacteroides. *Appl Environ Microbiol* 1981;41:1065-8. DOI PubMed PMC

27. Rakoff-Nahoum S, Foster KR, Comstock LE. The evolution of cooperation within the gut microbiota. *Nature* 2016;533:255-9. DOI PubMed PMC

28. Turroni F, Milani C, Duranti S, et al. Deciphering bifidobacterial-mediated metabolic interactions and their impact on gut microbiota by a multi-omics approach. *ISME J* 2016;10:1656-68. DOI PubMed PMC

29. Milani C, Lugli GA, Duranti S, et al. Bifidobacteria exhibit social behavior through carbohydrate resource sharing in the gut. *Sci Rep* 2015;5:15782. DOI PubMed PMC

30. Egan M, Motherway MO, Kilcoyne M, et al. Cross-feeding by Bifidobacterium breve UCC2003 during co-cultivation with Bifidobacterium bifidum PRL2010 in a mucin-based medium. *BMC Microbiol* 2014;14:282. DOI PubMed PMC

31. Turroni F, Bottacini F, Foroni E, et al. Genome analysis of Bifidobacterium bifidum PRL2010 reveals metabolic pathways for host-derived glycan foraging. *Proc Natl Acad Sci U S A* 2010;107:19514-9. DOI PubMed PMC

32. Hehemann JH, Correc G, Barbeyron T, Helbert W, Czjzek M, Michel G. Transfer of carbohydrate-active enzymes from marine bacteria to Japanese gut microbiota. *Nature* 2010;464:908-12. DOI PubMed

33. Fischbach MA, Sonnenburg JL. Eating for two: how metabolism establishes interspecies interactions in the gut. *Cell Host Microbe* 2011;10:336-47. DOI PubMed PMC

34. Rios-Covian D, Arboleya S, Hernandez-Barranco AM, et al. Interactions between Bifidobacterium and Bacteroides species in cofermentations are affected by carbon sources, including exopolysaccharides produced by bifidobacteria. *Appl Environ Microbiol* 2013;79:7518-24. DOI PubMed PMC

35. Rogowski A, Briggs JA, Mortimer JC, et al. Glycan complexity dictates microbial resource allocation in the large intestine. *Nat Commun* 2015;6:7481. DOI PubMed PMC

36. Zeybek N, Rastall RA, Buyukkileci AO. Utilization of xylan-type polysaccharides in co-culture fermentations of Bifidobacterium and Bacteroides species. *Carbohydr Polym* 2020;236:116076. DOI PubMed

37. Falony G, Lazidou K, Verschaeren A, Weckx S, Maes D, De Vuyst L. In vitro kinetic analysis of fermentation of prebiotic inulin-type fructans by Bifidobacterium species reveals four different phenotypes. *Appl Environ Microbiol* 2009;75:454-61. DOI PubMed PMC

38. Munoz J, James K, Bottacini F, Van Sinderen D. Biochemical analysis of cross-feeding behaviour between two common gut commensals when cultivated on plant-derived arabinogalactan. *Microb Biotechnol* 2020;13:1733-47. DOI PubMed PMC

39. Liu Y, Heath AL, Galland B, et al. Substrate use prioritization by a coculture of five species of gut bacteria fed mixtures of arabinoxylan, xyloglucan, β-glucan, and pectin. *Appl Environ Microbiol* 2020;86:e01905-19. DOI PubMed PMC

ARTICLE

Check for updates

Fungal β-glucan-facilitated cross-feeding activities between Bacteroides and Bifidobacterium species

Pedro Fernandez-Julia[1], Gary W. Black[1], William Cheung[1], Douwe Van Sinderen [2] & Jose Munoz-Munoz [1✉]

The human gut microbiota (HGM) is comprised of a very complex network of microorganisms, which interact with the host thereby impacting on host health and well-being. β-glucan has been established as a dietary polysaccharide supporting growth of particular gut-associated bacteria, including members of the genera *Bacteroides* and *Bifidobacterium*, the latter considered to represent beneficial or probiotic bacteria. However, the exact mechanism underpinning β-glucan metabolism by gut commensals is not fully understood. We show that mycoprotein represents an excellent source for β-glucan, which is consumed by certain *Bacteroides* species as primary degraders, such as *Bacteroides cellulosilyticus* WH2. The latter bacterium employs two extracellular, endo-acting enzymes, belonging to glycoside hydrolase families 30 and 157, to degrade mycoprotein-derived β-glucan, thereby releasing oligosaccharides into the growth medium. These released oligosaccharides can in turn be utilized by other gut microbes, such as *Bifidobacterium* and *Lactiplantibacillus*, which thus act as secondary degraders. We used a cross-feeding approach to track how both species are able to grow in co-culture.

[1] Microbial Enzymology Lab, Department of Applied Sciences, Northumbria University, Newcastle Upon Tyne NE1 8ST Tyne & Wear, England UK. [2] School of Microbiology & APC Microbiome Ireland, University College Cork, Cork, Ireland. ✉email: jose.munoz@northumbria.ac.uk

The human gut microbiota (HGM) is a complex ecosystem of microbes, which are purported to beneficially impact on human health. Dietary carbohydrates represent the main energy source for the human body, though we lack the enzymatic capabilities to degrade most of these glycans ourselves[1]. However, the HGM encodes an arsenal of carbohydrate active enzymes (CAZYmes) able to catabolize such carbohydrates[1]. The metabolic end products of glycan fermentation by the HGM are mostly SCFAs, such as propionate, acetate and butyrate, which have a variety of beneficial effects on the human host. Imbalance in the composition of the gut microbial community, sometimes referred to as dysbiosis, is a characteristic of Inflammatory Bowel Disease (IBD), colorectal cancer, obesity, *Clostridioides difficile* infections and, potentially, a wide range of other conditions[2–4].

As stated above, the HGM is a complex network of microbes representing approximately 10 trillion bacteria[5]. Nonetheless, just two phyla are dominant in this intricate bacterial community, i.e. Bacteroidota and Bacillota, complemented with representatives of several minor phyla, such as Actinomycetota or Verrucomicrobiota. Various members of the *Bacteroides* genus have been shown to contain specific clusters of co-regulated genes which metabolise a specific glycan, and which are called Polysaccharide Utilisation Loci (singular: PUL, plural: PULs). A given PUL contains the genes needed to sense, transport and degrade a particular glycan[6–8]. For example, the *Bacteroides thetaiotaomicron* (*Ba. thetaiotaomicron* VPI-5482, BT) genome harbours 96 different PULs, according to the CAZY database[9,10], while another *Bacteroides species*, *Ba. ovatus* ATCC8483 (Bacova), encompasses 115 different PULs. Generally, a cell surface-associated glycoside hydrolase (GH) or polysaccharide lyase (PL) initiates extracellular polysaccharide degradation allowing the release of the resulting oligosaccharides into the growth medium[11–17].

Members of the genus *Bifidobacterium* are particularly abundant in full-term, breast-fed infants, where they are believed to exert important beneficial effects[18–21]. The dominance of these bacteria in this niche is attributed, at least in part, to their ability to metabolise (particular) human milk oligosaccharides (HMOs) as a sole carbon and energy source[22]. Different bifidobacterial species have particular HMO consumption preferences, for example strains of *Bi. breve* and *Bi. longum* are known to internalise and metabolise Lacto-N-tetraose[23–26], while *Bi. catenulatum* subsp. *kashiwanohense* can use 2-fucosyllactose as a carbon source[19,27]. The prototypical strain *Bi. breve* UCC2003 has been shown to metabolise several HMOs and other dietary poly/oligosaccharides either on its own[23,28] or through cross-feeding involving other members of the gut microbiota; examples of such saccharidic substrates are mucin[29,30], arabinogalactan/galactan[31,32] and sialyllactose[20].

β-glucan is a complex glycan which has been explored as a potential prebiotic and which is particularly abundant in cereals and fungal cell walls[13,33–36]. Cereal-derived β-glucan, with a defined β-1,3/1,4-mixed linkage (Fig. 1A), has been employed to understand the molecular mechanisms by which certain *Bacteroides* species are able to sense, internalize and degrade this polymer[13,34–36]. For example, Bacova employs a PUL with a cell surface-associated glycoside hydrolase 16 (GH16) and a periplasmic GH3 to catalyse degradation of this mixed linkage cereal β-glucan[34–36].

Furthermore, a *Ba. uniformis* ATCC8492 PUL, which is involved in the metabolism of related β-1,3-glucans present in yeast and the seaweed glucan laminarin (Fig. 1A), is responsible for the initial degradation at the cell surface by a glycoside hydrolase 16 (GH16) and a GH158, and a subsequently acting periplasmic GH3[13]. In addition, *Ba. uniformis* strain JCM13288 can degrade laminarin, pustulan and porphyran β-glucans, employing two PULs encoding a GH16, GH30, GH158 and GH3,

and sharing oligosaccharides with other gut microbiota members, possibly supporting gut homeostasis[37].

Another type of β-1,6-glucan, which is found as linear glucan in the lichen *Lasallia pustulata* and as linear glucan but cross-linked with other cell wall components in the yeast *Saccharomyces cerevisiae* or in the almond mushroom (*Agaricus blazei*), is used by BT through a PUL involving just a surface-located GH30_3 and a periplasmic GH3[17,33]. Little is known about the degradation of fungal β-glucan, such as that derived from mycoprotein produced by *Fusarium venenatum*, a fungus employed by Quorn® as a functional food ingredient[38]. The chemical structure of this β-glucan consists of a linear β-1,3-glucan backbone carrying side chains of β-1,6-glucans, which makes it distinct from cereal β-glucan, or yeast β-glucan/laminarin, where either the core chain or the side chain linkages are different, respectively[13,34,39] (Fig. 1A).

Currently, there are only a few publications describing any health benefits elicited by Bacteroidota (in fact some species are considered opportunistic pathogens)[40,41]. However, a case can be made that certain *Bacteroides* species represent primary glycan degraders that allow carbohydrate cross-feeding by other, beneficial members of the microbiota, such as bifidobacteria (which are not known to be able to metabolise β-glucan directly). Such metabolic interactions occur between BT and *Bi. longum*, and between *Ba. cellulosilyticus* DSMZ14838 (Baccell DSMZ) and *Bi. breve* UCC2003 when grown on larch arabinogalactan protein (AGP) as the sole carbon source[31,42,43]. Other trophic interactions have been established between various species of *Bacteroides* and *Bifidobacterium*[39,44–48], but have yet to be defined for mycoprotein β-glucan.

In the current study, we performed a molecular characterization of mycoprotein and yeast β-glucan degradation by Bacova, *Ba. cellulosilyticus WH2* (Baccell WH2) and BT, highlighting the PUL architecture of these *Bacteroides spp.* In addition, we uncovered cross-feeding interactions between *Bacteroides*, as the primary degrader, and certain species of *Bifidobacterium* and *Lactiplantibacillus*, acting as secondary degraders of Mycoprotein-derived fungal β-glucan.

Results

Screening *Bacteroides* species for β-glucan metabolism. Certain members of the *Bacteroides* genus have been established as generalist fermenters of mixed linkage (barley) and yeast β-glucan[13,34–37]. The genomes of these *Bacteroides* species encompass various PULs (here referred to as glucan utilization loci or GULs) to degrade this complex glycan, employing encoded glycoside hydrolases for this metabolic process. To assess the ability of *Bacteroides* species to use fungal-derived β-glucan, we extracted this polysaccharide from mycoprotein of *Fusarium venenatum* (see "Materials and methods") and screened the 23 most prominent, gut-associated Bacteroidetes species for their ability to grow on this glycan as well as on β-glucan derived from yeast (Table S1). Under the (anaerobic) conditions used, *Ba. xylanisolvens*, *Ba. intestinalis*, Bacova, *Ba. fragilis*, *Ba. finegoldii*, *Ba. vulgatus*, *Ba. uniformis*, BT (partial growth)*, Dysgonomonas gadei*, *D. mossii* and two strains of Baccell (Baccell WH2 and Baccell DSMZ) were shown to metabolise β-glucan derived from mycoprotein. In addition, *Ba. vulgatus*, *Ba. uniformis*, Bacova, BT, *Dysgonomonas gadei*, *D. mossii* and both Baccell strains were able to utilise yeast β-glucan. Bacova has previously been shown to grow in barley-derived β-glucan as well[34,35], showing this species' broad ability to ferment β-glucans from different sources and chemical structures (Fig. 1A). Figure 1B shows the growth profile of Baccell WH2, Baccell DSMZ, BT and Bacova on β-glucan from mycoprotein (Fig. 1B). In addition to these growth experiments, we assessed growth of various *Bifidobacterium* strains on
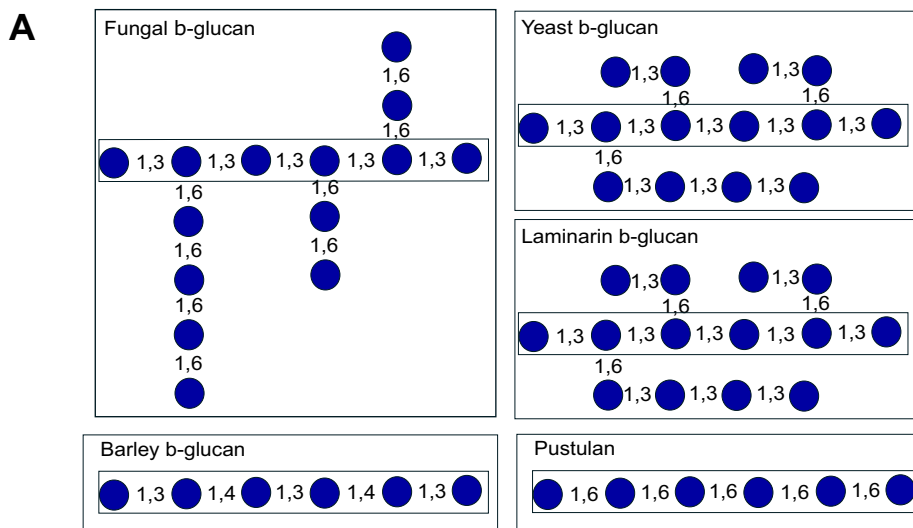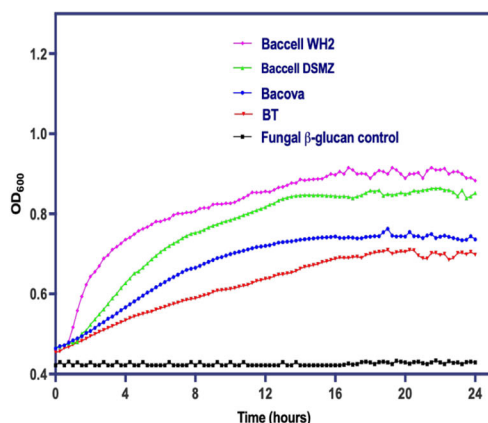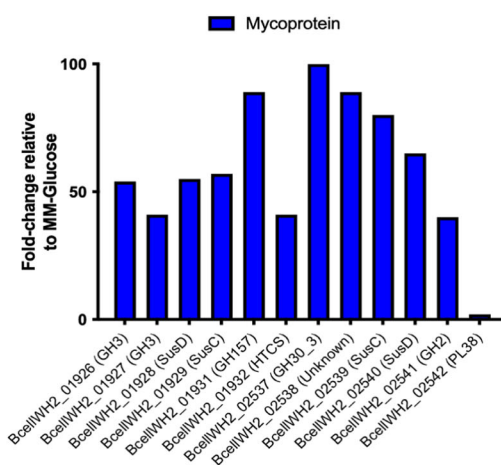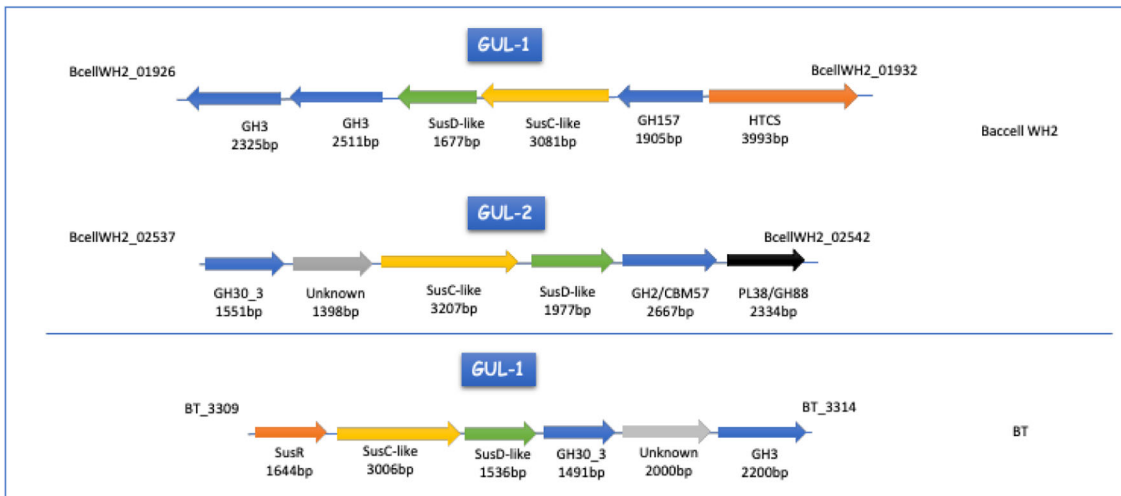
Fig. 1 Polysaccharide utilization systems in Bacteroides species for β-glucan degradation. A Structures of fungal (mycoprotein), yeast, laminarin, barley and pustulan β-glucan. **B** Growth *Bacteroides ovatus*, DSM, WH2 and BT on mycoprotein as measured on a plate reader. All growths have been produced in 3 different independent replicates ($n = 3$). **C** Number of proteins expressed by Baccell WH2 on the use of β-glucan from Mycoprotein as identified by proteome analysis. The proteomics have been produced in 3 different independent replicates ($n = 3$). **D** GUL structure in Baccell WH2 (GUL-1 and GUL-2) and BT acting on mycoprotein, yeast and pustulan.

mycoprotein-derived β-glucan, clearly showing a lack of ability by these strains to use this complex carbon source (Fig. S1A).

GUL regulation in *Bacteroides* and architecture. To further characterise growth of selected *Bacteroides* strains on particular β-glucans, we performed proteomics analysis on Baccell WH2 when grown on glucose (acting as reference) or mycoprotein-derived fungal β-glucan as carbon sources. We compared the generated proteome data of this bacterium when grown on either of these carbon sources to identify proteins that exhibit increased expression when the strain is grown on the complex polymer. As shown in Fig. 1C, this analysis revealed that all proteins encoded by two assigned GULs (named here as GUL-1 and GUL-2 and representing locus tags BcellWH2_01929-BcellWH2_01932 and BcellWH2_02537-BcellWH2_02542, respectively, see Fig. 1D) exhibit increased expression when Baccell WH2 was grown on mycoprotein-derived fungal β-glucan metabolism (when compared to growth on glucose). GUL-1 was predicted to encode two GH3 enzymes (BcellWH2_01926 and BcellWH2_01927) and a GH157 member (BcellWH2_01931), while the proteins encoded by locus tags BcellWH2_01928 and BcellWH2_01929 represent the SusC/D-like pair predicted to be involved in (polysaccharide) substrate binding and recognition at the bacterial cell surface (Fig. 1D). Furthermore, BcellWH2_01932 is predicted to represent the Hybrid Two Component System (HTCS) sensing system controlling transcriptional regulation of GUL-1. GUL-2 encodes a GH30_3 (BcellWH2_02537, a predicted endo-β-1,6-glucanase according to the CAZY database), a GH2 (BcellWH2_02541) and a protein without known function (BcellWH2_02538). In addition to these proteins, BcellWH2_02539 and BcellWH2_02540 represent the predicted the SusC/D pair in GUL2 (Fig. 1D). To confirm the proteomics data, we grew Baccell WH2 to mid-exponential and performed RT-qPCR on selected SusC/D pairs identified in the above described GULs (Fig. S1B). In addition, we also used this approach with BT and Bacova on the SusC/D pairs identified based on differential expression patterns when these two strains had been grown on beta-glucan from pustulan[17,34,35] (Fig. S1B). Since we observed differential expression based on RT-qPCR, it seems that their corresponding GULs, which are substantially different from that of Baccell WH2 in terms of their genetic structure and content, are also responsible for growth on fungal β-glucan. Figure 1D and S1C show the GUL architecture of BT, Bacova and Baccell WH2, and predicted functions pertaining to GUL regulation, β-glucan degradation and associated oligosaccharide intake. BT and Baccell WH2 employ a different GUL architecture for fungal β-glucan utilization (Fig. 1D), when compared to Bacova, which based on its expression profile appears to use the same GUL for fungal and barley β-glucan Figs. S1B and S1C.

As stated above, BT, Baccell WH2 and Bacova can metabolise fungal β-glucan. Based on qPCR performed on BT growing in a medium containing either fungal β-glucan or pustulan, this bacterium appears to employ the same GUL for either of these two carbon sources[17] (BT3309-BT3314, Fig. 1D and S1B). According to qPCR data obtained when Bacova is growing in a medium supplemented with either barley or fungal β-glucan (Fig. S1B), the bacterium was shown to employ the same GUL for either of these carbon sources, which contrasts with what we discovered for Baccell WH2, as this bacterium appears to employ distinct GULs to deconstruct either fungal or barley β-glucan (Fig. 1D and S1C)[49].

Dissecting the enzymes encoded by GUL-1 and GUL-2 that degrade fungal β-glucan. Following our observation that certain proteins encoded by, and their corresponding genes present in,

GUL-1 and GUL-2 of Baccell WH2 elicit increased expression when growing on fungal β-glucan, we wanted to confirm their involvement in this metabolic process. For this purpose, we recombinantly expressed the enzymes representing the putative GH157, GH30_3 and GH3 (Baccell WH2_01926) activities from GUL1/GUL2 to fully dissect the mechanism of degradation of this complex dietary carbon source. For this purpose, we incubated the expressed proteins with fungal β-glucan and revealed possible degradation products by means of HPLC chromatography. More specifically, Fig. 2A shows the HPLC chromatograms of BcellWH2_01931 and BcellWH2_02537 (representing predicted GH157 and GH30_3 activities, respectively) acting on fungal β-glucan.

The data presented in Fig. 2A and 2B confirmed that BcellWH2_01931 acts on fungal β-glucan (Fig. 2A) and the linear β-1,3-glucan from *Euglena glacialis* (Fig. 2B) initially releasing penta- and trisaccharides, which are converted to disaccharides and glucose upon longer incubation (16 h). However, we did not find any activity when the enzyme was incubated with pustulan. Table 1 lists the kinetic parameters (k_{cat}/K_m) of this protein acting on either substrate.

To validate the prediction that these enzymes are involved in fungal β-glucan metabolism, we performed protein location analysis by LipoP[50], indicating that BcellWH2_01931 (GH157) and BcellWH2_02537 (GH30_3) are located at the cell surface of Baccell WH2. Furthermore, according to the CAZY database, the GH157 enzyme was anticipated to act as an endo-β-1,3-glucanase, while the GH30_3 enzyme was expected to possess endo-β-1,6-glucanase activity as has been reported for other members of this CAZY family[17]. Like GH157, recombinantly expressed and purified GH30_3 was incubated with fungal β-glucan, linear β-1,3-glucan and pustulan (linear β-1,6-glucan), followed by HPLC analysis. Figure 2C and 2D show the associated chromatography results for this incubation experiment, confirming the β-1,6-glucanase activity with fungal β-glucan (Fig. 2C) and pustulan (Fig. 2D). In addition, GH30_3 didn't show any activity against linear β-1,3-glucan. Table 1 displays the catalytic parameters of this protein as measured by DNSA assays with fungal β-glucan and pustulan. BcellWH2_02537 showed activity parameters for β-glucan from *Fusarium venenatum* that are like those obtained for pustulan (k_{cat}/K_m of 2512 ± 28 and 1968 ± 17 mg ml^{-1} min^{-1}) suggesting that the enzyme does not require interactions with the β-(1,3)-glucan backbone. In addition, BcellWH2_02537 was shown to only exhibit activity on oligosaccharides larger than β-(1,6)-glucotriose indicating that, as in BT3312, the enzyme has 3 subsites in the active site (nomenclature established by Davies et al.)[51].

Finally, to fully understand how mycoprotein-derived β-glucan is metabolised by Baccell WH2, we recombinantly expressed the predicted GH3 and GH2 enzymes (as specified by BcellWH2_01926 and BcellWH2_02541, respectively), showing that both are able to act on the different oligosaccharides produced by the action of the GH157 and GH30_3 enzymes. BcellWH2_01926 (GH3) was able to degrade β-1,6-glucooligosaccharides released by GH30_3, while the GH2 enzyme (BcellWH2_02541) was shown to act on β-1,3-glucooligosaccharides (glucobiose and glucotriose), in both cases releasing glucose as the final product, which confirms the exo-acting mechanism for these enzymes (BcellWH2_01926 and BcellWH2_02541). Table 1 also displays the catalytic parameters of these two exo-glucosidases, which highlights that the activity of the GH2 enzyme is similar for β-1,3-glucobiose and β-1,3-glucotriose, suggesting 2 subsites in the active site.

In the case of BT, the GUL architecture is simpler than that observed for Baccell WH2 (Fig. 1D). For the former bacterium, only the GH30_3 (BT3312) and a GH3 (BT3314) have previously been described to be active on pustulan β-glucan[17]. To assess the
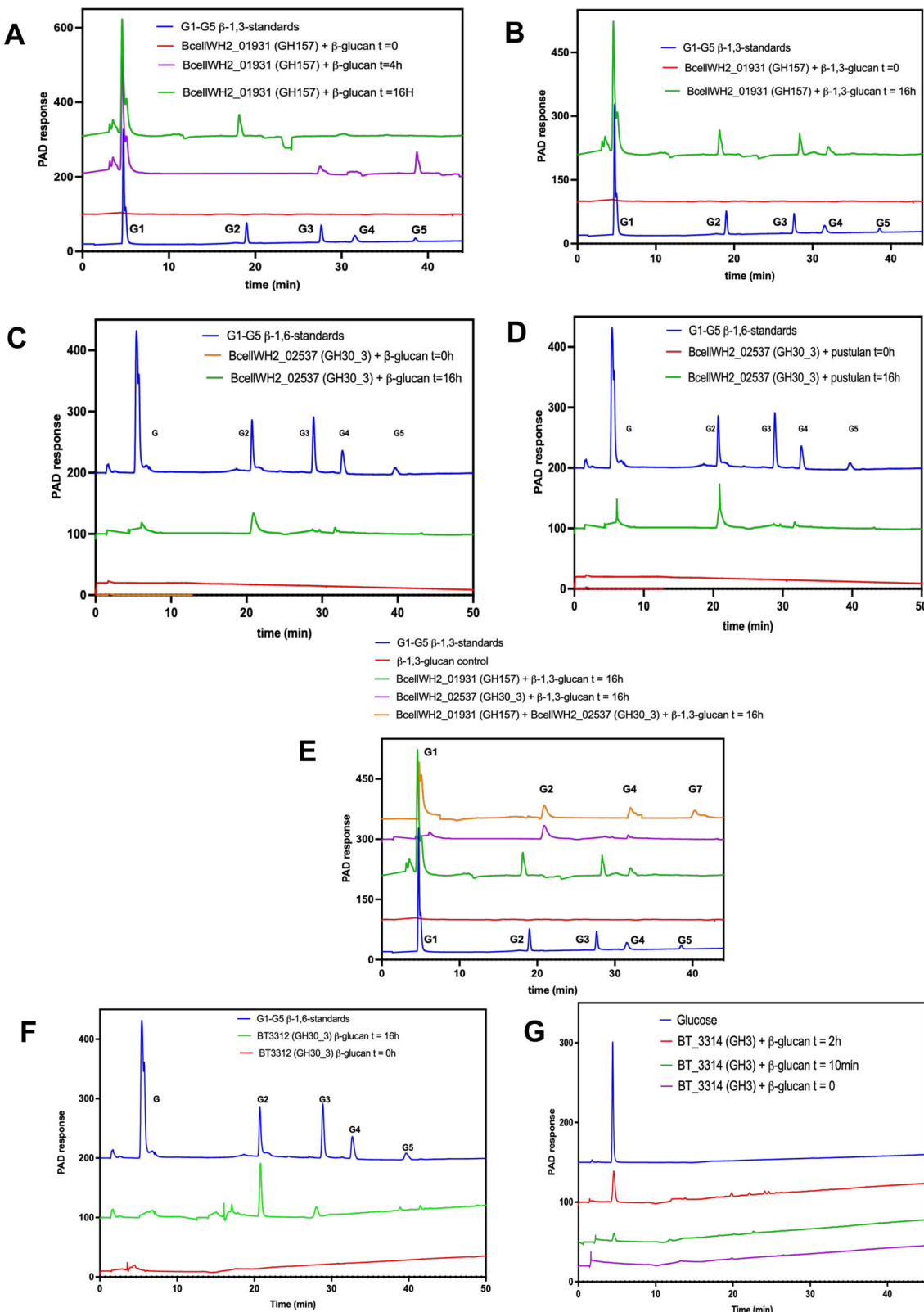
Fig. 2 HPLC analysis of the enzymatic reactions of glycoside hydrolases in Baccell WH2 and BT on fungal β-glucan. All HPLC experiments have been produced in 3 different independent replicates ($n = 3$). **A** Time course of BcellWH2_01931 (GH157) with mycoprotein β-glucan. **B** Time course of BcellWH2_01931 (GH157) with linear β-1,3-glucan. **C** Time course of BcellWH2_02537 (GH30_3) on mycoprotein β-glucan. **D** Time course of BcellWH2_02537 (GH30_3) with pustulan. **E** Time course of BcellWH2_01931 (GH157) and BcellWH2_02537 (GH30_3) together on linear β-1,3-glucan. **F** HPLC of BT3312 (GH30_3) on mycoprotein β-glucan. **G** HPLC of BT_3314 (GH3) on mycoprotein β-glucan.

Table 1 Kinetic parameters of GHs in Baccell WH2, BT and *Bi. breve UCC2003* acting different β-glucan substrates and gluco-oligosaccharides.

	Substrate	K_{cat}/K_m (mg/ml/min)	k_{cat}/K_m (µM/min)
Baccell WH2			
BcellWH2_01926 (GH3)	β-(1,6)glucobiose		10.2 ± 0.9
	β-(1,6)glucotriose		25.2 ± 1.8
BcellWH2_01931 (GH157)	*Fusarium* β-glucan	1069 ± 11	
	Linear β-(1,3)glucan	2611 ± 38	
	Pustulan	Not detectable	
BcellWH2_02537 (GH30_3)	*Fusarium* β-glucan	2512 ± 28	
	Pustulan	1968 ± 17	
	Linear β-(1,3)glucan	Not detectable	
	β-(1,6)glucotriose		2.5 ± 0.1
	β-(1,6)glucohexaose		9.8 ± 0.9
BcellWH2_02541 (GH2)	β-(1,3)glucobiose		18.1 ± 1.2
	β-(1,3)glucotriose		35.1 ± 2.9
BT			
BT3312 (GH30_3)	*Fusarium* β-glucan	2874 ± 35	
	Pustulan[a]	1776 ± 20	
	Linear β-(1,3)glucan	Not detectable	
	β-(1,6)glucotriose[a]		1.7 ± 0.1
	β-(1,6)glucohexaose[a]		6.0 ± 0.6
BT3314 (GH3)	β-(1,6)glucobiose[a]		5.6 ± 0.2
	β-(1,6)glucotriose[a]		6.7 ± 0.6
Bi. breve UCC2003			
Bbr_0109 (GH1)	β-(1,3)glucobiose		12.7 ± 1.8
	β-(1,4)glucobiose		8.1 ± 0.9
	β-(1,6)glucobiose		5.4 ± 0.6

[a]Data taken from Temple et al. as comparison[17].

catalytic activity of BT3312 on β-glucan from *Fusarium venenatum*, we performed enzymatic assays with this polysaccharide obtaining activity levels that are similar to those of BcellWH2_02537 ($2874 ± 35\ \mathrm{mg\ ml^{-1}\ min^{-1}}$ for BT3312 and $2512 ± 28\ \mathrm{mg\ ml^{-1}\ min^{-1}}$ for BcellWH2_02537) (Table 1). The BT3312 enzyme was shown to be active on fungal β-glucan side chains, thereby releasing particular β-1,6-oligosaccharides, which in turn can be hydrolysed by BT3314 as an exo-glucosidase to release glucose (Fig. 2F for BT3312, and Fig. 2G for BT3314). In the same way as Baccell WH2 enzymes, Table 1 shows the catalytic parameters for BT3312 and BT3314 on these substrates.

Structural modelling of GH157 and GH30_3 from Baccell WH2. To dissect the interactions of the Baccell WH2-encoded GH157 and GH30_3 enzymes with fungal β-glucan, we attempted to obtain crystals of the Baccell WH2 proteins. Unfortunately, despite screening multiple conditions we were unable to obtain suitable crystals. Instead, we obtained the structure of the GH30_3 protein by comparison to the crystal structure solved for BT3312 using the Phyre2 algorithm as a search platform[17,52]. Fig. S1D shows that the predicted structure is an (β/a)_8 barrel with the conserved retaining mechanism where two glutamic acids act as nucleophile (E339 and E347 for BT3312 and BcellWH2_02537, respectively) and acid/base (E238 and E247 for BT3312 and BcellWH2_02537, respectively). As indicated in this Figure, both proteins show a high level of sequence similarity (58.33% identical) and exhibit the same activity profile (Table 1). This indicates that the GH30_3 from Baccell WH2 contains only three major subsites in a similar manner to what has been described for BT3312[17]. Amino acids involved in the binding and catalysis are conserved in both proteins (Fig. S1E).

Oligosaccharides released into the cultivation medium. To investigate if Baccell WH2 and BT release oligosaccharides into

their cultivation medium when grown on fungal β-glucan, thereby perhaps allowing growth of other bacteria through cross-feeding activities, we obtained cell free growth medium following cultivation of these strains to the mid-exponential and stationary phase (Fig. 3). The presence of oligosaccharides released into the media by Baccell WH2 or BT was then assessed by HPLC (Fig. 3A, B). When these two bacterial species use mycoprotein as their sole carbon source (Fig. 3A), they were shown to release oligosaccharides into the media, but these were different in each case (Fig. 3B), which is consistent with their different GUL architecture and associated enzymes, thus confirming the distinct degradative strategy followed by each of these two species.

To investigate the nature of these oligosaccharides, we performed LC/MS to determine their mass. Figure 3C shows the HPLC profile of the purified main oligosaccharide released by Baccell WH2 and Fig. 3E the associated mass spectrum of this oligosaccharide confirming that this bacterium predominantly releases a heptasaccharide. These results are in concordance with the in vitro enzymatic digestion of fungal β-glucan because when we incubated this fungal carbon source with GH30_3 and GH157 together, the products generated by both enzymes were glucose, 1,6-β-glucobiose 1,3-β-glucotetraose and the heptasaccharide present in the growth medium generated by Baccell WH2 (Fig. 2E). Figure 3F displays the mass spectra of the main oligosaccharides released by BT in the growth medium, confirming the presence of a disaccharide as the main product, corresponding to 1,6-β-glucobiose as was indicated in the HPLC chromatogram (Fig. 3D).

Cross-feeding Bacteroides/Bifidobacterium/Lactiplantibacillus. After we confirmed the release of oligosaccharides into the growth medium by *Bacteroides* when grown on mycoprotein β-glucan, we hypothesised that this phenomenon would allow other gut commensals to cross-feed on such released oligosaccharides.
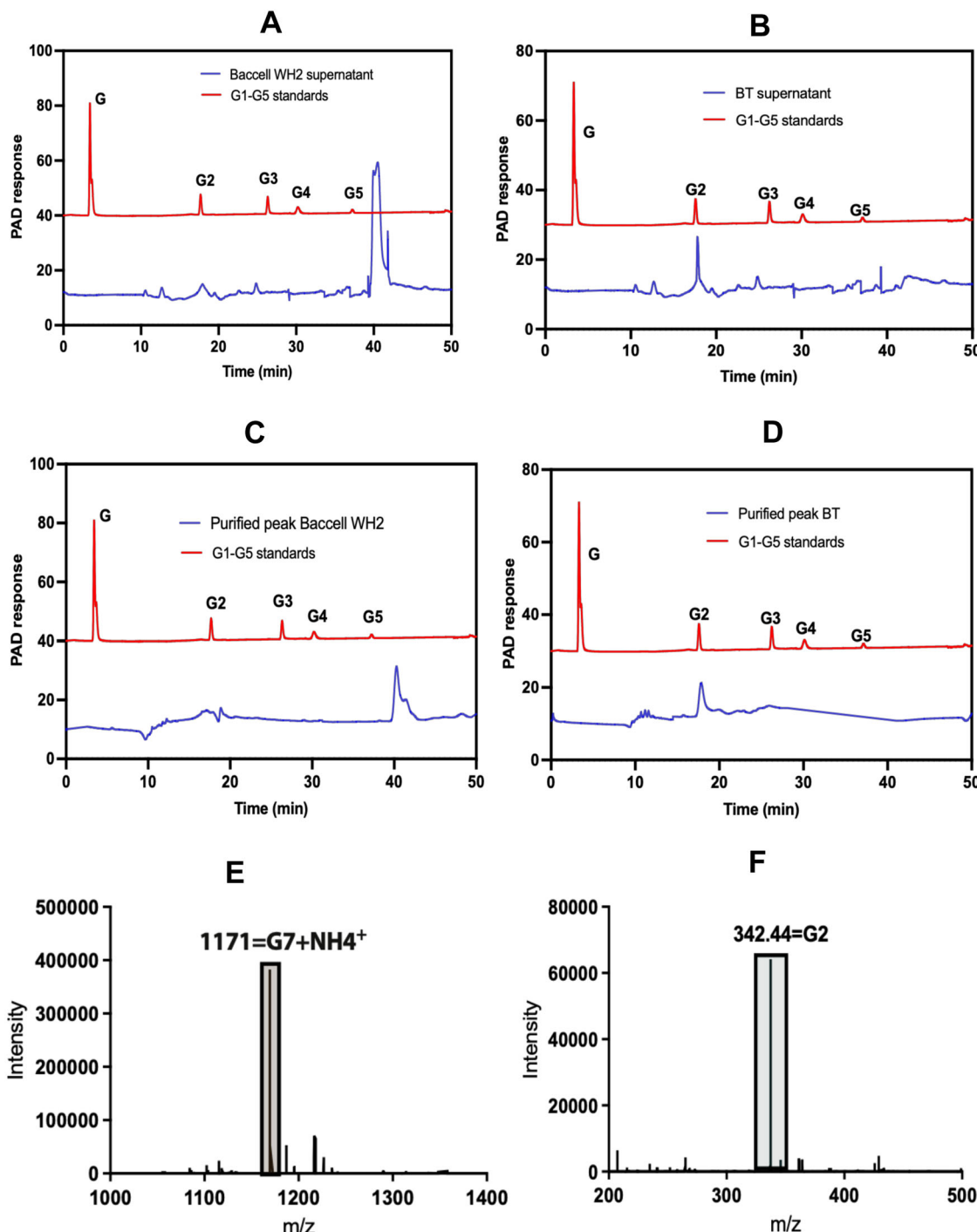
Fig. 3 Characterization of oligosaccharides released by Bacteroides when using β-1,3-glucan. A HPLC chromatogram of the growth media of Baccell WH2 on fungal β-glucan. **B** Same as Panel A with BT. **C** Purified oligosaccharide from Baccell WH2 after Gel Filtration (GF) column. **D** Purified oligosaccharide from BT after GF column. **E** LC/MS of Baccell WH2 supernatant grown on fungal β-glucan. **F** LC/MS of BT supernatant grown on fungal β-glucan. All HPLC and LC/MS experiments have been performed in 3 different independent replicates ($n = 3$).

Indeed, Fig. 4 shows that *Bifidobacterium strains* are able to grow when co-cultivated with *Bacteroides* on fungal β-glucan. We screened the overnight supernatant from Baccell WH2 and BT grown in β-glucan with several available *Bifidobacterium* and *Lactobacillus* strains showing that, in the case of Baccell WH2 supernatant, *Bi. breve* UCC2003, *Bi. longum* subsp. *longum* NCIMB 8809 and *Lb. plantarum* WCFS1 are unable to use intact β-glucan as a carbon source, yet that they can utilise the heptasaccharide released by Baccell WH2 (Fig. 4A). We confirmed

the ability of these strains to use the heptasaccharide testing the growth media before and after the *Bi. breve* UCC2003, *Bi. longum* subsp. *longum* NCIMB 8809 and *Lb. plantarum* WCFS1 growth. Figure 4B confirms the use of the heptasaccharide by *Bi. longum* subsp. *longum* NCIMB 8809, with *Bi. breve* UCC2003 and *Lb. plantarum* WCFS1 exhibiting a more modest ability to use the released oligosaccharide too. After 24 h fermentation, *Bi. longum* subsp. *longum* NCIMB 8809 reached a final optical density of 0.8 when using the supernatant from Baccell WH2. *Bi. breve* and *Lb.*

7
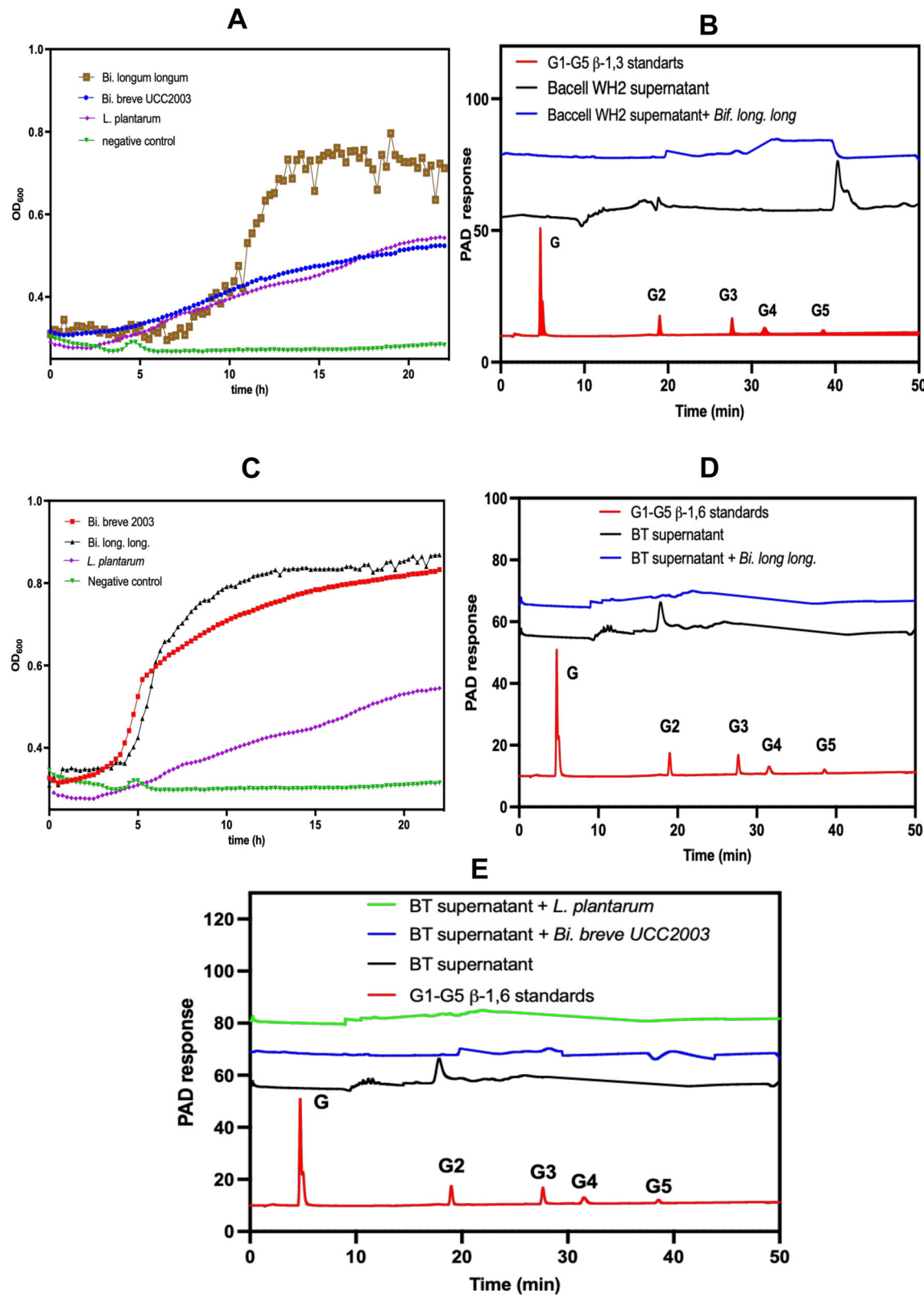
Fig. 4 Consumption of β-glucan oligosaccharides released by *Bacteroides* into the growth media by Bifidobacterium species. A Growth of *Bifidobacterium* with fungal β-glucan supernatant from Baccell WH2. **B** HPLC analysis of supernatants before and after growth of *Bifidobacterium longum subsp. longum* on supernatants from Baccell WH2. **C** Growth of *Bifidobacterium* with fungal β-glucan supernatant from BT. **D** HPLC analysis of supernatants before and after growth of *Bifidobacterium* longum *subspecie longum* on cell-free supernatant of BT grown on fungal β-glucan. **E** HPLC analysis of supernatants before and after growth of *Bi breve UCC2003* and *L. plantarum* on cell-free supernatants of BT grown on fungal β-glucan. All growths and HPLC experiments have been produced in 3 different independent replicates (*n* = 3).
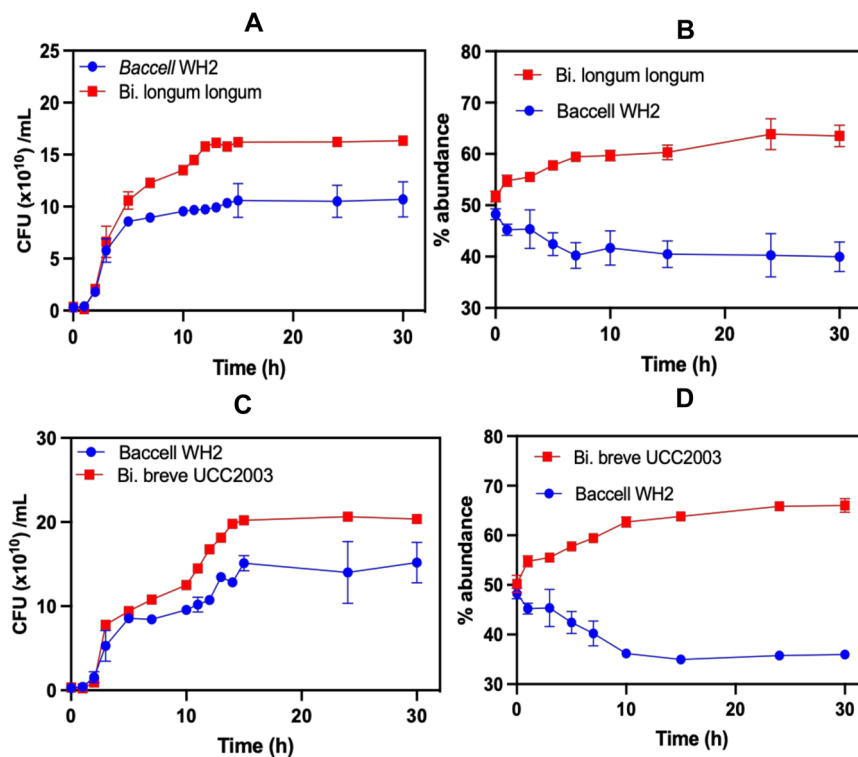
Fig. 5 Cross-feeding experiments between Baccell WH2 and *Bifidobacterium* and *Lactiplantibacillus spp*. A Colony forming units of Baccell WH2 + *Bi. longum subsp. longum*. **B** Percentage of Baccell WH2 + *Bi. longum subsp. longum*. **C** Colony forming units of Baccell WH2 + *Bi. Breve* UCC2003. **D** Percentage of Baccell WH2 + *Bi. breve* UCC2003. All cross-feeding experiments have been produced in 3 different independent replicates ($n = 3$).

plantarum were able to use these oligosaccharides but to a lesser degree, reaching a final optical density of 0.6.

When the supernatant of BT was used as carbon source for the screening of *Bi. breve* UCC2003, *Bi. longum* subsp. *longum* NCIMB 8809 and *Lb. plantarum* WCFS1, the disaccharide which is otherwise accumulating in the medium is now not present, indicating that this β-1,6-glucobiose is used by the bifidobacterial and *Lactiplantibacillus* strains to sustain their growth (Fig. 4C, D). Analysis of the growth medium by HPLC was also performed for *Bi. breve* UCC2003 and *Lb. plantarum* WCFS1 confirming their ability to use the β-1,6-glucobiose as carbon source (Fig. 4E).

To confirm this newly discovered cross-feeding interaction between *Bacteroides* and *Bifidobacterium* species, we performed cross-feeding experiments at different time points where we checked a co-culture of both species tracking the colony forming units and 16 S rRNA-based qPCR quantification of each species during growth (Figs. 5, 6). In this co-culture experiment, Baccell WH2 allowed *Bi. longum* subsp. *longum* NCIMB 8809 and *Bi. breve* UCC2003 to grow when both strains are cultivated with the intact fungal β-glucan as is obvious from viable count assessments (Fig. 5A for *Bi. longum* subsp. *longum* and 5 C for *Bi. breve*) and percentage of both bacteria in the co-culture (Fig. 5B for *Bi. longum* subsp. *longum* and 5D for *Bi. breve*). The observation of *Bifidobacterium* growth when in co-culture with Baccell WH2 in the presence of β-glucan agreed with the monoculture fermentation findings, when cell-free supernatant was used as carbon source, as displayed in Fig. 4.

Similarly, BT allowed growth of *Bi. breve* UCC2003 and *Bi. longum subsp. longum* NCIMB 8809 in co-culture as can be observed in Figs. 6A and 6C (colony forming units) and 6B and 6D (percentage), respectively. Again, it confirmed the ability of *Bacteroides* to allow for specific cross-feeding networks with *Bifidobacterium* strains in the gut when the former bacteria grow on dietary fungal β-glucan.

Finally, to expand this study with other commensal members of the human gut microbiota, we performed the co-culture experiment of Baccell WH2 and BT as primary and *Lactiplantibacillus plantarum* WCFS1 as a secondary degrader to confirm the ability of Baccel WH2 and BT to allow growth of this commensal. Figs. S2A and S2B for Baccell WH2 and Figs. S2C and S2D for BT showed this ability in co-culture too.

Ability of *Bi. breve* UCC2003 to utilize β-1,6-glucobiose. As stated above, *Bi. breve* UCC2003 can use glucobiose released by Baccell WH2 when grown on β-glucan. We conducted a bioinformatic analysis on the genome of the former bacterium to identify glycoside hydrolases that would allow *Bifidobacterium* to utilise this oligosaccharide. We identified a GH1 (Bbr_0109) which had previously been shown to act on cellobiose as substrate[53]. We hypothesised that this protein would act on gluco-oligosaccharides with different linkages as substrates. To prove our hypothesis, we recombinantly expressed the protein and performed enzymatic assays with β-1,4, β-1,3 and β-1,6-glucobiose as substrates of the enzyme. Bbr_0109 was active on β-1,4 and β-1,6-glucobiose as we expected, and this activity is shown by HPLC in Figs. S3A and S3B, respectively. In addition, we were able to characterise this activity and the kinetic parameters are calculated in Table 1. Bioinformatics analysis of the *Bi. longum subsp. longum* genome didn't reveal any homolog of Bbr_0109, or other candidate enzymes responsible for its ability to cross-feed on β-glucan-derived oligosaccharides and further work is therefore required to unravel the metabolic pathway responsible for this activity.

Metabolites released by *Bacteroides/Bifidobacterium* co-cultivation on β-glucan. After we confirmed the ability of *Bacteroides* to specifically allow *Bifidobacterium* growth when the
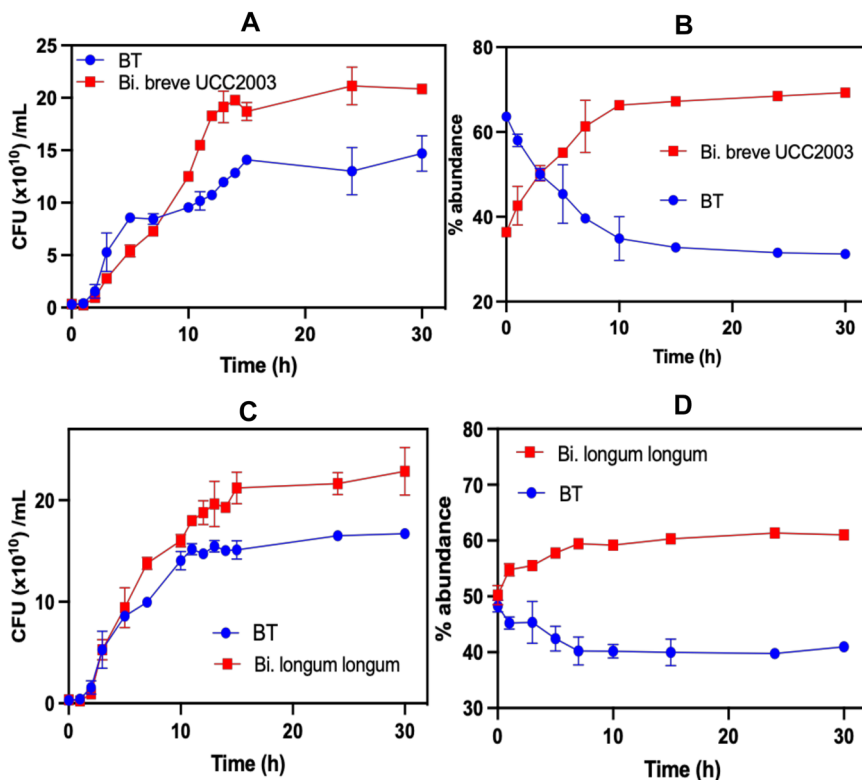
Fig. 6 Cross-feeding experiments between BT and *Bifidobacterium* and *Lactiplantibacillus* spp. A Colony forming units of BT + *Bi. breve* UCC2003. **B** Percentage of BT + *Bi. breve* UCC2003. **C** Colony forming units of BT + *Bi. longum* subsp. *longum*. **D** Percentage of BT + *Bi. longum* subsp. *longum*. All cross-feeding experiments have been produced in 3 different independent replicates (*n* = 3).

Table 2 Millimolar (mM) concentration of the metabolites generated in the cell-free supernatant of MM + 1% β-glucan, following 24 h incubation with Baccell WH2 and *B. breve* UCC2003.

	Succinate (mM)	Acetate (mM)	Lactate (mM)	Formate (mM)
No inoculum	ND	0.9 ± 0.1	0.10 ± 0.01	1.8 ± 0.2
Baccell WH2	78 ± 9.8	12 ± 2.2	ND	ND
B. breve UCC2003	ND	1.1 ± 0.1	3.5 ± 0.4	2.6 ± 0.3
Baccell WH2/*B. breve* UCC2003	99 ± 10.1	115 ± 16.2	21 ± 2.8	16 ± 1.9

Measures were made in triplicate.

former bacterium is cultivated on β-glucan, we performed a metabolomics analysis of the culture media to assess short chain fatty acid (SCFA)/lactate/succinate production by *Bacteroides* and *Bifidobacterium* in mono- and co-cultures. Table 2 lists the detected levels of acetate, butyrate, propionate, and lactate by these fermentations. Baccell WH2 was shown to produce succinate (78 mM) and acetate (12 mM) as main SCFAs produced in monoculture. As control, *Bi. longum* subsp. *longum* NCIMB 8809 failed to produce any significant amounts of SCFAs because of its inability to use the intact mycoprotein β-glucan. In contrast, in co-culture, acetate was the higher concentrated SCFA (115 mM) followed by succinate (99 mM) as consequence of the subsp. *longum* NCIMB 8809 growth. Finally, formate (16 mM) and lactate (21 mM) were also produced in co-culture because of the ability of *Bifidobacterium* to produce these metabolites.

Discussion

β-glucan has previously been demonstrated to act as a prebiotic carbohydrate with various reported beneficial outcomes for human health[54–57]. Recently, Dejean et al. (2020) showed the ability of *Bacteroides* strains to utilise β-(1,3)-glucans, such as that derived from yeast or algal laminarin[13]. These authors showed that *Bacteroides uniformis* ATCC 8492 employs a specific polysaccharide utilisation locus for the deconstruction of these β-(1,3)-glucans. This genetic locus encodes a cell surface-associated glycoside hydrolase family 158 (GH158) enzyme and a GH16 to initiate depolymerization of the polysaccharide to release oligosaccharides that are incorporated by the SusC/D-like pair into the periplasm where a GH3 (β-glucosidase) continues with the degradative process converting all oligosaccharides into glucose monomers, which then enter central glycolytic catabolism. Also in 2020, Singh et al.[37] showed the ability of *Bacteroides uniformis* JCM 13288 to degrade β-(1,3)-glucans with a similar enzymatic mechanism to the afore mentioned *Bacteroides uniformis* strain. However, these latter authors revealed an additional GH30 activity able to degrade β-(1,6)-glucan side chains of the molecule releasing β-1,6-glucobiose. In addition, they demonstrated that the oligosaccharides released by this *Ba. uniformis* strain can be used by other members of the gut microbiota, which either did not grow or grew poorly on laminarin.

In the case of barley β-glucan, Tamura et al.[34–36] showed that Bacova and Baccell WH2 use a surface associated GH16 enzyme (Bovatus_03149 and BcellWH2_04354) to initiate the degradative process. In addition, the same authors showed that there are two GH3 enzymes present in the periplasm of Bacova (Bovatus_03146 and Bovatus_03153) and one in that of Baccell WH2 (BcellWH2_4356) to complete the metabolism of barley β-glucan.

In the work described here, we reveal an alternative pathway followed by Baccell WH2 to degrade dietary fungal β-glucans,

such as the polysaccharide derived from *Fusarium venenatum*, the main ingredient employed in Quorn® products, where the chemical structure consists of a linear β-(1,3)-glucan backbone with β-(1,6)-glucan as side chains (Fig. 1A). For this metabolism, Baccell WH2 employs two GULs to degrade this complex glycan, as revealed by proteomics and confirmed by transcriptomics (Fig. 1C and S1B, respectively). Within these GULs, Baccell WH2 encodes a novel GH157 and a GH30_3, both predicted to be located at the cell surface, to start the degradation of the complex glycan. These GULs were also shown to encode additional glycoside hydrolases required to fully degrade the gluco-oligosaccharides released by the outer membrane surface proteins and incorporated into the periplasm by the SusC/D-like pairs. These periplasmic proteins represent typical β-glucosidases belonging to GH families 3 and 2. Finally, this GUL encodes a protein with an unknown function (BcellWH2_02538), with a predicted location to be in the surface of Baccell WH2. This protein is in a perfect location to be a Surface Glycan Binding Protein (SGBP), which has been shown to help the SusC/D-like pair in the binding of oligosaccharides at the bacterial cell surface[35,36,58]. The reason for the presence of three different β-glucosidases (two GH3 and one GH2) encoded by these GULs to target fungal β-glucan remains speculative to us. We postulate that Baccell WH2 could act on several types of β-glucans, not only fungal sources, with different chemical structures. For that reason, they use distinct β-glucosidases to hydrolyse different linkages in these gluco-oligosaccharides. However, we can't rule out the possibility that some of these β-glucosidases are redundant and the bacterium is evolving to remove some of these genes from its genome under the high selection pressure imposed by the gut environment.

Finally, we show that Baccell WH2 and BT can share oligosaccharides with other members of the gut microbiota, including commensals *Bifidobacterium* and *Lactiplantibacillus species*. In this respect, Baccell WH2 was shown to allow cross-feeding interactions with *Bi. longum* subsp. *longum, Bi. breve* UCC2003 and *Lactiplantibacillus plantarum* WCFS1 (Fig. 5 and S2). In addition, BT was shown to promote specific cross-feeding with *Bi. longum* subsp. *longum, Bi. breve* UCC2003 and *Lactiplantibacillus plantarum* WCFS1 (Fig. 6 and S2), enabling growth of both bacteria in co-culture. Since the oligosaccharides released by BT and Baccell WH are different (i.e. glucoheptasaccharide and glucobiose), it will select for specific interactions in the gut. *Bi. breve* UCC2003 encodes a GH1 (Bbr_0109) to degrade the glucobiose released by BT. This GH1 is very specific for glucobiose, being active on β-(1,3)glucobiose, β-(1,4)glucobiose and β-(1,6) glucobiose (Table 1). However, the inability to act on glucotriose or other longer oligosaccharides may explain the partial ability of *Bi. breve* to use the heptasaccharide released by Baccell WH2 and, as consequence, its inability to grow in Baccell WH2 supernatant. These specific interactions in the cross-feeding between *Bacteroides* and *Bifidobacterium* members have been shown for other polysaccharides such as arabinogalactan[31], arabinoxylan[48] or inulin[59].

In terms of β-glucan, little has been reported on cross-feeding interactions by members of the gut microbiota. As we stated above, Singh et al.[37] showed the ability of *Ba. uniformis* JCM 13288 to share gluco-oligosaccharides with *Blautia producta* JCM1471, *Ruminococcus faecis* JCM15917 *and Bifidobacterium adolescentis* JCM 1275 when they grow on laminarin as the sole carbon source. In addition, Centanni et al.[60] showed interactions between *Bacteroides ovatus*, *Subdoligranulum variabile*, and *Hungatella hathewayi* using barley β-glucan as a carbon source. They showed that *Ba. ovatus* released 3-O-β-cellobiosyl-d-glucose and 3-O-β-cellotriosyl-d-glucose into the medium as final products and these oligomers enabled growth of the other two

bacteria with preference for 3-O-β-cellotriosyl-d-glucose in the case of *Hungatella hathewayi*. However, to the best of our knowledge our study for the first time reveals detailed molecular interactions between different members of *Bacteroides spp*. and other human commensals (*Bifidobacterium* and *Lactiplantibacillus*) when using fungal β-glucan.

Finally, we have shown the ability of Baccell and *B. breve* UCC2003 to produce different SCFA in mono- and coculture as a result of β-glucan fermentation. Baccell produces acetate and succinate as main metabolites when grow in monoculture on β-glucan, whereas co-cultivation with *B. breve* UCC2003 was shown to result in the production of not only acetate and succinate but also lactate and formate, the latter from *Bifidobacterium* fermentation. This production is in accordance with other fermentative processes where *Bacteroides* produces acetate as the main SCFA[31]. Munoz et al. have reported on the production of lower levels of succinate (60 mM) for AGP fermentation than for β-glucan (78 mM, Table 2) when Baccell was cultivated in monocultures. However, the opposite effect is observed for acetate production as Baccell was shown to produce 24 mM and 12 mM acetate when cultivated on AGP or β-glucan, respectively[31]. However, SCFA production appears to be higher for all metabolites when Baccell was co-cultivated with *B. breve* UCC2003 in the presence of β-glucan (115, 99, 21 and 16 mM for acetate, succinate, lactate and formate, respectively), when compared to co-cultivation in the presence of AGP (94, 68, 6 and 6.9 mM for acetate, succinate, lactate and formate, respectively)[31].

All data presented in this work allowed us to obtain a general model for the degradation of fungal β-glucan in Baccell WH2 and its interaction with bifidobacteria as secondary degraders (Fig. S3C).

In conclusion, this paper shows the ability of different members of human gut *Bacteroides* strains to use dietary fungal β-glucan. We have shown that *Bacteroides* employs two main GULs to degrade this complex glycan with novel enzymatic activities and families discovered in those GULs and that they share oligosaccharides and *Bi. longum* subsp. *longum* and *Bi. breve* UCC2003 selectively where able to use them. Finally, we have shown the specific enzyme (Bbr_0109, GH1) encoded in *Bi. breve* UCC2003 responsible for the degradation of the oligosaccharide released by BT. Thus, the study provides evidence that fungal β-glucan utilisation genes are present not only into *Bacteroides* but also into Gram-positive bacteria. Diverse β-glucans GULs identified in this study may pave the way for the development of engineered functional foods for the improvement of human health through proper nutritional intervention therapy.

Methods

Reagents. Yeast and barley β-glucan tested in this study were purchased from Megazyme (Dublin, Ireland). D-Galactose and D-glucose were purchased from Sigma (United Kingdom). Luria-Bertani (LB) growth medium was purchased from Formedium (Norfolk, U.K.), reinforced clostridial agar from Oxoid Ltd. (Basingstoke, England) and Brain Heart Infusion from Sigma (United Kingdom). All reagents were of analytical grade.

Mycoprotein β-glucan extraction and purification. Cell wall material from *Fusarium venenatum* was extracted and the different glycan parts were purified according to a previously described method[61]. Briefly, cell wall material was alkaline extracted with 3% NaOH for 75 h obtaining two fractions: fraction 1 soluble in bases and fraction 2, insoluble in bases. Fraction 1 was shown to contain mannoproteins and β-1,6-1,3-glucan and fractions contained this β-1,6-1,3-glucan associated with chitin. Fraction 1 was neutralized with glacial acetic acid and centrifuged at $15,000 \times g$ during 30 min and the supernatant subjected to a 24 h dialysis. After dialysis, the mixture was freeze-dried prior to its use (Fig. S4A, B).

Growths, Proteomics and RT-qPCR
Growth. Ba. ovatus ATCC8483 (Bovatus), Ba. thetaiotaomicron VPI-5482 (BT), Ba. cellulosilyticus DSMZ14838 (Baccell DSM) and Ba. cellulosilyticus WH2 (Baccell WH2) are capable of growth on all carbon sources of interest in this study and,

therefore, were cultured directly in 3 ml of Minimal Media (MM) containing 1% (wt/vol) carbohydrate, as described above[48].

q-PCR. *Bacteroides sp.* were precultured on MM + Glucose, pelleted, washed, resuspended twice in MM without any carbon source, and inoculated to an A_{600} of ~0.3 in 4 ml of MM containing 1% (wt/vol) carbohydrate. Bacterial cultures were harvested in triplicate (at mid-log phase [A_{600}, ~0.6] after 5 h of incubation for Bovatus, BT, Baccell DSM and Baccell WH2, placed in RNA protect (Qiagen) for immediate stabilisation of RNA, and then stored at –20 °C. RNA was extracted and purified with the RNeasy minikit (Qiagen), and RNA purity was assessed by spectrophotometry. One μg of RNA was used for reverse transcription and synthesis of the cDNA (SuperScript VILO master mix; Invitrogen). Quantitative PCRs (20 μl final volume) using specific primers were performed with a SensiFast SYBR Lo-ROX kit (Bioline) on a 7500 Fast real-time PCR system (Applied Biosystems) (Table S2). Data were normalised to 16 S rRNA transcript levels, and changes in expression levels were calculated as fold change compared with levels for cultures of MM containing glucose.

Proteomics. Baccell WH2 was cultured in the same way as before with 1% β-glucan as complex polysaccharide and glucose as monosaccharide control. Bacterial cultures were harvested in triplicate after growth in MM+Glc or MM+β-glucan. Cells were collected by centrifugation (3,500 g, 15 min, 4 °C) and washed three times with PBS pH 7.4. Cell pellets were subsequently resuspended in 8 M urea buffer in 50 mM triethylammonium bicarbonate, containing 5 mM tris(2-carboxyethyl) phosphine. Cells were lysed via sonication using an ultrasonic homogenizer (Hielscher). Proteins were subsequently alkylated for 30 min at room temperature using 10 mM iodoacetamide in the dark. Protein concentration was determined using a Bradford protein assay (Thermo Fisher Scientific). Protein samples, containing 50 μg total protein, were diluted fivefold with 50 mM triethylammonium bicarbonate and protein digestion was performed at 37 °C for 18 h with shaking at 300 r.p.m. A protein to trypsin ratio of 50:1 was used. Trypsin digestion was stopped, and peptides were desalted as described above.

Mass spectrometry. Peptides were dissolved in 2% acetonitrile containing 0.1% trifluoroacetic acid, and each sample was independently analysed on an Orbitrap Fusion Lumos Tribrid mass spectrometer (Thermo Fisher Scientific), connected to an UltiMate 3000 RSLCnano System (Thermo Fisher Scientific). Peptides were injected on an Acclaim PepMap 100 C18 LC trap column (100 μm ID × 20 mm, 3 μm, 100 Å) followed by separation on an EASY-Spray nanoLC C18 column (75 μm × 500 mm, 2 μm, 100 Å) at a flow rate of 300 nlmin⁻¹. Solvent A was water containing 0.1% formic acid, and solvent B was 80% acetonitrile containing 0.1% formic acid. The gradient used for analysis of surface-shaved samples was as follows: solvent B was maintained at 3% for 6 min, followed by an increase from 3 to 35% B in 43 min, 35–90% B in 0.5 min, maintained at 90% B for 5.4 min, followed by a decrease to 3% in 0.1 min and equilibration at 3% for 10 min. The gradient used for analysis of proteome samples was as follows: solvent B was maintained at 3% for 6 min, followed by an increase from 3 to 35% B in 218 min, 35–90% B in 0.5 min, maintained at 90% B for 5 min, followed by a decrease to 3% in 0.5 min and equilibration at 3% for 10 min. The Orbitrap Fusion Lumos was operated in positive-ion data-dependent mode using a modified version of the recently described charge-ordered parallel ion analysis (CHOPIN) method for synchronized use of both the ion trap and the Orbitrap mass analysers. The CHOPIN method is derived from the 'Universal Method' developed by Thermo-Fisher, to extend the capabilities of mass analyser parallelization. The precursor ion scan (full scan) was performed in the Orbitrap in the range of 400–1600 *m/z* with a resolution of 120,000 at 200 *m/z*, an automatic gain control (AGC) target of 4 × 10⁵ and an ion injection time of 50 ms. MS/MS spectra of doubly charged precursor ions were acquired in the linear ion trap (IT) using rapid scan mode after collision-induced dissociation (CID) fragmentation. A CID collision energy of 32% was used, the AGC target was set to 2 × 10³ and a 300 ms injection time was allowed. Precursor ions with charge state 3–7 and with an intensity <5 × 10⁵ were also scheduled for analysis by CID/IT, as described above. Precursor ions with charge state 3–7 and with an intensity >5 × 10⁵ were, however, acquired in the Orbitrap (FT) with a resolution of 30,000 at 200 *m/z* after high-energy collisional dissociation (HCD). An HCD collision energy of 30% was used, the AGC target was set to 1 × 10⁴ and a 40 ms injection time was allowed. The number of MS/MS events between full scans was determined on-the-fly to maintain a 3 s fixed duty cycle. Dynamic exclusion of ions within a ± 10 p.p.m. *m/z* window was implemented using a 35 s exclusion duration. An electrospray voltage of 2.0 kV and capillary temperature of 275 °C, with no sheath and auxiliary gas flow, was used.

Mass spectrometry data analysis. All MS/MS spectra were analysed using Max-Quant 1.5.1.739 and searched against a database of *Bacteroides cellulosilyticus* MGS:158 (containing 4369 entries). Protein sequences were downloaded from Uniprot on 10 May 2020. Peak list generation was performed within MaxQuant and searches were performed using default parameters and the built-in Andromeda search engine. The enzyme specificity was set to consider fully tryptic peptides, and two missed cleavages were allowed. Oxidation of methionine, N-terminal acetylation and deamidation of asparagine and glutamine were allowed as variable modifications. A protein and peptide false discovery rate of less than 1% was

employed in MaxQuant. Proteins were confidently identified when they contained at least two unique tryptic peptides. Proteins that contained similar peptides and that could not be differentiated based on MS/MS analysis alone were grouped to satisfy the principles of parsimony. Reverse hits and contaminants were removed before downstream analysis. Skyline 4.1.0.11796 was used for extraction of ion chromatograms. Gene ontology enrichment was performed using PANTHER42 and subcellular protein localization prediction was performed using LocateP v243.

Cloning, expression and purification of recombinant proteins. The genes associated with the PULs described in Baccell WH2 [BccellWH2_01926 (GH3), BccellWH2_01931 (GH157), BaccellWH2_02537 (GH30_3)] and the proteins in BT [BT3312 (GH30_3) and BT3314 (GH3)] were amplified from Baccell WH2 and BT respectively using their genomic DNA as template and cloned into pET28a (Novagen) using NheI and XhoI restriction sites for production and purification of its encoded protein facilitated by the incorporation with an N-terminal His₆ tag (Table 2S). For this, *E. coli* TOP10 cells (ThermoFisher Scientific) were used. The recombinant construct was sequenced (Eurofins Genomics) to verify its genetic integrity and then used to transform *E. coli* BL21 (DE3) expression cells (Thermo-Fisher Scientific). Cells were cultured in Luria-Bertani (LB) medium containing 50 mg/ml kanamycin antibiotic to mid-log phase (A_{600nm} of ~0.6). Protein expression was induced by adding 0.1 mM isopropyl β-D-1-thiogalactopyranoside (IPTG) to cells followed by growth overnight at 16 °C. The next day, cells were harvested by centrifugation (4000 × g) and re-suspended in the Talon buffer (20 mM Tris/HCl pH 8.0 plus 100 mM NaCl). Resuspended cells were disrupted and centrifuged (16,000 × g) for 20 min at 4 °C, after which recombinant proteins were purified from the resulting cell free extract by immobilised metal affinity chromatography (IMAC) using Talon™, a cobalt-based matrix. In the process, the Cell Free Extract (CFE) was loaded on a column containing the Talon resin and then washed with a Talon buffer. Another wash was performed with Talon buffer containing 10 mM imidazole followed by recombinant protein elution with 100 mM imidazole. Purified proteins were then exchanged into a buffer of choice by standard dialysis.

Enzyme kinetics and product profile. All enzyme assays, unless otherwise stated, were carried out in a 20 mM sodium phosphate buffer, pH 7.0, containing 150 mM NaCl and performed in triplicate. Assays were carried out at 37 °C employing 1 μM each GH [BccellWH2_01926 (GH3), BccellWH2_01931 (GH157), BccellWH2_02537 (GH30_3), BcellWH2_02541 (GH2), BT3312 (GH30_3) and BT3314 (GH3)] in the presence of 150 μM β-glucan. Aliquots were taken over a 16 h time course, and samples and products were assessed by TLC and high-pressure anion exchange chromatography (HPAEC) with pulsed amperometric detection (PAD). Sugars (mono and short oligosaccharides) were separated on a Carbopac PA1 guard and analytical column in an isocratic program of 100 mM sodium hydroxide for 40 min and then with a 100% linear gradient of 500 mM sodium acetate over 60 min. Sugars were detected using the carbohydrate standard quad waveform for electrochemical detection at a gold working electrode with an Ag/AgCl pH reference electrode.

In the case of GH30_3 and GH157, polysaccharide hydrolysis was quantified using a DNSA (dinitrosalicylic acid) reducing-sugar assay[48]. Assays were conducted in a final volume of 1 ml at the optimum pH and 37 °C for 10 min. Reactions were terminated by the addition of an equal volume (1 ml) of DNSA reagent. Colour was developed by heating to 80 °C for 20 min before reading A_{540}. Glucose (25 to 150 μM) was used to generate a standard curve for quantitation. To determine Michaelis-Menten parameters, different concentrations of polysaccharide solutions were used over the range of 0.025 to 3 mg ml⁻¹ with the appropriate concentration of enzyme for 10 min, and the numbers of reducing ends released were quantified as described above. The values were plotted using linear regression giving k_{cat}/K_m as the slope of the line.

In the case of GH3s and GH2, the enzymatic assay was measured in the spectrophotometer at a wavelength of 340 nm measuring the releasing of glucose by the couple assay kit from Megazyme (Dublin, Ireland) for glucose release quantification.

Cross-feeding experiments. Before co-culture, Baccell WH2 and BT were grown in brain–heart infusion (BHI, Sigma Aldrich, UK) and washed twice in PBS. Monocultures of bifidobacterial strains were grown on Reinforced Clostridium Media (Oxoid, Basingstoke UK) and washed in PBS before being used to inoculate Minimal Media (MM) containing 1% Mycoprotein β-glucan[11]. Co-cultures were grown in inoculate Minimal Media containing 1% Mycoprotein β-glucan and the experiments were done in triplicate. Samples of 0.5 ml were taken at regular intervals during growth, which were serially diluted and plated onto BHI with agar and porcine haematin for determination of total CFUs per millilitre of the culture (Baccell WH2 and BT) and onto Reinforced Clostridium Media with 0.05% cysteine (for wild type bifidobacterial strains) and with 100 μg/ml erythromycin. *Lactiplantibacillus plantarum* WCSF4 was routinary grown on MRS media (Melford, U.K.) supplemented with vancomycin 10 μg/ml. Each Monoculture of *Bacteroides*, *Bifidobacterium* or *Lactiplantibacillus* was also plated for determination of CFUs per millilitre at intervals during cultivation.

Aliquots taken from mono and co-cultures were analysed by qPCR to quantify the ratio of each bacterial species during cultivation amplifying the 16 S rRNA gene

for each bacterium in the sample. We used specific primers (1 µM) for each bacterium for this qPCR and is shown in Table 2S.

Sugars (mixed type of oligosaccharides from growth media) were separated on a Carbopac PA200 guard and analytical column in an isocratic program of 100 mM sodium hydroxide for 40 min and then with a 100% linear gradient of 500 mM sodium acetate over a 60 min period. Sugars were detected using the carbohydrate standard quad waveform for electrochemical detection at a gold working electrode with an Ag/AgCl pH reference electrode.

Structural prediction with AlphaFold and Phyre2. 3-D structure of GH157 (BcellWH2_01931) was modelled using AlphaFold2 colab software We thank the AlphaFold team for developing an excellent model and open sourcing the software https://colab.research.google.com/github/sokrypton/ColabFold/blob/main/AlphaFold2.ipynb#scrollTo=UGUBLzB3C6WN). Bccell WH2_02537 (GH30_3) model was obtained using Phyre2 server[52]. Structures were visualised using Pymol (The PyMOL Molecular Graphic system, version 2.0 Schrodinger, LLC).

Metabolite analysis by high performance liquid chromatography (GC/MS). HPLC analysis was used to assess SCFA production by (cross-feeding) Baccell WH2 and Bi. Breve UCC2003. Growth medium supernatants from stationary phase (co-cultures) were sterilized (0.45 µM filter, Costart Spin-X column) and injected into an UltiMate® BioRS Thermo HPLC system (Thermo Fisher Scientific) with a refractive index detector system. This system was used to identify and calculate the production of acetate, lactate and butyrate as a result of carbohydrate fermentation. Concentrations were calculated based on known standards. Non-fermented medium containing LW-AG served as control. An Accucore™ C18 HPLC column was used and maintained at 65 °C. Elution was performed for 25 min using 10 mM H_2SO_4 solution at a constant flow rate of 0.6 ml min^{-1}.

LC/MS of the oligosaccharides released by Baccell WH2 and BT. The sample containing the oligosaccharides generated from the supernatant from Baccell WH2 and BT grown on β-glucan was diluted 1:10 (v/v) with Buffer B (85% acetonitrile/15% 50 mM ammonium formate in water, pH 4.7) and 0.5 µl was analysed by liquid chromatography–mass spectrometry analysis via elution from a ZIC-HILIC (SeQuant, 3.5 µm, 200 Å, 150 × 0.3 mm, Merck) capillary column. The column was connected to a NanoAcquity HPLC system (Waters) and heated to 35 °C with an elution gradient as follows: 100% Buffer B for 5 min, followed by a gradient to 25% Buffer B/75% Buffer A (50 mM ammonium formate in water, pH 4.7) over 40 min. The flow rate was 50 µl min-1 and 10 column volumes of Buffer B equilibration was performed between injections. MS data were collected using a Bruker Impact II QT of mass spectrometer operated in positive ion mode, 50–2000 m/z, with capillary voltage and temperature settings of 2800 V and 200 °C respectively, together with a drying gas flow and nebulizer pressure of 6 l min^{-1} and 0.4 bar. The MS data were analysed using Compass DataAnalysis software (Bruker).

Reporting summary. Further information on research design is available in the Nature Portfolio Reporting Summary linked to this article.

Data availability

All proteomic data are deposited in PeptideAtlas (identifier PASS04831, raw data for blank, glucose and mycoprotein β-glucan as carbon sources). All data generated during this study are included in this published article (and its supplementary information files). All source data underlying the graphs and charts can be found in Supplementary Data 1. Original SDS gels are available in Fig. S5. Further raw data is available upon request.

References

1. Wardman, J. F., Bains, R. K., Rahfeld, P. & Withers, S. G. Carbohydrate-active enzymes (CAZymes) in the gut microbiome. *Nat. Rev. Microbiol.*, https://doi.org/10.1038/s41579-022-00712-1 (2022).
2. de Vadder, F. & Mithieux, G. Gut-brain signaling in energy homeostasis: the unexpected role of microbiota-derived succinate. *J. Endocrinol.* **236**, 105–108 (2018).
3. Yang, J. & Yu, J. The association of diet, gut microbiota and colorectal cancer: what we eat may imply what we get. *Protein Cell.* **9**, 474–487 (2018).
4. Cani, P. D. Human gut microbiome: hopes, threats and promises. *Gut* **67**, 1716–1725 (2018).
5. Briggs, J. A., Grondin, J. M. & Brumer, H. Communal living: glycan utilization by the human gut microbiota. *Environ. Microbiol.* **23**, 15–35 (2021).
6. Feng, J. et al. Polysaccharide utilization loci in *Bacteroides* determine population fitness and community-level interactions. *Cell Host Microbe* **30**, 200–215 (2022).
7. Grondin, J. M., Tamura, K., Déjean, G., Abbott, D. W. & Brumer, H. Polysaccharide utilization loci: fueling microbial communities. *J. Bacteriol.* **199**, e00860–00816 (2017).
8. Luis, A. S. et al. Dietary pectic glycans are degraded by coordinated enzyme pathways in human colonic. *Bacteroides. Nat. Microbiol.* **3**, 210–219 (2018).
9. Drula, E. et al. The carbohydrate-active enzyme database: functions and literature. *Nucleic Acids Res.* **50**, 571–577 (2022).
10. Terrapon, N. et al. PULDB: the expanded database of polysaccharide utilization loci. *Nucleic Acids Res.* **46**, D667–D668 (2018).
11. Bågenholm, V. et al. Galactomannan catabolism conferred by a polysaccharide utilization locus of *Bacteroides ovatus*: enzyme synergy and crystal structure of a β-mannanase. *J. Biol. Chem.* **292**, 229–243 (2017).
12. Cartmell, A. et al. A surface endogalactanase in *Bacteroides thetaiotaomicron* confers keystone status for arabinogalactan degradation. *Nat. Microbiol.* **3**, 1314–1326 (2018).
13. Déjean, G. et al. Synergy between cell surface glycosidases and glycan-binding proteins dictates the utilization of specific beta(1,3)-glucans by human gut *Bacteroides*. *mBio* **11**, e00095–00020 (2020).
14. Foley, M. H. et al. A cell-surface GH9 endo-glucanase coordinates with surface glycan-binding proteins to mediate xyloglucan uptake in the gut symbiont *Bacteroides ovatus*. *J. Mol. Biol.* **431**, 981–995 (2019).
15. Rawat, P. S., Seyed Hameed, A. S., Meng, X. & Liu, W. Utilization of glycosaminoglycans by the human gut microbiota: participating bacteria and their enzymatic machineries. *Gut Microbes* **14**, 2068367 (2022).
16. Robb, C. S. et al. Metabolism of a hybrid algal galactan by members of the human gut microbiome. *Nat. Chem. Biol.* **18**, 501–510 (2022).
17. Temple, M. J. et al. A Bacteroidetes locus dedicated to fungal 1,6-β-glucan degradation: Unique substrate conformation drives specificity of the key endo-1,6-β-glucanase. *J. Biol. Chem.* **292**, 10639–10650 (2017).
18. Alessandri, G., Ossiprandi, M. C., MacSharry, J., van Sinderen, D. & Ventura, M. Bifidobacterial dialogue with its human host and consequent modulation of the immune system. *Front. Immunol.* **10**, 2348 (2019).
19. James, K. et al. Metabolism of the predominant human milk oligosaccharide fucosyllactose by an infant gut commensal. *Sci. Rep.* **9**, 15427 (2019).
20. O'Connell Motherway, M. et al. Carbohydrate syntrophy enhances the establishment of *Bifidobacterium breve* UCC2003 in the neonatal gut. *Sci. Rep.* **8**, 10627 (2018).
21. Turroni, F. et al. The infant gut microbiome as a microbial organ influencing host well-being. *Ital. J. Pediatr.* **46**, 16 (2020).
22. Sakanaka et al. Evolutionary adaptation in fucosyllactose uptake systems supports bifidobacterial-infant symbiosis. *Sci. Adv.* **5**, eaaw7696 (2019).
23. James, K., Motherway, M. O., Bottacini, F. & van Sinderen, D. *Bifidobacterium breve* UCC2003 metabolises the human milk oligosaccharides lacto-N-tetraose and lacto-N-neo-tetraose through overlapping, yet distinct pathways. *Sci. Rep.* **6**, 38560 (2016).
24. James, K., O'Connell Motherway, M., Penno, C., O'Brien, R. L. & van Sinderen, D. *Bifidobacterium breve* UCC2003 employs multiple transcriptional regulators to control metabolism of particular human milk oligosaccharides. *Appl. Environ. Microbiol.* **84**, https://doi.org/10.1128/aem.02774-17 (2018).
25. Özcan, E. S. & Sela, D. A. Inefficient metabolism of the human milk oligosaccharides lacto-n-tetraose and lacto-n-neotetraose shifts *Bifidobacterium longum* subsp. *infantis* Physiology. *Front. Nutr.* **5**, 46 (2018).
26. Sakurama, H. et al. Lacto-N-biosidase encoded by a novel gene of *Bifidobacterium longum* subspecies *longum* shows unique substrate specificity and requires a designated chaperone for its active expression. *J. Biol. Chem.* **288**, 25194–25206 (2013).
27. Bunesova, V., Lacroix, C. & Schwab, C. Fucosyllactose and L-fucose utilization of infant *Bifidobacterium longum* and *Bifidobacterium kashiwanohense*. *BMC Microbiol.* **16**, 248 (2016).
28. Walsh, C., Lane, J. A., van Sinderen, D. & Hickey, R. M. Human milk oligosaccharide-sharing by a consortium of infant derived *Bifidobacterium* species. *Sci. Rep.* **12**, 4143 (2022).
29. Bunesova, V., Lacroix, C. & Schwab, C. Mucin cross-feeding of infant bifidobacteria and *Eubacterium hallii*. *Microb. Ecol.* **75**, 228–238 (2018).
30. Egan, M. et al. Cross-feeding by *Bifidobacterium breve* UCC2003 during co-cultivation with *Bifidobacterium bifidum* PRL2010 in a mucin-based medium. *BMC Microbiol.* **14**, 282 (2014).
31. Munoz, J., James, K., Bottacini, F. & Van Sinderen, D. Biochemical analysis of cross-feeding behaviour between two common gut commensals when cultivated on plant-derived arabinogalactan. *Microb. Biotechnol.* **13**, 1733–1747 (2020).
32. O'Connell Motherway, M., Fitzgerald, G. F. & van Sinderen, D. Metabolism of a plant derived galactose-containing polysaccharide by *Bifidobacterium breve* UCC2003. *Microb. Biotechnol.* **4**, 403–416 (2011).

33. Golisch, B., Lei, Z., Tamura, K. & Brumer, H. Configured for the human gut microbiota: molecular mechanisms of dietary β-glucan utilization. *ACS Chem. Biol.* **16**, 2087–2102 (2021).

34. Tamura, K. et al. Molecular mechanism by which prominent human gut bacteroidetes utilize mixed-linkage beta-glucans, major health-promoting cereal polysaccharides. *Cell Rep.* **21**, 417–430 (2017).

35. Tamura, K., Dejean, G., Van Petegem, F. & Brumer, H. Distinct protein architectures mediate species-specific beta-glucan binding and metabolism in the human gut microbiota. *J. Biol. Chem.* **296**, 100415 (2021).

36. Tamura, K. et al. Surface glycan-binding proteins are essential for cereal beta-glucan utilization by the human gut symbiont *Bacteroides ovatus*. *Cell Mol. Life Sci.* **76**, 4319–4340 (2019).

37. Singh, R. P., Rajarammohan, S., Thakur, R. & Hassan, M. Linear and branched β-Glucans degrading enzymes from versatile *Bacteroides uniformis* JCM 13288(T) and their roles in cooperation with gut bacteria. *Gut Microbes* **12**, 1–18 (2020).

38. Finnigan, T. J. A. et al. Mycoprotein: the future of nutritious nonmeat protein, a symposium review. *Curr. Dev. Nutr.* **3**, nzz021 (2019).

39. Fernandez-Julia, P. J., Munoz-Munoz, J. & van Sinderen, D. A comprehensive review on the impact of β-glucan metabolism by *Bacteroides* and *Bifidobacterium* species as members of the gut microbiota. *Int. J. Biol. Macromol.* **181**, 877–889 (2021).

40. Frankfater, C. F. et al. Lipidome of the Bacteroides genus containing new petidolipid and sphingolipid families revealed by multiple-stage mass spectrometry. *Biochemistry* **62**, 1160–1180 (2023).

41. Guo, Y. et al. Screening and epitope characterization of diagnostic nanobody against total and activated Bacteroides fragilis toxin. *Front. Immonol.* **14**, 1065274 (2023).

42. Degnan, B. A. & Macfarlane, G. T. Arabinogalactan utilization in continuous cultures of *Bifidobacterium longum*: effect of co-culture with *Bacteroides thetaiotaomicron*. *Anaerobe* **1**, 103–112 (1995).

43. Wang, Y. & LaPointe, G. Arabinogalactan utilization by *Bifidobacterium longum* subsp. *longum* NCC 2705 and *Bacteroides caccae* ATCC 43185 in monoculture and coculture. *Microorganisms* **8**, https://doi.org/10.3390/microorganisms8111703 (2020).

44. Fischbach, M. A. & Sonnenburg, J. L. Eating for two: how metabolism establishes interspecies interactions in the gut. *Cell Host Microbe* **10**, 336–347 (2011).

45. Higashi, B., Mariano, T. B., de Abreu Filho, B. A., Gonçalves, R. A. C. & de Oliveira, A. J. B. Effects of fructans and probiotics on the inhibition of *Klebsiella oxytoca* and the production of short-chain fatty acids assessed by NMR spectroscopy. *Carbohydr. Polym.* **248**, 116832 (2020).

46. Higashi, B., Mariano, T. B., Alves de Abreu Filho, B., Gonçalves, R. A. C. & Braz de Oliveira, A. J. Corrigendum to: "Effects of fructans and probiotics on the inhibition of *Klebsiella oxytoca* and the production of short-chain fatty acids assessed by NMR spectroscopy". *Carbohydr. Polym.* **260**, 117568 (2021).

47. Rios-Covian, D. et al. Interactions between *Bifidobacterium* and *Bacteroides* species in cofermentations are affected by carbon sources, including exopolysaccharides produced by 34ifidobacterial. *Appl. Environ. Microbiol.* **79**, 7518–7524 (2013).

48. Rogowski, A. et al. Glycan complexity dictates microbial resource allocation in the large intestine. *Nat. Commun.* **6**, 7481 (2015).

49. McNulty, N. P. et al. Effects of diet on resource utilization by a model human gut microbiota containing Bacteroides cellulosilyticus WH2, a symbiont with an extensive glycobiome. *Plos Biol.* **11**, e1001637 (2013).

50. Rahman, O., Cummings, S. P., Harrington, D. J. & Sutcliffe, I. C. Methods for the bioinformatic identification of bacterial lipoproteins encoded in the genomes of Gram-positive bacteria. *World J. Microbiol. Biotechnol.* **24**, 2377–2382 (2008).

51. Davies, G. J., Wilson, K. S. & Henrissat, B. Nomenclature for sugar-binding subsites in glycosyl hydrolases. *Biochem. J.* **321**, 557–559 (1997).

52. Kelley, L. A. et al. The Phyre2 web portal for protein modelling, prediction and analysis. *Nature* **10**, 845–858 (2015).

53. Pokusaeva, K. et al. Cellodextrin utilization by *Bifidobacterium breve* UCC2003. *Appl. Environ. Microbiol.* **77**, 1681–1690 (2011).

54. Abdi, R. & Joye, I. J. Prebiotic potential of cereal components. *Foods* **10**, https://doi.org/10.3390/foods10102338 (2021).

55. Ciecierska, A., Drywień, M. E., Hamulka, J. & Sadkowski, T. Nutraceutical functions of beta-glucans in human nutrition. *Rocz. Panstw. Zakl. Hig.* **70**, 315–324 (2019).

56. Cloetens, L., Ulmius, M., Johansson-Persson, A., Akesson, B. & Onning, G. Role of dietary beta-glucans in the prevention of the metabolic syndrome. *Nutr. Rev.* **70**, 444–458 (2012).

57. Mo, X. et al. Insoluble yeast β-glucan attenuates high-fat diet-induced obesity by regulating gut microbiota and its metabolites. *Carbohydr. Polym.* **281**, 119046 (2022).

58. Correia, V. G. et al. Mapping molecular recognition of β1,3-1,4-glucans by a surface glycan-binding protein from the human gut symbiont *Bacteroides ovatus*. *Microbiol. Spectr.* **9**, e0182621 (2021).

59. Rakoff-Nahoum, S., Coyne, M. J. & Comstock, L. E. An ecological network of polysaccharide utilization among human intestinal symbionts. *Curr. Biol.* **24**, 40–49 (2014).

60. Centanni, M., Sims, I. M., Bell, T. J., Biswas, A. & Tannock, G. W. Sharing a β-Glucan Meal: Transcriptomic Eavesdropping on a *Bacteroides ovatus*-Subdoligranulum variabile-Hungatella hathewayi Consortium. *Appl. Environ. Microbiol.* **86**, https://doi.org/10.1128/aem.01651-20 (2020).

61. Bzducha-Wróbel, A., Błażejak, S. & Tkacz, K. Cell wall structure of selected yeast species as a factor of magnesium binding ability. *Eur. Food Res. Technol.* **235**, 355–366 (2012).

Acknowledgements

Author contributions

P.F.-J. cloned, expressed, and purified recombinant enzymes; conducted and analysed kinetics for hydrolysis of polysaccharides, oligosaccharides, and chromogenic substrates; determined hydrolysis products in the HPLC; performed growth curves of all anaerobic bacteria; carried out cross-feeding experiments; and wrote the article. W.C. conducted and analysed the proteomics data and wrote the proteomics section in the manuscript. G.B., D.V.S. and J.M.-M. designed and directed research and co-wrote the article with input from all authors.

Competing interests

The authors declare no competing interests.

Additional information

Supplementary information The online version contains supplementary material available at https://doi.org/10.1038/s42003-023-04970-4.

Correspondence and requests for materials should be addressed to Jose Munoz-Munoz.

Peer review information *Communications Biology* thanks the anonymous reviewers for their contribution to the peer review of this work. Primary Handling Editors: Tobias Goris. A peer review file is available.

Reprints and permission information is available at http://www.nature.com/reprints

Publisher's note Springer Nature remains neutral with regard to jurisdictional claims in published maps and institutional affiliations.

List of primers

Bacteroides celulosyliticus WH2

	Sequence (5'→3')
Bccell WH2_01926 (GH3)	Forward: GCGGCGGCTAGCCAGGAAAAGGCAAATACC (% GC: 60, Melting Temperature: 76.2 °C) Reverse: GCGGCGCTCGAGCTATTGTAAGACAGTAAA (% GC: 50, Melting Temperature: 72.1 °C) Annealing temperature: 72 °C
Bccell WH2_01931 (GH157)	Forward: GCGGCGGCTAGCCAATTCAGTTCTTCTCCG (% GC: 60, Melting Temperature: 76.2 °C) Reverse: GCGGCGCTCGAGTCATGTCAGCAACATCTT (% GC: 57, Melting Temperature: 54.9 °C) Annealing temperature: 72 °C
Bccell WH2_02537 (GH30_3)	Forward: GCGGCGGCTAGCTGCGGATCGGACCACAAT (% GC: 67, Melting Temperature: 79 °C) Reverse: GCGGCGCTCGAGTTATTTCCACTTGAAAGA (% GC: 50, Melting Temperature: 72.1 °C) Annealing temperature: 72 °C
Bccell WH2_02538 (unknown)	Forward: GCGGCGGCTAGCGATGAGATTGACCAGTTC (% GC: 60, Melting Temperature: 76.2 °C) Reverse: GCGGCGCTCGAGTCATTCGCCCATTTCGTA (% GC: 60, Melting Temperature 76.2 °C) Annealing temperature: 72 °C
Bccell WH2_02541 (GH2)	Forward: GCGGCGGAATTCCAACATGAGAGCAAAACG (% GC: 53, Melting Temperature: 73.3 °C) Reverse: GCGGCGCTCGAGTTAATAAAGTTTCCTGAG (% GC: 52, Melting Temperature: 72.1 °C) Annealing temperature: 72 °C
Primers for qPCR cross feeding	Forward: AGCAGGCGGAATTCGATAAG (% GC: 50, Melting Temperature: 65 °C) Reverse: UGTGTACAGTGCCAGGCATAA (%GC: 48, Melting Temperature 66 °C) Annealing temperature: 66 °C

Bacteroides thetaiotaomicron VPI 5482

BT3312 (GH30_3)	Forward: GCGGCGGCTAGCAATAGTGATGATGCGGAA (% GC: 57, Melting Temperature: 74,9 °C) Reverse: GCGGCGCTCGAGTTACTTTGACTTTGCCCAACG

	(% GC: 58, Melting Temperature: 77.8 °C) Annealing temperature: 72 °C
BT3313 (unkown)	Forward: GCGGCTAGCGATGACGAGTTCCTTCCC (% GC: 63, Melting Temperature: 74.4 °C) XhoReverse: GCGGCGCTCGAGTTACTTCTTCACAACAGA (% GC: 53, Melting Temperature: 73.3 °C) Annealing temperature: 72 °C
BT3314 (GH3)	Forward: GCGGCGGCTAGCCAGACACCAGTATATCTA (% GC: 57, Melting Temperature: 74.9 °C) Reverse: GCGGCGCTCGAGCTATCTCAACTCAAATGG (% GC: 57, Melting Temperature: 74.9 °C) Annealing temperature: 72 °C
Primers for qPCR cross feeding	Forward: AGGTGCAGGCAACCT (% GC: 60, Melting Temperature: 64 °C) Reverse: AATTCCCGTTCTCCATGTCC (% GC: 50, Melting Temperature: 65 °C) Annealing temperature: 65 °C
Bifidobacterium breve UCC2003	
Bbr_0109 (GH1)	Forward: GCGGCGGCTAGC ATGACATTCGTTTTTCCG (% GC: 57, Melting Temperature: 77 °C) Reverse: GCGGCGCTCGAG TCA GAT TCC TTC CTG GAT (% GC: 60, Melting Temperature: 79 °C) Annealing temperature: 72 °C
Primers for qPCR cross feeding	Forward: AGAGTTTGATCCTGGCTCAG (% GC: 50, Melting Temperature: 64 °C) Reverse: CTACGGCTACCTTGTTACGA (% GC: 50, Melting Temperature: 64 °C) Annealing temperature: 65 °C
Bifidobacterium longum subsp. longum	
Primers for qPCR cross feeding	Forward: AGAGTTTGATCCTGGCTCAG (% GC: 50, Melting Temperature: 64 °C) °C Reverse: CTACGGCTACCTTGTTACGA (% GC: 50, Melting Temperature: 64 °C) °C Annealing temperature: 65 °C
Bifidobacterium longum **subsp**. *infantis*	
Primers for qPCR cross feeding	Forward: AGAGTTTGATCCTGGCTCAG (% GC: 50, Melting Temperature: 64 °C) Reverse: CTACGGCTACCTTGTTACGA

	°(% GC: 50, Melting Temperature: 64 °C) Annealing temperature: 65 °C
***Lactiplantibacillus plantarum* WCFS1**	
Primers for qPCR cross feeding	Forward: CACCGCTACACATGGAG (% GC: 59, Melting Temperature: 63 °C) Reverse: CCACCGCTACACATGGAGTTCCACT (% GC: 56, Melting Temperature: 73 °C) Annealing temperature 64 °C